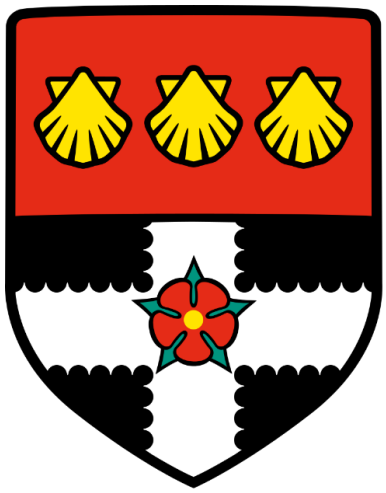

Watercress as a nutritional adjuvant treatment in breast cancer

A thesis submitted for the degree of Doctor of Philosophy

Department of Food and Nutritional Sciences

Natasa Giallourou

June 2017

To my parents,

my guardian angels.

Declaration of ownership

‘Declaration:

I confirm that this is my own work and the use of all material from other sources has been properly and fully acknowledged.’

Acknowledgments

First and foremost I would like to thank my supervisor Dr Jonathan Swann for his support and guidance. He has been a continuous source of motivation and inspiration and I will be forever grateful for everything he has done for me.

Great thanks to Dr Daniel Commane for 'adopting' me halfway through my PhD and most importantly for helping me realise and understand the importance of patience and perseverance in research. In addition, I am thankful to Dr Niamh Harbourne (University College Dublin) for her supervision and great support throughout my PhD.

Furthermore, I am grateful to Prof Ian Rowland for offering me the opportunity to work at the University of Reading and for his invaluable contribution in this project. A big thank you to my industrial supervisor Dr Steve Rothwell for his continuous help and support and for being a perfect example of how one can be endlessly passionate about their job.

Many thanks to Prof Graham Packham (University of Southampton) for hosting me in his lab and to Prof Ketan Patel (University of Reading) for giving me the chance to be a part of his projects.

I would like to acknowledge my sponsors - the University of Reading and the Agriculture and Horticulture Development Board (AHDB) for funding my PhD.

My PhD experience would not have been the same without a few special friends from the University of Reading. I am very thankful to everyone in 2-1 for all the great moments and particularly Roberta and Caroline for supporting me through it all. Special thanks to Petra, Katerina, Vangelis and Panos for making the past three years unforgettable.

I would especially like to thank my boyfriend, Panayiotis, for his patience, support and unconditional love over the past three years. Thank you for brightening my life and making my heart smile. I am also extremely grateful to his family for everything they have offered to me and for being so helpful during my thesis write up.

Words cannot express my gratitude to my family. Special thanks to my grandparents for their lifelong love and support. I hope I made you proud. Thank you to my little sister Maria for being my best friend and to my brother Christos for being by my side. Lastly and most importantly, I wish to thank my parents. Thank you for teaching me what hard work looks like and to appreciate the ways in which it pays off in the end. Thank you for reminding me that everything in life happens for a reason and for always being by my side, supporting me in fulfilling my dreams. Thank you for your unwavering love. I owe you everything I am today, and everything I am working on becoming. Σας αγαπώ!

Abstract

Breast cancer is a leading cause of cancer related mortality globally, and epidemiological studies suggest a link between healthy nutrition and cancer prevention. Members of the Brassicaceae family, including watercress, have been extensively studied for their anti-cancer and anti-genotoxic potential. Watercress has a complex phytonutrient profile characterised by high levels of carotenoids, flavonols and glucosinolates Extracts of watercress exhibit strong antioxidant capacity *in vitro*. Watercress and its components have been associated with the inhibition of the three stages of carcinogenesis: initiation, proliferation and metastasis in *in vitro* cancer cell models. Phenethyl isothiocyanate (PEITC) is a glucosinolate break-down product and watercress is the richest dietary source of it. It has received considerable attention for its anti-cancer properties and has been tested in a number of clinical trials.

In this thesis, the effects of crude watercress extract and PEITC on the metabolic and phenotypic responses in breast cancer and healthy breast tissue cell lines were examined. Radiotherapy is the most common treatment modality for breast cancer patients, it functions by killing cancer cells but it simultaneously damages healthy tissues. We set out to examine synergistic responses to irradiation and watercress/ or PEITC exposures in breast cancer cells and we further investigated whether watercress or PEITC can be protective against radiation induced collateral damage.

Watercress and PEITC effectively modulated important cancer cell metabolic pathways associated with anti-cancer endpoints such as cell cycle arrest and DNA damage. In this thesis, PEITC has been shown to enhance the sensitivity of cancer cells to irradiation making the cancer killing process more effective, whereas watercress can protect healthy breast cells from radiation induced damage. These observations appear to be mediated by the ability of PEITC and other phytochemicals in watercress to interact with the antioxidant glutathione. The results obtained from this work remain to be validated in a clinical setting.

Table of Contents

List of abbreviations

°C	Degrees Celsius
1D	One dimensional
^{1}H	Proton (Hydrogen)
4-AB	4 - aminobutyrate
4-HGB	4-hydroxyglucobrassicin
4-HNE	4-hydroxy nonenal
4-MGB	4-methoxyglucobrassicin
µM	Micromolar
AAE	Ascorbic acid equivalents
ACLY	ATP citrate lyase
ADP	Adenosine diphoshate
AHDB	Agriculture and Horticulture Development Board
AIF	Apoptosis inducing factor
AKT	Protein kinase B
AMP	Adenosine monophosphate
AMPK	AMP-activated protein kinase
ANOVA	Analysis of variance
ARE	Antioxidant response element
ATCC	American Type Culture Collection
ATP	Adenosine triphosphate
AXP	Adenosine X phosphate
BD	Boiled
BITC	Benzyl-isothiocyanate
BMI	Body mass index
CG	Cycteinglycinase
CO_2	Carbon dioxide
COX	Cyclooxygenase
CPMG	Carr-Purcell-Meiboom-Gill
CYP	Cytochrome P450
D_2O	Deuterium oxide
DA	Discriminant analysis
DAPI	4',6-Diamidino-2-Phenylindole, Dihydrochloride
DCIS	Ductal carcinoma *in situ*
DMEM	Dulbecco's modified Eagle's medium
DMSO	Dimethyl sulfoxide
DNA	Deoxyribonucleic acid
DW	Dry weight
EBCTCG	Early Breast Cancer Trialists' Collaborative Group
EDTA	Ethylenediaminetetraacetic acid
EGF	Oestrogen growth factor
EGFR	Oestrogen growth factor receptor
ER	Oestrogen receptor

ERK	Extracellular signal-regulated kinases
FAD	Flavin adenine dinucleotide
FBS	Fetal bovine serum
FID	Free induction decay
FRAP	Ferric reducing antioxidant power
FW	Fresh weight
g	grams or gravity
GAE	Gallic acid equivalents
GCL	Glutathione cysteine ligase
GLS	Glucosinolate
GPC	Glycerophosphocholine
GPX	Glutathione peroxidase
GR	Glutathione reductase
GSH	Glutathione
GSSG	Oxidised glutathione
GST	Glutathione S-transferase
H_2O	Water
H_2O_2	Hydrogen Peroxide
HDL	High density lipoprotein
HER	Human epidermal growth factor receptor
HIF	Hypoxia inducible factor
HPLC	High performance liquid chromatography
HR-MAS	High resolution-Magic angle spinning
HSC-3	Human oral squamous cell carcinoma
HT-29	Human colon adenocarcinoma cells
IG	Isorhamnetin glucoside
iNOS	Inducible nitric oxide synthase
IR	Irradiation
ITC	Isothiocyanate
JNK	Jun amino-terminal kinases
KDG	Kampferol 3-diGlc-7-Glc
KFTG	Kampferol 3-(fer-triGlc)-7 Glc;
KSG	Kampferol 3-(sinp-Glc)-4'Glc
KSTG	K 3-(sinp-triGlc)-7-Glc
LC	Liquid chromatography
LCIS	Lobular carcinoma *in situ*
LKB	Liver kinase B
LMA	Low melting point agarose
MAPK	Mitogen-activated protein kinase
MCF	Michigan Cancer Foundation
mg	milligrams
MHz	megahertz
mM	Millimolar
MRP1	Multidrug resistance-associated protein 1
MS	Mass spectrometry

MTBE	Methyl tert- butyl ether
MTT	3-(4,5-dimethylthiazol-2-yl)-2,5-diphenyltetrazolium bromide
MW	Microwaved
NAC	N-acetyl cysteine
NAD	Nicotinamide adenine dinucleotide
NADPH	Nicotinamide adenine dinucleotide phosphate
ND	Not detected
NFκB	Nuclear factor kappa-light-chain-enhancer of activated B cells
nM	nanomolar
NMNA	N-methyl-nicotinic acid
NMR	Nuclear magnetic resonance
NNK	Nicotine-derived nitrosamine ketone
Noesy	Nuclear Overhauser effect spectroscopy
NSCLC	Non-small cell lung cancer
O_2	Oxygen
OPLS	Orthogonal projections to latent structures
OPLS-DA	Orthogonal projections to latent structures – discriminant analysis
ORAC	Oxygen radical absorbance capacity
OSC	Orthogonal signal corection
PARP	Poly (ADP-ribose) polymerase
PBS	Phosphate buffer saline
PC	Phosphocholine
PCA	Principal component analysis
PDH	Pyruvate dehydrogenase
PEITC	Phenethyl-isothiocyanate
PI	Propidium iodide
PLS	Projections to latent structures
ppm	parts per million
PR	Progesterone receptor
PTEN	Phosphatase and tensin homologue
Q^2Y	Predictive ability parameter of OPLS-DA model
QCSG	Quercitin 3-(caf-Glc)-3'-(sinp-Glc)-4'-Glc
R	Correlation value
R^2	Coefficient of covariance
R^2Y	''Goodness of fit'' parameter of OPLS-DA model
RD	Relaxation delay
RF	Radiofrequency
ROS	Reactive oxygen species
rpm	revolutions per minute
RSPA	Recursive segment-wise peak alignment
RT	Radiotherapy
SAM	S-Adenosyl methionine
SD	Standard deviation
SEM	Standard error of the mean
SOD	Superoxide dismutase

T_1	Spin-lattice relaxation time
T_2	Spin-spin relacation time
TCA	Tricarboxylic acid
TMAO	Trimethylamine-N-Oxide
TPTZ	2,4,6-Tris(2-pyridyl)-*s*-triazine
TRAIL	TNF-related apoptosis-inducing ligand
TSP	3-(trimethylsilyl)-[2,2,3,3,-$^{2}H_4$]-propionic acid
TXI	Triple resonance inverse (probe)
UDP	Uridine diphosphate
UV	Ultraviolet
VEGF	Vascular endothelial growth factor
VLDL	Very low-density lipoprotein
WX	Watercress
XIAP	X-linked inhibitor of apoptosis

List of figures

List of tables

1 Introduction

1.1 Molecular basis of cancer

Cancer is often defined as a disease of uncontrolled and abnormal proliferation of cells that leads to tumour formation. It is the result of a multistep process involving genetic mutations as well as epigenetic changes progressively driving the transformation of healthy cells to malignant derivatives. It has been postulated that cancer cells acquire a number of gain of function traits during malignant transformation, indicative of the high complexity of this disease (Fig. 1.1). The hallmarks include increased proliferative activity, evasion of growth suppressors, induction of angiogenesis, activation of invasion and metastasis, resistance to cell death and the enabling of replicative immortality [1]. Enabling characteristics, which facilitate tumor progression, involve inflammation and genomic instability that expedites the acquisition of the aforementioned hallmarks. Advances in the field of cancer research over the past decade have led to consideration of the importance of previously understudied cancer traits for sustaining tumour cells in vivo. Notably the ability of cancer cells to evade challenges from the immune system and to reprogram their metabolism to establish as tumours [2].

1.2 Breast cancer

Breast cancer is the most common type of cancer amongst women in the United Kingdom (UK), with nearly 53,700 new cases in 2013 and a one in eight estimated lifetime risk of diagnosis (Cancer Research UK, 2016). The UK 10 year survival rate is increasing and the treatment curative is 78% of all women affected by breast cancer. The decline in breast cancer associated mortality is likely due to improved drug

treatment despite breast cancer incidence rates increasing in recent years. A national screening program means that the majority of the breast cancer cases are now diagnosed at an early stage.

Genetic predisposition has been identified in individuals with mutations in the *BRCA1*, *BRCA2, PTEN* and *TP53* genes but these mutations account for only a small percentage of all breast cancers. This suggests that the majority of cases are caused by a complex combination of environmental and inherited factors [3].

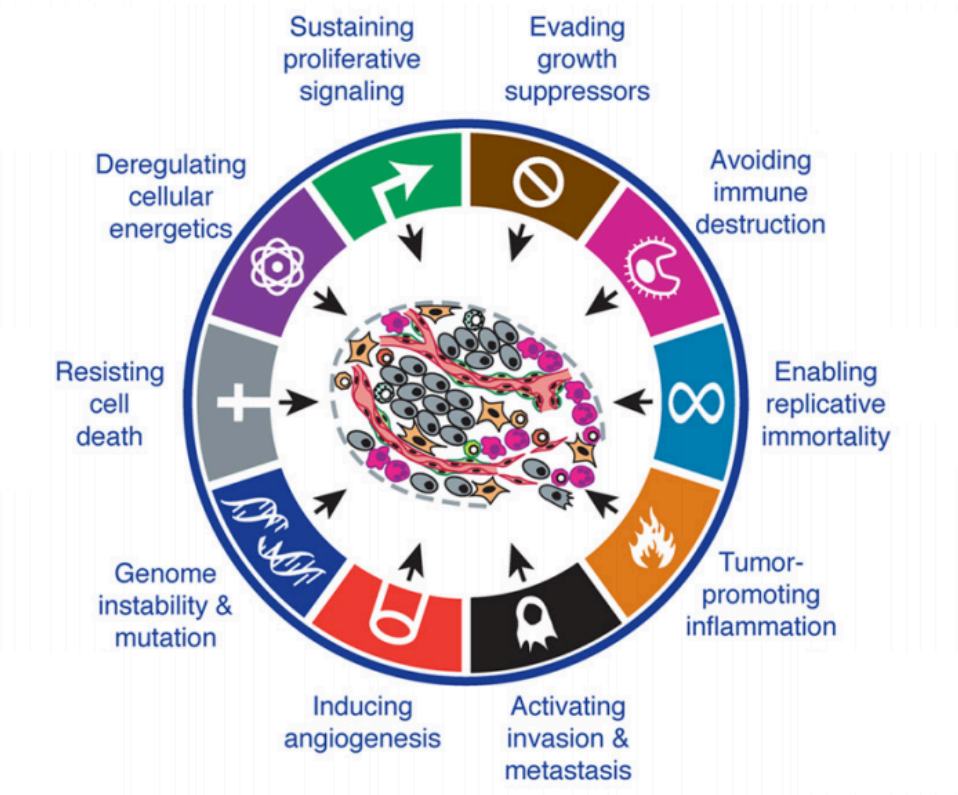

Figure 1.1 The established hallmarks of cancer

Figure adapted from [2]

1.2.1 Subtypes of breast cancer

Breast cancer is a multifaceted disease and is characterised by many subtypes with different clinical and molecular features that can have different prognostic attributes and therapeutic implications. Breast cancer can be invasive or non-invasive. Adenocarcinomas are the most common form of invasive breast cancer and can be either ductal or lobular accounting for approximately 85% and 15% of invasive adenocarcinomas respectively [4] (Fig. 1.2 depicts the structure of a healthy human breast).

In addition to invasive breast cancer, non-invasive forms can appear with ductal carcinoma *in situ* (DCIS) which is the most common type, and lobular carcinoma *in situ* (LCIS). LCIS is rare in comparison to DCIS and is considered as an increased risk factor for invasive breast cancer rather than as a direct precursor lesion [5]

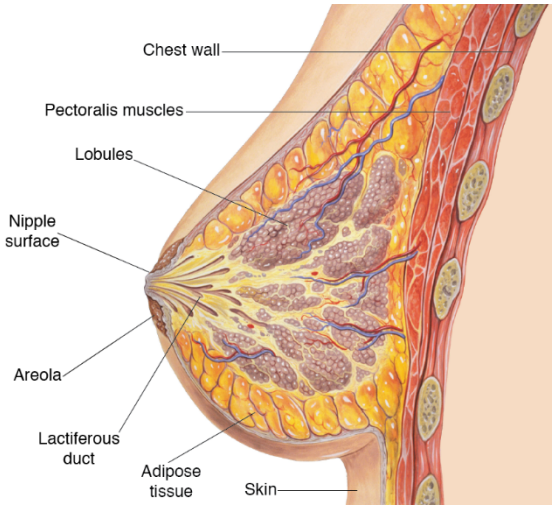

Figure 1.2 Anatomy of the normal human breast

[By Andrewmeyerson (Own work); adapted to add labels [CC BY-SA 3.0, (http://creativecommons.org/licenses/by-sa/3.0)], via Wikimedia Commons Andrewmeyerson]

1.2.2 Hormone receptors status and their relevance to treatment

Hormone receptor status is the major biomarker for breast cancer prognosis and response to therapy. Oestrogen receptors (ER) are cellular proteins and are activated by the lipophilic steroid, oestrogen. Binding of oestrogen to ER results in a variety of signalling cascades involved in DNA synthesis, cell division and the formation of proteins including the progesterone receptor (PR). Breast cancer is often characterised by higher levels of expression of ER and PR compared to healthy tissue and the presence of these receptors (referred to as ER+ or PR+) is generally linked with positive prognosis and increased rates of successful endocrine therapy.

Tamoxifen is the primary drug administered to pre-menopausal women with an ER positive status. It is a selective oestrogen receptor modulator that acts by binding to ER resulting in conformational changes in the protein and antagonistically inhibiting transcription of oestrogen responsive genes, eventually halting cell division [6]. For ER+ post-menopausal breast cancer patients, aromatase inhibitors are being given as adjuvant therapy for the inhibition of oestrogen synthesis. Aromatase catalyses the conversion of androgens to oestrogens; its inactivation thereby reduces the mitogenic effects of oestrogens. There are three aromatase inhibitors namely anastrozole, exemestane and letrozole that are widely used in the clinical setting [7].

Overexpression of the human epidermal growth factor 2 (HER2) is indicative of a more aggressive form of breast cancer with poor prognosis and it is found at increased levels in 25-30% of all breast cancer cases [8, 9]. Activation of HER2, and of other members of the human epidermal growth factor family (HER), by ligands like epidermal growth factor, initiates a signal cascade that alters gene expression

affecting biological functions related to proliferation and migration. Trastuzumab (Herceptin) is used as a treatment for breast cancer patients overexpressing HER2. It is involved in the regulation of proliferation and apoptosis; cancer cells treated with Herceptin exhibit G1 cell cycle arrest [10, 11].

Triple negative cancers do not express ER, PR and do not overexpress HER2. These types of cancer are exceptionally aggressive, they do not respond to endocrine treatment and are correlated with poor prognosis [12]. Chemotherapy is the chosen treatment modality in these cases [13].

1.2.3 Radiotherapy

Adjuvant radiotherapy is a crucial element for the treatment of breast cancer. It has been used for over 50 years and is undeniably a positive intervention recommended to a substantial proportion of patients [14] (the process of radiotherapy is depicted in Fig. 1.3). Results from the Early Breast Cancer Trialists' Collaborative Group (EBCTCG) study of 45,000 women with breast cancer in 86 randomised trials, suggest that radiotherapy following breast conserving surgery reduced the 5 year recurrence rate by 15.7% and the 15 year breast cancer mortality by 4.2% [15].

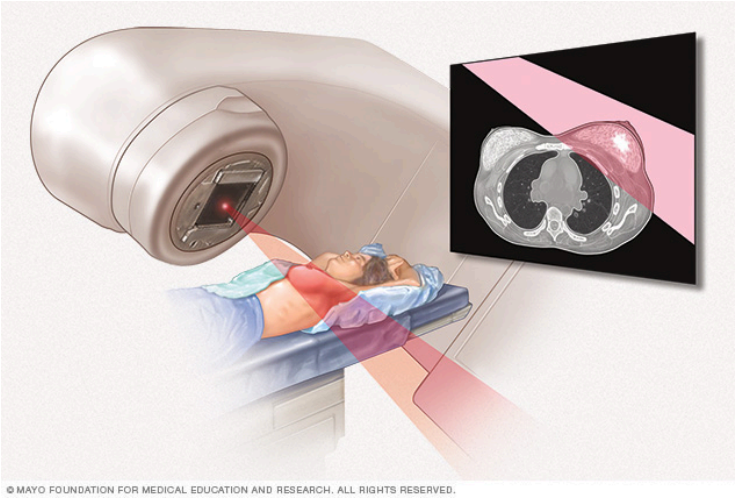

Figure 1.3 Linear accelerator delivering high-energy x-rays to the target cancer site. Figure adapted from [16]

The goal of radiotherapy is to damage the DNA and kill cancer cells inducing cell death. Charged energy particles and photons can induce direct or indirect ionisation of the atoms that make up DNA nucleotides. Indirect ionisation stems from the radiolysis of water molecules inside the cell, which then results in the rapid formation of reactive free radicals, mainly hydroxyl radicals that can in turn induce damage to DNA and cellular compartments (Fig. 1.4). Direct ionisation by charged particles usually causes double strand DNA breaks but single strand breaks are also a common outcome. Double strand breaks cause substantially more genomic instability than single strand breaks and are more likely to result in cell death or poor DNA repair. Radiotherapy has the potential to induce a broad range of damage to DNA in addition to single and double strand breaks, including base pair alterations, destruction of sugars and interstrand crosslinks [17]. Radiation sequelae include activation of signal transduction pathways for cell cycle arrest, allowing for DNA repair, or in some

instances where the damage is too high, for apoptotic machinery to be employed to prevent further DNA replication [18]. The susceptibility of breast cancer cells to ionising radiation depends to a great extent on the rate of cell proliferation, the total dose of radiation, the fractionation plan and on the capacity of these cells to repair DNA damage [19].

Non-cancerous cells are unavoidably affected in the course of radiotherapy treatment however healthy cells are better equipped to scavenge the radiation induced damage and may have more efficient DNA repair meachinery [20]. Side effects of radiotherapy can be divided into acute and late. Acute side effects include mainly skin reactions and are extremely common among patients receiving radiotherapy [14]. Late side effects include hyperpigmentation, skin fibrosis and potential influence on lung and heart tissues. Cardiac damage has been linked to radiotherapy during breast cancer, as have radiation induced sarcomas and lung cancers, due to the proximity of these tissues to the breast [15, 21]. Fractionation of the total radiation dose is therefore employed allowing the healthy cells to recover between treatments. The need for radio-protective agents is of paramount importance for oncologists especially in cases of radio-resistant tumours where higher doses of radiation have to be administered to the patient.

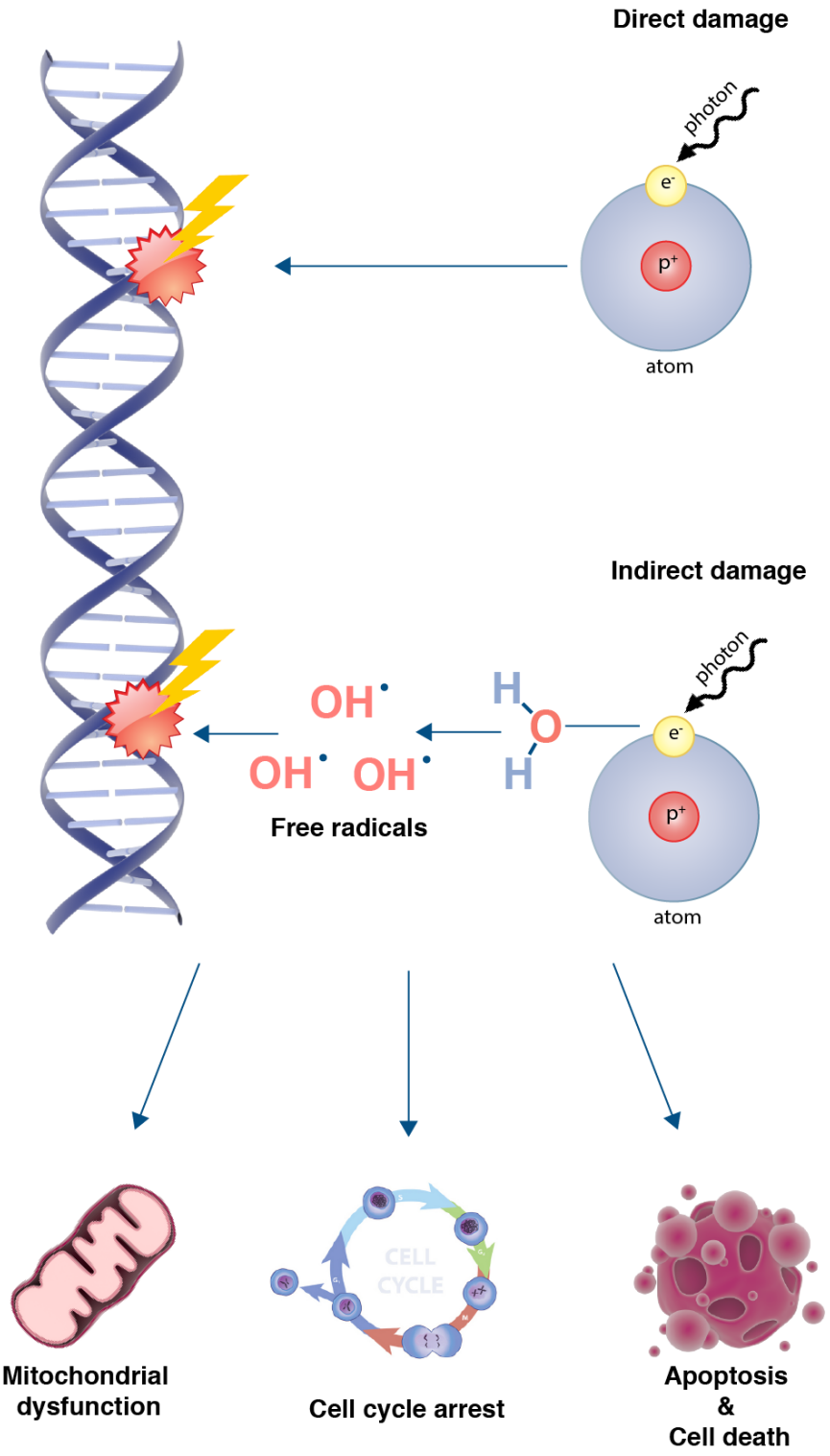

Figure 1.4 Direct and indirect DNA damage induced by ionising radiation and the consequences on cellular functions

1.3 Cancer cell metabolism

The metabolic activities of cancer cells are dissimilar to those of normal cells. [2]. Cancer cells undergo metabolic reprogramming, acquiring distinct metabolic features resulting in enhanced or suppressed activity of conventional metabolic pathways. Reprogrammed tumour cell metabolism modifies cellular fitness in such a manner that presents a selective advantage during the acquisition of malignant properties therefore; deregulated cancer metabolism constitutes one of cancer's established hallmarks

The metabolic phenotype of cancer cells is shaped by a complex combination of intrinsic and extrinsic molecular events involving genetic mutations and interactions with the microenvironment. Inherently, proliferating cells have to alter their metabolism to meet three basic needs: a) rapid generation of ATP to sustain their energy status, b) upregulated biosynthesis of macromolecules for biomass increase c) strict maintenance of redox status (Fig.1.5) [22]. To support the essential requirements for growth and proliferation, cancer cells rewire the metabolism of all major groups of macromolecules: carbohydrates, proteins, lipids, and nucleic acids [23].

Growth and survival of cancer cells are processes regulated by oncogenic signalling pathways, which are activated by the loss of function of tumour suppressor genes like p53 or the activation of oncogenes, like PI3K; this can strongly influence cell metabolism. Cell signalling modifications influence metabolism in order to maintain function through increases in the rate of cell proliferation. Coupled with the genetic alterations that modify cancer cell metabolism, metabolic interactions with the microenvironment constitute a major determinant of the metabolic phenotype of

cancer cells. Interestingly, a range of genetically stable cell lines (fibroblasts, endothelial cells and components of the immune system) alter their metabolic phenotype when residing in the vicinity of a growing cancer [24].

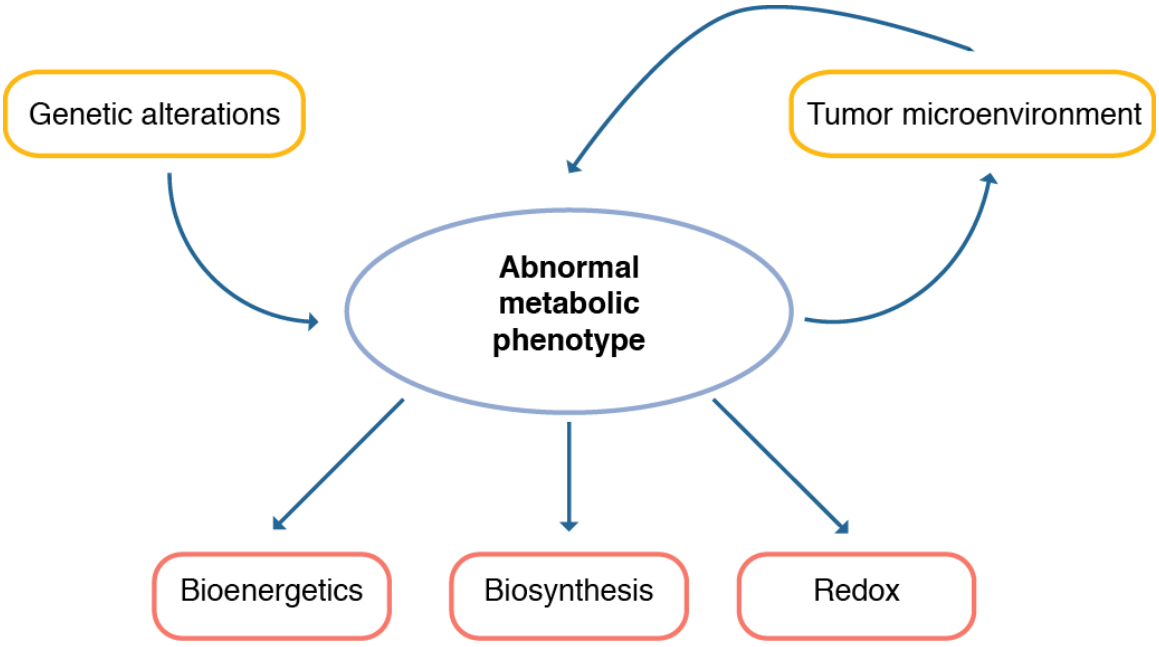

Figure 1.5 Causal elements shaping the cancer metabolic phenotype

Genetic alterations control cancer cell metabolism along with signals from the tumour microenvironment. The abnormal metabolic phenotype of cancer cells ultimately satisfies the energy requirements of the cells in the form of ATP; it maintains their biosynthetic capacity for cell proliferation and ensures maintenance of appropriate redox status.

Cancer cells modify the metabolic configuration of the extracellular milieu as a result of their enhanced substrate uptake, catabolism and export of metabolites, thereby influencing the phenotype of local normal cells. Reciprocally, the microenvironment can induce shifts in the metabolism and signalling cascades in the cancer cells *per se* [25]. The abnormal vasculature of tumours in combination with the innately altered cancer cell metabolism generates a spatial and temporal

heterogeneity in oxygen concentration, pH, as well as the availability of several nutrients like glucose and glutamine, which are all essential requirements for tumour progression [22]. Solid tumours need to adapt to these stressful and dynamic microenvironment features, developing strategies, which feed into the cancer cells' distorted metabolic phenotype by altering cell signalling, transcriptional regulation and redox balance contributing to tumour growth and dissemination [26].

1.3.1 Glycolysis

Cell proliferation is a process during which cells have increased requirements for nutrients and it also induces shifts in the manner nutrients are utilised to meet cellular needs. Non-proliferating cells in differentiated tissues utilise glucose to generate acetyl-CoA in the mitochondrial space, which is oxidised in the tricarboxylic acid (TCA) cycle under normoxic conditions. The oxidative reactions of the TCA cycle give rise to NAD^+/NADH and FAD/$FADH_2$ that then fuel the electron transport chain and ATP is produced through oxidative phosphorylation. The net energy yield of oxidative phosphorylation is 36 ATP molecules. Under insufficient oxygen conditions, differentiated cells undergo anaerobic glycolysis, converting glucose to lactate yielding two ATP molecules (Fig. 1.6).

The carbon economy of tumour cells differs significantly from that of differentiated cells. Cancer cells reprogram their biochemical pathways to fulfil their needs during cancer progression. Carbon is shuttled to the biosynthesis of macromolecules like fatty acids, cholesterol, sugars, nucleotides and non-essential amino acids [25]. Cancer cells undergo glycolysis even in the presence of oxygen; a

process defined as the Warburg effect and is one of the best-studied metabolic characteristics in cancer cells [27]. Under adequate oxygen concentrations, tumour cells generate ATP via glycolysis, shifting the primary ATP generation from oxidative phosphorylation. The majority of glucose is therefore converted to lactate with only a minor percentage (~5%) of pyruvate being metabolised in the TCA cycle [28]. ATP generation through glycolysis is a fast process compared to oxidative phosphorylation but it is far less efficient in terms of ATP yield. Therefore, cancer cells exhibit excessively high rates of glycolysis to cover their bioenergetics, biosynthetic and redox needs resulting in the high accumulation of lactate (Fig. 1.6).

The explanation behind the paradoxical switch of rapidly proliferating cells to the less efficient glycolysis is still unclear. It is proposed that because the metabolic requirements of cancer cells extend beyond ATP, glycolysis presents a biosynthetic advantage for these cells through the branching pathways like pentose phosphate pathway and one-carbon metabolism running parallel to glycolysis giving rise to a high flux of carbon sources [28] (Fig. 1.7)

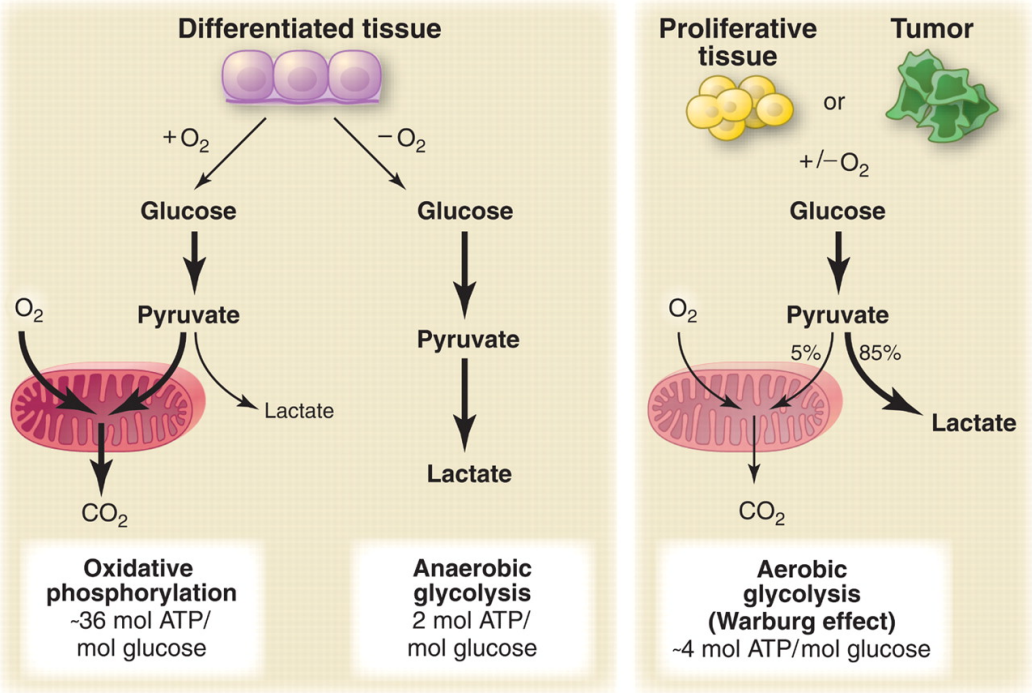

Figure 1.6 Schematic representation of the oxidative and glycolytic metabolic phenotypes of differentiated and proliferative tissues respectively.

In the presence of oxygen, non-proliferating (differentiated) tissues first metabolize glucose to pyruvate via glycolysis and then completely oxidize most of that pyruvate in the mitochondria to CO_2 during the process of oxidative phosphorylation. Because oxygen is required as the final electron acceptor to completely oxidize the glucose, oxygen is essential for this process. When oxygen is limiting, cells can redirect the pyruvate generated by glycolysis away from mitochondrial oxidative phosphorylation by generating lactate (anaerobic glycolysis). This generation of lactate during anaerobic glycolysis allows glycolysis to continue (by cycling NADH back to NAD+), but results in minimal ATP production when compared with oxidative phosphorylation. Warburg observed that cancer cells tend to convert most glucose to lactate regardless of whether oxygen is present (aerobic glycolysis). This property is shared by normal proliferative tissues. Mitochondria remain functional and some oxidative phosphorylation continues in both cancer cells and normal proliferating cells. Nevertheless, aerobic glycolysis is less efficient than oxidative phosphorylation for generating ATP. In proliferating cells, ~10% of the glucose is diverted into biosynthetic pathways upstream of pyruvate production. Figure and legend adapted from [28]

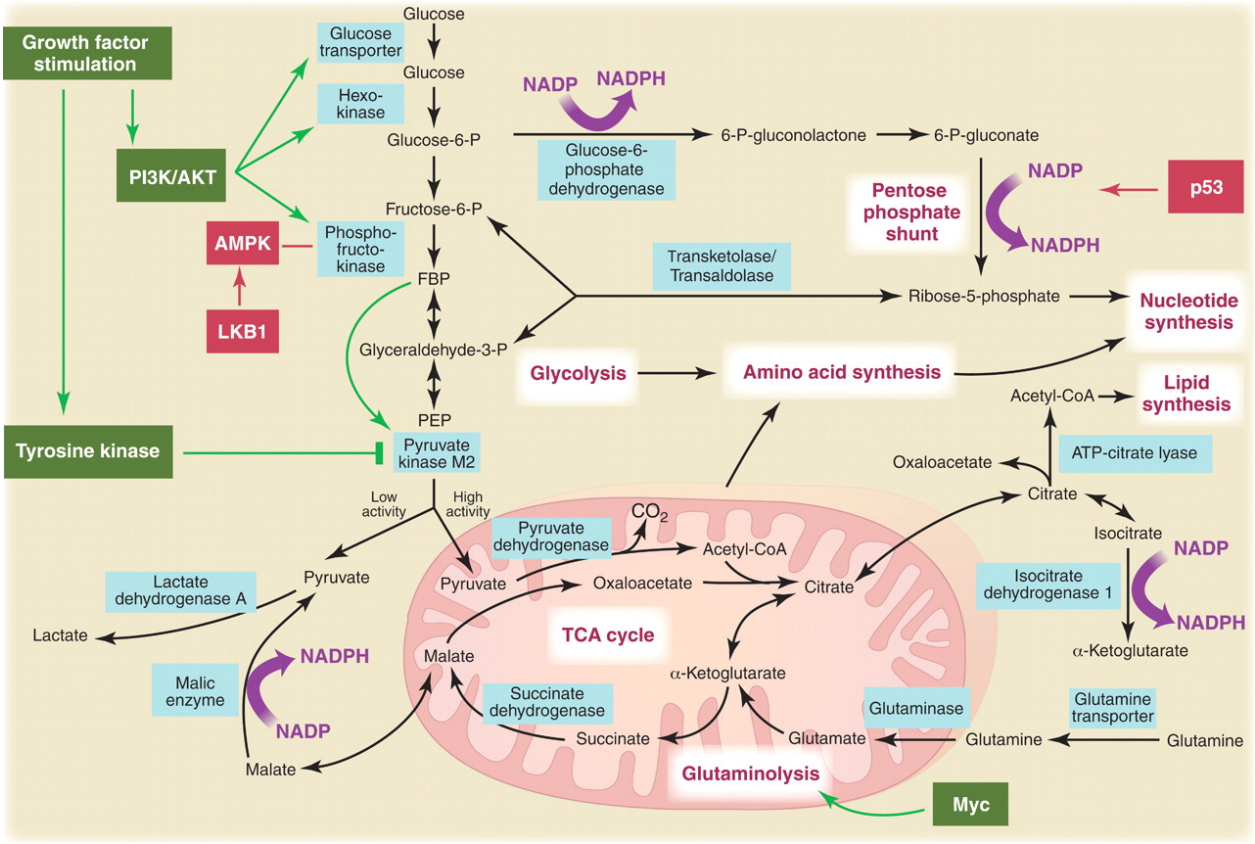

Figure 1.7 Metabolic pathways active in proliferating cells

Metabolic pathways active in proliferating cells are directly controlled by signalling pathways involving known oncogenes and tumor suppressor genes. This schematic shows our current understanding of how glycolysis, oxidative phosphorylation, the pentose phosphate pathway, and glutamine metabolism are interconnected in proliferating cells. This metabolic wiring allows for both NADPH production and acetyl-CoA flux to the cytosol for lipid synthesis. Key steps in these metabolic pathways can be influenced by signalling pathways known to be important for cell proliferation. Activation of growth factor receptors leads to both tyrosine kinase signalling and PI3K activation. Via AKT, PI3K activation stimulates glucose uptake and flux through the early part of glycolysis. Tyrosine kinase signalling negatively regulates flux through the late steps of glycolysis, making glycolytic intermediates available for macromolecular synthesis as well as supporting NADPH production. Myc drives glutamine metabolism, which also supports NADPH production. LKB1/AMPK signalling and p53 decrease metabolic flux through glycolysis in response to cell stress. Decreased glycolytic flux in response to LKB/AMPK or p53 may be an adaptive response to shut off proliferative metabolism during periods of low energy availability or oxidative stress. Tumor suppressors are shown in red, and oncogenes are in green. Key metabolic pathways are labeled in purple with white boxes, and the enzymes controlling critical steps in these pathways are shown in blue. Some of these enzymes are candidates as novel therapeutic targets in cancer. Figure and legend adapted from [28]

1.3.2 Glutaminolysis

Tumour cells are highly dependent on glutamine for macromolecular biosynthesis as well as robust cell proliferation. Glutamine is intracellularly converted to glutamate by the action of glutaminase. Glutamate can then be converted to α-ketoglutarate via glutamate dehydrogenase and incorporated into the TCA cycle. Through this process of anaplerosis, glutamate can serve as a carbon and nitrogen source for the production of nonessential amino acids, purines, pyrimidines, nucleotides and lipids [25, 29]. The enzyme glutathione cysteine ligase (GCL) can also convert glutamate directly to glutathione which is the most significant antioxidant in cells and has a major role in the management of cellular redox status [30].

1.3.3 Fatty acid synthesis

Biosynthesis and turnover of fatty acids is often increased in tumour cells to meet the anabolic requirements of rapidly proliferating cells. Lipids are shuttled towards the formation of cellular membranes and signalling molecules. *De novo* biochemical synthesis of fatty acids requires reducing power coming from NADPH as well as acetyl-CoA, which is the major lipogenic substrate unit. In the process of fatty acid synthesis acetyl-CoA comes from citrate formed in the TCA cycle in the mitochondria and is converted to acetyl-CoA by the action of ATP citrate lyase (ACLY). In nutrient-scarce circumstances (which is usually the case *in vivo*), cancer cells have higher rates of glycolysis. As such, pyruvate is preferentially converted to lactate rather than being oxidised in the TCA cycle to provide citrate for fatty acid synthesis via acetyl-CoA. Instead extracellular acetate has been shown to be the source of acetyl-CoA for *de*

novo fatty acid synthesis in a variety of hypoxic brain tumours [31-33]. Acetate can hence nourish stressed tumour cells.

1.3.4 Choline metabolism

Malignant transformation during carcinogenesis is characterised by active choline metabolism as observed by increased levels of choline-containing metabolites as well as choline breakdown products like phospholipids [34]. Phospholipids such as phosphocholine, phosphatidylcholine, along with phosphatidylethanolamine and other neutral lipids are the constituents of the lipid bilayer of cellular membranes and have a vital role in the maintenance of membrane integrity. Up-regulated choline metabolism is central to sustaining cancer cell proliferation and can also be influenced by the tumour microenvironment. Hypoxic conditions as well as low extracellular pH have been found to induce shifts in the concentrations of total choline, phosphocholine and glycerophosphocholine [35, 36]. Furthermore, oncogenes, cytokines and growth factors can affect choline metabolism [34]. Because choline-containing metabolites are detectable by non-invasive spectroscopic methods, these compounds may form a non-invasive biomarker of cell transformation, the stage of cancer development, as well as response to therapy [37].

1.3.5 ROS and cancer

Reactive oxygen species (ROS) are a natural by-product of cell metabolism and can have pleiotropic effects in all aspects of cell survival. The fate of cells relies heavily on the levels at which ROS are present (Fig. 1.8). Low abundance of intracellular ROS (yellow area) presents a benefit for cell proliferation and successful progression through survival pathways as a result of post-translational modifications [38, 39]. Conversely, if the levels of ROS become extremely high (pink area in Fig. 1.8) this causes detrimental oxidative stress via macromolecular damage, senescence [40] and loss of mitochondrial membrane potential leading to apoptosis [41]; a collection of events that can have lethal effects on cells. To counter the outcomes of oxidative stress, cancer cells increase their antioxidant content (mainly GSH), limiting the accumulation of ROS at excessively high levels preventing irreparable damage [42]. Naturally, proliferating cells acquire oncogenic mutations, which favour anomalous energy metabolism and protein translation leading to aberrantly increased ROS [43]. Through further mutations and adjustments, cancer cells tightly orchestrate the cycling of ROS and antioxidant production in a manner that permits cell survival and maintenance of ROS at moderate quantities (blue area). This remarkable regulation of ROS not only protects cancer cells from catastrophic oxidative damage but also ensures that they will benefit from ROS driven mutagenic episodes, which favour tumour progression.

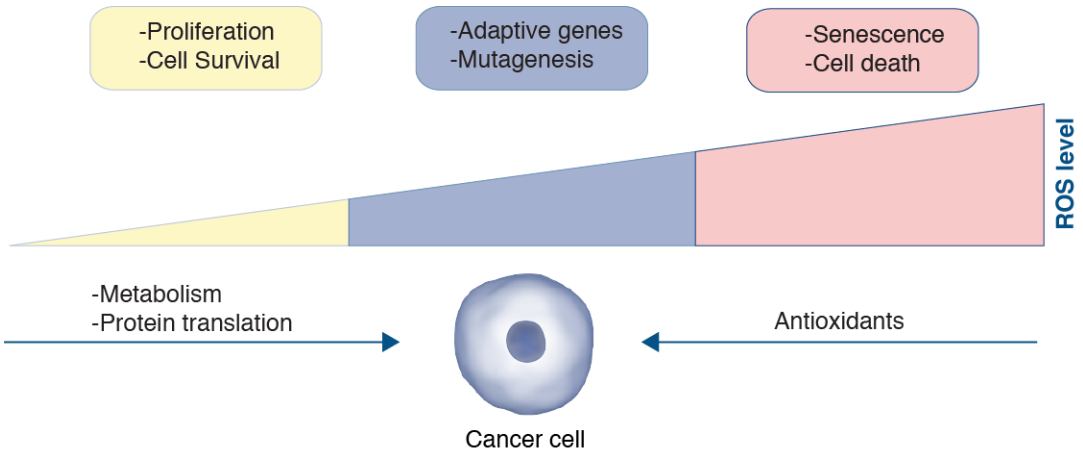

Figure 1.8 Schematic representation of the influence of ROS levels on cell fate.

1.3.6 Glutathione

Glutathione (GSH) is a tripeptide made of glutamate, cysteine and glycine. It has a critical role in cancer through its role as an intracellular ROS scavenger, controlling the intracellular redox state. Many cultured cancer cell lines demonstrate increased intracellular GSH concentrations [44]. GSH scavenging of ROS is mediated by glutathione peroxidase. Upon donating its exposed sulfhydryl group, GSH becomes reactive and reacts with other glutathione molecules forming glutathione disulphide (GSSG), the oxidised form of glutathione. The glutathione pool is maintained mainly in a reduced state via the action of glutathione reductase (GR), which has a great affinity for GSSG. NADPH is the source of reducing equivalents for GSH regeneration from its oxidised equivalent and this reaction is catalysed by GR (Fig. 1.9). NADPH is formed through the pentose phosphate pathway, from the glycolysis-derived glucose-6-phosphate.

Figure 1.9 Glutathione 'recycling' between its reduced and oxidised state

1.3.7 Metabolic biomarkers of breast cancer

Breast cancer tissue metabolomic analyses using primarily HR-MAS NMR have revealed important metabolic features of the disease that correlate with *in vivo* observations. The potential biomarkers unveiled thus far appear to be robust, with particular interest in the changes in choline metabolism during cancer. The list of potential biomarkers from cancer tissue biopsies also includes glycine as a choline breakdown product, lactate as a marker of glycolytic metabolism, taurine and several lipids [45-47]. The metabolic alterations during breast cancer are highly multifaceted and are interrelated with genetics and receptor status.

Urine and blood are the most commonly used biofluids for diagnostic purposes. Review of the available literature revealed potential metabolic signatures in breast cancer, however no definitive consensus on potential biomarkers. Possible metabolic biomarkers from blood include histidine, proline, phenylalanine, glutamate, 3-hydroxybutyrate, lactate and lipids [48-50]. Studies examining potential breast cancer biomarkers in urine are very limited for conclusive results.

Studies exploring potential breast cancer biomarkers in breast tissue, serum and urine in the last 25 years have been recently reviewed by Gunther UL, 2015 [37]

1.4 Watercress

Watercress (*Nasturtium officinale*) belongs to the family of Brassicaceae together with broccoli, cabbage, mustard and Brussels sprouts. It is a perennial herb, grown in aquatic or semi-aquatic conditions originating in Europe but also cultivated in Asia and the Americas. Watercress has been known since the first century AD mainly for its medicinal purposes besides being consumed as a raw salad crop [51]. While still being eaten as a raw vegetable in salads, watercress is becoming increasingly popular in cooked foods. The rising interest in healthy diets and the shift towards natural foods in the last decade has put watercress under the 'microscope' of the nutritional science community as well as the health-conscious public. Watercress is a known rich source of phytochemicals such as glucosinolates, carotenoids, flavonols, vitamins and minerals and recent studies have provided evidence for potential chemopreventive properties of watercress [52, 53]

1.4.1 Phytochemical components of watercress

1.4.1.1 Glucosinolates

Glucosinolates are plant secondary metabolites, found predominantly in cruciferous vegetables of the Brassicaceae family. They are nitrogen and sulfur-containing glycosides - β-thioglycoside, *N*-hydroxysulfates - along with a variable amino acid derived R-group. Glucosinolate metabolism is driven by the action of a β-thioglycosidase enzyme, myrosinase, in glucosinolate containing plants. This enzyme is located in a different cellular compartment of the plant to the glucosinolates [54] Glucosinolates are stable compounds that exist in the cytoplasm of the plant cell.

However, when the plant tissue is damaged such as upon cooking, cutting, mastication or digestion, an enzyme-substrate interaction occurs resulting in the hydrolysis of the glucosinolates and the formation of a range of bioactive products including isothiocyanates, thiocyanates and nitriles (Fig. 1.10) [54]. Table 1.1 summarises the glucosinolates commonly found in watercress along with their respective isothiocyanates.

The chemical structure and proportion of these breakdown products are dependent upon the hydrolysis conditions like temperature and pH, as well as the R-group nature of the glucosinolate. In humans the conversion of glucosinolates to their hydrolysis products can also be driven by the gut microbiota, which possess a low-level myrosinase activity [55]. The distinctive bitter and pungent taste and aroma of cruciferous vegetables is attributed mainly to isothiocyanates generated from glucosinolates and it is suggested that this is adapted as a defense mechanism by the plants, making them unattractive to predators [56]

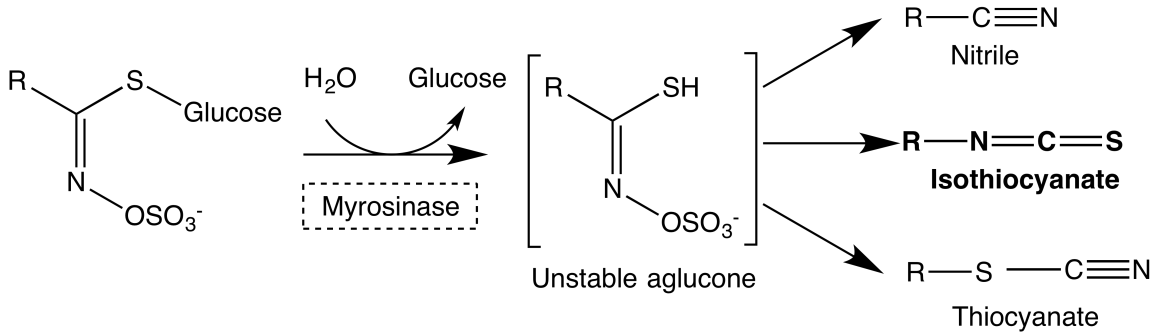

Figure 1.10 Glucosinolate hydrolysis via myrosinase reaction

Figure adapted from [56]

Table 1.1 Glucosinolate and isoothiocyanate content of watercress. Reported values were obtained from Gill *et al.* [57] represent mean ± SD from 8 replicates and Rose *et al*. [58] mean ± SE from 12 replicates.

GLUCOSINOLATE		ISOTHIOCYANATE	
Chemical Name	**Common Name**	**Chemical Name**	**µmol/g DW**
2-Phenylethyl-GLS	Gluconasturtiin	2-Phenethyl-ICT	17.98 ± 4.31[57], 23.7 ± 0.64 [58]
6-Methylsulfinylhexyl-GLS	Glucohesperin	6-Methylsulfinylhexyl-ICT	0.2 ± 0.00[58]
7-Methylsulfinylheptyl-GLS	Glucoibarin	7-Methylsulfinylheptyl-ICT	1.07 ± 0.03 [57], 3.9 ± 0.09 [58]
8-Methylsulfinyloctyl-GLS	Glucohirsutin	8-Methylsulfinyloctyl-ICT	0.68 ± 0.15[57], 2.1 ± 0.05[58]
7-Methylthioheptyl-GLS	-	7-Methylthioheptyl-ICT	1.8 ± 0.14[58]
8-Methylthiooctyl-GLS	-	8-Methylthiooctyl-ICT	0.8 ± 0.06[58]
4-Methoxy-3-indolylmethyl-GLS	4-Methoxyglucobrassin	4-Methoxy-3indolylmethyl-ICT	0.79 ± 0.05[57]
3-Indolylmethyl-GLS	Glucobrassicin	Indole-3-carbinol*	0.43 ± 0.26[57]

1.4.1.2 Isothiocyanates

Watercress is the source of a number of glucosinolates, which can be further hydrolysed to their respective isothiocyanates. Phenethyl isothiocyanate (PEITC) is the most abundant isothiocyanate derived from watercress and watercress is the richest dietary source of this compound. This isothiocyanate is the result of the myrosinase enzymatic conversion of gluconasturtiin. Other naturally occurring isothiocyanates include sulforaphane prevalent in broccoli and allyl-isothiocyanate that occurs in mustard (Fig. 1.11).

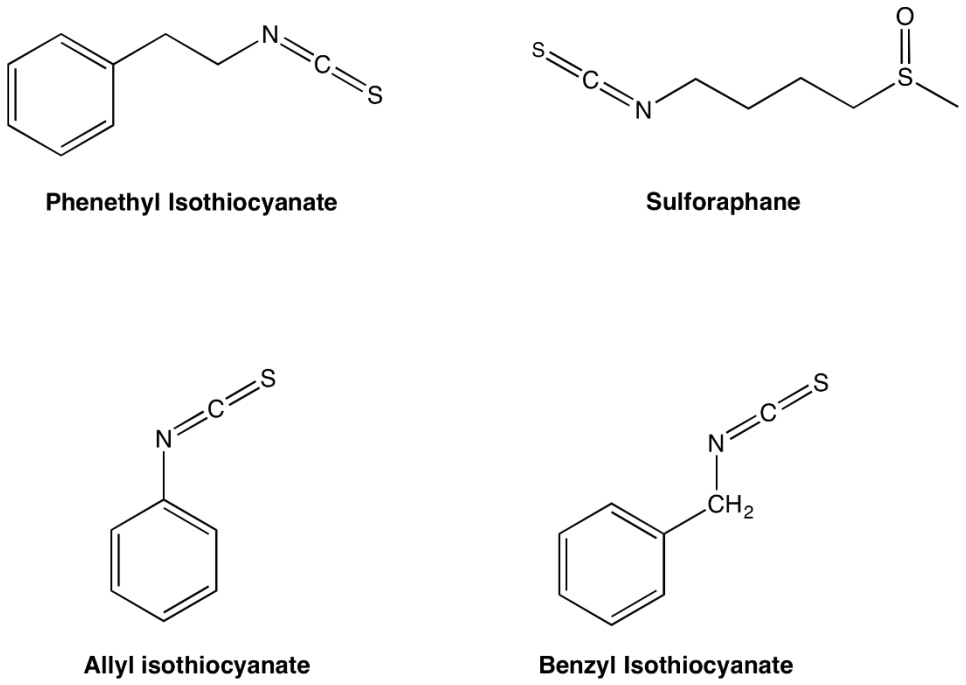

Figure 1.11 Chemical structures of common ITCs

Isothiocyanates are electrophilic compounds with the general chemical formula R-N=C=S. Their biological properties are underlined by their highly electrophilic central carbon unit [59]. As a result, isothiocyanates can rapidly conjugate

with thiol groups like cysteine and lysine via thiocarbamoylation (Fig. 1.12). For this reaction the thiol group is converted to a thiolate ion, allowing for the nucleophilic attack on the carbon atom. This will break one of the N=C double bonds so that nitrogen can attract a hydrogen giving a thiol-isothiocyanate conjugate [60].

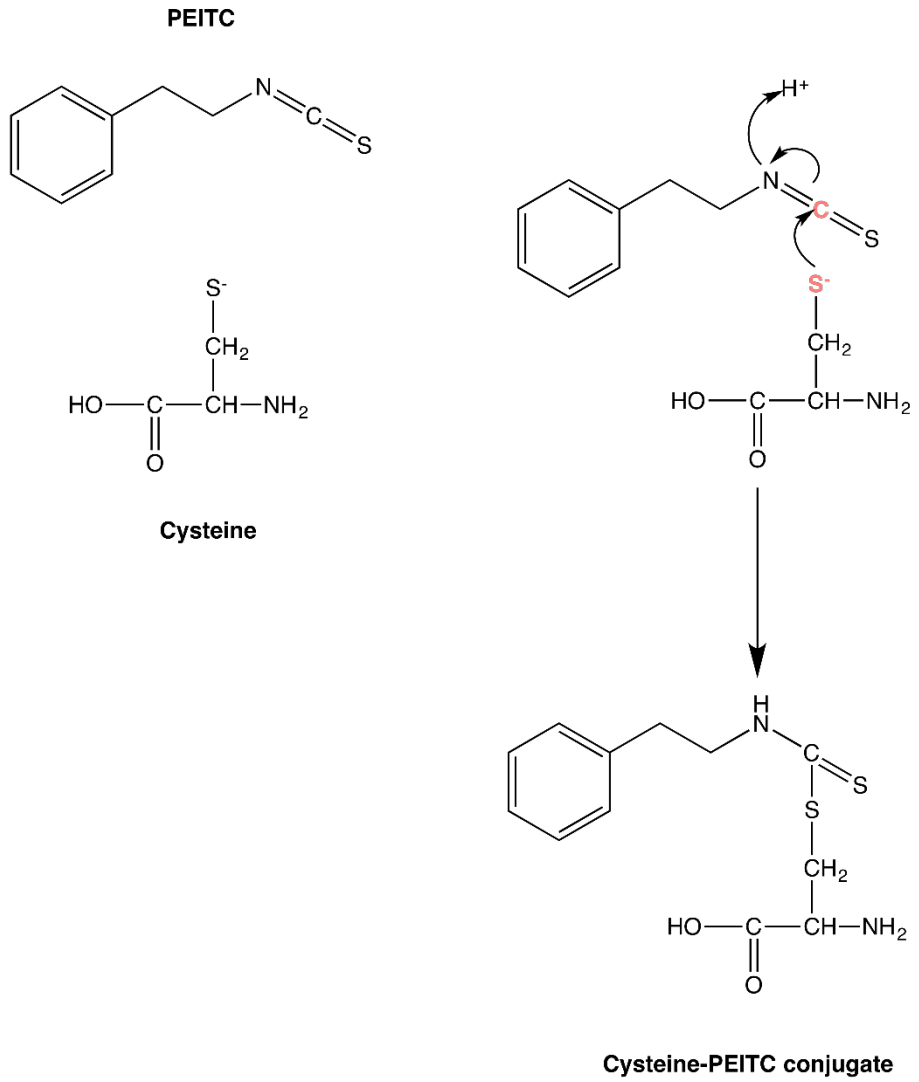

Figure 1.12 PEITC thiocarbamoylation reaction

The most abundant intracellular thiol is GSH that also acts as the major antioxidant therefore ITCs strongly interact with GSH. ITCs including PEITC passively diffuse across the plasma membrane and enter the intracellular space where they bind

to glutathione forming an ITC-GSH conjugate, which is then exported outside the cell through efflux pumps. Extracellularly, the exported conjugate dissociates releasing a free ITC and a GSH molecule. ITCs can then re-enter the cell and conjugate to more thiol containing peptides (Fig. 1.13). This process eventually depletes the cell of its glutathione content, and results in the accumulation of ITCs intracellularly [61]. Glutathione depletion can result in excessively high ROS concentrations that can lead to substantial cell damage.

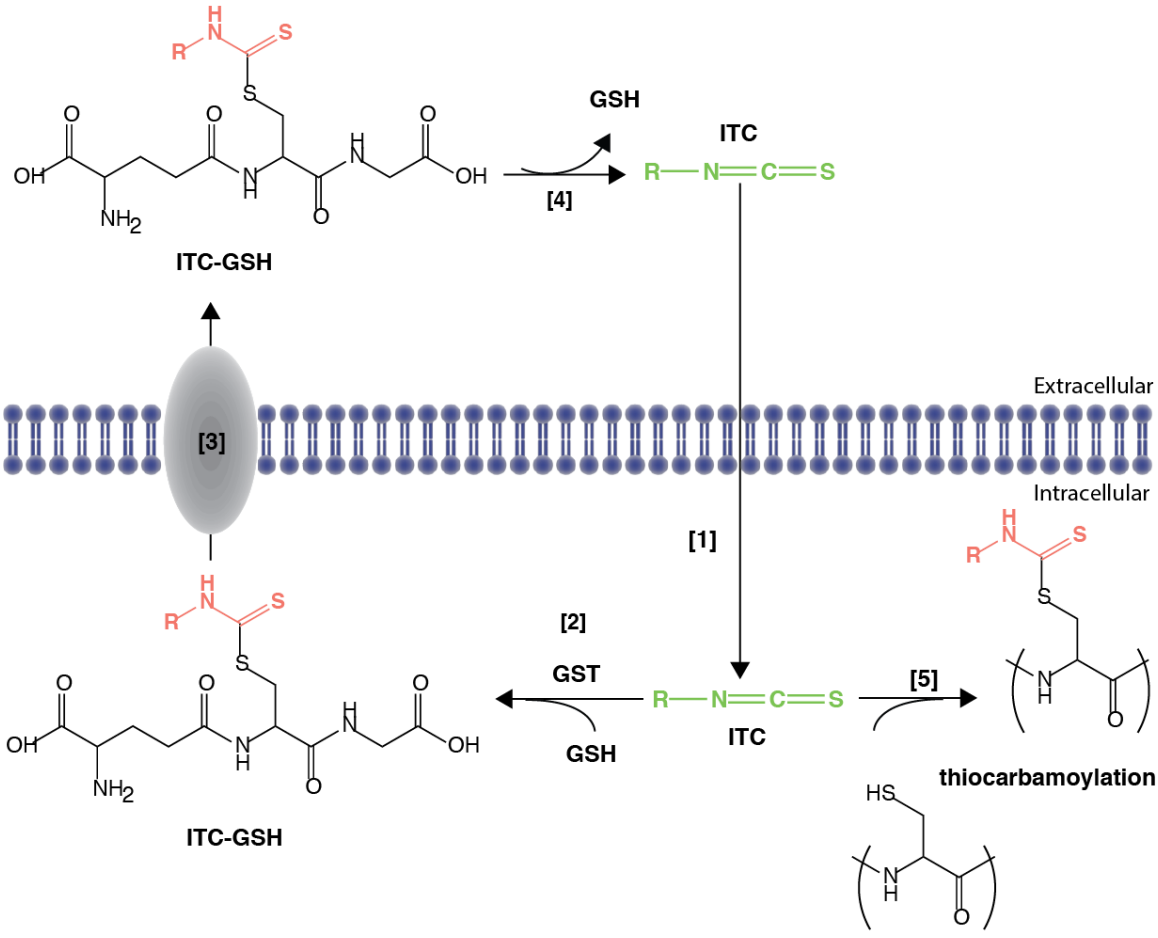

Figure 1.13 Intracellular accumulation of ITCs

Isothiocyanates diffuse across the plasma membranes (1) and once located in the intracellular space they bind to thiol groups in glutathione (GSH), upon the action of glutathione-S-transferase (GST) (2). The glutathione-isothiocyanate conjugate is then exported from the cells via efflux pumps (3). The conjugate is hydrolysed extracellularly (4) giving rise to a free isothiocyanate, which can then re-enter the cell. This cycle results in a rapid accumulation of

isothiocyanates and the concurrent depletion of intracellular glutathione, allowing isothiocyanates to bind via thiol groups to other proteins (5) via thiocarbamoylation. Figure adapted from [61].

1.4.1.2.1 Metabolism of isothiocyanates

PEITC, and all isothiocyanates, passively diffuse across the plasma membrane into the cell where it reversibly conjugates with glutathione forming a glutathione dithiocarbamate (Fig. 1.14). The PEITC-GSH conjugate can be expelled from the cells by transporters, like multidrug resistance protein 1 (MRP1), and enter the mercapturic acid pathway for further metabolism. Extracellularly, the PEITC conjugate undergoes a series of enzymatic modifications forming PEITC-cysteine-glycine via the action of γ-glutamyltransferase (γGTP), followed by cleavage of the glycine residue by cycteinglycinase (CG) giving PEITC-cysteine conjugate. This conjugate is then transported to the liver where it gets acetylated by *N*-acetyltransferases to mercapturic acid namely PEITC-*N*-acetylcysteine conjugate (PEITC-NAC). Upon acetylation, the conjugate is transported to the kidneys and eliminated via urine excretion [62].

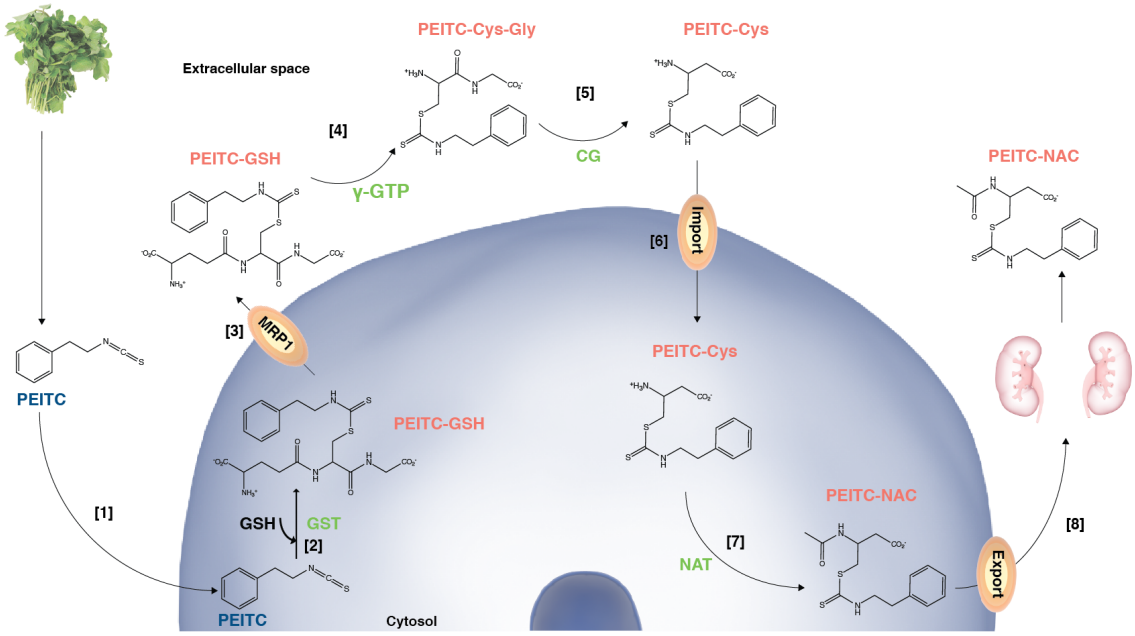

Figure 1.14 Schematic representation of the mercapturic acid pathway for the metabolism of PEITC.

Following ingestion of watercress gluconasturtiin is hydrolysed to PEITC by the action of myrosinase. After diffusion into the cells [1] PEITC conjugates with glutathione via GST action forming a glutathione dithiocarbamate conjugate [2]. The PEITC-GSH conjugate can be expelled from the cells by MRP1 [3] and enter the mercapturic acid for further metabolism. PEITC-GSH conjugate undergoes a series of enzymatic modifications [4-5] resulting in the formation of a PEITC-cysteine conjugate, which is transported [6] and metabolised in the liver and converted to mercapturic acid [7] (PEITC-NAC conjugate). The PEITC-NAC conjugate goes to the kidneys and is excreted in urine. Urinary ITC-NACs serve as a marker of ITCs bioavailability.
Figure adapted from [63] and [62].

Isothiocyanates are detectable in the urine in their NAC conjugate form and recovery of these molecules in urine is therefore commonly used to study the bioavailability of isothiocyanates. A study observed that the isothiocyanate-NAC conjugates are biologically active and their properties are similar to that of the parent compounds, possibly prolonging the effects of isothiocyanates at the systemic level [64]. A study examined the urinary excretion of PEITC-NAC following consumption of 30 g of watercress containing 21.6 mg of gluconasturtiin (equivalent to 7.6 mg of

PEITC), of which 30-67% was recovered as PEITC-NAC in urine [65]. The concentration of PEITC-NAC in the urine peaked between 2-4 hours and was not present in the urine by 24 hours, indicating rapid metabolic clearance of PEITC.

It is important to highlight the role of GST in isothiocyanate metabolism and effective chemoprevention by isothiocyanates overall. Some epidemiological data suggest that the anticancer properties of isothiocyanates are greater in individuals bearing *GSTM1* or *GTT1* null-null genotypes compared to those with a positive *GSTM1* or *GTT1* genotype due to the impaired metabolism of isothiocyanates in these individuals [66]. However some studies noted a greater risk reduction in individuals with the most active or expressed genotypes [67, 68]. Loss of GST enzymatic activity would result in a limited conjugation of isothiocyanates to glutathione and subsequent elimination from the cells, extending their presence in the system possibly enhancing their protective effects *in vivo*. Some evidence supports this hypothesis [69], however in a study where volunteers consumed 200 ml of watercress juice no effect of *GSTT1* or *GSTM1* status was observed on isothiocyanate conjugates excretion [70].

1.4.1.3 Watercress polyphenols

Flavonoids are a diverse group of polyphenolic compounds, ubiquitously found in the plant kingdom mainly as glycosides. Watercress contains molecules from the flavone and flavonol subgroups (Table 2) as well as other phenolics, hydroxycinnamic acid derivatives, in high concentrations [52]. Flavonoids have received intense interest due to their potential favourable effects on human health. They can act as direct

antioxidants *in vitro* [71, 72] and indirectly through the stimulation of detoxification enzymes like the cytochrome P450. Flavonoids also inhibit tumor proliferation and induce apoptosis [73]. Collectively, these actions may be associated with a decreased risk of cancer, cardiovascular disease and chronic inflammation [74]

Table 1.2 Flavonoid content of watercress. Data obtained from the USDA Nutrient Data Laboratory [75]. Data represent mean ± SE of nutrient values reported in different studies.

Flavonoids	mg/100g FW
Flavones	
Apigenin	0.0 ± 0.00
Luteolin	0.0 ± 0.01
Flavonols	
Kaempferol	23.0 ± 3.66
Myricetin	0.2 ± 0.05
Quercetin	30.0 ± 6.74

1.4.1.4 Carotenoids

Carotenoids are isoprenoid, lipid-soluble pigments found in the chloroplasts of photosynthetic organisms. This class of phytochemicals can be divided into two main groups: the oxygenated xanthophylls like lutein and zeaxanthin, and the carotenes that are un-oxygenated like α-carotene and β-carotene. Numerous health benefits are attributed to dietary carotenoids, including antioxidant and anti-carcinogenic activities [76]. Watercress is an exceptional source of carotenoids with concentrations ranging from 2.5 to 5.9 mg β-carotene/100g fresh weight (FW) and 5.77 to 10.71 mg lutein/100 g FW [75, 77]. Gill *et al.* [57] have shown that adults who consumed 85 g of

raw watercress for eight weeks had significantly higher concentrations of lutein and β-carotene in their plasma. This is likely related to the concurrent reduction in markers of DNA damage in their lymphocytes. This may be attributed to the antioxidant effect of carotenoids in combination with other health promoting compounds in watercress.

1.5 Anti-cancer potential of PEITC

1.5.1 Chemopreventive agent

Phase I (Cytochrome P450 (CYP)) drug metabolising enzymes (DMEs) activate dietary pro-carcinogens through oxidation, reduction or hydrolysis creating electrophilic intermediates which may form adducts in DNA [78].

PEITC has been shown to have a dual effect on the expression and activity of DMEs. In primary hepatocytes PEITC induced up-regulation of the expression of CYP1A1 and CYP1A2, both of which are carcinogen-activating enzymes [79]. However, in baculovirus-infected insect cells carrying human CYP isoforms, PEITC was found to completely inhibit a range of CYPs including CYP1A2 [80]. Further studies support the notion that PEITC can be a potent inhibitor of phase I CYPs including CYP2E1, CYP3A4 and CYP2A3 [81-83].

Data from human and rodent studies provide evidence for the inhibition of carcinogen-induced carcinogenesis by PEITC. In a recent phase II clinical trial conducted by Yuan *et al.* [84] eighty-two smokers, smoking only deuterated NNK cigarettes for the duration of the study, were randomly assigned to a placebo and a PEITC receiving group. The metabolic activation of NNK, a nicotine-derived potent lung carcinogen, was significantly reduced by PEITC treatment as measured by the

urinary excretion of NNK metabolites. It is worth noting that the effect was stronger in subjects with the null genotype of both the GSTM1 and the GSTT1 polymorphisms, as well as in women. Similar results were obtained from earlier rodent studies where NNK treated animals receiving a diet rich in PEITC developed significantly fewer lung tumours than those without the PEITC intervention [85]. Further to this, pre-treatment of mice with PEITC for a week followed by NNK administration, resulted in increased urinary excretion of NNK derivatives in comparison to the non-PEITC treated animals and correlated with a reduced tumour burden [86]. The chemopreventive effects of PEITC are therefore suggested to be a result of its potential to modulate the activity of phase I and phase II DMEs.

Phase II enzymes constitute a protective mechanism of the cells through their role as detoxifying agents of reactive phase I metabolites. They conjugate compounds with large polar molecules like glutathione, glucuronide or sulfate limiting the biotransformation of damaging carcinogens and facilitating their elimination through the urine or bile [87]. Isothiocyanates including PEITC can induce the expression of phase II DMEs with known chemopreventive properties such as glutathione S-transferase (GST), NAD(P)H:quinone oxoreductase 1 (NQO1) and UDP-glucuronosyltransferase (UGT) [88].

A number of studies have demonstrated the potential of PEITC to induce the activity of phase II enzymes. PEITC treatment significantly increased the induction of GST isoenzymes in a murine liver [89] and along similar lines hepatic activity of GST was stimulated by PEITC administration in rats but with no effect in the lungs or kidneys [90]. Treatment of human liver biopsies with increasing concentrations of

PEITC showed a varied response in the induction of phase II enzymes characterised by inter-individual and inter-enzyme variation [91].

1.5.2 Cell proliferation

Cancer cells are characterised by up-regulated pro-proliferative signals in order to generate new cells, expand in size and establish as tumours. Activation of the Ras family of proteins is vital to sustain proliferation and PEITC has been shown to inhibit several components of the Ras family including the Akt (protein kinase B). Akt has a central role in apoptosis and cell proliferation and it is overactive in many types of cancers. PEITC has been shown to inhibit its activity in a number of models including breast cancer [92-95]. It has been suggested that this is mediated through inhibition of the epidermal growth factor receptor (EGFR) and of HER2; both of which are significant regulators of Akt [93, 96, 97].

1.5.3 Cell cycle arrest

Cell cycle progression involves a series of processes, which direct dividing and proliferating cells through the G, S, G2 and M phases. It is mediated by the activation of cyclin dependent kinases (Cdk) and their associated cyclins and PEITC can modulate cell cycle and inhibit proliferation of cancer cells by targeting this complex [98].

PEITC has been shown to induce cell cycle arrest at the G1/S phase, the growth and proliferation phase. The G1 checkpoint is the point of assessment of adequate nutrients and growth factors and detection of DNA damage levels. If a cell carries substantial amount of damaged DNA this signals the delay or arrest of the cell cycle in G1 repressing the transition to the subsequent phases. In the case of cancer, the cell

cycle process is deregulated resulting in different growth characteristics in these cells, and ultimately uncontrolled cell proliferation.

In HT-29 colon cancer cells, PEITC induced G1 cell cycle arrest by down-regulating cyclin A, D and E [99]. PEITC has also been shown to inhibit the growth of oral squamous carcinoma HSC-3 cells through G1/S cell cycle arrest mediated by reductions in the levels of Cdk2, Cdk6 and their associated cyclins with concomitant increases in the expression of protein levels of cyclin-dependent kinase inhibitors p15, p53, p27 and p21 [100]. Arrest in the S phase of the cell cycle has also been observed, upon PEITC treatment in sarcoma cells and this observation was associated with a reduction in protein levels of cyclin A, the S phase cyclin regulator [101]. PEITC-induced cell cycle arrest in the G2/M phase is related to the down-regulation of Cdk1, cyclin B1 and the cell division cycle 25C (Cdc5C) [102, 103]. Cdk1 forms complexes with cyclin B. Subsequently; Cdc25C targets this complex for dephosphorylation of Cdk1 promoting its activation, which is necessary for transition into mitosis (M phase). Cell cycle arrest by PEITC is the result of a decrease of the levels of Cdk1 or cyclin B or by inhibition of Cdk1 phosphorylation [102].

1.5.4 Tumour Metastasis

Healthy cells, once they have specialised and differentiated do not migrate to other tissues and remain in the organ or tissues they have specialised for. In cancer, cells reverse from their differentiated state and behave like pluripotent cells, invading blood circulation and metastasise to secondary organs from their original primary location, resulting in extensive spread of cancer. Cancer invasion and metastasis is

associated with a much poorer prognosis and increased mortality. Development of anti-invasive and anti-metastatic therapies is therefore an important target of cancer research. A number of studies have shown that PEITC can significantly suppress invasion and negatively influence metastasis. This activity was related to the attenuation of the protein and mRNA expression of matrix metalloproteinases that are known to promote cell migration, invasion and proliferation [103-105]. Interestingly, Gupta *et al.* [96] have demonstrated the anti-metastatic potential of PEITC *in vivo* in a breast cancer metastasis mouse model. In this model, MDA-MB-231 brain seeking breast cancer cells were injected into the left ventricle of the heart of female mice and a part of these cells migrated to the brain through blood circulation and established as metastatic tumours [96]. Oral administration of the mice with 10 μM of PEITC significantly prevented the migration of the breast cancer cells to the brain of these animals. Additionally, in a secondary experiment PEITC administration following tumour cell implantation, limited the growth of the metastasized tumours in the brain area and also prolonged the survival of the mice with cancer [96].

1.5.5 Angiogenesis

A recognised mechanism by which PEITC inhibits growth and survival of established cancer cells is through the inhibition of angiogenesis. This is a hallmark in the process of tumour progression during which new blood vessels are formed from existing vasculature to meet the increasing demands of cancer cells for nutrients and oxygen [61]. A study explored the impact of PEITC on a specific pathway central to angiogenesis by exposing human MCF-7 breast cancer cells to PEITC and measuring

hypoxia-inducible factor 1α (HIF-1α) signalling activity [106]. HIF-1α stimulates the expression of the vascular endothelial growth factor (VEGF), a master regulator of angiogenesis. PEITC was shown to be an effective inhibitor of HIF-1α protein expression, which is stably expressed in hypoxic conditions, contributing to the anti-angiogenic properties of ITCs. To further substantiate the data obtained from this study Alwi *et al.* [107] demonstrated that, similar to PEITC, crude watercress extracts inhibited cancer cell growth and HIF activity *in vitro*. Furthermore, 6 to 8 hours after dietary intake of 80 g watercress by four healthy human volunteers, peripheral blood cells exhibited significantly attenuated HIF signalling activity, suggesting that dietary intake of watercress may be sufficient to modulate potential anti-cancer pathways [107]

1.5.6 Apoptosis

Apoptosis is a critical process to ensure clearance of non-functional, damaged or aged cells. Cells undergo apoptosis when proliferation can no longer be controlled by the cell cycle checkpoints. Defects in the apoptotic pathway can lead to cancer formation, and pro-apoptotic therapies present attractive targets in cancer research.

PEITC induces apoptosis in several cancer cell lines via the intrinsic and extrinsic pathways [108-112]. Mitochondria are the central organelle mediating signal transduction apoptotic pathways and have a major role in the intrinsic apoptosis pathway [113, 114]. PEITC is a potent intracellular ROS generator inducing oxidative mitochondrial damage [115-117]. These observations are likely to be a result of the continuous intracellular conjugation of PEITC with glutathione and subsequent export

outside the cell, diminishing the cell of its antioxidant potential leading to increased ROS and oxidative damage [118]. Additionally, ROS accumulation as a result of PEITC treatment can result in lipid peroxidation of the mitochondrial membrane accompanied by loss of the mitochondrial integrity, which triggers the release of apoptosis inducing factor (AIF) and of cytochrome *c* [116]. This leads to caspase cleavage and activation that eventually elicits apoptotic events. PEITC treatment reduces the levels of the anti-apoptotic proteins Bcl-2 and Bcl-xL, which are overexpressed in cancer and can inhibit the activation of the pro-apoptotic Bax protein and the release of cytochrome *c* with an immediate effect on the caspase cascade and activation of the apoptosis pathway [100, 112, 119].

PEITC-mediated apoptosis can also ensue via the extrinsic pathway through its interaction with the tumour necrosis factor related apoptosis-inducing ligand (TRAIL) and the elevated expression of death receptors, which bind to TRAIL and lead to apoptosis exclusively in cancer cells [120, 121]. The predominant apoptosis pathway induced by PEITC can vary between different cell types [98].

1.6 Health implications of watercress consumption

Research has highlighted a promising chemopreventive role of watercress and its components. Boyd *et al.* [53] showed inhibition of three stages of carcinogenesis: initiation, proliferation and metastasis in HT29 colon cancer cells after incubation with watercress extract. In the same study, watercress extract appeared to be protective against oxidative DNA damage induced by genotoxic compounds like 4-hydroxy nonenal (4-HNE), faecal water and hydrogen peroxide (H_2O_2). Inhibition of cell cycle

progression at the S phase of these cells was also observed as well as suppressed invasion of HT115 cells (a highly invasive colon cancer cell line) through matrigel. Along similar lines, Kassie *et al.* [122] showed that pretreatment of hepatoma Hep G2 cells with watercress extract, reduced the genotoxic effects of benzo(a)pyrene (B(a)P) in DNA damage measurements. In the same study, treatment of the cells with the watercress extract significantly increased the activity of drug metabolising enzymes GST and CYP1A1. However this effect cannot solely be attributed to the reduction of DNA damage, since garden cress in the same study setting also protected against B(a)P but had no observable effect of the activity of GST or CYP1A1 [122]. These results cannot be attributed to PEITC since it was not detected in the watercress extract by LC-MS. Kassie *et al.* did detect PEITC using gas chromatography, but when it was added to Hep 2G cells in similar concentrations as those present in the extract, it was not protective against B(a)P induced genotoxicity. It can therefore be suggested that phytochemicals present in watercress, other than PEITC, can have chemopreventive effects and that this impact is not restricted to modifications to drug metabolizing enzymes.

Evidence was also provided that isothiocyanates other than PEITC possess anti-genotoxic and anti-carcinogenic properties [58]. The compounds 7-methylthioheptyl-ICT and 8-methylthiooctyl-ICT were found to be present in watercress at concentrations three times lower than PEITC. These components were shown to have a much stronger potency for inducing quinone reductase activity in murine hepatoma Hepa 1c1c7 cells compared to PEITC, providing further evidence for the ability of watercress to induce phase II enzymes.

Additional information derived from a study conducted by Gill *et al.* [57] during which 60 volunteers consumed 85 g of raw watercress for eight weeks; showed a decrease in markers of DNA damage in lymphocytes with concomitant increases in circulating β-carotene and lutein. Reduced DNA damage was much greater in smokers, suggesting that increased smoking-derived ROS led to lower antioxidant status and they therefore benefited more from watercress-derived antioxidants than non-smoking individuals. The activity of two detoxifying enzymes namely, superoxide dismutase (SOD) and glutathione peroxidase (GPX) were analysed in this study, with insignificant differences between the control and intervention phase of the study providing further evidence that cruciferous vegetables may not exert their chemopreventive effects via modulation of SOD and GPX [123]. A minor but significant increase was observed in GPX and SOD only in individuals with the *GSTM1* null phenotype [124].

A study by Hecht *et al.* [125] provides further evidence to support the chemopreventative effects of watercress. In this work the consumption of 56.8 g of watercress for three days was found to inhibit the metabolic activation of a tobacco-specific lung carcinogen NNK in a group of smokers. This anti-carcinogenic observation was attributed to PEITC activity, due to notable shifts in the urinary excretion of PEITC-NAC, which correlated with elevated urinary detoxification metabolites that are used as biomarkers of NNK oxidative metabolism.

On the basis of the evidence currently available, it seems fair to suggest that watercress supplementation may further prove useful in the modulation of cancer progression and disease recurrence. The metabolic and molecular mechanism behind

its potential mechanism of action are not yet fully understood.

1.7 Epidemiological data for the chemopreventive impact of cruciferous vegetables consumption

Population studies from different geographical locations provide contradicting evidence for the inverse relationship between the risk of developing cancer and increased dietary intake of cruciferous vegetables. Despite the fact that these studies do not provide direct correlation between cancer occurrence and specific ITCs, a number of them suggest a correlation between total ITCs intake from dietary sources and reduced risk of certain types of cancer. Total ITCs are however an arguable measurement as there are numerous variables biasing their calculation such as variety of cultivar, growth period, climate and harvest method [63]. Further to this, different cooking regimes can have a crucial impact on the ITC content of cruciferous vegetables.

Epidemiological studies in the Netherlands [126], United States [127] and across Europe [128] analysed the daily consumption of cruciferous vegetables and found insignificant or modest associations with prostate cancer risk. Cohort studies in the United States and the Netherlands found no evidence for inverse correlation between colorectal cancer and cruciferous vegetable dietary intake [129-131]. In contrast, the Netherlands Cohort Study on Diet and Cancer concluded that individuals with high intake of cruciferous vegetables (more than 3 servings per day) had a reduced risk of colon cancer compared to those with a lower intake [132].

Varying results from epidemiological studies also arise in the case of lung cancer [133-135]. The majority of these studies report little or no association between lung cancer risk and cruciferous vegetables but one study based on the Nurses' Health Study and the Health Professionals' Follow up Study suggested that women consuming over four portions of cruciferous vegetables weekly had a lower risk of developing lung cancer (relative risk = 0.74, 95% CI = 0.68-1.20) [136].

Regarding breast cancer, a meta-analysis carried out from 17 studies (14 case-control and 3 cohort studies) evaluating breast cancer risk in association with vegetables intake, suggested that consumption can reduce 25% of the breast cancer risk (relative risk = 0.75, 95% CI = 0.66-0.85) [137]. However, a meta-analysis of seven large prospective studies performed in the United States, Canada, Sweden and the Netherlands did not show any association [138]. Total intake of cruciferous vegetables was not significantly associated with reduced risk of breast cancer in pre or post menopausal women irrespective of a monthly serving exceeding 1000 g with odds ratios of 0.7 (95% CI = 0.5-1.2) and 0.8 (95% CI = 0.6-1.2) respectively [139]. Interestingly, examination of a cohort of breast cancer survivors showed reduced cancer recurrence correlating with dietary cruciferous vegetables intake [140].

This heterogeneous body of evidence can be a result of a number of confounding factors in the studies like the differences in the subject population, duration of cruciferous vegetables dietary intake, age of the subjects as well as differences in the isothiocyanate content of the reported vegetables. It is also important to note that people's food and lifestyle habits have significanltly changed over the past decade a factor which can have a major effect on the outcomes of

studies with wider durations. Epidemiological studies can also be confounded by the participants' reporting bias.

Consequently, based on the current epidemiological data and the lack of long term chronic human clinical trials in the literature, no definitive conclusions can be drawn about the effective protection of cruciferous vegetables and cancer risk

1.8 Thesis framework

On the basis of the reviewed literature herein it is apparent that watercress and PEITC potentially modulate a range of factors implicated in cancer onset and progression and are influential in the efficacy of cancer treatment. Characterising the biochemical effects of watercress components and PEITC on cellular energetics is key to understanding the mechanisms through which they exert their beneficial effects. As such, a central aim of this thesis is to define the metabolic impact of watercress and PEITC exposures on breast cancer and healthy cells lines.

Further we aim is to assess the potential of watercress and PEITC to act as radiosensitising or radioprotective agents in breast tumour or normal cells respectively. The relevance of the obtained data will be evaluated in a human clinical trial involving breast cancer patients consuming watercress during radiotherapy.

1.8.1 Aims

1. Investigate the impact of watercress and PEITC on the metabolome of breast cancer and healthy breast cells
2. Evaluate the interactions between watercress or PEITC with ionising radiation on markers of cellular function and metabolism of breast cancer and healthy breast cells
3. Examine the effects of domestic cooking methods on the phytochemical profile of watercress and formulate recommendations for optimal preparation to maximise nutrient ingestion
4. Assess the metabonomic impact of watercress consumption during radiotherapy treatment in breast cancer patients

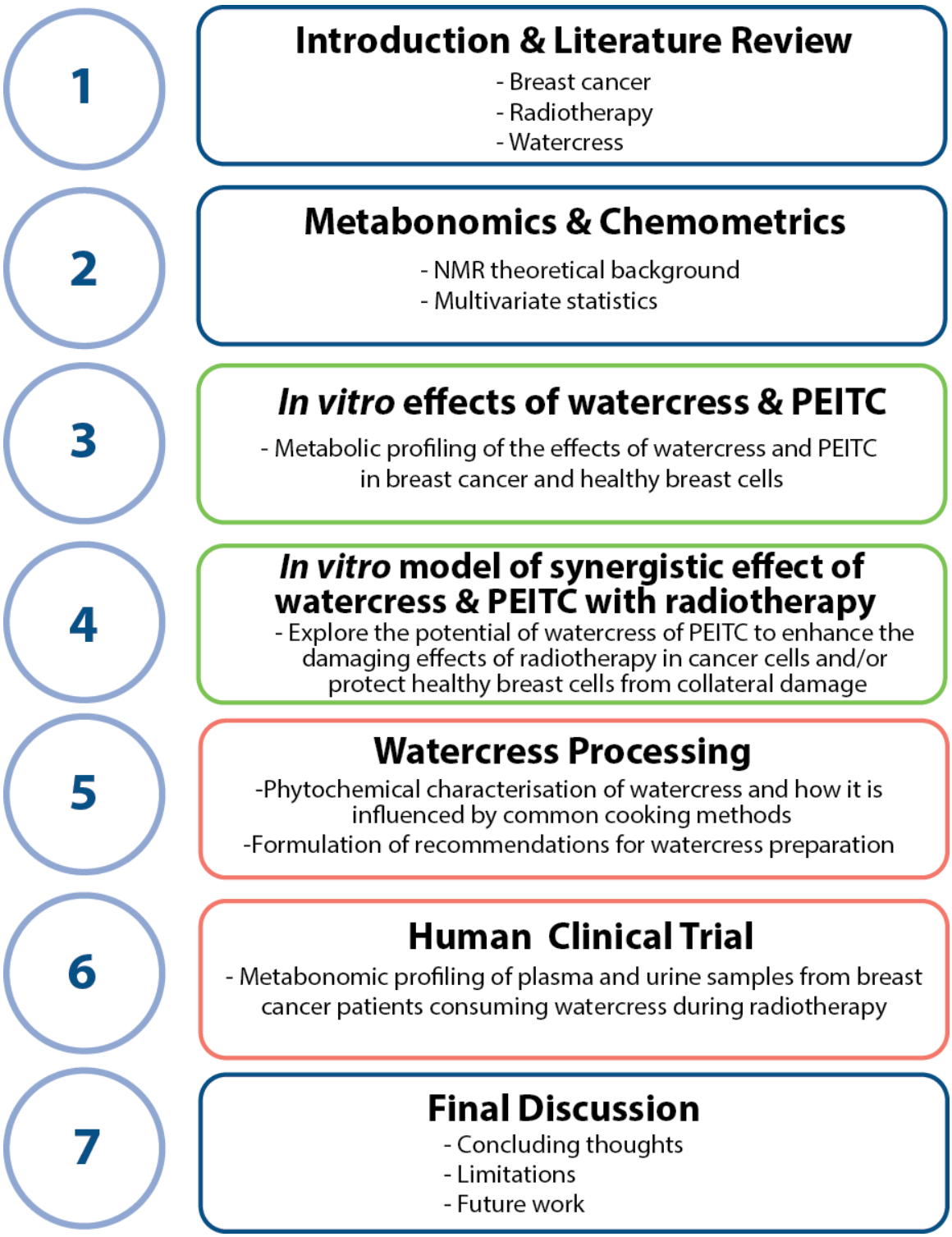
1
Introduction & Literature Review
- Breast cancer
- Radiotherapy
- Watercress
2
Metabonomics & Chemometrics
- NMR theoretical background
- Multivariate statistics
3
In vitro effects of watercress & PEITC
- Metabolic profiling of the effects of watercress and PEITC in breast cancer and healthy breast cells
4
In vitro model of synergistic effect of watercress & PEITC with radiotherapy
- Explore the potential of watercress of PEITC to enhance the damaging effects of radiotherapy in cancer cells and/or protect healthy breast cells from collateral damage
5
Watercress Processing
-Phytochemical characterisation of watercress and how it is influenced by common cooking methods
-Formulation of recommendations for watercress preparation
6
Human Clinical Trial
- Metabonomic profiling of plasma and urine samples from breast cancer patients consuming watercress during radiotherapy
7
Final Discussion
- Concluding thoughts
- Limitations
- Future work

2 Metabonomics and Chemometrics

2.1 Metabonomics

Metabonomics is a term first coined in 1999 and is defined as 'the quantitative measurement of the dynamic multiparametric metabolic response of living systems to pathophysiological stimuli or genetic modification' [141]. Metabolic profiling is facilitated by analytical platforms like NMR spectroscopy and mass spectrometry (MS) and aims at the coverage of the complete spectrum of metabolites, the metabolome, in a given biological sample. This collection of metabolites serves as a direct snapshot of the biochemical activity in a system [142] and provides information on physiological status and perturbations arising from exogenous stimuli like diet and the gut microbiome [143]. Metabolic profiling approaches are versatile in that they can be applied in several biological matrices such as urine, plasma, homogenised or intact tissues and cells [144, 145]. Metabonomics is a top-down 'systems level', dynamic approach and it is being used as an increasingly popular tool in the fields of medicine for diagnostic [146] and prognostic [147] purposes as well as in nutritional sciences [148] and toxicology [149].

Metabonomic data are interpreted and latent information is extracted using multivariate statistical analysis. Statistical interpretation is naturally followed by biological interpretation, which often generates new hypotheses for exploration. A metabolic change can be probed by further experiments to assess its validity as a functional biomarker. Validation of biomarkers with diagnostic value is of paramount importance, and it is often performed in an independent cohort of experimental samples to establish the biological basis of a molecule that serves as a potential biomarker.

Integration of metabonomic data with 'omic' data derived from other platforms or data from large-scale consortia projects, can provide a richer and more comprehensive understanding of complex diseases by exploring the interactions between genetic, metabolic and other physiological shifts in a system.

2.2 ^{1}H Nuclear magnetic resonance (NMR) spectroscopy

^{1}H NMR spectroscopy is an analytical method facilitating the profiling of a vast array of low molecular weight compounds (<1000 Daltons), in bio-fluids, tissues and cells [145]. This technique benefits from high reproducibility and simple sample preparation as well as short experiment times. NMR-based metabolic profiling is an invaluable tool in the field of metabonomics capturing and delivering highly informative snapshots regarding the metabolic state of the sample under study.

2.2.1 The NMR Spectrometer

An NMR spectrometer is comprised of a superconducting magnet, made of coils of superconducting wire, which is cooled using liquid helium to temperatures very close to absolute zero, to enable a strong magnetic field. A central component of the NMR instrumentation is the probe, which accommodates the NMR sample tube and facilitates the generation and transmittance of the radiofrequency pulse to the sample. The signal from the excited nuclei is detected by the probe and through the receiver coil surrounding the sample. Figure 2.1 depicts the components of an NMR superconducting magnet.

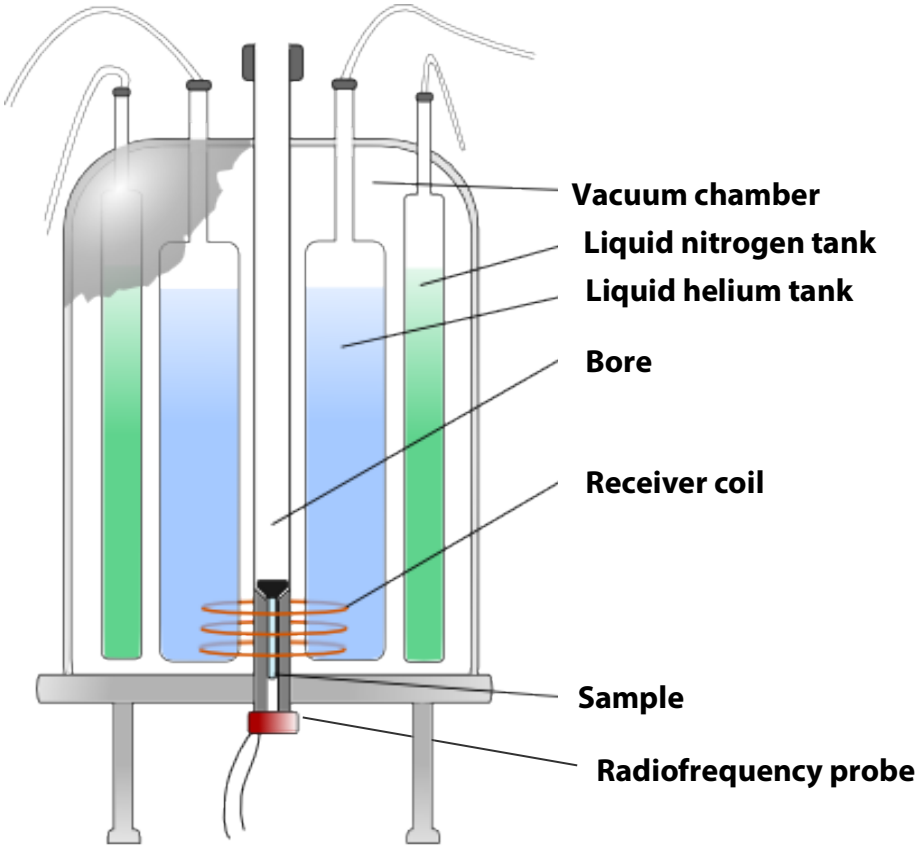

Figure 2.1 Internal configuration of an NMR spectrometer.

Inside the magnet a liquid nitrogen tank is located, whose main function is to insulate the inner liquid helium tank. At the centre of the electromagnet there is the bore, a long tube from the top of which the sample is inserted and sits in the probe.

2.2.2 Principles of ^{1}H NMR spectroscopy

The principle of NMR spectroscopy is based in the physical properties of the atomic nuclei that are composed of protons and neutrons. The nuclear property of interest in NMR experiments is the nuclear angular momentum spin quantum number (I), commonly referred to as nuclear spin. This number depends on the number of protons (atomic number) and the number of neutrons (atomic mass) [150]. If the number of neutrons and protons are both even, then the nucleus has I=0 (e.g. ^{12}C, ^{16}O, ^{32}S). In cases where the number of neutrons and

the number of protons is odd, then the nucleus has I=1/2 (e.g. ^{1}H, ^{13}C, ^{31}P). When the number of neutrons and the number of protons are both odd then the nucleus has I=1.

Any nucleus with a spin quantum number (I) different from zero can be analysed using NMR spectroscopy. Proportional to the nuclear spin is the magnetic moment (μ), which is the vector of the positive charge of the nucleus as a result of nuclear spinning and of the angular momentum through the gyromagnetic ratio (γ). The gyromagnetic ratio is a fundamental constant, unique to each nucleus. It can therefore be deduced that if a nucleus, with I =0 will not have a magnetic moment and will not be detected by NMR. Some of the isotopes used in NMR spectroscopy in biological applications are those with I =1/2 such as ^{1}H, ^{13}C, ^{15}N, ^{31}P. Hydrogen (^{1}H) is the most commonly used atom in metabolic profiling, since it is the most abundant element in biological molecules. The natural abundance of ^{1}H is 99.98%, substantially higher than that of ^{13}C, which is 1.1%.

When a magnetic field is applied to nuclei with a spin quantum I>0, the nuclear moments of spins will orient themselves and the number of possible energy levels can be calculated by the equation: 2I+1. The magnetic quantum number m_I designates these energy levels of nuclei. The spin quantum number (I) of ^{1}H is equal to 1/2 and will therefore have two possible orientations (energy states) in the presence of a magnetic field (Fig. 2.2). Upon transition from a random to an oriented state, the nuclei spin around the axis of the applied magnetic field in a motion known as the Larmor precession with a frequency ν and an angular speed ω_o [150].

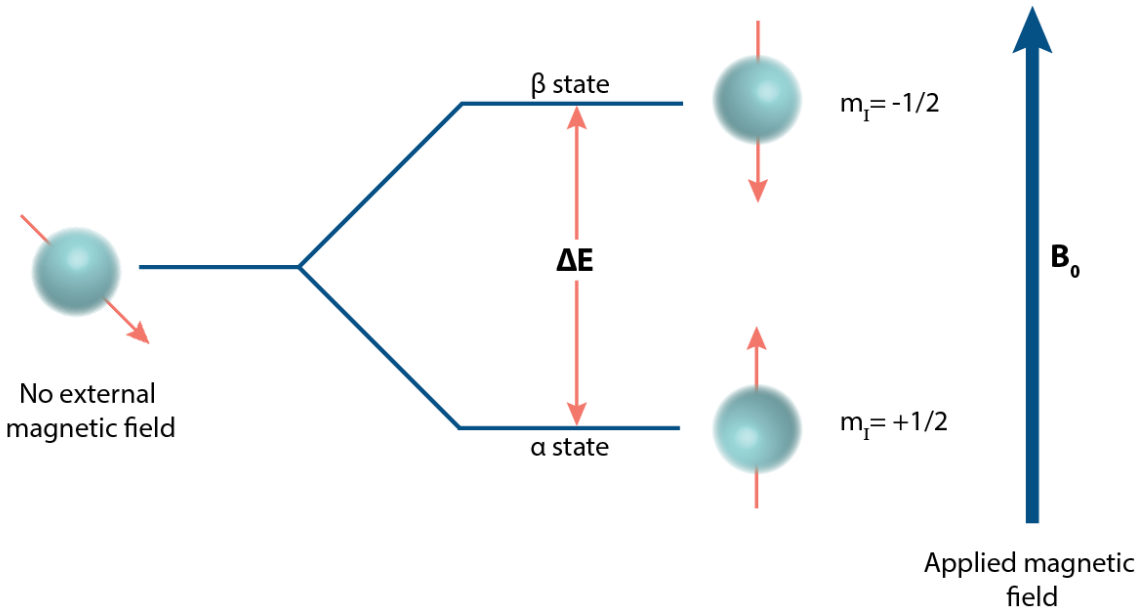

Figure 2.2 Energy levels of a nucleus with a spin quantum number 1/2

Schematic representation of the energy level of a nucleus with I =1/2 and transition upon application of an external magnetic field B_0. The nucleus aligns with or against the applied magnetic field in a low (α, m_I=+1/2) or high (β, m_I=-1/2) energy state respectively. The difference between the two energy states is described as ΔE.

The population of the protons between the two energy states is given by the Boltzmann distribution:

$$\frac{N_\alpha}{N_\beta} = e^{-\Delta E/KT}$$

N_α and N_β represent the number of nuclei that occupy the lower and upper energy state respectively; K is the Boltzmann constant and T the absolute temperature in degrees Kelvin. ΔE is the energy difference between the two energy states α and β and the energy required for the transition (flipping) of the nuclear spins.

It is important to note that there will be a slight excess of nuclei in the lower energy state at thermal equilibrium. The net absorption of energy by the nuclei that change spin

states will in turn give an NMR signal. The energy needed for the flipping between the two orientations is provided by electromagnetic radiation and can be calculated using the following equation:

$$\Delta E = \nu h = \gamma h B_0 / 2\pi$$

Where ν is the Larmor frequency; h is the Planck's constant; γ corresponds to the gyromagnetic ratio (unique for each nucleus and defines the direction of the spin) and B_0 is the strength of the external magnetic field.

ΔE is equal to νh meaning that electromagnetic radiation is proportional to the resonance frequency. This means that an exact frequency should be applied for the nuclei to resonate (flip) between the energy levels, and allow for an NMR signal to be detected. In addition, considering that ΔE is directly related to the applied magnetic field (B_0) the Larmor frequency (resonance) will also be proportional to B_0.

Energy for the excitation of nuclei is provided in the form of radiofrequency (RF) pulses during an NMR experiment. The RF pulses used interact with all the nuclei of an isotope in a sample. The fact that there are differences in the population distribution of nuclei in the two energy levels, and therefore different Larmor frequencies, creates a net magnetisation vector M_0 in the same direction as B_0 (z-axis) (Fig. 2.3a). Application of a short 90° RF pulse rotates the magnetisation vector away from the z-axis to the x-y plane (Fig. 2.3b). When the pulse stops, the nuclei will relax and return to equilibrium (Fig. 2.3c). During the precession movement back to z-axis, the magnetisation vector will release an oscillating voltage, detected by the receiver coil and amplified by the receiver. This detectable NMR signal is know as free induction decay (FID) and it represents the sum of these oscilations. The speed of relaxation

and the RF pulse determines the differences between molecules. The FID recorded in a time domain is converted into the frequency domain and into an NMR spectrum by Fourier transformation (Fig. 2.3d).

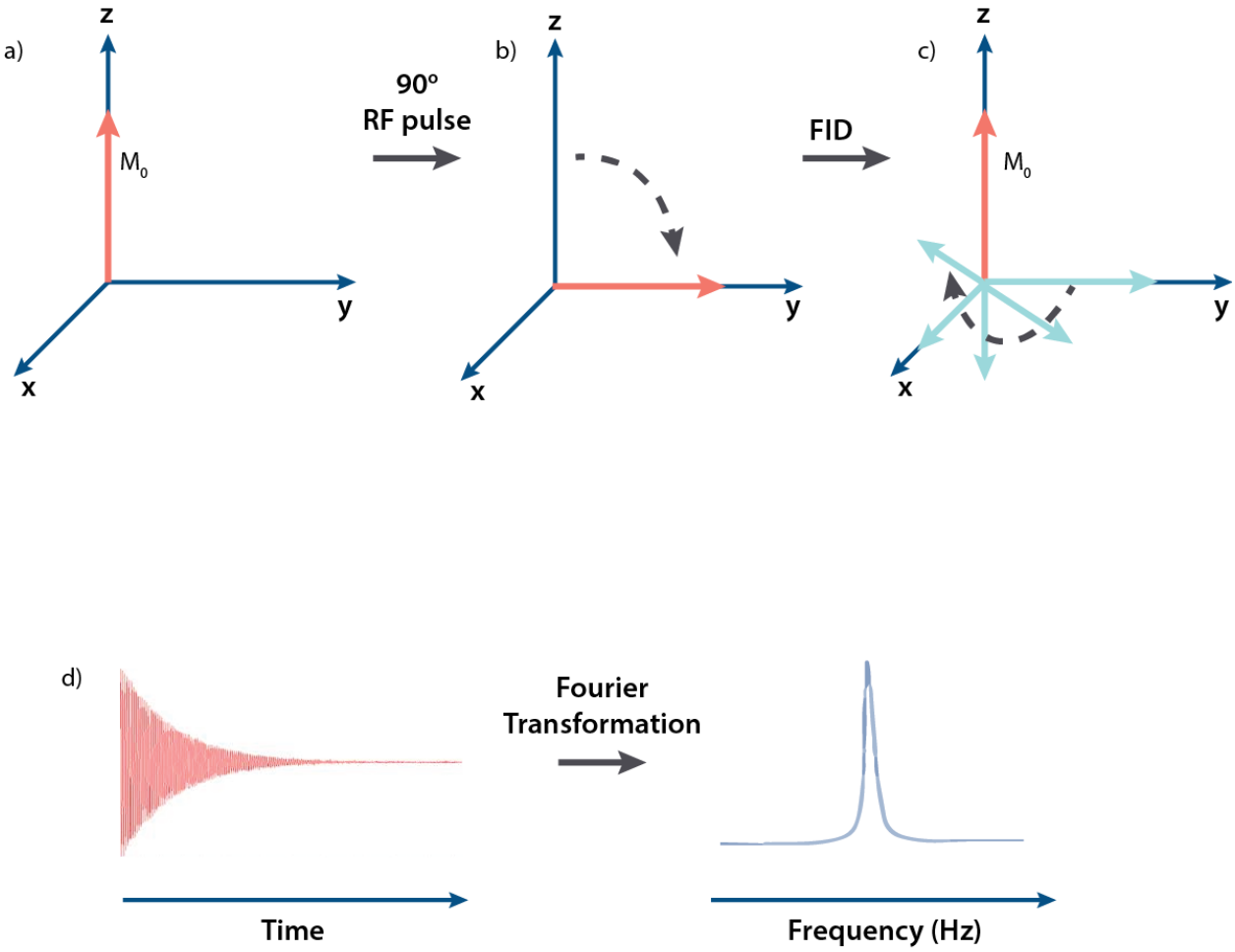

Figure 2.3 The NMR signal acquisition process

a) Precession of the magnetisation vector around the z-axis b) application of a 90° RF pulse causes a transition of the vector along the x-y plane c) release of RF pulse and free induction decay to return back to equilibrium d) signal acquisition and Fourier transformation.

Relaxation describes the process during which excited nuclei release their previously absorbed energy and return to equilibrium. The relaxation of the nuclear spin magnetisation is not an intrinsic characteristic of excited nuclei but is facilitated by two processes: the spin-lattice (longitudinal) relaxation time (T_1) and the spin-spin (transverse) relaxation time (T_2). During spin lattice relaxation, nuclei in a higher energy state release energy to the lattice (the sample in which the nuclei are held) and lose energy returning to the lower state. This process happens exponentially with time and it is essentially the time constant for a nucleus to return to its equilibrium state (z axis).

For spin-spin relaxation to occur, inter-nuclei interactions take place during which there is an exchange of energy between nuclear spins in the higher and lower energy state. T_2 is therefore defined as the time constant for the nuclear spins to lose energy in the XY plane [150].

2.2.2.1 Chemical shift

A property of NMR spectroscopy that can provide further structural and conformational details about a molecule, is that each nucleus experiences the applied magnetic field (B_0) differently resulting in distinct resonance frequencies. The electron cloud surrounding the interrogated nucleus influences this effect, in that the external applied magnetic field (B_0) will generate a local magnetic field in the electron cloud, which will be smaller, and in the opposite direction of B_0. This phenomenon is known as nuclear shielding and essentially reduces the magnetic field experienced by the nucleus. The extent to which each nucleus will be shielded depends on the electronegativity of the atoms in the molecule. For instance, if a proton nucleus is bound to a highly electronegative atom like oxygen, it will have a lower

electron density because the oxygen nucleus will attract more electrons. This will decrease the shielding of the proton nucleus against B_0 and result in the protons experiencing a higher overall magnetic field and resonating at higher frequencies. On the contrary, proton nuclei of a methyl group will have a greater electron density leading to a higher degree of shielding, a weaker experienced magnetic field and therefore a lower resonance frequency.

Nuclear shielding essentially corresponds to the difference between the applied and the experienced magnetic field by the nucleus. The chemical shift (δ) can be defined by the following formula:

$$\delta(\text{ppm}) = \frac{[(\upsilon_{\text{observed}} - \upsilon_{\text{reference}})\,(Hz)]\; x\; 10^6}{Spectrometer\ frequency\ (Hz)}$$

Where $\upsilon_{observed}$ is the resonance frequency of the samples proton nucleus, and $\upsilon_{reference}$ is the resonance frequency of a reference nucleus. In the NMR experiments described in this thesis the reference compound used is 3-(trimethylsilyl)-[2,2,3,3,-$^2H_4$]-propionic acid (TSP). TSP is a highly shielded compound, meaning that it absorbs energy at low frequency therefore its resonance does not overlap with the resonances of other metabolites in the sample of interest. Molecules are characterised by their chemical shift relative to the reference compound in an experiment rather than the frequency of the line due to the fact that different applied magnetic fields can cause the observed peaks to appear at slightly different frequencies, but the position in relation to the reference compound peak is always constant when expressed as the chemical shift (ppm).

2.2.2.2 The spin-spin coupling

The spin-spin coupling (or J coupling) phenomenon occurs extensively when two nuclei are in close proximity, and serve as minor independent magnetic fields. Adjacent nuclei in the

same molecule interact with each other, as well as with the external applied magnetic field, resulting in the splitting of the NMR signal and subsequent spectral peak multiplicity. NMR spectra are characterised by the presence of not only singlet peaks, but also doublets, triplets and multiplets. Spin-spin coupling occurs when adjacent protons affect the NMR signal as such, that splitting of the resonance peak occurs into further components. The peak pattern of shape and intensity is in accordance with Pascal's triangle (Fig. 2.4). If all couplings to a particular proton are the same there will be 2nI+1 peaks, where I is the spin quantum number and n is the number of adjacent nuclei (n + 1 for ^{1}H I = 1/2).

In ^{1}H NMR spectroscopy, spin-spin coupling is observed in protons that are up to three bonds apart, but any unsaturated bonds can influence the distance up to which the electron exchange occurs [150]. *J* coupling interactions are not affected by the applied magnetic field in a given sample, meaning that the observed peak patterns are constant regardless of the external magnetic field strength [151]. This feature of NMR spectroscopy is of great importance for molecular structure characterisation since it depends on chemical bonds, coupled nuclei, the distance of the interacting bonds as well as the dihedral angles between the bonds.

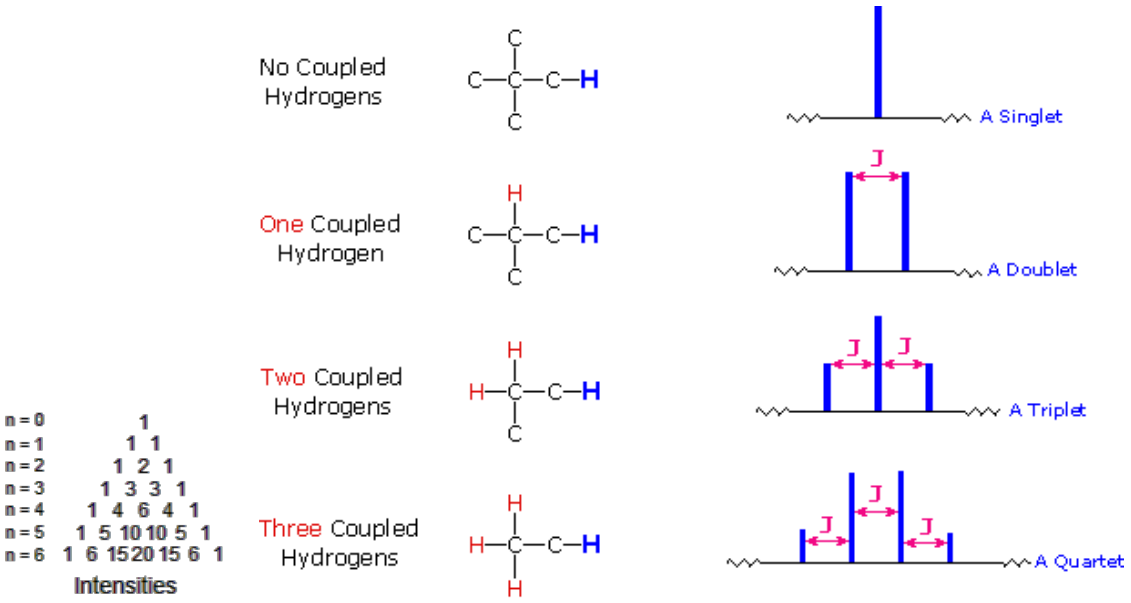

Figure 2.4 Example of *J* coupling in the generation of different peak shapes and intensities following the Pascal's triangle (n; number of adjacent nuclei) [152]

2.2.3 Pulse sequences

A single pulse sequence employed in 1D NMR experiments can be broken down into several sections. The preparation time, also known as the relaxation delay (s), the pulse width (µs) and lastly the acquisition time. During the relaxation delay (RD) the spin system is prepared for the spins to reach equilibrium. This is an important step to ensure maximum signal to noise ratio. Insufficient relaxation of the spin system will result in poor quality peaks. For a complete spin system relaxation, RD lasts about four to five times the T1 relaxation time. Following RD is the pulse width during which the radiofrequency generator is rapidly turned on and then off (5-15 µs) and this results in the perturbation of the spin system. Subsequently, the signal from the excited spins relaxing back to their original state (FID) is recorded during the acquisition period. The pulse sequence is repeated multiple times during an experiment to compensate

for the rather low sensitivity of the NMR compared to other spectroscopy based methods. Increasing the number of acquired scans increases the signal to noise ratio.

Pulse sequences in NMR experiments can be modified accordingly, to facilitate the metabolic profile acquisition from different samples. The following two sections describe the pulse sequences used in this thesis.

2.2.3.1 Standard one-dimensional solvent suppression pulse sequence

One-dimensional experiments with water pre-saturation allow for the acquisition of the resonance of all ^{1}H-containing molecules in a given sample including signals from small molecules as well as broad signals from larger molecules. This type of pulse sequence is used for the acquisition of spectra from urine samples, aqueous tissue extracts as well as cell extracts, which are characterised by a poor macromolecular content. The water resonance is irradiated during this sequence with a low power continuous wave for pre-saturation and attenuation of the resonance before acquisition [153]. Figure 2.5 shows a representative 1H NMR spectrum obtained from the hydrophilic fraction of cell extracts using a standard one-dimensional pulse sequence.

2.2.3.2 The Carr-Purcell-Meiboom-Gill (CPMG) pulse sequence

This experiment is particularly relevant for samples with substantial macromolecular content such as tissue extracts and plasma samples. The CPMG spin-echo pulse sequence attenuates the signals of macromolecules like proteins and lipids, allowing for a better signal acquisition from small molecules (carbohydrates, amino acids, nucleic acids). The pulse sequence is as follows: RD - 90° - $(t$ -180° – $t)_n$ – 90° -acquire; where t is the spin- echo delay, n represents the number of loop and 180° is the 180° radiofrequency pulse [145]. During the CPMG pulse

sequence the amplitude of the received signal decays over time as a result of the T_2 relaxation. Naturally, larger molecules have faster T_2 relaxation therefore their signal decays first and their resonance weakens.

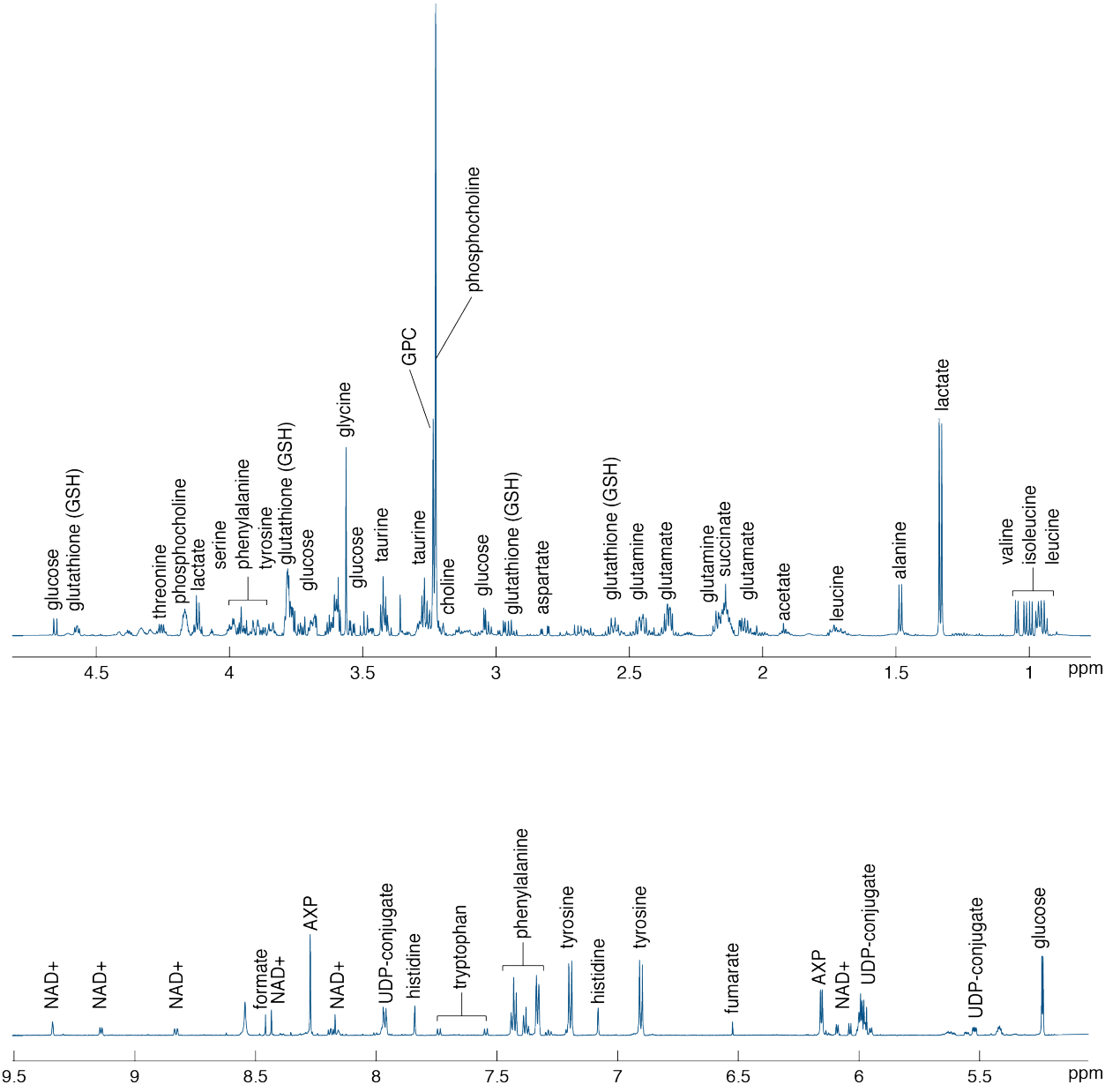

Figure 2.5 Representative ^{1}H NMR spectrum of the hydrophilic metabolites extracted from untreated MCF-7 cells

2.3 Chemometrics

Metabonomic analytical platforms generate thousands of signals from metabolic fingerprinting. Multivariate data analysis is the ideal tool to be used in instances where the number of variables obtained substantially exceeds the number of samples, which is a typical case in metabonomics. Univariate statistical analyses lack the ability to account for multicolinearities, where highly correlated variables can mutually define and predict a class, rendering the analysis less robust than multivariate statistical analyses.

The purpose of multivariate statistics undertaken for large datasets is to summarise and visualise the main sources of variation in the data and facilitate the extraction of useful information from such complex datasets, usually in the form of plots and model summary statistics. Unsupervised and supervised modelling methods are used in metabonomics to facilitate biological interpretation and biomarker discovery.

2.3.1 Unsupervised methods – Principal components analysis

Principal component analysis (PCA) is an unsupervised method of multivariate data analysis meaning that no existing hypothesis of the dataset is needed for model generation. It is a data projection-based method facilitating the representation of a multivariate dataset matrix (X) consisted of n rows (samples) and *k* columns (variables) by reducing the large dimensionality of the dataset while maintaining important information for data interpretation. In PCA, each observation is represented by one point in as many dimensions as there are variables, and placed on the plane according to the variables values.

PCA calculates the line of least squares, which passes through the origin. The first fitted line is called the first principal component (PC1) in the multidimensional space, and this

will be in the direction that explains the greatest degree of variation in the dataset. A single principal component cannot adequately explain the variation in a model of biological data. Therefore, subsequent principal components are implemented to further explain the variation and are calculated orthogonally to the previous principal component. Figure 2.6 shows how PC1 and PC2 form a model plane in the multivariate space, on which every observation is projected.

PCA is interpreted by the scores and loadings plots. From each principal component, the respective scores and loadings can be produced. Scores represent the projections of the observations on the corresponding principal component. Scores plots (graphical representation of the projection-score value (t)) reveal any existing similarity or difference among the samples in the new reduced dimensional space as a function of the variance explained by each of the principal components calculated. PCA constitutes a useful tool for the detection of outliers in the dataset matrix. Loadings (P) are the cosine angle of a variable from a specific principal component. It calculated to examine the degree of contribution of each variable (for NMR spectral data each variable corresponds to a signal and therefore a metabolite) to the model for each of the principal component, and allows for the identification of the metabolites driving any specific patterns observed in the scores plot. The matrix is therefore modelled by the equation:

$$X = TP' + E$$

X represents the metabolite data; T is the scores; P transposed represents the loadings and E is the residuals. The residuals represent the deviation between the true position of a data-

point and the position projected on the model plane, and constitute the part of the dataset matrix that cannot be explained by the model.

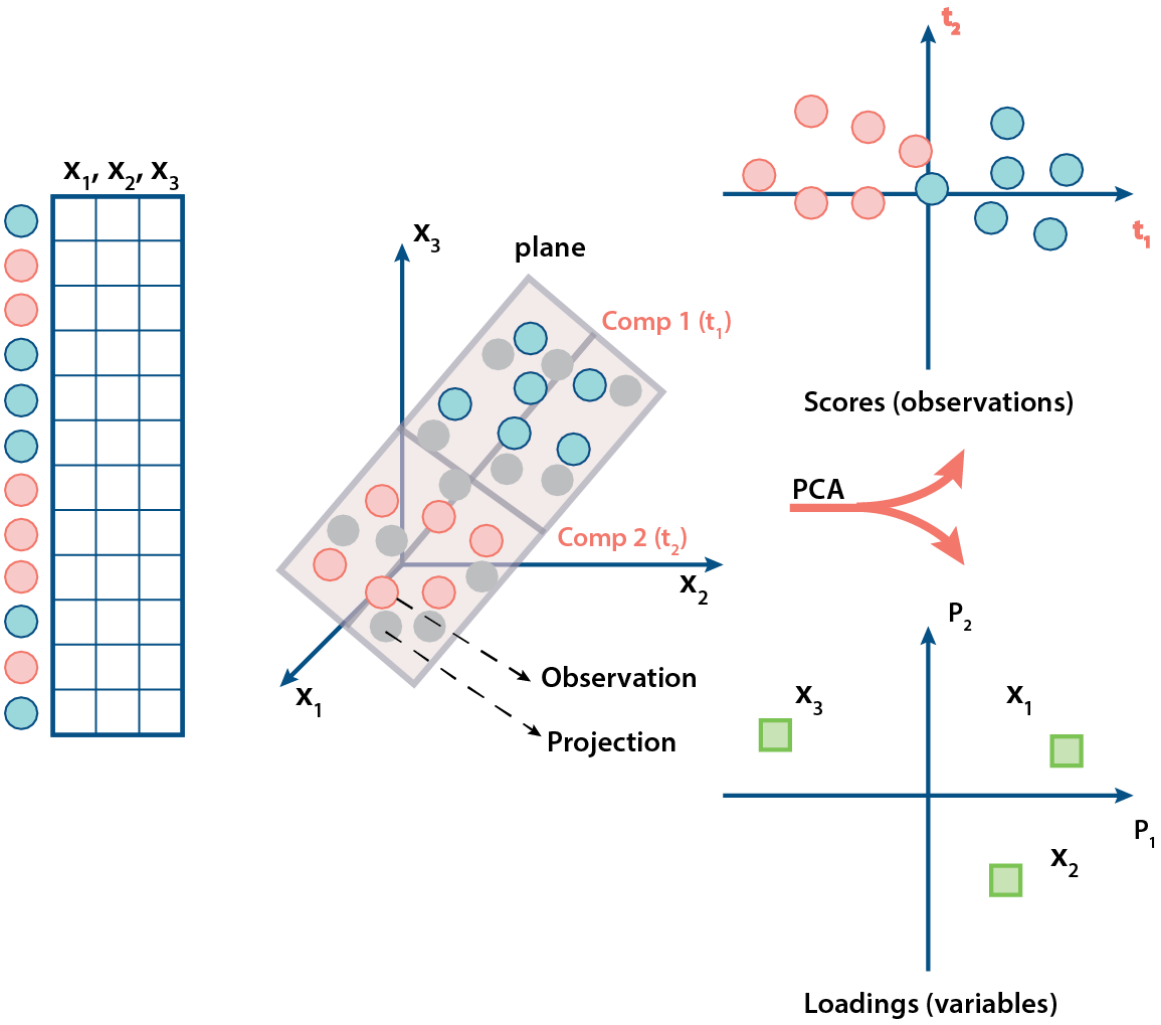

Figure 2.6 Geometric representation of the PCA process [154]

Variables in the X matrix (X_1, X_2, X_3) that contains 12 samples are placed in a lower dimension plane. Each dimension represents one variable. The scores and loadings plots are provided from the model plane. Scores plots provide information on any existing groupings, trends or outliers in the dataset and the loadings plots explains the contribution of each of the variables (X_1, X_2, X_3) in the model.

2.3.2 Centring & Scaling

In metabonomic datasets variables can have considerably different ranges and this can modify the quality and the quantity of information obtained by a statistical model. PCA, like all projection-based methods, is sensitive to scaling of the variables, meaning that the variables with highest value range will substantially influence and dominate the model [154]. In order to adjust for this, two data modification methods are employed prior to model construction; mean centring and scaling (Fig. 2.7).

Mean centring is a data pre-processing method, which, as the name suggests, ensures that the mean of each variable is centred on the origin of the axes. This is achieved by calculating the mean of each of the variables and subtracting it from the value of each variable, thus removing the mean trajectory from the dataset [154, 155]. The interpretation of the obtained result will be relative to the spread around the mean and all of the variables will have the same reference point. The first principal component will therefore represent the covariance in the dataset and will not be dominated by the mean of each variable.

Scaling of data adjusts the weight of each variable on each axis, and prevents the skewed interpretation of the results as a consequence of differences in the range of values for each of the variables. In unit variance scaling the value of each variable is divided by its standard deviation, hence variables have equal variances and no variable can dominate over any other.

Pareto scaling is a scaling method used in metabonomic data analysis, and is calculated by dividing each variable by the square root of its standard deviation [154]. It minimises the differences in the range of the variables values, while maintaining the order of

the starting variance of each variable. Pareto scaling up-weights medium features without inflating baseline noise, which is the case in unit variance scaling [156].

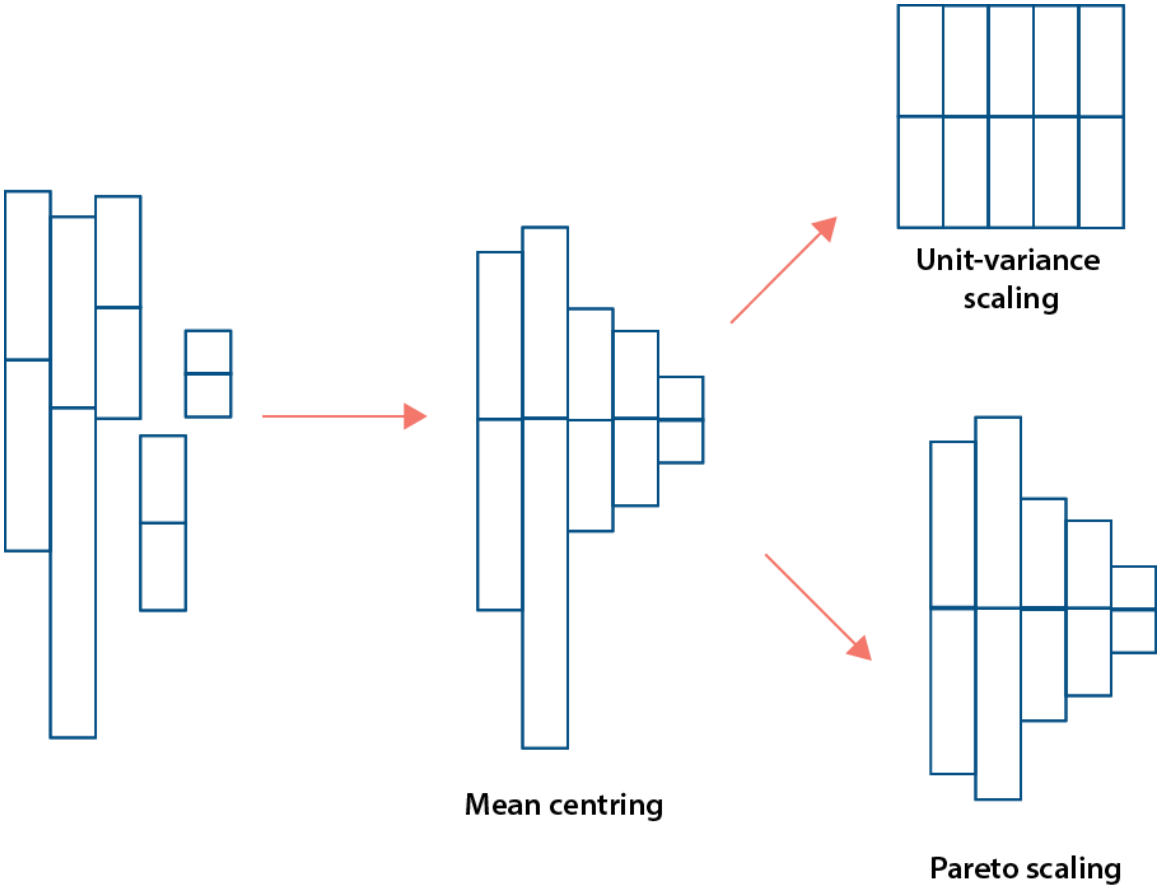

Figure 2.7 Schematic representation of the effect of mean-centring and scaling methods on data

2.3.3 Supervised methods – Projections to latent structures and Orthogonal projections to latent structures

While PCA is an unsupervised method of data modelling, projections to latent structures (PLS) method and its iterations are supervised methods, meaning that *a priori* knowledge is required for model construction. In these methods a response variable (Y) is implemented corresponding to continuous or discrete variables such as age, gender or treatment group. When the Y matrix contains discrete data, discriminant analysis is performed (PLS-DA).

PLS method relates matrices X (predictor, metabolite data) and Y (response variable to be predicted) aiming to explain the maximum covariance between the two and allow for any true metabolic variation related to a response variable to be shown (Fig. 2.8). This method is particularly useful in metabonomic studies where the number of variables surpasses the number of observations. Similarly to PCA, the first PLS component calculated in the X and Y multivariate space must describe the maximum variation within the matrices and therefore maximise the covariance of the scores t1 and u1 (Fig. 2.8). Further components are calculated perpendicular to the previous one. The new PLS model can be expressed by the following equations:

$$X = TP' + E$$

$$Y = UC' + F$$

Where T and U correspond to the matrix of scores that summarise the X and Y variables respectively. P' and C' represent the loadings for the correlation between X and Y and the score vectors U and T respectively. E and F are the residual matrices.

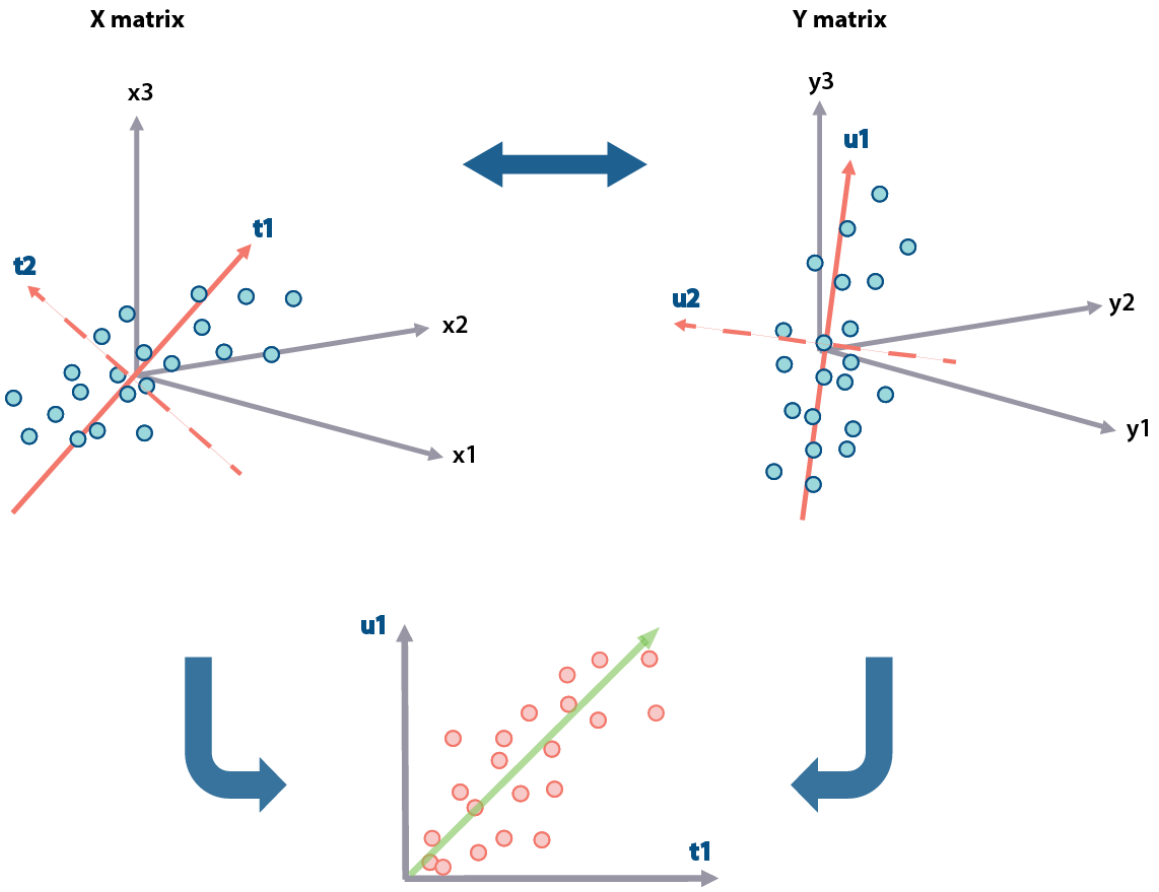

Figure 2.8 Schematic representation of the principle of PLS model

Orthogonal projections to latent structures (OPLS) and orthogonal projections to latent structures – discriminant analysis (OPLS-DA) are variants of the PLS models facilitating the filtering of extraneous variation irrelevant to the biological class. Variable (X) matrices obtained from NMR metabolic profiling often contain variation that is uncorrelated to the Y matrix that can introduce noise in the PLS/ PLS-DA model and compromise its interpretability (e.g. instrumental issues, sampling problems and uncontrolled sources of biological variation). In OPLS and OPLS-DA models an integrated Orthogonal Signal Correlation (OSC) filter is implemented during model construction. This added orthogonal component divides the X matrix variation into a predictive component (variation correlating between X and Y)

and an orthogonal component that accounts for the variance that is uncorrelated to Y [154]. It therefore describes the unwanted systematic variation unrelated to the biological variation (Y). This partitioning of the X matrix variation positively impacts model interpretation by separating between-class and within-class variation, something that cannot be facilitated by PLS models [154, 157].

Similarly to PCA, loadings in OPLS-DA are displayed in the form of a pseudo-NMR spectrum, plotting the covariance between the metabolites and the Y matrix (classes). OPLS-DA covariance plots are obtained by back-scaling the unit-variance scaled model (multiplying the model coefficients by the standard deviation of the corresponding variable) to a correlation matrix [157, 158]. The pseudo-spectrum is coloured with scale; the colour of each resonance on the plot is the square of the correlation of each metabolite with the class relationship (R^2: the proportion of the X matrix predictable by Y).

2.3.3.1 Model diagnostics and validation

PLS and its derivative models are prone to over-fitting. This phenomenon occurs when a model despite its apparent ability for fitting training data, it has a poor predictive ability for future observations and therefore predicts noise or random error. R^2Y represents the proportion of X needed to describe Y, and this value is known as the 'goodness of fit' [159]. It signifies the ability of the model to fully characterise the dataset, therefore a high R^2Y value suggests a low residual value. In order to overcome the problem of over-fitting, a cross validation step is implemented in the data analysis to assess the true predictive ability of a model. Cross validation is performed by removing $1/7^{th}$ of the X matrix, and using the remaining data to predict the missing values back into the model. If the interrogated model is

valid it will accurately predict the missing data. This procedure is repeated until every observation has been back-predicted once. Cross validation facilitates the determination of the Q^2Y value, which represents the predictive power of the model i.e. how well X predicts Y in the model.

In most cases, R^2 value is expected to be higher than Q^2 as the model complexity increases but the difference should not be more than 0.2-0.3. R^2 will continue to increase with complexity due to greater variation explained by the model. On the contrary, Q^2 value will reach a peak when the model is saturated, in terms of the number of fitted components, and will then start to decline. This is a result of the fact that when additional variation is added to the model, the more noise is added too leading to a reduction in the predictive ability of the model.

2.3.3.2 Permutation testing

A permutation test is used to calculate the significance of the estimated predictive power Q^2Y of the model, to validate the model. Here, data are shuffled (permutated) resulting in the random assignment of observations in correct or incorrect classes. Virtual OPLS-DA models are then constructed based on the newly generated dataset, and the R^2Y and Q^2Y values are obtained. The Y matrix is normally permutated 1000 times and the R^2Y and Q^2Y values are ranked. The rank of the Q^2Y from the real model against the virtual random models provides a significance value. The real model is considered significant if its Q^2Y value ranks within the top 5% of the Q^2Y values obtained from the virtual models ($p < 0.05$). Hence a genuine association exists between the metabolites and the response measure.

3 Characterising the metabolic perturbations induced by watercress and phenethyl isothiocyanate exposure in MCF-7 and MCF-10A cells

Hypothesis

It is hypothesised that phenethyl isothiocyanate (PEITC) and the watercress extract will induce significant metabolic modifications with anti-carcinogenic potential in breast cancer cells and that these effects will be different from those in healthy breast cells.

Aims

- Characterise the basal metabolic profiles of MCF-7 and MCF-10A cells.
- Investigate the metabolic response of MCF-7 and MCF-10A cells in response to crude watercress extract and PEITC.
- Study how crude watercress extract and PEITC influence markers of cellular genotoxicity.

Objectives

- ^{1}H NMR metabonomics and multivariate statistics will be used to characterise the metabolic profiles of the two cell lines following exposure to different doses of the watercress extract and PEITC.
- Treatment genotoxicity will be evaluated by measuring DNA damage using the Comet assay, assessing cell cycle stages using flow cytometry and measuring mitochondrial membrane potential.

3.1 Introduction

Watercress (*Nasturtium officinale*) belongs to the family of *Brassicaceae* together with broccoli, Brussel sprouts and kale. Epidemiological studies suggest a link between the consumption of Brassica vegetables and a reduced risk for many types of cancers [160] including breast cancer [161, 162]. Watercress has a complex phytochemical profile characterised by high levels of carotenoids, flavonols and glucosinolates [163] and extracts of watercress exhibit strong antioxidant capacity *in vitro* [52, 57]. Watercress and its components have been associated with the inhibition of the three stages of carcinogenesis: initiation, proliferation and metastasis in *in vitro* cancer cell models [53, 58, 164].

Plant tissue damage such as cutting or chewing, induces the release of the plant enzyme myrosinase (β-thioglucoside glycohydrolase; EC 3.2.3.1), which hydrolyses glucosinolates present in the tissue, forming reactive isothiocyanates [63]. It is this group of bioactive compounds that have received considerable attention for their potential anti-cancer properties. Watercress is particularly rich in gluconasturtiin, which is the glucosinolate precursor to phenethyl isothiocyanate (PEITC). Research has highlighted promising chemopreventive and chemotherapeutic activities of PEITC. Due to its highly electrophilic nature PEITC reacts with cellular thiols via thiocarbamoylation and after its cellular uptake it reacts with glutathione (GSH), which is the major intracellular antioxidant [60, 108, 165] depleting cells of their GSH content. GSH has a vital role in the maintenance of cellular redox status [30] and tight regulation of intracellular reactive oxygen species (ROS) through the induction of antioxidant mechanisms is central to cancer cell survival. Low levels of ROS can have a proliferative advantage for cancer cells [166]. Excessively high levels of ROS though, will result in disruptions in redox balance can lead to mitochondrial damage underpinned by

oxidative stress, and ultimately cancer cell death [22]. To manage this, cancer cells use antioxidants such as GSH, to prevent ROS from accumulating at detrimentally high levels. Malignant cells are commonly characterised by elevated ROS levels compared to non-cancerous cells [166] PEITC treatment has therefore a selective detrimental effect on cancer cells since they rely on their antioxidant mechanisms for survival and PEITC depletes the cellular levels of their main antioxidant, GSH.

At the cellular level PEITC has been extensively shown to have direct anti-cancer effects in *in vitro* cancer models. It causes cell cycle arrest in a wide variety of cell lines and it is a potent inducer of apoptosis [99, 102, 108]. PEITC increases the activity of Nrf2, a key transcription factor relevant to the activation of oxidant/electrophile response genes mediating chemopreventive functions [167]. PEITC also inactivates the nuclear factor kappa B (NF-kB) pathway affecting important steps in carcinogenesis including, inflammation, cancer cell survival, differentiation and proliferation [168-170]. Inflammation is a central process in cancer development and PEITC has been shown to decrease the expression of inducible nitric oxide synthase (iNOS) and cyclooxygenase-2 (COX-2) resulting in an attenuated secretion of pro-inflammatory mediators [171]. Other targets of PEITC include the hypoxia inducible factor (HIF) [106] negatively regulating angiogenesis as well as inhibiting mTOR, which plays a key anabolic role in translation and functions as a vital metabolic integration point joining nutrient availability with growth signals [22, 95]

Metabolic regulation is a determining element of the cell growth machinery and cancer cells have adapted to several oncogenic signals to modify their metabolic phenotype as such, to support their needs for growth, survival and malignant transformation. Core

cancer cell metabolism serves the three basic needs of proliferating cells: i) rapid ATP generation to sustain energy status, ii) increased need for the biosynthesis of macromolecules, proteins, lipids and nucleotides, iii) maintenance of appropriate cellular redox status.

To our knowledge, limited work has been done on the effects of PEITC and of crude watercress extract on cancer cell energetics and metabolism. PEITC impacts a great range of oncogenes and tumour suppressor genes, which can all cause shifts in intracellular signalling pathways involved in cancer cell metabolism. It is therefore central to get an insight into the effect of such a bioactive compound on the global metabolic profile of cancer cells. This chapter will investigate the biochemical response of MCF-7 breast cancer cells to increasing doses of watercress extract and to PEITC using ^{1}H NMR metabonomics. This will then be compared to the metabolic response of immortalised but non-tumorigenic MCF-10A cells to the same treatments. Biochemical observations will be related to inducible cancer related phenotypic changes in cell behaviour.

3.2 Materials and methods

5.1.1 Cell Culture

The MCF-7 human breast adenocarcinoma cell line was purchased from the American Type Culture Collection (ATCC) (LGC standards, Middlesex, UK). Cells were cultured in Dulbecco's Modified Eagle's Medium (DMEM; Lonza Group Ltd, Basel, Switzerland) supplemented with 10% (v/v) foetal bovine serum (FBS; Lonza Group Ltd), 2 mM glutamine (Thermo Fisher Scientific, Loughborough, UK), 50 U/ml penicillin and 50 U/ml streptomycin (Thermo Fisher Scientific, Loughborough, UK) and 1% non-essential amino acids (Sigma-Aldrich, Dorset, UK).

The MCF-10A, non-tumorigenic breast epithelial cell line was kindly provided from Prof. Graham Packham (University of Southampton, Southampton, UK). Cells were maintained in Ham's F12:DMEM (1:1) (Lonza Group Ltd), 20 ng/ml epidermal growth factor (EGF) (PeproTech, London, UK), 0.1 µg/ml cholera toxin (Sigma-Adrich), 10 µg/ml insulin (Invitrogen), 500 ng/ml hydrocortisone (Sigma-Aldrich), 5% horse serum (Invitrogen) and 50 U/ml penicillin and 50 U/ml streptomycin (Thermo Fisher Scientific, Loughborough, UK).

Cells were grown in an incubator at 37 ^{o}C with 5% CO_2 and 95% humidity in 75 cm^2 culture flasks and were routinely passaged at approximately 70% confluency. The medium was changed every 2-3 days. For passaging, cells were washed with phosphate buffer saline (PBS; Lonza Group Ltd) before detaching with 5ml of Trypsin-Versene® (EDTA) mixture (Lonza Group Ltd) for 3-5 mins for MCF-7 cells and 18-20 mins for MCF-10A cells. Media (5 ml) was then added to the cells to inactivate the trypsin and the cell suspensions were centrifuged at 300 *g* for 3 mins. Cell pellets were resuspended in complete media in the flask and incubated.

5.1.2 Compounds and Extracts

3.2.1.1 Analytical grade compounds

Phenethyl isothiocyanate (PEITC) was purchased from Sigma (Dorset, UK). PEITC stock solution (30 mM) was made up in DMSO fresh on the day of use.

3.2.1.2 Watercress extracts

Fresh watercress samples were obtained directly from Vitacress Salads Ltd. (Andover, UK). Samples were snap frozen in liquid nitrogen and stored at -80 ºC. 2 g of leaf and 2 g of stem were weighed and placed in a 20 ml syringe (BD Biosciences, Oxford, UK) that had had the plunger removed and a circular 25 mm glass microfiber filter (Whatman, Dassel, Germany) placed at the bottom. The syringe was then placed inside a 50 ml centrifuge tube without the lid and centrifuged at 1500 *g* for 30 mins to collect the extract. This crude watercress extract was then filtered through a 0.22 µm filter and used in the cultures.

5.1.3 Cell proliferation

For the determination of cell proliferation MCF-7 and MCF-10A cells were seeded in 96-well microplates at $5x10^3$ cells per well and incubated at 37 ºC with 5% CO_2 and 95% humidity for 24 hours. Cells were exposed to the watercress extract at 6.25, 12.5, 25 and 50 µl/ml and PEITC at 5, 10, 20, 30 µM for 24 hours. The treatments were then removed by aspiration. Cells were permeabilised with 100 µl of ice-cold methanol for 5 mins at room temperature. Methanol was removed and the plates were allowed to air dry for 15 mins in a hood, followed by addition of 100 µl of DAPI in PBS (70 µl of 30mM DAPI stock solution in 10.43 ml of PBS). Cells were incubated in the dark for 30 mins at 37 ºC and absoprtion was measured using GENios microplate reader (TECAN Group Ltd., Mannedorf, Switzerland) with absorbance at 340 nm

and emission at 465 nm. The experiment was performed in triplicate with three technical replicates per experiment.

5.1.4 NMR Metabonomics

The metabolic profiles of MCF-7 and MCF-10A cells were analysed using ^{1}H NMR spectroscopy. Cells were seeded at $1x10^{5}$ cells per well into six well plates and treated at 80% confluency. Cells were exposed to the watercress extract at 6.25, 12.5, 25 and 50 µl/ml and PEITC at 5, 10, 20, 30 µM for 24 hours. Media was transferred into eppendorf tubes and cells on the surface of the plate were washed twice using 1 ml cold (4°C) PBS and were quenched using 1 ml of ice-cold methanol (maintained on dry ice). Cells were allowed to lyse for 2 mins and were detached from the plate using a cell scraper and transferred into an Eppendorf tube. Methanol quenching was repeated to maximise metabolite recovery. A vacuum concentrator (SpeedVac) was used to dry down the cell suspensions before reconstitution in 80 µl of phosphate buffer (pH 7.4) in 100% deuterium oxide containing 1 mM of the internal standard, 3-(trimethylsilyl)-[2,2,3,3,-$^{2}H_{4}$]-propionic acid (TSP).

For every sample, a standard one-dimensional NMR spectrum was acquired using a 600 MHz Bruker NMR spectrometer, with water peak suppression using a standard pulse sequence (recycle delay (RD)-90°-t1–90°-tm-90°-acquire free induction decay (FID) RD= 4s, t_1=8.62 µs, t_m= 100 ms). For each spectrum 256 scans and 8 dummy scans were obtained, collected in 64K data points with a spectral width of 12.001 ppm. ^{1}H NMR spectra were manually corrected for phase and baseline distortions and referenced to the TSP singlet at δ 0.0. Spectra were digitized using an in-house MatLab (version R2012a, The Mathworks, Inc.; Natwick, MA) script. Metabolites were identified using an in-house database of standards and

Chenomx NMR suite (version 7.7, Chenomx Inc). Multivariate modelling, including principal component analysis (PCA) and orthogonal projections to latent structures discriminant analysis (OPLS-DA), was performed on the samples using in house scripts

5.1.5 Cell Cycle

MCF-7 and MCF-10A cells were seeded at a $1x10^5$ cells per well in six well plates and incubated as required. The cells were then exposed to the watercress extract and PEITC at 6.25, 12.5, 25, 50 µl/ml and 5, 10, 20, 30 µM, respectively for 24 hours. Following treatment removal, the cells were washed with cold PBS (4°C) and harvested by trypsinisation. Cells were pelleted by centrifugation at 300 *g* for 3 mins and the supernatant was discarded. The cell tissue was then resuspended in 200 µl of cold PBS and fixed with drop-wise addition of 70% (v/v) fresh ice-cold methanol. The samples were then stored at -20 °C until analysis.

On the day of the analysis, samples were centrifuged at 300 *g* for 3 mins and the supernatants were discarded. The cell pellets were then resuspended in 200 µl of PBS and 25 µl of 1 mg/ml RNAse was added to the suspensions. The samples were incubated at 37°C for 30 mins and 2.5 µl of 400 µg/ml of PI dye were added to the cells which were then incubated for a further 30 mins at room temperature under dark conditions. The final volume of the cell suspensions was adjusted to 600 µl with PBS. Cellular DNA content of 15,000 cells was quantified via flow cytometry. The flow cytometry analysis was performed using the FL2 channel on a BD Accuri™ C6 flow cytometer (Germany). Data analysis was facilitated using the Flow Jo software (version 7.6, Tree star Inc, Oregon, USA). Cell cycle progression was evaluated accounting for the percentage of cells in each of the phases Gap0/1 (G0/1), Synthesis (S), Gap2/mitosis (G2/M) and apoptotic cells (sub G0/1). The principle of the cell

cycle analysis is based on the fluorescence intensity of the PI nuclear dye that is proportional to the DNA concentration of the cell.

5.1.6 Comet Assay

The Comet assay is used for the measurement of DNA strand breaks in single cells. MCF-7 and MCF-10A cells were seeded in T25 cells culture flasks at a concentration of $1x10^6$ and maintained at 37 °C with 5% CO_2 and 95% humidity. The cells were then exposed to the watercress extract and PEITC at 6.25, 12.5, 25, 50 µl/ml and 5, 10, 20, 30 µM, respectively for 24 hours. The treatment solutions were then removed via aspiration followed by washing with PBS and detaching from the cell culture flask with trypsin. Cell suspensions were adjusted to a concentration of $1x10^6$ cells/ml.

Following the treatments, 20 µl of the cell suspensions were resuspended in 200 µl of warm low melting point agarose (LMA) (0.85% w/v) and applied 75 µl of this was dispensed on Comet Slides (Trevigen). The LMA was allowed to solidify at 4°C for 15 mins. The slides were then transferred into a staining jar, lysis buffer (2.5M NaCl, 0.1M EDTA, 0.01M Tris and 1% (v/v) Triton X – added just prior to use – pH 10) was added and the cells were allowed to lyse for 1 hour at 4°C).

Following lysis of the cells, the slides were placed in a horizontal electrophoresis tank and incubated for 20 mins in alkaline buffer (0.3M NaOH, 1mM EDTA – pH 13) at 4°C in dark conditions. Electrophoresis was carried out at 26 V, 300 mA for 30 mins at 4°C. Immediately after electrophoresis the slides were washed in neutralising buffer (0.4M Tris – pH 7.5) three times for 5 mins.

The slides were then stained with 10 µl of ethidium bromide (20 µl/ml) and DNA migration from the nucleus was visualized with a fluorescence microscope (Olympus BX51). The computer-based image analysis software, Komet 4.0 (Andor Technology, South Windsor, CT) was used to calculate the proportion of DNA that had migrated from the head to the tail of the comet (% tail DNA). The mean value from 100 randomly scored cells was taken as an index of damage for each replicate well.

5.1.7 Mitochondrial membrane potential assay

Mitochondrial membrane potential was assessed using the JC-10 mitochondrial membrane potential kit according to the manufacturer's instructions (Sigma, Dorset, UK). Briefly, $1x10^4$ MCF-7 and MCF-10A cells were seeded in a 96 well plate and allowed to attach overnight. The cells were then exposed to the watercress extract at 6.25, 12.5, 25 and 50 µl/ml and PEITC at 5, 10, 20, 30 µM for 24 hours. JC-10 dye-loading solution (50 µl) was added to each well and incubated for 60 mins before measuring fluorescent intensities (Ex/Em= 485/520 nm and Ex/Em=544/590 nm). The shifts of mitochondrial membrane potential were measured as the ratio between aggregate (Em =520 nm) and monomeric forms (Em =590 nm) of the JC-10 dye using FLUOstar Omega (Isogen Life Science, De Meer, the Netherlands). Increasing ratio indicates mitochondrial membrane depolarization and damage.

3.3 Results

5.1.8 Cell Proliferation

Cytotoxicity of increasing doses of the crude watercress extract and PEITC was assessed in MCF-7 and MCF-10A cells. The dose response curves for cytotoxicity as assessed by DAPI staining are presented in Fig. 3.1 (A-D). Treatment with the watercress extract did not impact MCF-10A proliferation but caused a 20% and 25% decrease in proliferation in MCF-7 cells treated with 25 and 50 µl/ml of the extract, respectively. PEITC caused a significant decrease in cell proliferation in MCF-7 cells reaching up to 46% in the highest PEITC dose (30 µM). Treatment of the MCF-10A cells with 30 µM of PEITC showed evidence of cytotoxicity compared to the untreated cells.

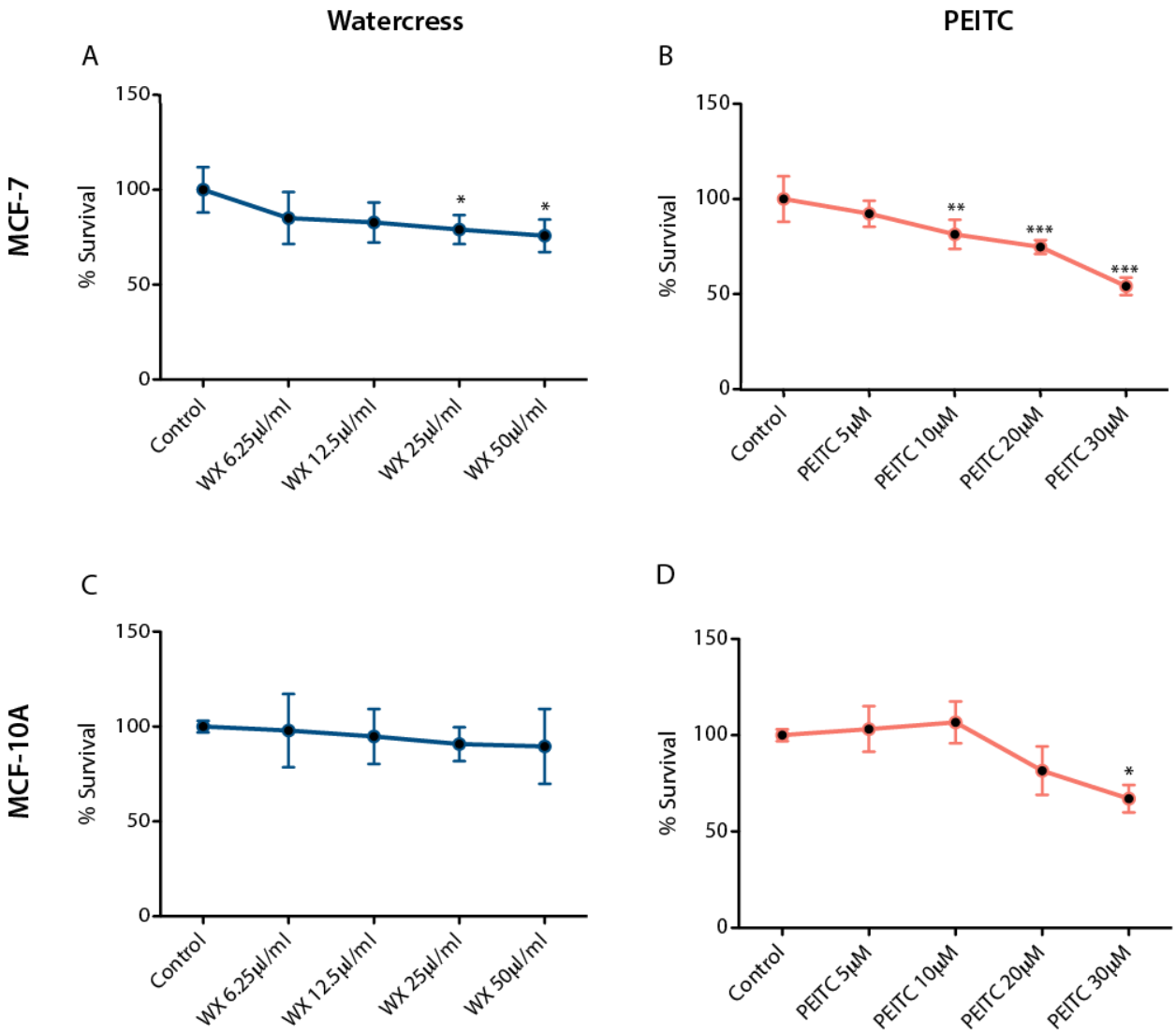

Figure 3.1 Cytotoxicity of the crude watercress extract and PEITC in MCF-7 (A&B) and MCF-10A (C&D) cells.

Data presented as mean ± SEM percentage cell survival. Statistically significant differences between control and treated cells are indicated *p<0.05, **p<0.01, ***p<0.001 after one-way ANOVA followed by Dunnett's multiple comparison test. Data shown represent the average of three independent experiments with three replicates per sample. WX, watercress.

5.1.9 Comparative metabonomic profiling of MCF-7 and MCF-10A cells

Metabolic profiles were acquired from the hydrophilic methanol extracts of MCF-7 and MCF-10A cells using ^{1}H NMR spectroscopy. Principal components analysis (PCA) was applied to the baseline metabolic profiles of MCF7 and MCF-10A cells to observe the main drivers of variation within the metabolic data. From the scores plot obtained from this PCA model (Figure 3.2A) clear separation was observed between the two cell lines in the first principal component (PC1). This indicates that the tumorigenic difference of the cell lines is the main source of variation accounting for 22% of the total variation within the data (metabolites). The loadings plot for PC1 from this model (Fig. 3.2B) indicates that this variation was explained by an increased amount of lactate, phosphocholine and glycine in the MCF-7 cells compared to the MCF-10A.

An orthogonal projection to latent structures discriminant analysis (OPLS-DA) model was built to make a pair-wise comparison between the two cell lines. An OPLS-DA model with strong predictive ability ($Q^2\hat{Y} = 0.56$, $R^2\hat{Y} = 0.98$) was obtained and validated by permutation testing (1000 permutations; $p = 0.001$). The correlation coefficients plot from this model is presented in Fig. 3.3. MCF-7 cells contained greater amounts of lactate, the amino acids alanine, glutamine, glutamate, methionine serine and glycine. MCF-10A cells contained higher amounts glucose, myo-inositol, choline and creatine phosphate compared to the MCF-7, threonine, as well as phosphocholine.

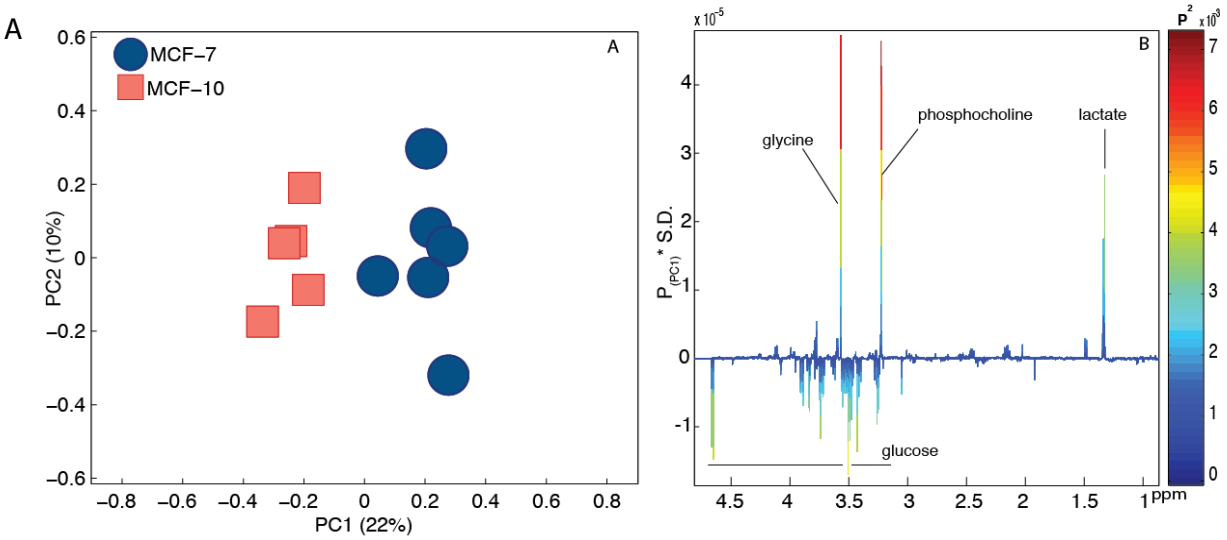

Figure 3.2 Comparison of the metabolic profile obtained from the two cell lines. (A) PCA scores plot (PC1 vs PC2). (B) PCA loadings plot of PC1.

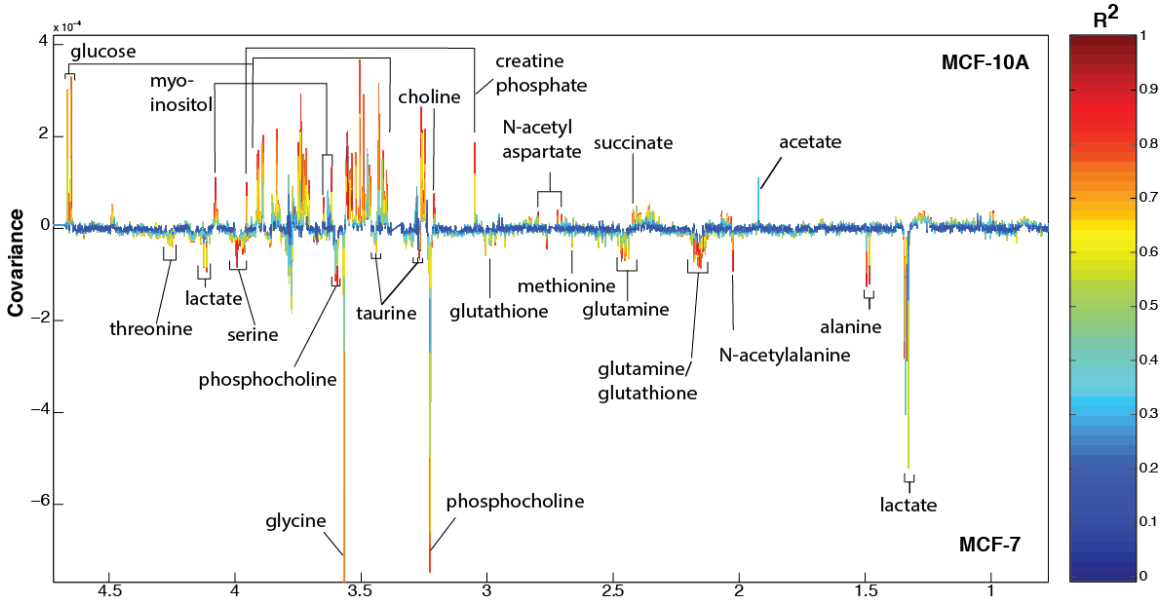

Figure 3.3 OPLS-DA model identifying metabolic associations with cell type. GPC, glycerophosphocholine.

($Q^2\hat{Y} = 0.56$, $R^2\hat{Y} = 0.98$, $p = 0.001$)

5.1.10 Metabolic profiling with increasing doses of crude watercress extract

5.1.11 MCF-7

PCA was performed on untreated samples and samples treated with increasing doses of the watercress extract. A clear clustering was observed between the low and the high treatment doses on the first principal component representing 17% of the variation (Fig. 3.4A). No observable separation was observed between the untreated samples and those treated with the two lower doses (6.25 and 12.5 µl/ml) of the watercress extract. This metabolic transition from low to high doses was explained by increases in the intracellular lactate content of the cells (Fig. 3.4B). Valid OPLS-DA models with good predictive ability ($Q^2\hat{Y}$) were returned for all the pair-wise comparisons of control MCF-7 cells and cells treated with the different watercress extract doses (Table 3.1).

Watercress treatment of the MCF-7 cells caused a number of metabolic perturbations including an increase in lactate production at the highest dose (50 µl/ml), elevated amino acid abundance (valine, leucine, isoleucine, alanine, asparagine) and also an increase in the glutathione content of these cells. Significant increases of NAD+ were also observed accompanied by increased AXP (indistinguishable spectral differences between AMP and ADP) and essentially a lower ATP content (Fig. 3.5).

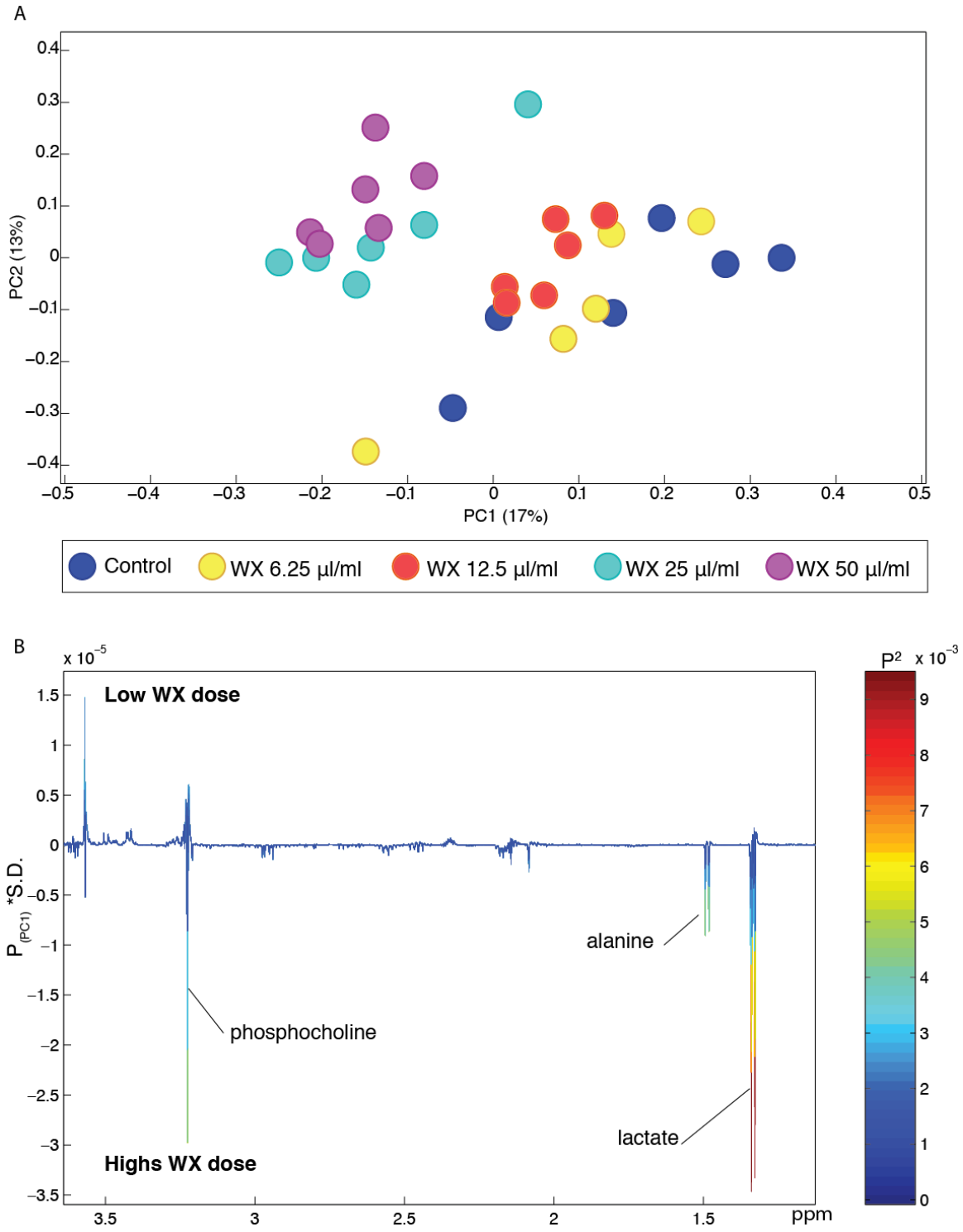

Figure 3.4 (A) PCA scores plot of the MCF-7 cells treated with increasing concentrations of the watercress extract for 24 hours. (B) PCA loadings plot of PC1

Table 3.1 Summary of the OPLS-DA models returned for the comparisons between untreated control cells against cells treated with the watercress extract (6.25 -50 µl/ml) and PEITC (5-30µM) for 24 hours from both MCF-7 and MCF-10A cells.

Treatment	$R^2\hat{Y}$	$Q^2\hat{Y}$	P-value
MCF-7			
Control vs WX 6.25	0.9579	0.4645	0.006
Control vs WX 12.5	0.9871	0.4948	0.002
Control vs WX 25	0.9666	0.7333	0.001
Control vs WX 50	0.9716	0.7525	0.001
Control vs PEITC 5	0.9809	0.4917	0.002
Control vs PEITC 10	0.9884	0.9056	0.002
Control vs PEITC 20	0.9709	0.9317	0.001
Control vs PEITC 30	0.9978	0.9041	0.001
MCF-10A			
Control vs WX 6.25	0.9250	0.4678	0.018
Control vs WX 12.5	0.9344	0.5708	0.004
Control vs WX 25	0.9639	0.7038	0.001
Control vs WX 50	0.9782	0.8248	0.001
Control vs PEITC 5	0.9774	0.0520	0.590
Control vs PEITC 10	0.8776	0.2292	0.250
Control vs PEITC 20	0.9079	0.6422	0.001
Control vs PEITC 30	0.9538	0.8483	0.001

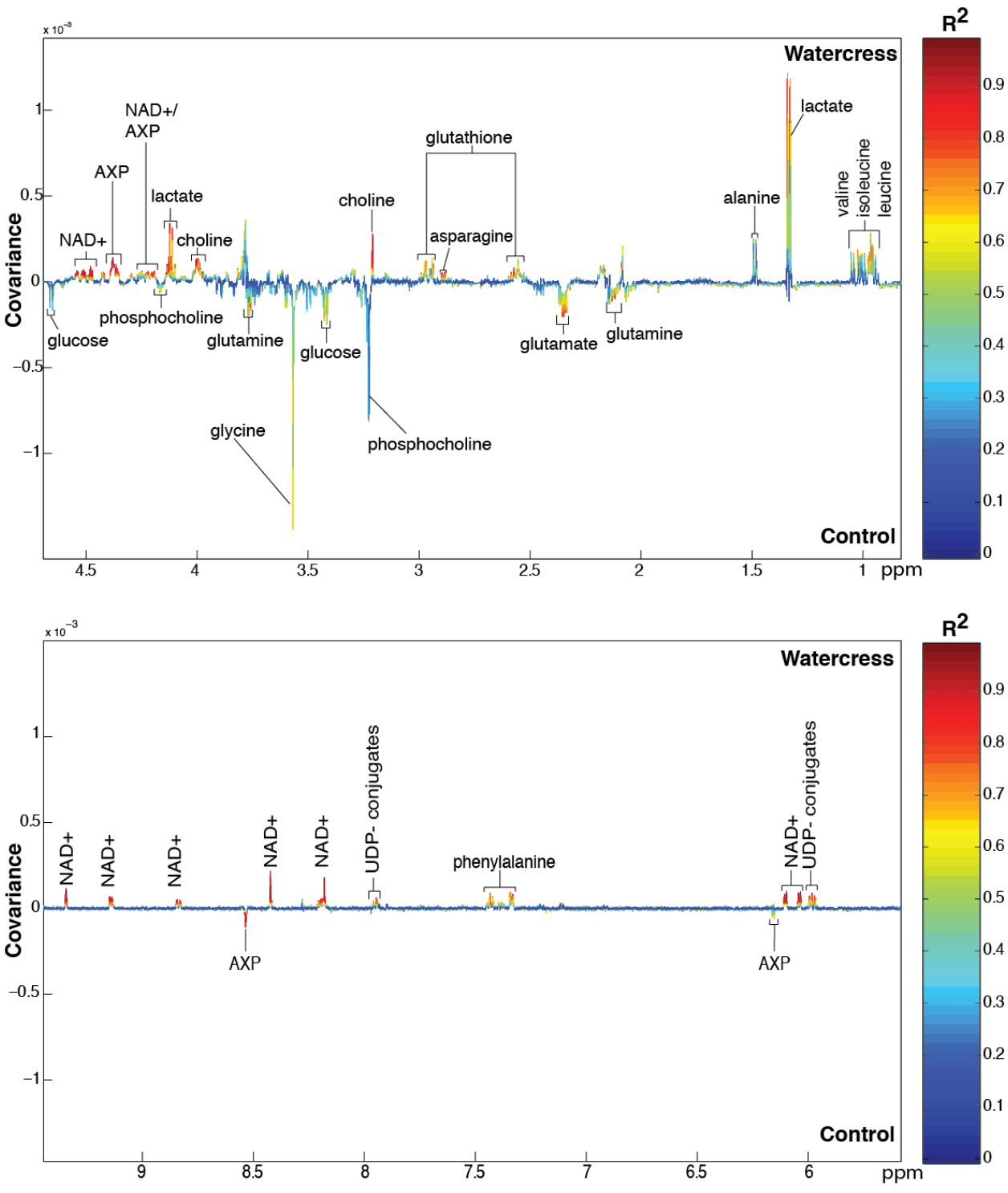

Figure 3.5 OPLS-DA coefficients plot comparing the metabolic profiles of untreated control MCF-7 cells and the highest dose of WX (50 µl/ml) treated cells. (AXP: indistinguishable difference between AMP, ADP, ATP)

5.1.12 MCF-10A

Treatment of MCF-10A cells with the watercress extract caused a metabolic transition from the low to high doses as observed in the PCA scores plot with the different groups separating along PC1 (Fig. 3.6A). Similarly to the MCF-7 cells, increased lactate explained the variation across the treatment groups (Fig. 3.6B). An OPLS-DA model was constructed to probe for discriminating features between control and watercress treated cell samples (50 µl/ml). As expected, the model was dominated by elevated lactate in the watercress treated cells with concomitant increases in acetate, succinate and 4-aminobuturate (4-AB) as well as choline and glycerophosphocholine. The metabolic profile of the untreated MCF-10A cells contained higher phosphocholine, the amino acids valine, leucine, isoleucine, glutamate, glutamine, methionine and glutathione compared to the watercress treated samples (Fig. 3.7).

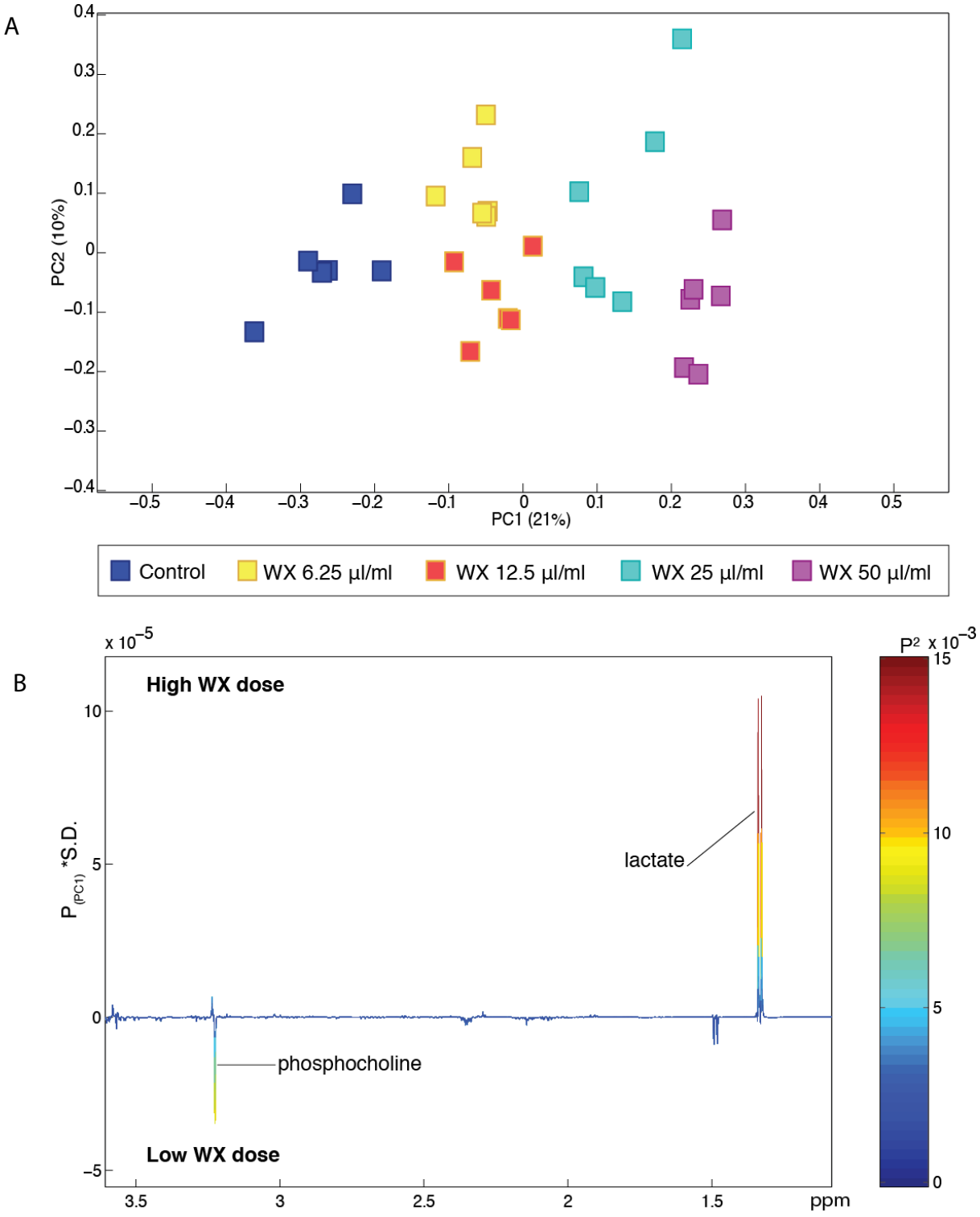

Figure 3.6 (A) PCA scores plot of the MCF-10A cells treated with increasing concentrations of the watercress extract for 24 hours. (B) PCA loadings plot of PC1.

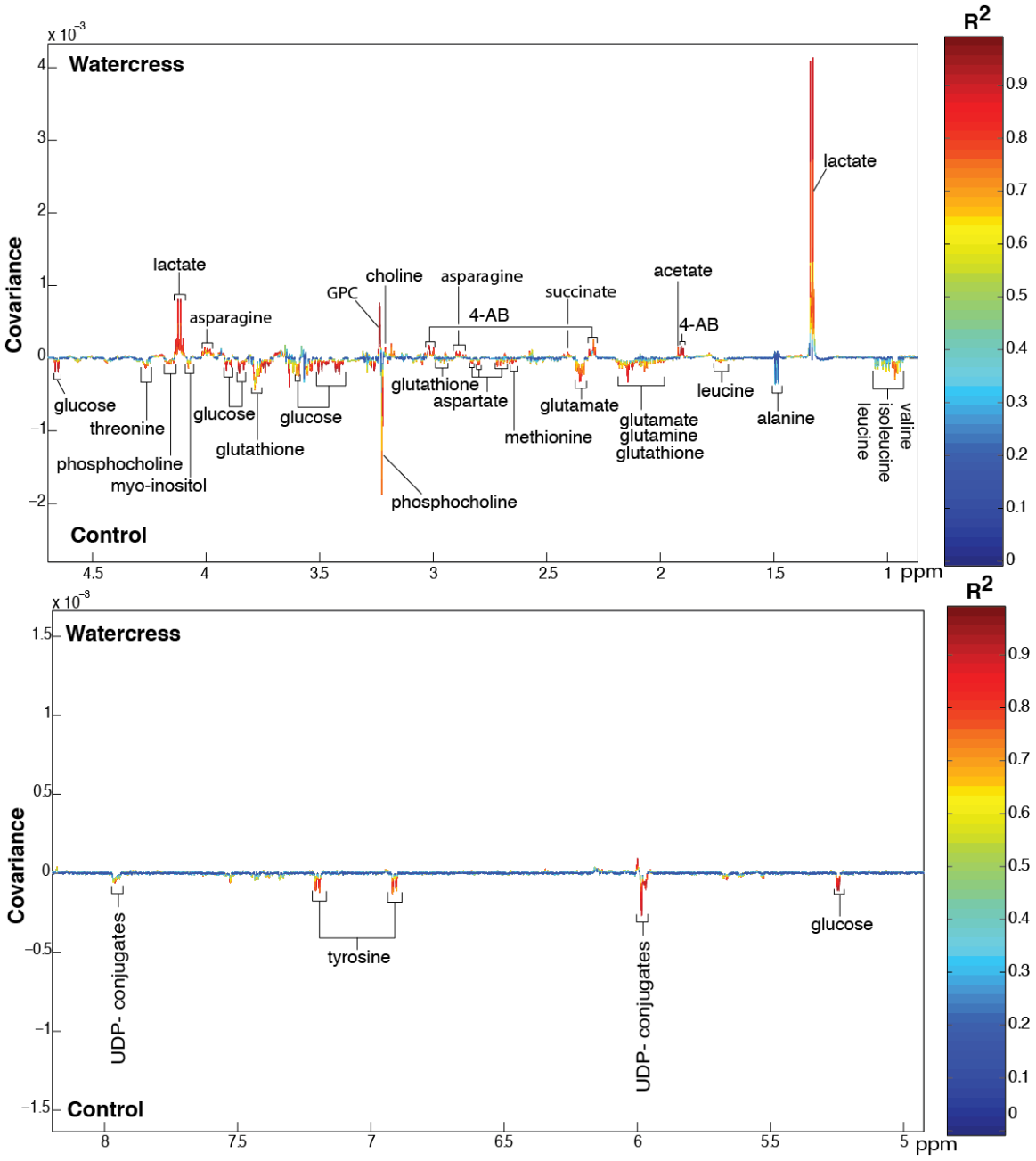

Figure 3.7 OPLS-DA coefficients plot comparing the metabolic profiles of untreated control MCF-10A cells and WX (50 µl/ml) treated cells. GPC, glycerophosphocholine, 4-AB, 4-aminobutyrate.

5.1.13 Metabolic profiling with increasing doses of PEITC

5.1.14 MCF-7

PCA of untreated and increasing PEITC dose data from MCF-7 cells revealed separation in the first principal component based on the PEITC dose representing 42% of the variance in the dataset (Fig. 3.8A). PCA demonstrated a metabolic trajectory between low and high doses of PEITC driven by lower phosphocholine in the high dose samples compared to the control and low dose samples (Fig. 3.8B).

OPLS-DA models were constructed for a pair-wise evaluation of the effect of the four PEITC dose treatments compared to control treatment in the MCF-7 cells. Valid models with good predictive ability ($Q^2\hat{Y}$) were returned for the comparisons between control and treated MCF-7 cells (Table 3.1). PEITC treatment induced a strong perturbation in the biochemical signature of these cells in a dose dependent manner. Following the high dose exposure to PEITC lactate, valine, leucine, isoleucine, methionine and threonine, glutamate and glutamine were increased compared to the control treatment and low dose samples. PEITC significantly decreased the amount of choline-related metabolites, phosphocholine and glycerophosphocholine and glycine. MCF-7 cells treated with a high PEITC dose exhibited a characteristic depletion in their glutathione content and taurine to a lesser extent (Fig. 3.9). Interestingly, PEITC appears to have a biphasic effect on glutathione, which increases with low PEITC exposure but is depleted with the high dose treatment.

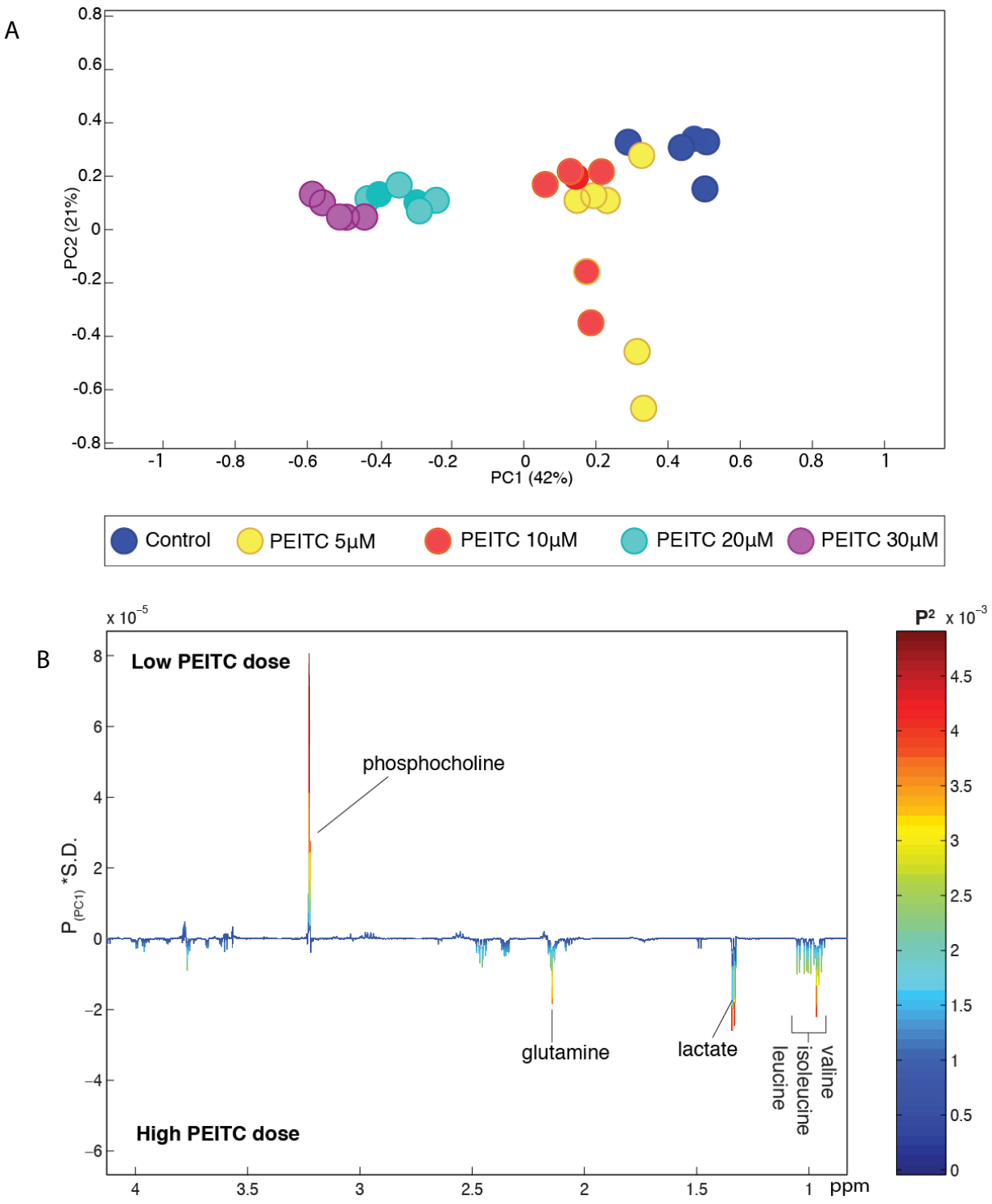

Figure 3.8 (A) PCA scores plot of the MCF-7 cells treated with increasing concentrations of PEITC for 24 hours. (B) PCA loadings plot of PC1.

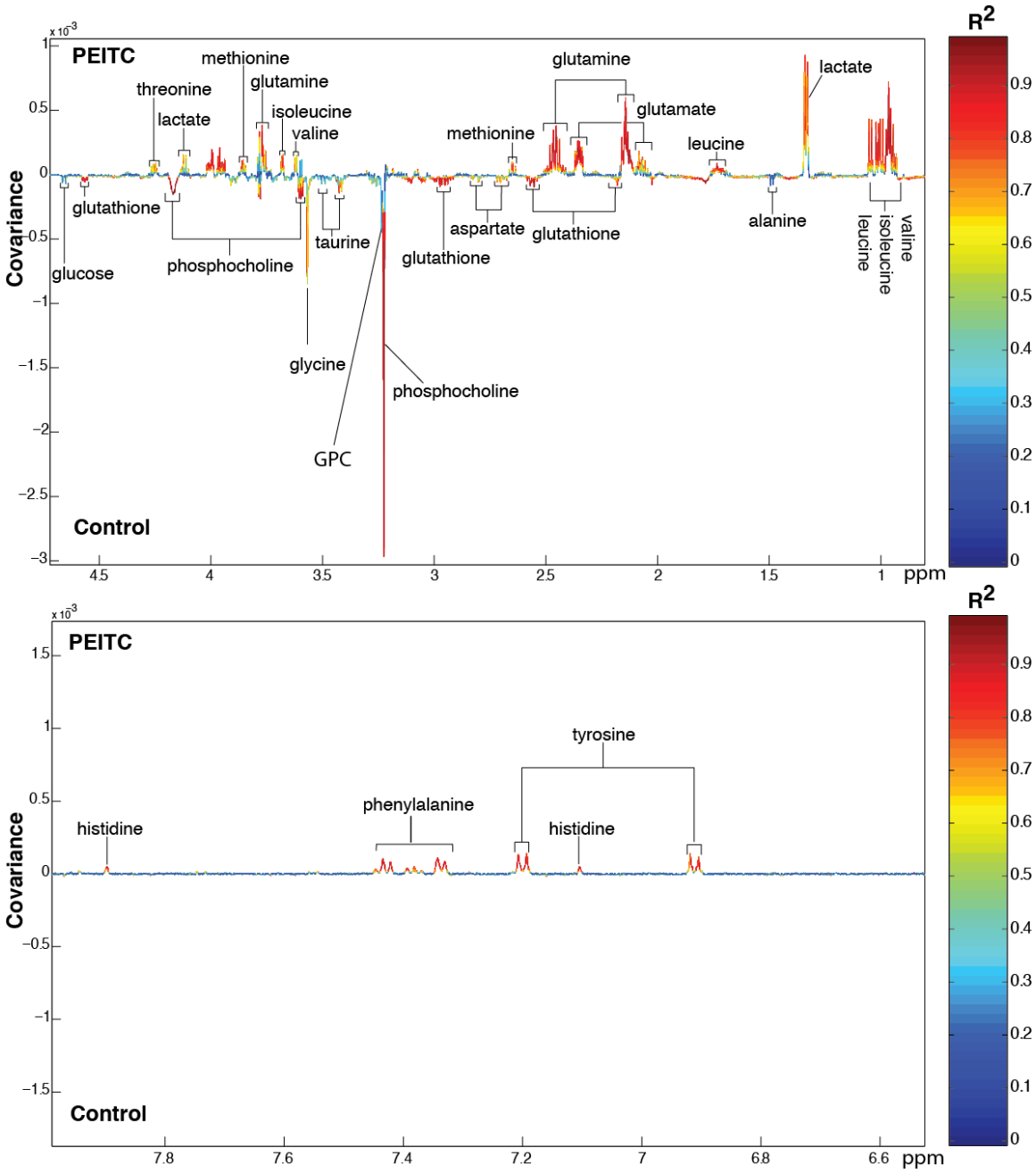

Figure 3.9 OPLS-DA coefficients plot comparing the metabolic profiles of untreated control MCF-7 cells and PEITC (30 μM) treated cells.

5.1.15 MCF-10A

The metabolic response of MCF-10A cells to PEITC was found to differ compared to that of MCF-7 cells. A dose dependent effect was observed with no discernible differences between control samples and those treated with the 5 or 10 μM of PEITC. Clustering of the cells treated with 30 μM of PEITC was observed on the first principal component (Fig. 3.10A) and was driven by decreased levels of alanine and phosphocholine in these samples (Fig. 3.10B).

Pairwise OPLS-DA models were constructed comparing the effect of the four PEITC dose treatments with the control treatment in the MCF-10A cells. The low doses of PEITC (5 and 10 μM) did not have a significant impact on the metabolic profile of the MCF-10A cells. On the contrary, the models built for the pair-wise evaluation of the effects of the two highest PEITC dose treatments were of strong predictive ability (PEITC 20μM, $Q^2Y = 0.64$, PEITC 30μM, $Q^2Y = 0.85$) and valid upon permutation testing (PEITC 20μM, $p = 0.001$, PEITC 30μM, $p = 0.001$). MCF-10A cell respond to PEITC treatment with reductions in their amino acid pool (valine, leucine, isoleucine, threonine, alanine, glutamate, glutamine, methionine) and phosphocholine and glycine abundance (Fig. 3.11). Strikingly, the higher doses of PEITC did not cause depletion in the levels of glutathione or taurine as it was the case in the MCF-7 cells but rather increased their levels.

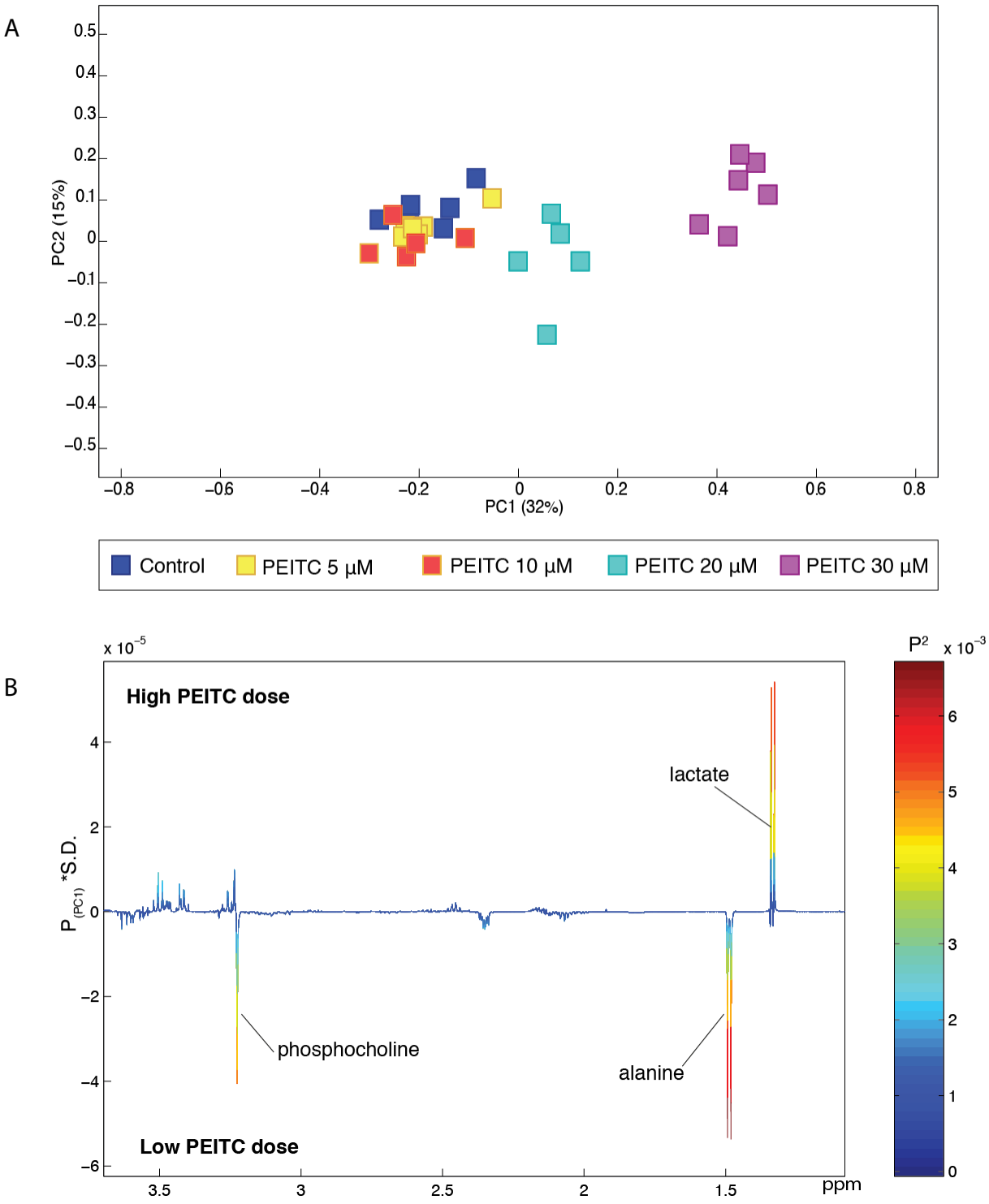

Figure 3.10 A) PCA scores plot of the MCF-10A cells treated with increasing concentrations of PEITC for 24 hours. (B) PCA loadings plot of PC1

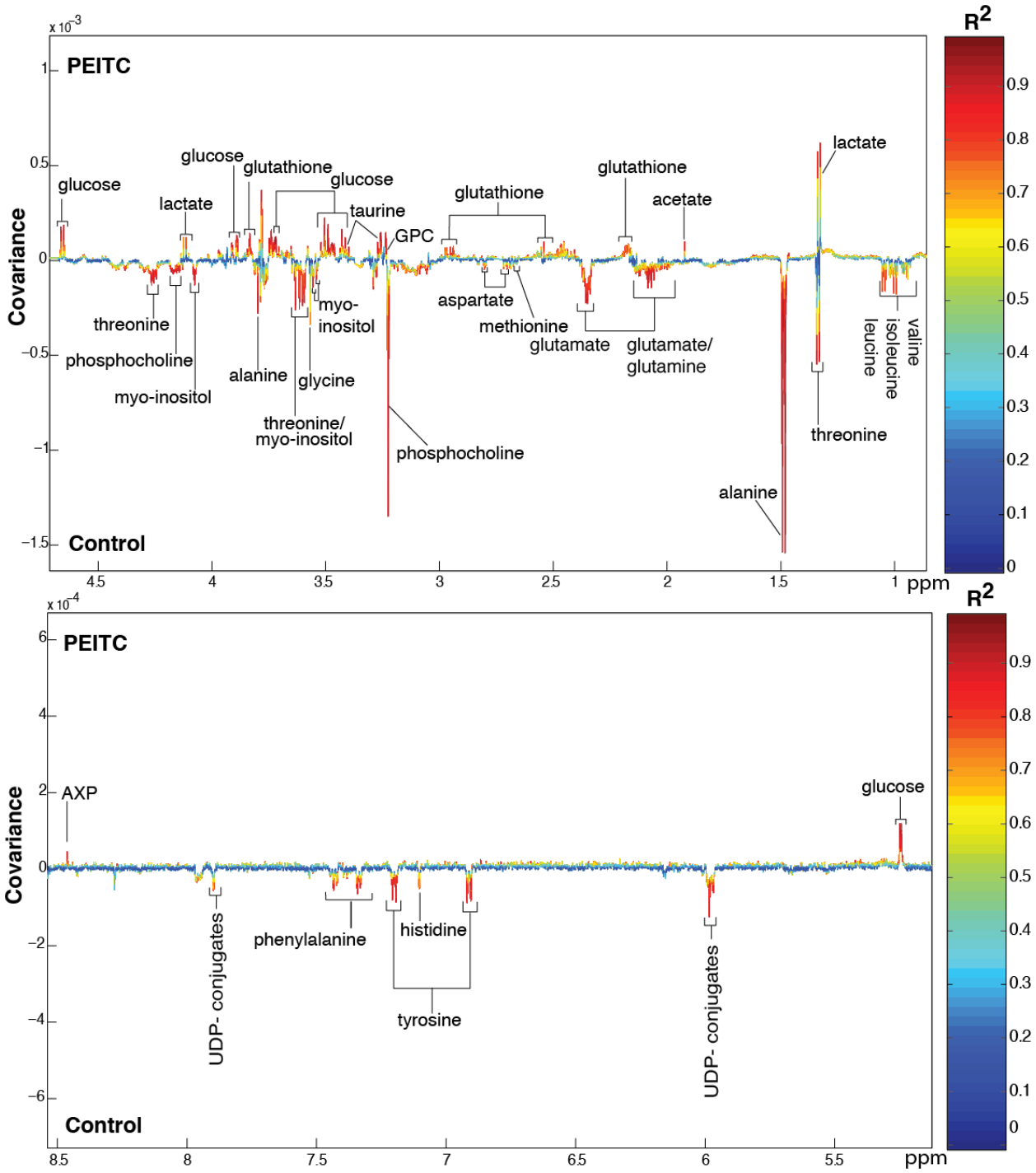

Figure 3.11 OPLS-DA coefficients plot comparing the metabolic profiles of untreated control MCF-10A cells and PEITC (30 μM) treated cells.

5.1.16 *In vitro* effects of watercress and PEITC in MCF-7 and MCF-10A cells

The metabolic alterations observed from the OPLS-DA models were used to perform unsupervised hierarchical clustering of the metabolites by integrating the corresponding peaks. The results are summarised in Fig 3.12A and Fig 3.12B. A clear metabolic separation of all treatments and doses was observed in the MCF-7 cells but the response of the MCF-10A cells to the different treatments was varied and characterised by some overlap. No observable effects of the low PEITC doses were noted in the MCF-10A cells. MCF-7 cells respond to watercress and PEITC treatments by shifting their metabolic phenotype in an anti-parallel manner. Metabolites like glutathione, aspartate, glycine, phosphocholine and alanine are significantly lower in the MCF-7 cells treated with the higher doses of PEITC but are found in higher levels in the watercress treated cells. In addition, amino acids (threonine, glutamine, methionine, tyrosine, phenylalanine, leucine, isoleucine, valine and histidine) are characteristically elevated in the PEITC treated MCF-7 cells whereas their levels are lower in the watercress treated groups. Comparing the metabolic profiles of the two treated cell lines reveals significant differences in the response of cancer and non-transformed cells upon watercress and PEITC exposure with a more uniform response in the MCF-7 cells.

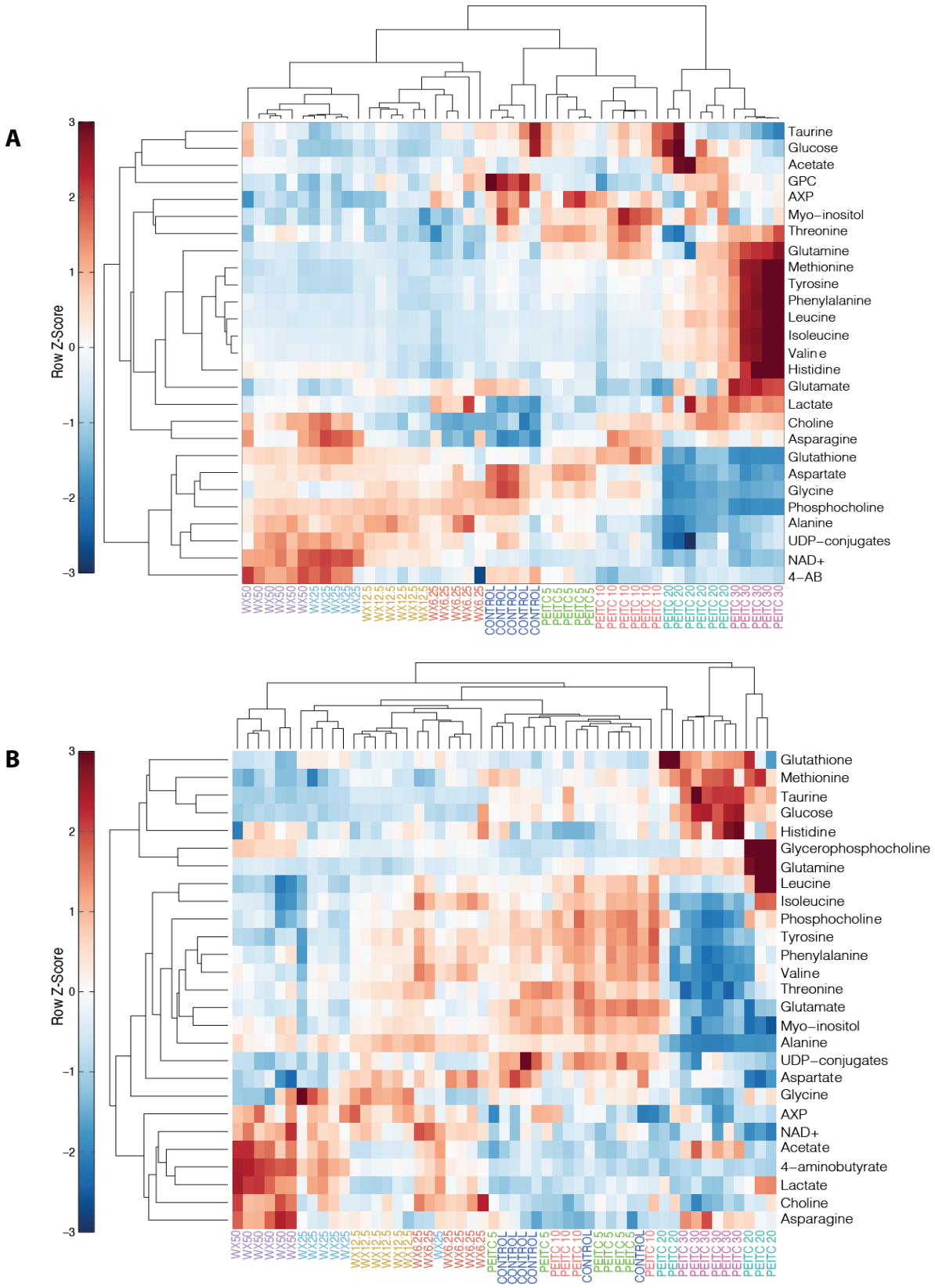

Figure 3.12 Unsupervised hierarchical clustering heat-map of metabolites from MCF-7 (A) and MCF-10A (B) cells treated with watercress extract or PEITC at increasing concentrations. Each row represents a metabolite and each column represents a sample. The row Z-score

(scaled expression value) of each metabolite is plotted in red-blue colour. The red colour indicates metabolites that are high in abundance and blue indicates metabolites low in abundance

5.1.17 Cell cycle analysis

Propidium iodide staining was used to assess the impact of watercress extract and PEITC on the cell cycle distribution of MCF-7 and MCF-10A cells.

At the basal level, untreated MCF-7 cells had 10% greater cell distribution in the S phase and 8% in the G2 phase as compared to untreated MCF-10A cells. In MCF-7 cells (Fig. 3.13) watercress (50 µl/ml) caused a significant 11% reduction in the G1 phase and a parallel increase in the proportion of the cells in the S phase. PEITC induced a cell cycle arrest at the G1 phase only at the highest doses (20 and 30 µM) with concomitant decrease in the proportion of cells in the S phase.

A similar effect of the watercress extract was observed with the MCF-10A cells with an 8% reduction of cells in the G1 phase and a 4% increase of cells in the S phase (50 µl/ml). In contrast, PEITC did not induce a cell cycle arrest at the G1 stage as observed in the MCF-7 cells. PEITC caused a significant increase in the percentage of cells in the S and G2 phase and a concomitant decrease of the cells in the G1 phase only at the two highest doses.

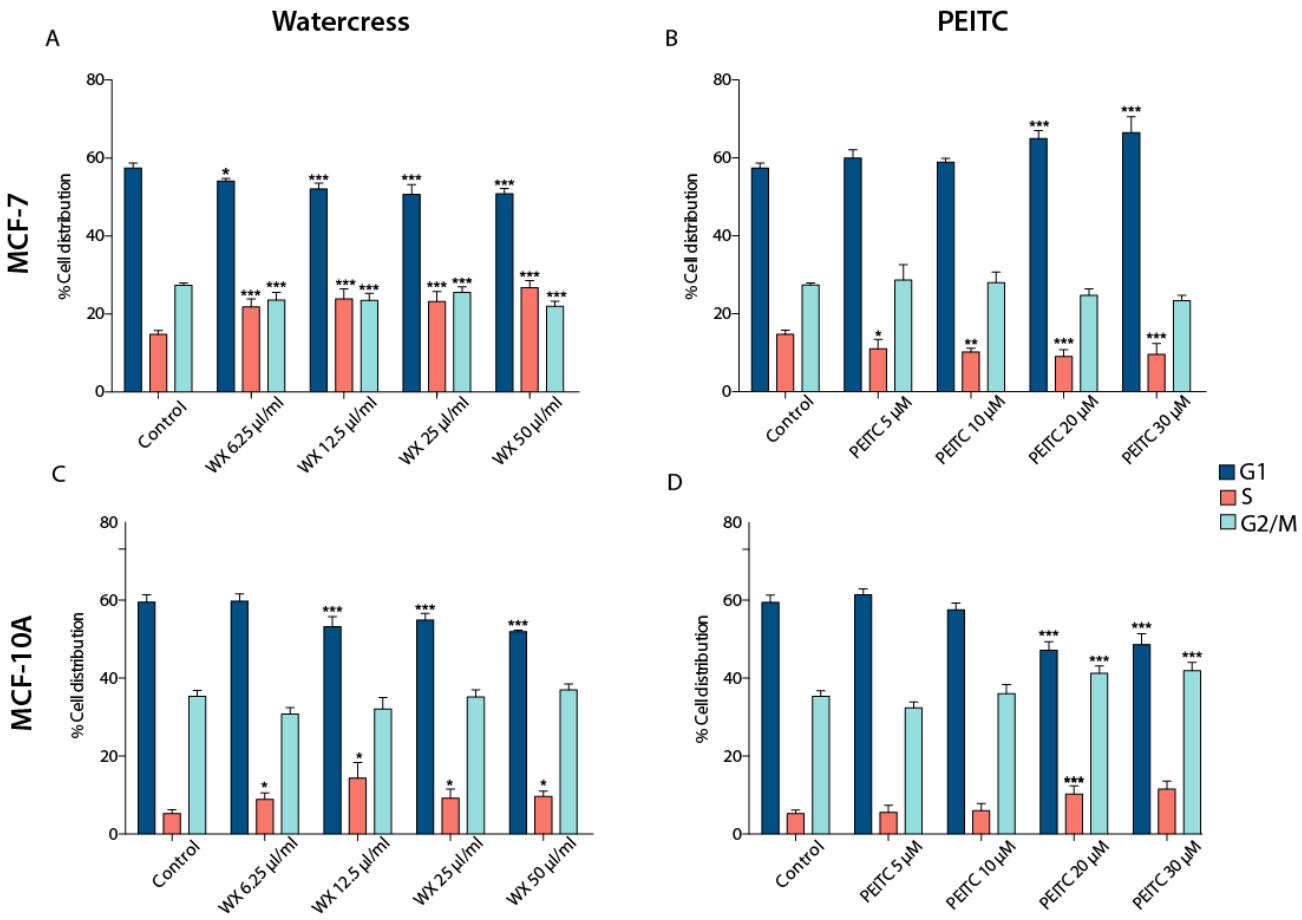

Figure 3.13 Cell cycle analysis of MCF-7 (A&B) and MCF-10A (C&D) exposed to a range of crude watercress extracts (0-50 µl/ml) and PEITC (0-30µM) for 24 hours.

Data presented as mean ± SEM percentage cell survival. Statistically significant differences between control and treated cells are indicated *p<0.05, **p<0.01, ***p<0.001 after one-way ANOVA followed by Dunnett's multiple comparison test. Data shown represent the average of three independent experiments with three replicates per sample. WX, watercress.

5.1.18 DNA oxidative damage

MCF-10A cells possessed slightly lower basal DNA damage (8.8 ± 1.4%) compared to MCF-7 cells (13.6 ± 1.6%) (Fig.3.14). Crude watercress extract did not induce any significant genotoxic effects in either cell line at any of the concentrations tested. PEITC on the other hand was genotoxic in both cell lines at 20 and 30 µM with significantly increased % tail DNA. In MCF-7 cells PEITC 20 µM and 30 µM caused 14.1% and 19.2% additional damage

respectively. In MCF-10A cells the same treatments induced a further 4.7% and 8.2% damage respectively.

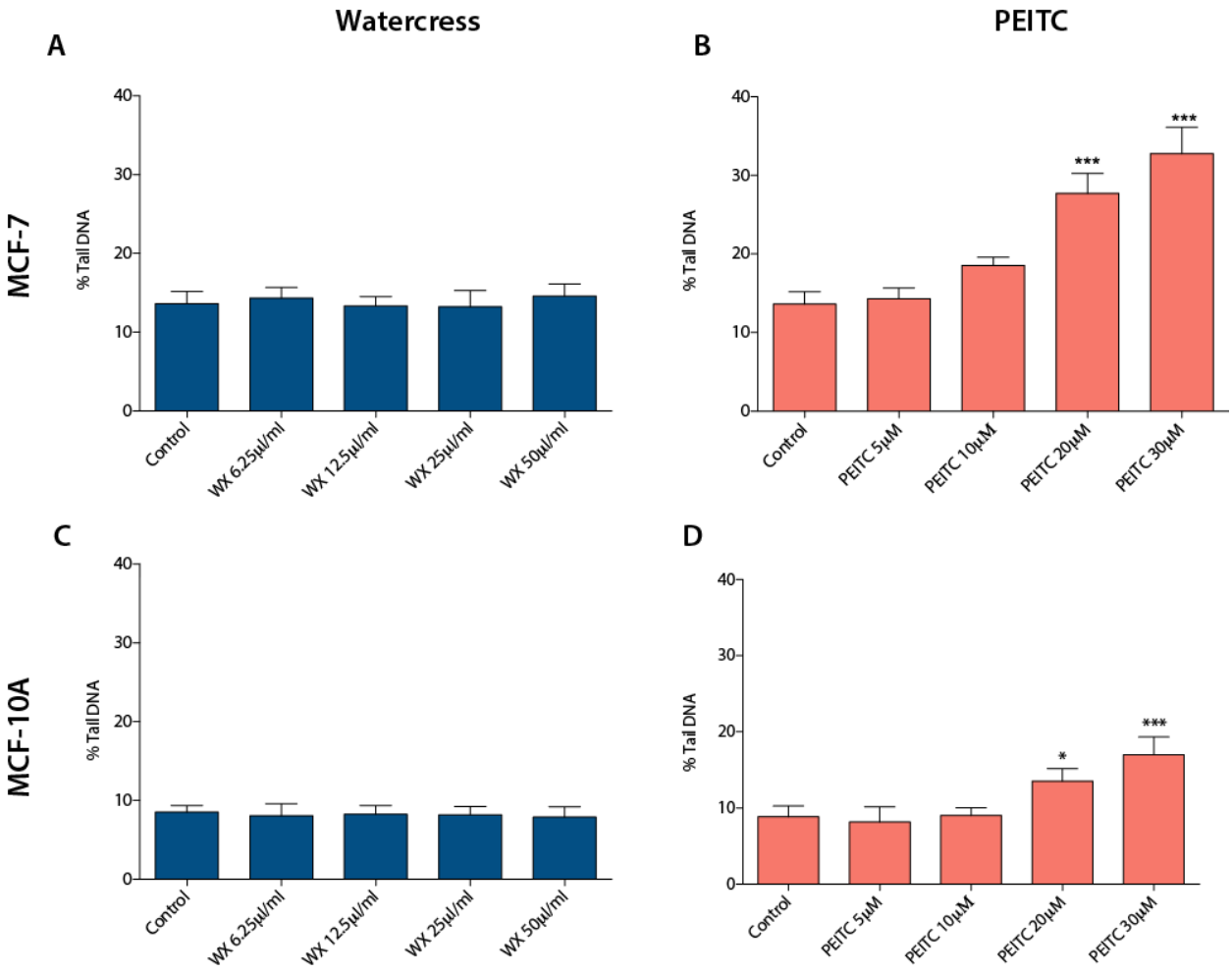

Figure 3.14 Genotoxic effects of the crude watercress extract and PEITC on MCF-7 (A&B) and MCF-10A (C&D) cells after a 24-hour incubation.

Data presented as mean ± SEM percentage cell survival. Statistically significant differences between control and treated cells are indicated *p<0.05, **p<0.01, ***p<0.001 after one-way ANOVA followed by Dunnett's multiple comparison test. Data shown represent the average of three independent experiments with three replicates per sample. WX, watercress.

5.1.19 Mitochondrial membrane potential

The impact of increasing doses of the crude watercress extract and PEITC on the mitochondrial membrane potential was assessed by fluorescent JC-10. Crude watercress extract did not affect the membrane potential of MCF-10A cells but induced significant increase in the polarisation of the mitochondrial membrane of MCF-7 cells (Fig.3.15). A remarkable loss of mitochondrial membrane potential was observed in the PEITC treated groups with the polarisation increasing by 148% in the highest PEITC dose in MCF-7 cells. MCF-10A cells were more resistant to the lower doses of PEITC but showed 65% and 115% increase in polarisation in the two high PEITC doses respectively.

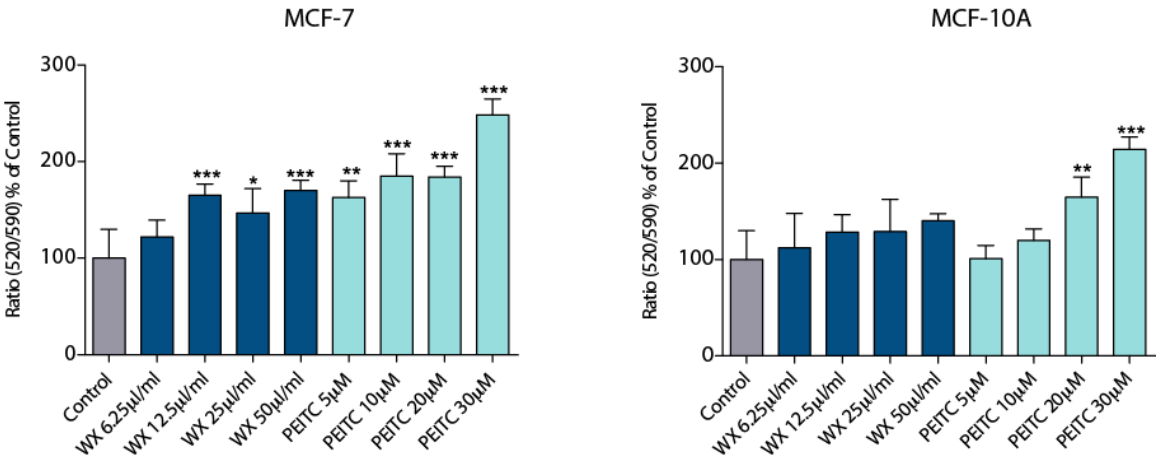

Figure 3.15 Impact of PEITC and the crude watercress extract on the mitochondrial membrane potential of MCF-7 and MCF-10A cells as evaluated by increased JC-10 monomer/aggregate ratio (520/590 nm).

Data presented as mean ± SEM percentage cell survival. Statistically significant differences between control and treated cells are indicated *p<0.05, **p<0.01, ***p<0.001 after one-way ANOVA followed by Dunnett's multiple comparison test. Data shown represent the average of three independent experiments with three replicates per sample. WX, watercress.

3.4 Discussion

Crude watercress extract and PEITC induced a range of phenotypic changes in cell behaviour both in MCF-7 and MCF-10A cells. PEITC G1 cell cycle arrest in MCF-7 cells was accompanied by significant decreases in cell proliferation as well as elevated DNA damage in this cell line. DNA damage can lead to the activation of the tumour suppressor p53, which can then induce the expression of p21 that then binds to G1/S cyclin-dependent kinases (Cdk) inhibiting their activity and arresting the cells in the G1 phase [100]. PEITC was also shown to cause loss of the mitochondrial membrane potential in agreement with other studies [111, 117], which is considered the trigger for further downstream events in the apoptotic cascade. Crude watercress extract caused an accumulation of cells in the S phase of the cell cycle in MCF-7 cells. Our results are corroborated by those of Boyd *et al*. [53] who also observed cell cycle delay in the S phase of HT-29 cells treated with a watercress extract. Watercress is known to inhibit Cdk gene expression preventing the cells from progressing through the cell cycle. The watercress extract also caused minor decreases in cell proliferation and mitochondrial potential without however having a genotoxic effect in either cell line. MCF-10A cells were highly resistant to any watercress driven phenotypic changes in cell progression and also less sensitive to the genotoxic PEITC effects. It should be noted though that the high dose of PEITC is cytotoxic to MCF-10A cells, suggesting a hormetic role for this ICT.

^{1}H-NMR spectroscopy based metabonomics was successfully applied to tumorigenic MCF-7 and non-tumorigenic MCF-10A breast cells to examine the fundamental differences in their metabolic phenotype. The biochemical impact of crude watercress extract and PEITC was then examined on these two cell lines. To our knowledge this is the first study looking at

the comparative metabolic responses of these cell lines to bioactive compounds of nutritional importance.

Metabolic phenotype of MCF7 and MCF-10A

Through basal metabolic profiling it was possible to differentiate between the cancerous MCF-7 cell line and the non-transformed MCF-10A cell line. As expected the cancerous MCF-7 cell line appeared to be more reliant on glycolysis for energy generation as indicated by the higher content of lactate. Similarly, greater amounts of phosphocholine were measured in the MCF-7 cells, relative to the non-transformed cells. This may be an adaptation to the higher cell proliferation rate and the demand for the synthesis of new cellular membranes, and it may be coupled to sparing of fatty acids in a glycolytic cellular environment.

MCF-7 cells also contained higher levels of glutamine. Glutamine is interchangeable with glutamate and alpha glutarate in the TCA cycle, which may be redundant in these cells, it also acts as a precursor in the biosynthesis of nucleotides and as an amino acid for protein synthesis. Higher amounts of the antioxidants glutathione and taurine were also observed in the MCF-7 cells. These compounds serve as antioxidants and their increased abundance facilitates the maintenance of appropriate cellular redox status by keeping the amount of ROS at a level that enables cell proliferation and survival.

Glutathione

The MCF-7 breast cancer cells exhibited non-linear but dose-dependent changes in glutathione concentrations in response to watercress and PEITC treatments. PEITC appears to induce a biphasic response in the glutathione abundance of MCF-7 cells, with increased concentrations at low doses and depletion at the two higher doses. The ability of isothiocyanates to act as both pro-oxidants and indirect antioxidants may explain the dose-

dependent fluctuations in cellular glutathione content. Prolonged exposure to low isothiocyanate concentrations can induce phase II enzymes, which regulate antioxidant gene expression [56] potentially explaining the increase in glutathione observed in the MCF-7 cells treated with the lower doses of PEITC. PEITC effectively depletes cells of glutathione by continued intracellular conjugation and efflux hence disabling the glutathione antioxidant system [60, 165]. Glutathione depletion accompanied by compromised mitochondrial function ultimately results in excessive oxidative stress, as demonstrated by the increased levels of DNA damage with higher PEITC exposure and this may help explain the observed cell cycle arrest and cell cytotoxicity in the PEITC treated MCF-7 cells. Interestingly, PEITC did not deplete MCF-10A cells of glutathione and these cells were also less sensitive to PEITC induced DNA damage. PEITC has previously been shown to selectively kill cancer cells with lower antioxidant status over non-tumorigenic cell lines [116, 172, 173]

Glutathione increased in MCF-7 cells with increasing concentrations of the watercress extract. This is likely to be a result of the complex mixture of compounds in the watercress extract such as phenolics and flavonoids with proven antioxidant properties. Flavonoids increase the expression of γ-glutamylcysteine synthetase, which is directly proportional to elevated glutathione levels [174]. Watercress is also a rich source of folate [75] which can be used in one-carbon metabolism pathway, adding to the cellular glutathione pool.

Energy status, glycolysis and mitochondrial function

The ''Warburg effect'' is a well established metabolic phenotype observed in cancer cells. It postulates that tumour cells generate ATP through enhanced glycolysis rather than oxidative phosphorylation, characterised by higher lactate as seen here in MCF-7 cells, even when oxygen is not a limiting factor and although they possess the functional properties to

maintain oxidative phosphorylation. As a result the majority of the glucose is converted to lactate via glycolysis, providing a rapid source of ATP. However, this is a far less efficient process in terms of ATP molecules produced per mol of glucose input.

Results from the mitochondrial membrane potential assay indicate that the watercress extract and PEITC significantly compromise mitochondrial function. Oxidative phosphorylation can therefore no longer occur in the mitochondria resulting in cellular energy depletion. Up-regulated glycolysis, evidenced by increased lactate levels, is an essential adaptation to cope with the limited capacity for ATP generation through oxidative phosphorylation. Pyruvate dehydrogenase (PDH) kinase is inhibited by increasing concentrations of ROS, which may increase as a result of the observed glutathione depletion [175]. PDH kinase catalyses the conversion of pyruvate to acetyl-coA dictating the rate at which the TCA cycle occurs and its inhibition may therefore favour lactate production [175].

One-carbon metabolism

Significant decreases in glycine were observed in MCF-7 cells treated with the higher concentrations of both the PEITC and the watercress extract. Rapidly dividing cells rely heavily on the maintenance of their biosynthetic potential as well as redox status for survival. Continuous shuttling of carbon molecules in the one-carbon metabolism pathway, which has a central role in cell proliferation and cancer progression, ensures the availability of the building blocks necessary for the construction of new cellular components. This also sustains the formation of reducing power compounds for redox balance. Upon conversion from serine, glycine enters the glycine cleavage system and fuels the folate cycle of the one-carbon metabolic network. Following a series of reduction and methylation reactions, the folate cycle is coupled to the methionine cycle. The two interconnected cycles constitute one-carbon

metabolism, the product of which is a multitude of compounds for synthesis of macromolecules like proteins, lipids and nucleotides necessary for cell growth [176].

Glycine has a multifaceted role in cancer cell proliferation and survival. It is involved in purine and nucleotide biosynthesis, which forms the basis of DNA synthesis and repair that is a central metabolic feature of cell proliferation. Data from a mathematical modelling study in 60 cell lines (NCI60 panel) suggest that glycine metabolism is positively correlated with increased proliferation rates and provides further evidence on its role in purine, ATP and NADPH synthesis [177]. Consequently, reductions in glycine content with PEITC treatment is consistent with impaired cell survival observed in our results.

Cellular redox balance is also regulated by glycine/one-carbon metabolism via glutathione synthesis and maintenance of $NADP^+$/NADPH ratio. Therefore, glutathione depletion by PEITC can be a combined result of both conjugation followed by extracellular transport of glutathione as well as a consequence of reduced synthesis of this antioxidant due to lack of glycine uptake and conversion.

Antagonising glycine uptake and its mitochondrial biosynthesis in HeLa cells and in a range of other cells resulted in compromised proliferation by prolongation of the G1 phase of the cell cycle without any observed effect on protein synthesis, consistent with a defect in nucleotide synthesis through one carbon metabolism [178]. Consistently, in our study, PEITC caused a significant cell cycle prolongation in the G1 phase of the MCF-7 cells suggesting that glycine reductions are likely to be contributing to this effect.

Threonine and methionine also have an important role in one-carbon metabolism. Interestingly the higher doses of PEITC increase the abundance of these amino acids in MCF-7 cells but not in the MCF10A cells. Threonine, apart from serine, acts as a glycine precursor and

is introduced into the one-carbon metabolism pathway via the glycine cleavage system [179]. Methionine *per se* is necessary for protein synthesis, but adenylation of methionine gives rise to S-adenosylmethionine (SAM), which in turn acts as a methyl donor in a number of metabolic pathways as well as reactions that produce phospholipid head groups for new cell membrane composition [176]. SAM is also involved in glutathione synthesis through transsulfuration reactions.

Accumulation of these amino acids in the PEITC treated MCF-7 cells is suggestive of a blockage in one-carbon metabolism pathway resulting in the inability of these cells to maintain their needs in macromolecules necessary for proliferation.

Collectively, these observations provide novel evidence for the impact of PEITC and watercress in negatively regulating one-carbon metabolism, further substantiating their role as anti-cancer agents.

Lipid metabolism and inflammation

A prominent target of the crude watercress extract and of PEITC is lipid and phospholipid metabolism. Major shifts were observed in both cell lines upon treatments involving choline, phosphocholine and glycerophosphocholine. Phosphocholine is a major constituent of cell membranes therefore reduced levels of phosphocholine are directly related to loss of cell membrane homeostasis and compromised cell proliferation and viability. Elevated phosphocholine levels are positively correlated with the expression of COX-2 enzyme, which is a pro-inflammatory marker [180]. PEITC has been shown to down regulate the expression and activity of COX-2 [171], which is associated with the inactivation of NF-κB. It is plausible that reduced phosphocholine observed here reflects COX-2 inhibition as part of an anti-

inflammatory phenotype in cancer cells. The role of choline metabolism in cancer is highly complex and merits further investigation both in *in vitro* and *in vivo* models.

Amino acid metabolism

PEITC and watercress strongly interact with the metabolism of amino acids in both cell lines. PEITC at the higher doses, but not watercress, induced a strikingly selective increase in the pool of amino acids in MCF-7 cells, but not in the MCF-10A cells, including branched chain amino acids (valine, leucine, isoleucine) and glutamine.

Glutamine and protein translation

Glutamine together with glucose represents the two molecules that appear to be the most important for cellular metabolic needs. Catabolism of glutamine supplies the cells with carbon, nitrogen, energy molecules and reducing equivalents to sustain cancer cell growth and proliferation. In the process of glutaminolysis, glutamine is converted to glutamate by the action of glutaminase enzymes. Glutamate can then be directly converted to glutathione by the enzyme glutathione cysteine ligase (GCL), which in turn regulates the cellular redox status. Glutaminolysis can also yield substrates to refuel the TCA cycle. These anaplerotic reactions maintain the carbon levels needed for the TCA cycle to preserve its function as a biosynthetic 'hub' [22]. Increases in the amino acid levels of the cells treated with watercress and PEITC suggest that they are not being used for maintaining TCA function which ultimately results in energy depletion and cease in proliferation.

Glutamine is an essential amino acid for biosynthesis establishes and is a key component for the protein translational requirements of cancer cells. mTORC1 is master regulator of translation, which is inhibited by PEITC [95, 181] but is positively regulated by the abundance of glutamine. It is therefore unlikely that PEITC exhibits its inhibitory effects on

mTORC1 via glutamine. PEITC causes mitochondrial damage that essentially increases the AMP/ATP ratio due to energy depletion, which in turn activates AMPK. AMPK acts upstream of mTORC1, ultimately inactivating it and suppressing translation. MCF-10A cells have a lower basal mTORC1 activity as compared to the MCF-7 cells [182] suggesting that PEITC has a stronger affinity for cells with increased rates of translation.

3.5 Conclusions

^{1}H-NMR metabonomics has been successfully applied in profiling and distinguishing between tumorigenic and non-transformed cells as well as mapping the responses of MCF-7 and MCF-10A breast cells to PEITC and crude watercress extract. Our results suggest that the most prominent metabolic targets of the two treatments include glutathione metabolism, energy metabolism as well as phospholipid and amino acid metabolism. Metabolic biomarkers identified in this study provide further evidence on the biphasic impact that PEITC has on the oxidative status on breast cancer cells and that the observed effects are distinct between malignant and normal cells. Watercress and PEITC can induce significant changes in the cancer cell metabonome accompanied by genotoxic effects such as cell cycle arrest, mitochondrial damage and oxidative stress. Collectively, these can potentially result in increased sensitivity to radiation and DNA damaging chemotherapeutic drugs.

4 Sensitisation of human breast cell lines to ionising radiation by phenethyl isothiocyanate and watercress extract

Hypothesis

It is hypothesised that phenethyl isothiocyanate (PEITC) sensitises cancer (MCF-7) cells, but not healthy (MCF-10A) cells, to ionising radiation (IR) and that watercress extract protects healthy cells from IR induced collateral damage while enhancing the deleterious effects of IR in cancer cells.

Aims

- Examine the combined effect of PEITC or watercress pre-treatment with IR on physiological parameters of cell function and genotoxicity
- Characterise the metabolic response of MCF-7 and MCF-10A cell lines to IR.
- Investigate how the metabolic profile of the MCF-7 and MCF-10A cells mediated by IR exposure following pre-treatment with PEITC or with watercress

Objectives

- MCF-7 and MCF-10A cells will be exposed to X-ray IR and DNA damage levels will be measured using the Comet assay, and cell cycle progression will be assessed using flow cytometry.
- ^{1}H NMR metabonomics and multivariate statistics will be used to define the metabolic variation between cell type, PEITC or watercress pre-treatment and IR.

4.1 Introduction

Breast cancer represents a leading cause of cancer related mortalities globally. Nearly 250,000 new breast cancer cases are projected to occur solely in the United States in 2016 accounting for over 40,000 deaths [183]. In the United Kingdom (UK), breast cancer is the most common type of cancer in women, with nearly 53,700 new cases in 2013 and a one in eight estimated lifetime risk of diagnosis (Cancer Research UK, 2016). Radiotherapy is a primary treatment modality for many breast cancer patients and it aims to damage cellular DNA. Fractionated delivery of high-energy X-ray beams generates within the targeted tissue highly reactive free radicals, which cause DNA damage via lipid peroxidation or oxidative cellular respiration. Radiation-induced damage activates several signal transduction pathways whose primary role is to detect genomic injury leading to cell cycle arrest, where DNA is repaired or, in occasions of substantial damage, endogenous apoptotic machinery of cells is triggered to inhibit further replication of the damaged DNA [184]. Radiotherapy is indisputably a positive intervention [14] however as its primary mode of action is the killing of cancer cells to prevent replication, other non-cancerous cells can be affected as well. Therapeutic selectivity is therefore a vital issue in cancer therapy, and essentially an ideal anticancer agent should be toxic to cancerous cells but exert minimum toxicity in healthy cells.

Dietary isothiocyanates have been widely studied for their anti-cancer role as well as their ability to act as radiosensitisers and radioprotective agents. Benzyl isothiocyanate sensitises human pancreatic cancer cells to X-ray irradiation by inducing apoptosis [185] and allyl isothiocyanate exerts synergistic effects with IR against lung cancer cells [186]. Sulforaphane, a broccoli derived isothiocyanate, has been shown to mitigate genotoxicity induced by γ-radiation in human lymphocytes *in vitro* [187].

PEITC has been extensively shown to have direct anti-cancer effects in *in vitro* cancer models. It possesses genotoxic properties causing cell cycle arrest and mitochondrial damage in a wide variety of cell lines and it is a potent inducer of apoptosis [99, 102, 108, 188]. Combined treatment of cancer cells with PEITC along with established chemotherapeutic agents such as cisplatin and doxorubicin potentiates their cancer-killing properties [189, 190] providing preliminary evidence for the use of PEITC as an adjuvant treatment during radiotherapy in breast cancer patients. PEITC, due to its highly electrophilic nature reacts with cellular thiols via thiocarbamoylation. After its cellular uptake it also reacts with glutathione (GSH), the major intracellular antioxidant, depleting cells of their GSH content and impacting cell survival [60, 108, 165]. As radiotherapy works primarily by inducing DNA damage through the formation of free radicals, the ability of PEITC to deplete the radical scavenger GSH is likely to contribute to its radiosensitising properties.

Epidemiological studies suggest a link between the consumption of Brassica vegetables, which are the main dietary source of isothiocyanates, and a reduced risk for many types of cancers [160] including breast cancer [161, 162]. Watercress is the main dietary source of PEITC as well as a rich source of other phytochemicals such as carotenoids and flavonols, and it has been shown to have anti-cancer properties by inhibiting initiation, proliferation and metastasis *in vitro* [53, 58, 164].

We previously showed that PEITC and watercress are potent modulators of the cellular metabolic landscape and can affect cellular physiology (Chapter 3). In this study we examined the DNA damage response, cell cycle arrest and the metabolic impact of PEITC or watercress extract combined with X-ray irradiation exposure on cancerous and non-transformed breast cells.

4.2 Materials and methods

4.2.1 Cell Culture

The MCF-7 human breast adenocarcinoma cell line was used as a breast cancer model. The cells were purchased from the American Type Culture Collection (ATCC) (LGC standards, Middlesex, UK). Cells were cultured in Dulbecco's Modified Eagle's Medium (DMEM; Lonza Group Ltd, Basel, Switzerland) supplemented with 10% (v/v) foetal bovine serum (FBS; Lonza Group Ltd), 2mM glutamine (Thermo Fisher Scientific, Loughborough, UK), 50 U/ml penicillin and 50 U/ml streptomycin (Thermo Fisher Scientific, Loughborough, UK) and 1% non-essential amino acids (Sigma-Aldrich, Dorset, UK).

The MCF-10A is a non-tumorigenic breast epithelial cell line used as a model of typical breast function. The cells were kindly donated by Prof. Graham Packham (University of Southampton, Southampton, UK). Cells were maintained in Ham's F12:DMEM (1:1) (Lonza Group Ltd), 20 ng/ml epidermal growth factor (EGF) (PeproTech, London, UK), 0.1 µg/ml cholera toxin (Sigma-Aldrich), 10 µg/ml insulin (Invitrogen), 500 ng/ml hydrocortisone (Sigma-Aldrich), 5% horse serum (Invitrogen) and 50 U/ml penicillin and 50 U/ml streptomycin (Thermo Fisher Scientific, Loughborough, UK).

Cells were grown in an incubator at 37°C with 5% CO_2 and 95% humidity in 75 cm^2 culture flasks and were routinely passaged at approximately 70% confluency. The medium was changed every 2-3 days. For passage, cells were washed with phosphate buffer saline (PBS; Lonza Group Ltd) before adding 5ml of Trypsin-Versene® (EDTA) mixture (Lonza Group Ltd) and allowing the cells to detach for 3-5 mins for MCF-7 cells and 18-20 mins for MCF-10A cells. 5 ml of medium was then added to the cells to inactivate the trypsin and the cell

suspensions were centrifuged at 300g for 3 mins. Cell pellets were then resuspended in complete media in the flask and incubated.

4.2.2 Compounds and Extracts

4.2.2.1 Analytical grade compounds

Phenethyl isothiocyanate (PEITC) was purchased from Sigma-Aldrich (Dorset, UK). 20 mM PEITC stock solution was made up in DMSO fresh on the day of use.

4.2.2.2 Watercress extracts

Fresh watercress samples were obtained directly from Vitacress Salads Ltd. (Andover, UK). Samples were snap frozen in liquid nitrogen and stored at -80 ^{o}C. Leaves (2 g) and stems (2 g) were weighed and placed in a 20 ml syringe (BD Biosciences, Oxford, UK) that had had the plunger removed and a circular 25 mm glass microfiber filter (Whatman, Dassel, Germany) placed at the bottom. The syringe was then placed inside a 50 ml centrifuge tube without the lid and centrifuged at 2600 rpm for 30 mins at 4 ^{o}C to collect the extract. This crude watercress extract was then filtered through a 0.22 µm filter (Whatman) and used in the cultures.

4.2.3 Irradiation

MCF-7 and MCF-10A cells were plated in the respective culture plates for each experiment and next day were treated with the crude watercress or PEITC for 24 hours. At the end of the treatment period the cells were exposed to 5 Gy X-ray radiation using an orthovoltage X-ray unit (Gulmay Medical D3225, Xstrahl, UK). The irradiator was at a stable distance from the cell culture plates and the irradiator field was approximately 20 x 20 cm. The cell culture plates were placed in the centre of the irradiation field.

Following radiation treatment cells were returned in the incubator and were allowed to rest for 1 hour. The cells were then collected and used in the experiments.

4.2.4 Cell viability

Cell viability was assessed using the MTT (3-[4,5- dimethylthiazol-2-yl]-2,5-diphenyl tetrazolium bromide) based *in vitro* toxicology assay kit (Sigma-Aldrich, Dorset, UK) according to the manufacturers instructions. Briefly, $5x10^3$ MCF-7 or MCF-10A cells were seeded in 96 well plates. Cells were allowed to attach overnight and were then treated with PEITC (10, 20 µM) or the watercress extract (12.5, 50 µl/ml) for 24 hours. Three hours before the end of the treatment duration cell were irradiated and allowed to rest as described above. Two hours before the end of duration of the treatment MTT solution was added to each well equal to 10% of the culture medium volume and the cells were incubated for the remaining 2 hours. Following MTT incubation, the formazan crystals formed were dissolved in MTT solubilisation solution equal to the original culture medium volume. Plates were shaken to enhance dissolution and absorbance was measured at 570 nm and 690 nm (background absorbance)

4.2.5 Cell Cycle

Cell cycle progression was evaluated accounting for the percentage of cells in each of the phases Gap0/1 (G0/1), Synthesis (S), Gap2/mitosis (G2/M) and apoptotic cells (sub G0/1). The principle of the cell cycle analysis is based on the fluorescence intensity of the PI nuclear dye that is proportional to the DNA concentration of the cell. MCF-7 and MCF-10A cells were seeded at a $1x10^5$ cells per well in 6 well plates and incubated as required. The cells were then exposed to the watercress extract and PEITC at 12.5, 50 µl/ml and 10, 20, respectively for 24 hours and then irradiated with 5 Gy IR and allowed to rest for 1 hour. Following treatment

removal, the cells were washed with cold PBS (4°C) and harvested by trypsinisation. Cells were pelleted by centrifugation (brand) at 300g for 3 mins and the supernatant was discarded. Cells were resuspended in 200 µl of cold PBS and fixed with drop-wise addition of 70% (v/v) fresh ice-cold methanol (1 ml). The samples were then stored at -20°C until analysis.

On the day of the analysis, the samples were centrifuged at 300g for 3 mins and the supernatants were discarded. Cell pellets were then resuspended in 200 µl of PBS and 25 µl of 1 mg/ml RNAse was added to the suspensions. The samples were incubated at 37°C for 30 mins and then 2.5 µl of 400 µg/ml of PI dye was added to the cells and samples were incubated for a further 30 mins at room temperature under dark conditions. The final volume of the cell suspensions was adjusted to 600 µl with PBS. Cellular DNA content of 15,000 cells was quantified via flow cytometry. The flow cytometry analysis was performed using the FL2 channel on a BD Accuri™ C6 flow cytometer (Germany). Data analysis was facilitated using the Flow Jo software (version 7.6, Tree star Inc, Oregon, USA).

4.2.6 Comet Assay

The Comet assay is a semi-quantitative measure of DNA strand breaks in single cells. MCF-7 and MCF-10A cells were seeded in T25 cells culture flasks at a concentration of $1x10^6$ and maintained at 37°C with 5% CO_2 and 95% humidity. The cells were then exposed to the watercress extract and PEITC at 12.5, 50 µl/ml and 10, 20µM, respectively for 24 hours. Cells were then irradiated as explained above. The treatment solutions were then removed via aspiration followed by washing with PBS and detaching from the cell culture flask with trypsin. Cell suspensions were adjusted to a concentration of $1x10^6$ cells/ml.

Following the treatments, 20 µl of the cell suspensions were resuspended in 200 µl of warm low melting point agarose (LMA) (0.85% w/v) and applied 75 µl of this was dispensed on Comet Slides (Trevigen). The LMA was allowed to solidify at 4°C for 15 mins. The slides were then transferred into a staining jar, lysis buffer (2.5M NaCl, 0.1M EDTA, 0.01M Tris and 1% (v/v) Triton X – added just prior to use – pH 10) was added and the cells were allowed to lyse for 1 hour at 4°C).

Following lysis of the cells, the slides were placed in a horizontal electrophoresis tank and incubated for 20 mins in alkaline buffer (0.3M NaOH, 1mM EDTA – pH 13) at 4°C in dark conditions. Electrophoresis was carried out at 26 V, 300 mA for 30 mins at 4°C. Immediately after electrophoresis the slides were washed in neutralising buffer (0.4M Tris – pH 7.5) three times for 5 mins.

The slides were then stained with 10 µl of ethidium bromide (20 µl/ml) and DNA migration from the nucleus was visualized with a fluorescence microscope (Olympus BX51). The computer-based image analysis software, Komet 4.0 (Andor Technology, South Windsor, CT) was used to calculate the proportion of DNA that had migrated from the head to the tail of the comet (% tail DNA). The mean value from 100 randomly scored cells was taken as an index of damage for each replicate well.

4.2.7 ^{1}H NMR spectroscopy-based metabonomics

The metabolic profiles of MCF-7 and MCF-10A cells were analysed using ^{1}H NMR spectroscopy. Cells were seeded at $1x10^{5}$ cells per well into 6 well plates and treated at 80% confluency. The cells were then exposed to the watercress extract at 12.5 or 50 µl/ml of extract and PEITC at 10 or 20 µM for 24 hours and treated with IR following the method

described above. Media was transferred into eppendorf tubes and cells on the surface of the plate were washed twice using 1 ml cold (4°C) PBS and were then quenched using 1 ml of ice-cold methanol (maintained on dry ice). The cells were allowed to lyse for 2 minutes and were detached from the plate using a Starstedt cell scraper and transferred into an eppendorf tube. Methanol quenching was repeated to maximise metabolite recovery. A vacuum concentrator (SpeedVac) was used to dry down the cell suspensions before reconstitution in 80 µl of phosphate buffer (pH 7.4) in 100% deuterium oxide containing 1 mM of the internal standard, 3-(trimethylsilyl)-[2,2,3,3,-$^{2}H_4$]-propionic acid (TSP).

For every sample, a standard one-dimensional NMR spectrum was acquired using a 600 MHz Bruker NMR spectrometer, with water peak suppression using a standard pulse sequence (recycle delay (RD)-90°-t_1–90°-t_m-90°-acquire free induction decay (FID), RD= 4s, t_1=28.96 µs, t_m= 100 ms). For each spectrum 256 scans and 8 dummy scans were obtained, collected in 64K data points with a spectral width of 12.001 ppm. ^{1}H NMR spectra were manually corrected for phase and baseline distortions and referenced to the TSP singlet at δ 0.0. Spectra were digitized using an in-house MatLab (version R2012a, The Mathworks, Inc.; Natwick, MA) script. Metabolites were using an in-house database of standards and Chenomx NMR suite (version 7.7, Chenomx Inc). Multivariate modelling, including principal component analysis (PCA) and orthogonal projections to latent structures discriminant analysis (OPLS-DA), was performed on the samples using in house scripts.

4.3 Results

4.3.1 Cell viability

The impact of combined IR and PEITC or watercress treatment on cell survival was assessed using the MTT assay. At the dose applied IR decreased mean cell survival in both cell lines, although this was not statistically significant ($p>0.05$). Significant decreases in the survival of both cell lines were observed with PEITC pre-treatment prior to IR (Fig. 4.1). At 20μM of PETIC cell viability was decreased by 86 % in MCF-7 ($p<0.01$) and 66 % in MCF-10A ($p<0.05$) relative to IR alone. 10 μM of PEITC did not affect MCF-10A cell viability. Exposure to the watercress prior to IR did not have an impact on cell viability in MFC-10A cells compared to irradiated cells. Combined exposure to both doses of watercress and IR resulted in significant decrease in cell viability of MCF-7 cells when compared to the non-irradiated controls ($p<0.01$).

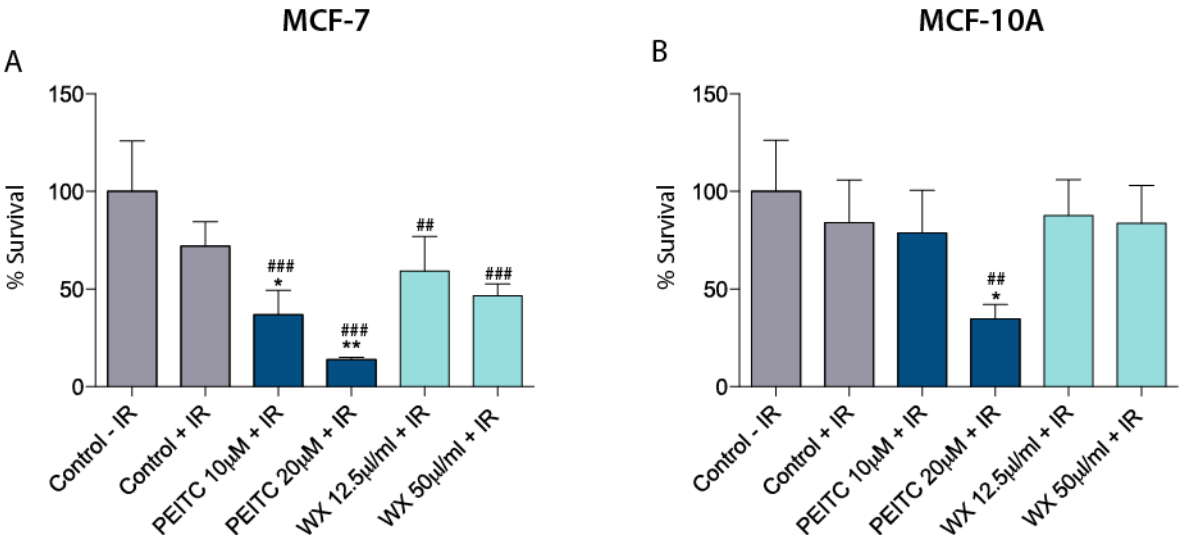

Figure 4.1 Effect of PEITC and watercress extract (WX) pretreatment (24 hours) combined with 5 Gy of IR on MCF-7 (A) and MCF-10A (B) cell viability.

Statistically significant differences between groups are indicated as follows: ##$p<0.01$, ###$p<0.01$ for comparisons to 'Control – IR' *$p<0.05$, **$p<0.01$ for comparisons to 'Control+IR' after one-way ANOVA followed by Dunnett's multiple comparison test. Data shown represent

the average of three independent experiments with three replicates per sample. WX, watercress.

4.3.2 Cell cycle analysis

Cell cycle kinetics were assessed using propidium iodide staining; the MCF-7 cultures had a much higher number of cells in S-phase than was observed with the MCF-10A cells, this is consistent with a higher proliferative capacity for the cancer cell line. The response to a 5 Gy IR dose also differed; in the MCF-7 cells there was an accumulation of cells in G2 arrest coupled to a decrease in the number of cells in S phase. In contrast the MCF-10A cells responded to IR by increasing the proportion of cells in the G1 phase of the cell cycle (~6%) (Fig. 4.2B) coupled to an 11% reduction in the percentage of cells in G2.

Pre-treatment of MCF-7 and MCF-10A cells with the watercress extract or with PEITC differentially sensitised cells to a subsequent dose of 5 Gy IR, (Fig. 4.2A and 4.2B). In the MCF-7 cells pre-treatment with PEITC (20 μM) led to a further reduction in the number of irradiated cells in S-phase, and an accumulation of irradiated cells in G1 cell cycle arrest with a reduction in the proportion of cells in G2 relative to non-pretreated irradiated controls. The same dose of PEITC alone caused a 7.6% increase in the proportion of the cells in G1 phase but when combined with IR the proportion increased to 18.4% (Fig. 4.2C). In the MCF-10A cells, PEITC caused a minor decrease in the proportion of the cells on the G2 phase coupled to an increase in the percentage of the cells in the S phase.

In contrast to PEITC, watercress increased the percentage of IR cells in S phase in both cell lines. In the MCF-7 cells this was coupled to a decrease in the proportion of cells in G2, whereas in the MCF-10A cells the proportion of cells in G1. These observations were not observed in non-irradiated watercress treated cells.

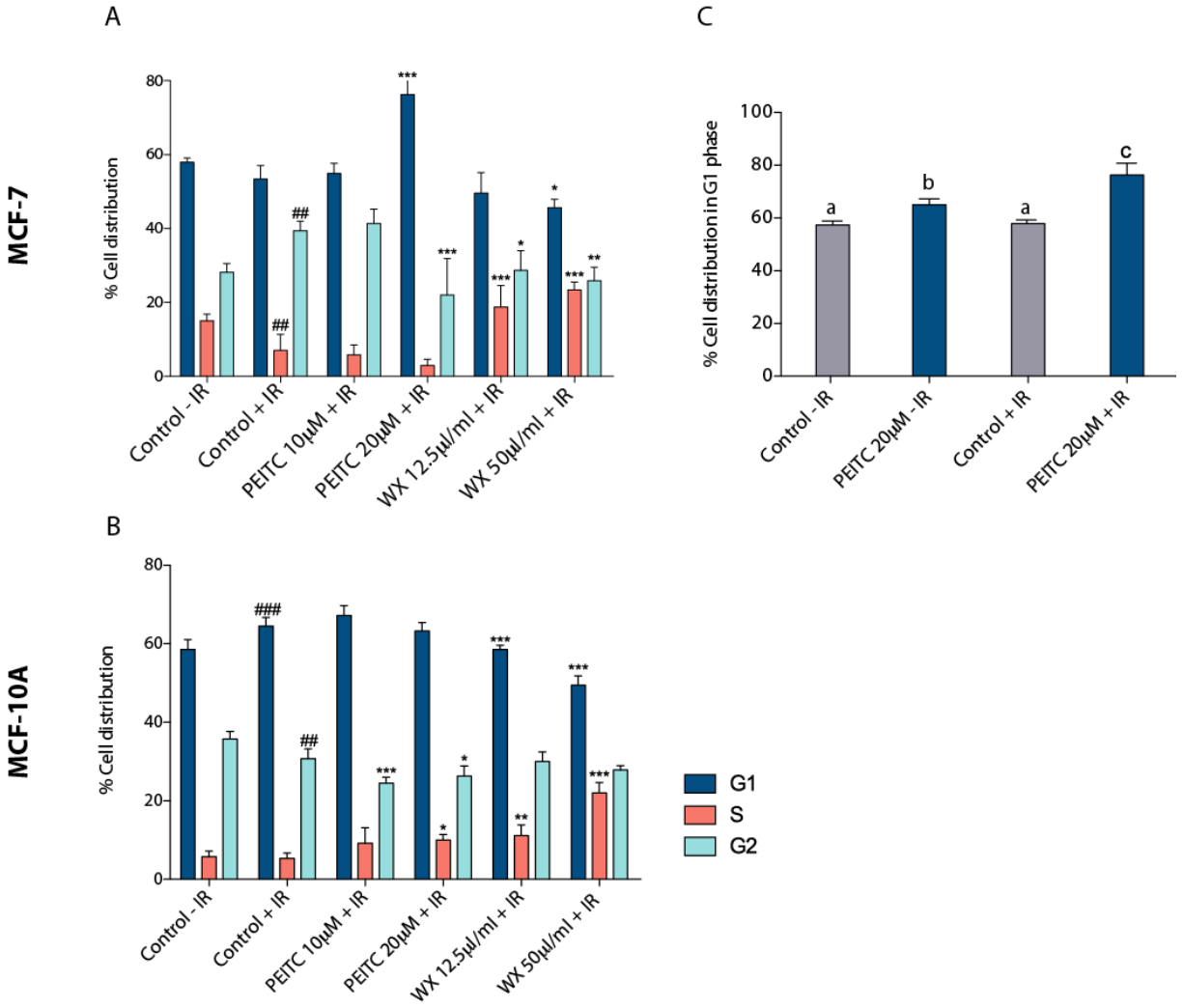

Figure 4.2 Cell cycle analysis of MCF-7 (A) and MCF-10A (B) cells exposed to 5 Gy of IR following a 24 hour pre-treatment with PEITC or crude watercress extract. Statistically significant differences between irradiated control and treated cells are indicated *p<0.05, **p<0.01, ***p<0.001 and significant differences between non-irradiated and irradiated cells are indicated ##p<0.01, ### p<0.001 after one-way ANOVA followed by Dunnett's multiple comparison test. (C) % Distribution of MCF-7 cells in G1 upon treatment with PEITC or IR. Different letters suggest statistical significance (p<0.05).

Data shown represent the average of three independent experiments + SEM with two replicates per sample. WX, watercress**.**

4.3.3 DNA oxidative damage

To further assess if the observed cell cycle arrest was a response to DNA damage, MCF-7 and MCF-10A cells were treated with PEITC and the crude watercress extract for 24 hours followed by exposure to 5 Gy of IR and DNA lesions were quantified using the Comet assay. IR induced a 39 % increase in tail DNA in MCF-7 cells and pre-treatment with 20 μM of PEITC significantly increased the damage by a further 15 % resulting in a final 66% tail DNA content (Fig. 4.3). Exposure of the MCF-7 cells to 50 μl/ml of the watercress extract also increased DNA damage levels by 7% compared to the irradiated but non-treated control cells.

MCF-10A cells exhibited sensitivity to IR but to a lesser extent than the cancerous cells. IR induced an 11% increase in tail DNA in these cells. Following a 24 hour pretreatment with 10 μM of PEITC and 50 μl/ml of watercress extract reduced the comet tail from 19.37% in the irradiated cells to 13.88% and 10.5% respectively. The highest dose of PEITC combined with 5 Gy of IR was genotoxic to the non-tumorigenic cells resulting in a final 44 % tail DNA.

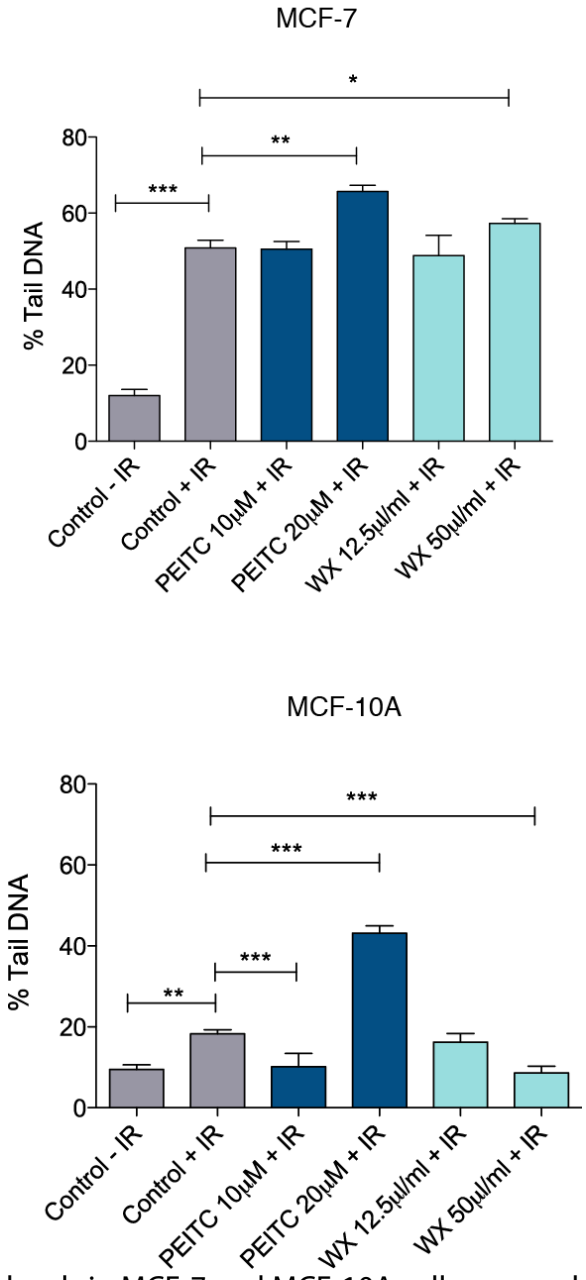

Figure 4.3 DNA damage levels in MCF-7 and MCF-10A cells exposed to 5 Gy of IR following 24 hour pre-treatment with PEITC or crude watercress extract. Statistically significant differences between groups are indicated as follows *p<0.05, **p<0.01, ***p<0.001 after one-way ANOVA followed by Dunnett's multiple comparison test.. Data shown represent the average of three independent experiments + SEM with two replicates per sample. WX, watercress.

4.3.4 Metabonomic profiling of MCF-7 and MCF-10A cells in response to IR exposure

MCF-7

Metabolic profiles were obtained from the cell extracts of MCF-7 cells exposed to 5 Gy IR and of untreated control cells. Principal component analysis (PCA) was applied to these profiles to reveal the main source of variation within the metabolic data. The scores plot obtained from the PCA model (Fig. 4.4A) showed a separation between the two groups along the first principal component, indicating that IR exposure is responsible for the largest amount of variance in the data. The loadings plot for PC1 from this model (Fig.4.4B) shows that phosphocholine and glycine explained the variation in the model being present in lower amounts in the irradiated MCF-7 cells.

An orthogonal projections to latent structures discriminant analysis (OPLS-DA) model was constructed to perform a pair-wise comparison between the untreated and irradiated cells. A valid OPLS-DA model with good predictive ability ($Q^2\hat{Y}$=0.462) was obtained and validated by permutation testing (1000 permutations; p=0.005). The metabolites associated with IR in MCF-7 cells are shown in the coefficients plot extracted from the OPLS-DA model (Fig. 4.5). Irradiated MCF-7 cells contained lower amounts of glutathione and phosphocholine as well as glutamine and glutamate, but had higher amounts of lactate, taurine and glucose compared to the non irradiated cells.

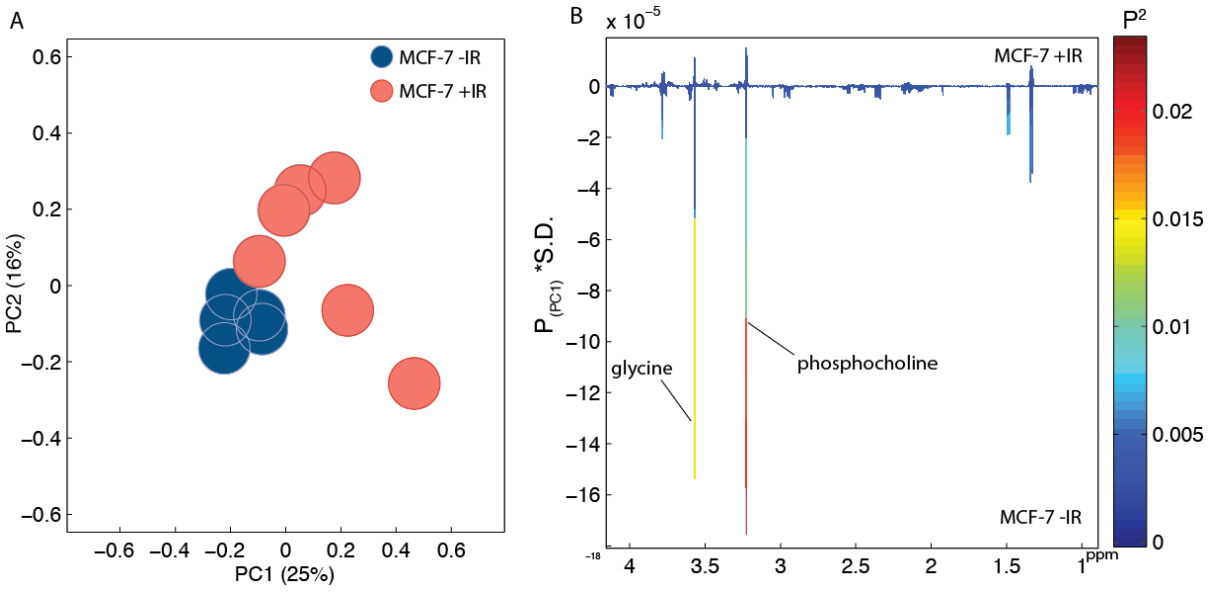

Figure 4.4 (A) PCA scores plot of MCF-7 untreated cells and cells exposed to 5 Gy IR. (B) PCA loadings plot for PC1.

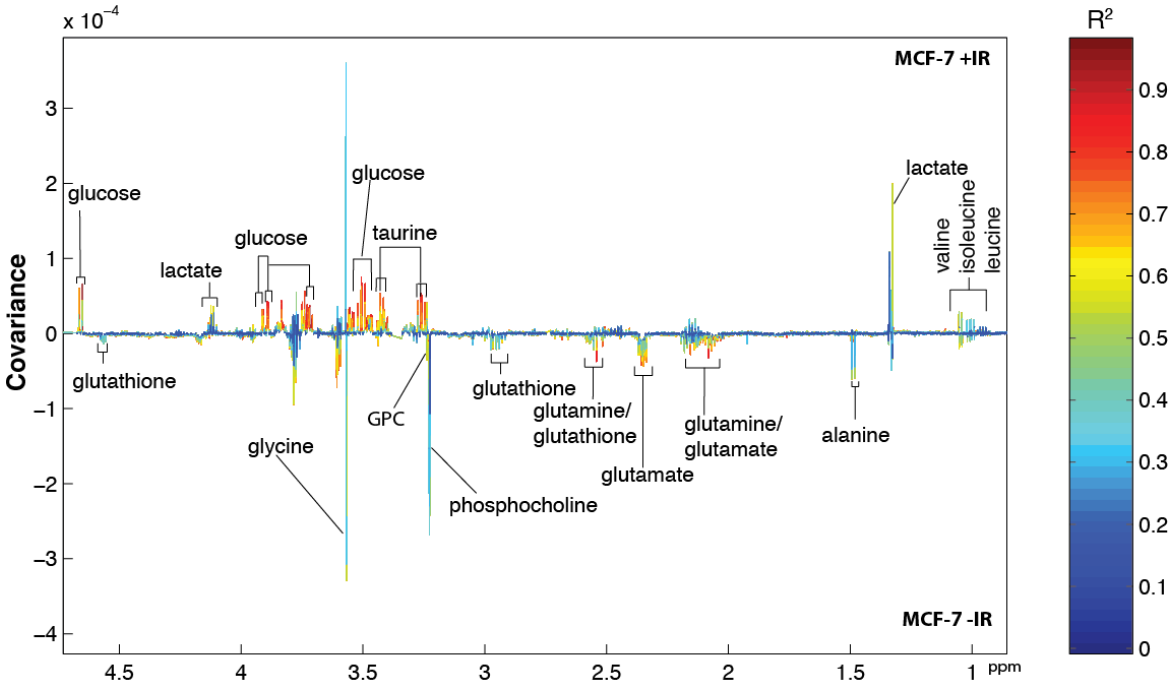

Figure 4.5 Correlation coefficients plot obtained from the OPLS-DA model identifying metabolic changes in the MCF-7 cells induced by 5 Gy of IR exposure. GPC, glycerophosphocholine

MCF-10A

Exposure of MCF-10 A cells to IR caused a uniform metabolic response in these cells, indicated by the tight clustering in the PCA scores plot (Fig. 4.6A). Clear separation can be seen in the first principal component, which explains 47% of the total variation within the data. In contrast to the MCF-7 cells, irradiated MCF-10A cells had higher amounts of phosphocholine (Fig. 4.6B).

An OPLS-DA model with strong predictive ability ($Q^2\hat{Y}$=0.87) and valid upon permutation testing (p=0.001) was constructed to probe for the discriminating features between non-irradiated and irradiated MCF-10A cells (Fig. 4.7). The non-tumorigenic cells response to irradiation exposure is characterised by an increase in glutathione, this is in stark contrast to the irradiated cancer cells. Irradiation treatment also causes increases in the lactate, phosphocholine and amino acid (valine, isoleucine, leucine, alanine, threonine) content of these cells.

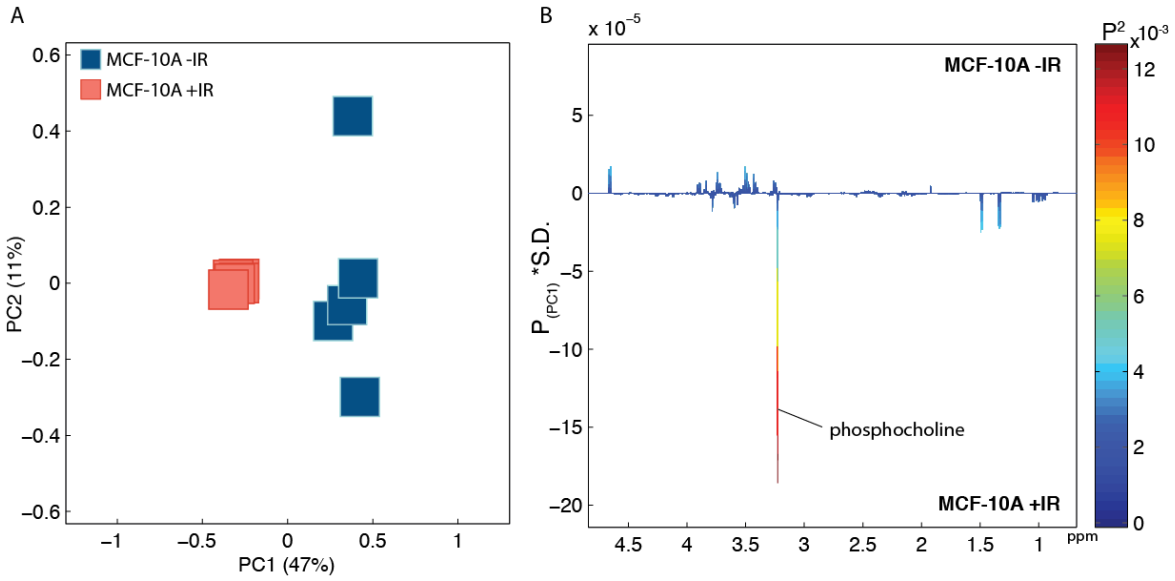

Figure 4.6 (A) PCA scores plot of MCF-10A untreated cells and cells exposed to 5 Gy IR. (B) PCA loadings plot for PC1.

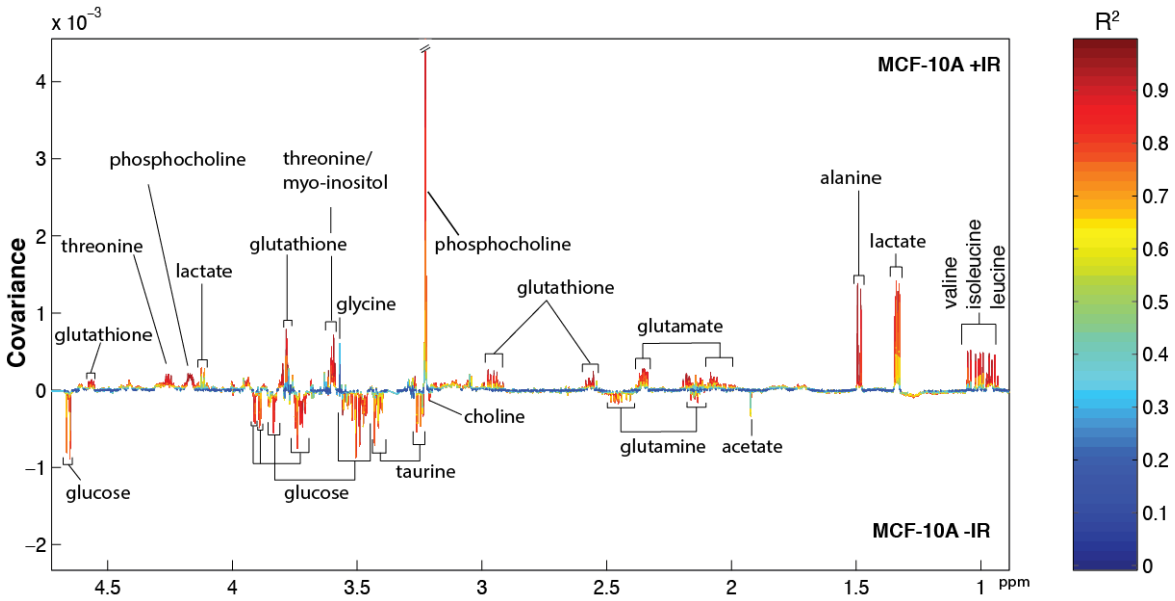

Figure 4.7 OPLS-DA model constructed on the metabolic profiles of cell extracts obtained from control and irradiated (5 Gy IR exposure) MCF-10A cells. GPC, glycerophosphocholine

4.3.5 Comparative metabolic impact of IR in MCF-7 and MCF-10A cells

Comparing the metabolic profiles of irradiated MCF-7 and MCF-10A cells returned a significant OPLS-DA model ($Q^2\hat{Y}$=0.895, p= 0.001) (Fig. S1-appendix). Following irradiation the metabolic differences between the cell types were consistent with the differences observed pre-treatment with higher levels of lactate, alanine, glutamine, and glycine in the irradiated MCF-7 cells compared to irradiated MCF-10A cells. The major difference, as observed in the metabolic associations (correlation coefficients) summarised in Fig. 4.8, lies in the glutathione shifts between the two cell lines. At baseline, MCF-7 cells contained higher amounts of glutathione compared to MCF-10A cells however, post IR this was reversed with MCF-10A cells containing significantly higher glutathione. In addition, MCF-10A cells had significantly lower amounts of phosphocholine pre-IR compared to MCF-7 cells, but this difference was no longer significant post IR suggesting a higher phosphocholine utilisation rate by the non-tumorigenic cell line upon IR exposure.

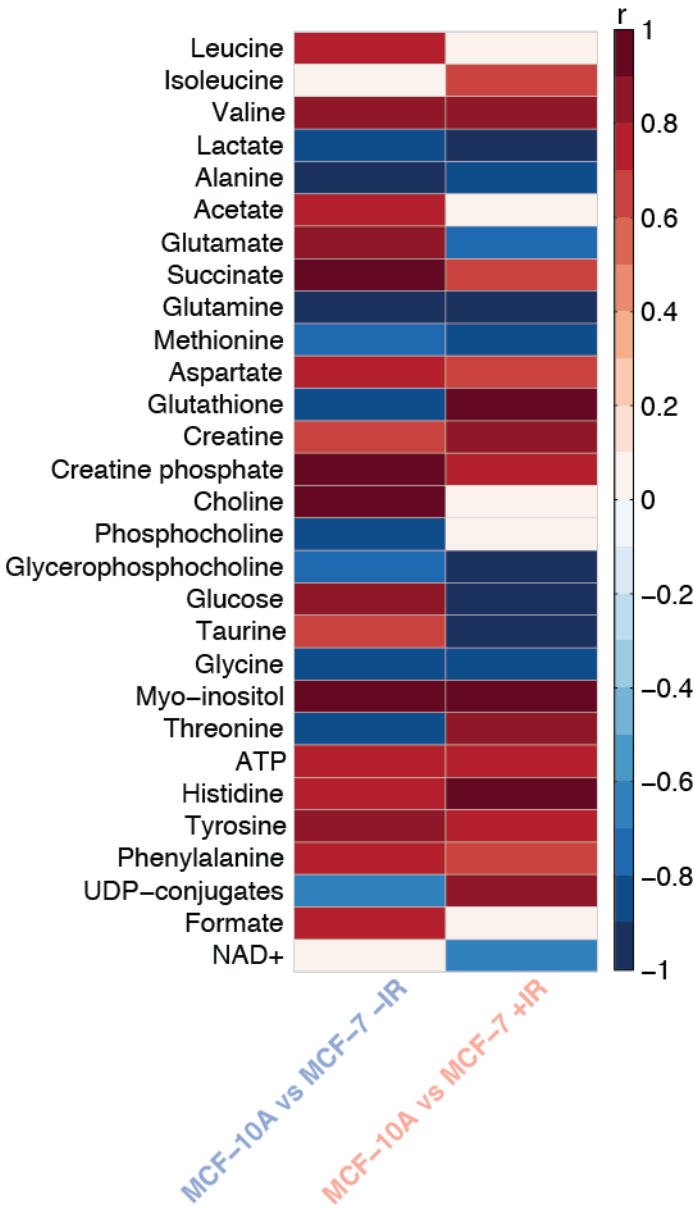

Figure 4.8 Summary of the significant metabolic alterations identified from the OPLS-DA models comparing metabolic profiles of MCF-7 and MCF-10A cells with (+IR) and without (-IR) radiation exposure (*n* = 5-6). Colours indicate the correlation coefficient (r) extracted from the OPLS-DA model. Red indicates metabolites that are present in higher amounts in MCF-10A cells and blue indicates metabolites that are present in lower amounts in MCF-10A cells compared to MCF-7 cells.

4.3.6 Metabolic perturbations induced by IR combined with PEITC or watercress extract pre-treatment

Valid OPLS-DA models with good predictive ability ($Q^2\hat{Y}$) were returned for all the pair-wise comparisons between irradiated MCF-7 and MCF-10A cells pre-treated with the different PEITC and watercress extract concentrations (Table 4.1). The metabolic associations between cell type and treatment and how these associations change after exposure to IR are presented in Fig. 4.9.

Table 4.1 Summary of the OPLS-DA models returned for the comparisons between irradiated control cells against cells treated with the watercress extract (12.5 or 50 µl/ml) and PEITC (10 or 20 µM) for 24 hours from both MCF-7 and MCF-10A cells.

Treatment	$R^2\hat{Y}$	$Q^2\hat{Y}$	P-value
MCF-7			
Control + IR vs WX 12.5 µl/ml	0.9650	0.6166	0.001
Control + IR vs WX 50 µl/ml	0.9749	0.6806	0.001
Control + IR vs PEITC 10µM	0.9614	0.8218	0.001
Control + IR vs PEITC 20µM	0.9410	0.6577	0.001
MCF-10A			
Control + IR vs WX 12.5 µl/ml	0.9589	0.6869	0.003
Control + IR vs WX 50 µl/ml	0.9949	0.6136	0.001
Control + IR vs PEITC 10µM	0.9259	0.7119	0.001
Control + IR vs PEITC 20µM	0.9735	0.9497	0.001

The most striking observation of the impact of the pre-treatment with PEITC or the watercress extract followed by IR, was the shift in glutathione levels in both cell lines.

We previously observed a biphasic response of MCF-7 to PEITC doses with regards to glutathione. Low PEITC exposure (10 µM) increased the glutathione content of these cells but

was depleted by the high PEITC dose (20 μM). This effect of PEITC in MCF-7 cells was the same after exposure to IR. Interestingly, in MCF-10A cells, PEITC increased glutathione at both low and high doses, but glutathione was significantly decreased after exposure of the PEITC pre-treated cells to IR.

Crude watercress extract treament alone, caused an increase in glutathione in MCF-7 cells and this effect persisted following IR. In contrast, a reduction in GSH was seen in MCF-10A cells following watercress treatment but was elevated when the watercress treatment was followed by IR.

A great range of metabolic associations established during the pre-treatment of both cell lines with watercress extract and PEITC remained largely unchanged following exposure of the cells to IR including shifts in lactate, choline, taurine, glycine, UDP-conjugates as well as changes in cellular amino acid pools (Fig. 4.10). It should also be noted, that the metabolic signature of the MCF-10A cells pre-treated with the high PEITC dose (20 μM) combined with IR, is suggestive of a metabolic shut-down in these cells, with the majority of the metabolites being depleted.

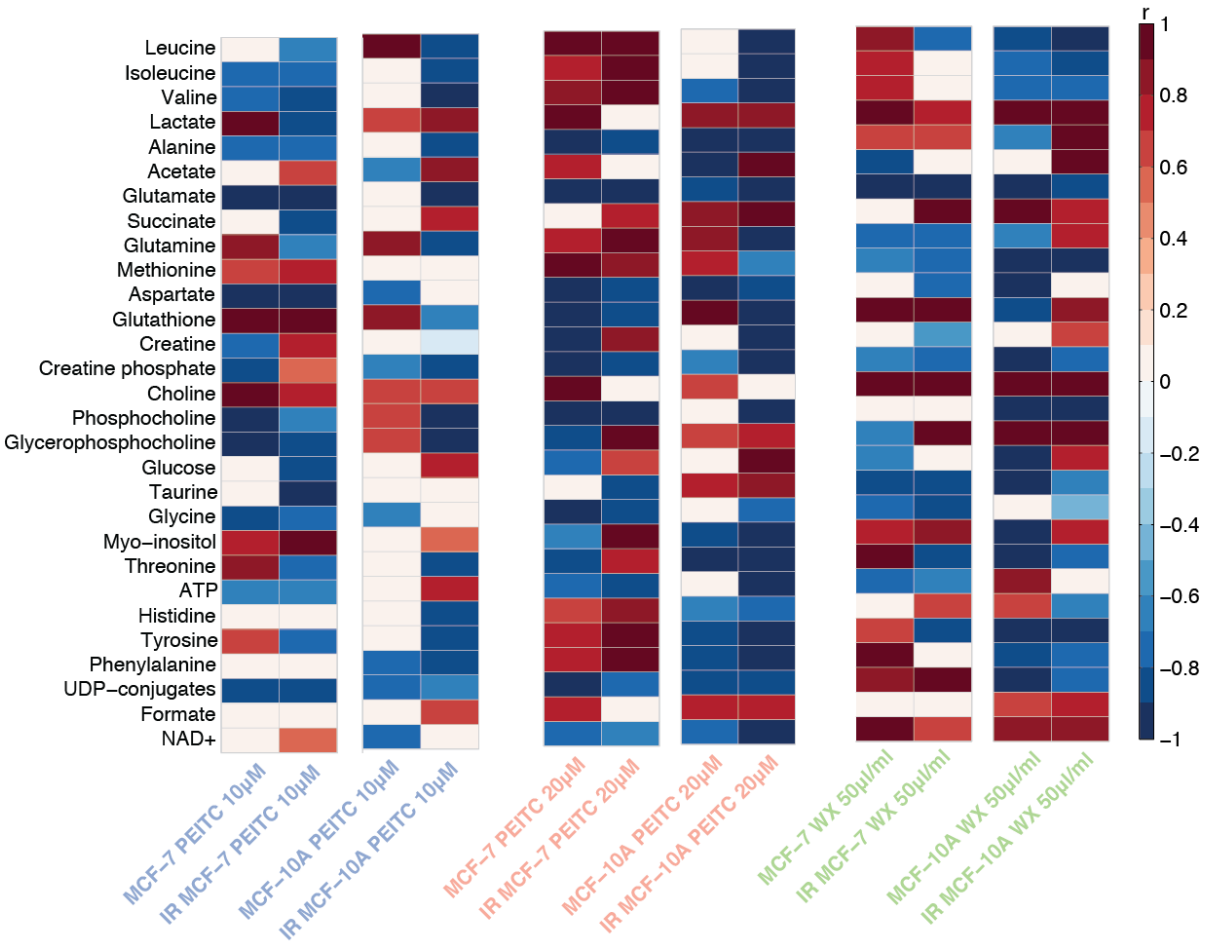

Figure 4.9 Summary of the metabolites associated with the OPLS-DA models given by the correlation coefficient (r) with the response variable, in this case PEITC or watercress (WX) treatment and IR (n = 5-6) in comparison to non-irradiated control or irradiated control cells. The red colour indicates metabolites that are positively correlated with the respective treatment (PEITC or WX) and blue colour indicates a negative correlation between metabolites and treatment.

4.4 Discussion

Radiotherapy is an important treatment modality in breast cancer. Cancer cells posses several aberrant signalling pathways that can result in drug resistance or failure of therapeutic outcomes. Current research suggests that combination therapy can kill cancer cells more efficiently via diverse mechanisms simultaneously [191]. Isothiocyanates such as PEITC have a range of cellular targets for cancer-related outcomes [191]. This property makes PEITC and its dietary source watercress, highly desirable for combinatorial therapeutic methods, assuming it does not decrease the effectiveness of radiotherapy or enhance its negative effects on local healthy tissue.

The aim of this study was to examine the impact of PEITC and of crude watercress extract combined with IR on cancerous and non-cancerous cells. To our knowledge this is the first study examining this concept. Our observations suggest that PEITC can sensitise MCF-7 cells towards IR induced damage but can also harm MCF-10A cells to a lesser extent. The watercress extract appears to be protective in MCF-10A rescuing them from IR oxidative damage. The potential mechanism of action explaining our observations involves the ability of watercress and PEITC to interact with glutathione, modifying the anti-oxidant potential of the cell lines.

In the cancerous MCF-7 cells IR caused G2 cell cycle arrest as a result of increases in DNA damage levels but no significant impact of IR on cell survival was observed, suggesting a potential resistance of these cells to IR killing. Our results are consistent with those of Jänicke *et al.* [192] who observed the same cell cycle arrest and failure of IR to activate the mitochondrial intrinsic apoptosis pathway. Pre-treatment with PEITC results in significant G1 arrest parallel to increased DNA damage and significant compromise of cell viability. These

observed effects are likely to be mediated by the ability of PEITC to further induce p53 activity in MCF-7 cells [193] which is a potent regulator of G1 cell cycle arrest. PEITC can also induce apoptosis from the mitochondria in breast cancer cells by caspase activation as well as changes in the Bac/Bcl-2 ratio following the release of cytochrome *c*, all significant elements of the intrinsic apoptotic pathway [119].

At the biochemical level, different responses were observed in glutathione abundance following IR exposure in MCF-7 versus MCF-10A cells. Treatment of MCF-7 cells with IR resulted in intracellular glutathione depletion in agreement with other studies where important decreases in glutathione were observed in cancer cells exposed to IR [63, 194, 195]. In contrast, MCF-10A cells responded to IR induced stress by increasing their glutathione content. IR generates reactive oxygen species (ROS), which are quenched in part through the glutathione response reducing the potential of ROS to exert oxidative DNA damage. Elevations in intracellular glutathione in MCF-10A cells can be considered part of a protective response by up-regulating the metabolic anti-oxidant capacity of these cells. This may explain their ability to better recover from IR induced damage compared to MCF-7 cells, and which may explain the lower levels of DNA damage observed in the healthy cells in this study.

MCF-10A cells respond to low dose PEITC treatment (10 μM) by elevating their glutathione content. When these cells are exposed to IR and PEITC (10 μM), glutathione is depleted contrary to the cancer cells. Depleted glutathione pools suggest increased utilisation of glutathione for IR-derived ROS scavenging purposes, explaining the decreased DNA damage levels in these cells.

Pre-treatment of MCF-10A cells with the watercress extract also appeared to be protective when the cells were exposed to IR, evidenced by the reduced levels of DNA

damage. Watercress extract has been shown to possess anti-genotoxic properties in several *in vitro* models where cells have been challenged with known genotoxic agents [53, 122]. The combined treatment of MCF-10A cells with the watercress extract and IR appears to increase the glutathione content of these cells, suggestive of enhanced anti-oxidant activity and hence a protective effect. It can be argued that other anti-oxidant compounds present in watercress spare some of the glutathione in these cells.

The protective effect of watercress in healthy cells observed here is unlikely to be a result of PEITC or any other ITC since they are not present in the extract, as a result of the high volatility of these compounds as well as the snap freezing of the plant material, which inactivates the myrosinase enzyme. PEITC alone was found to be genotoxic at high concentrations in the healthy cells therefore, the anti-genotoxic effect of the watercress extract can be attributed to the great range of other phytochemical present such as phenolics and carotenoids (phytochemical profiling of watercress described in Chapter 5).

The metabolic signatures of MCF-7 cells indicate that glutathione depletion is a major target for PEITC, which can lead to the build up of intracellular ROS resulting in cell damage. Elevated ROS is a characteristic outcome of IR exposure and combined with the glutathione depleting property of PEITC can be exploited for cancer cell killing. Indeed, our results suggest that PEITC treatment can sensitise cells to IR induced damage as observed from G1 cell cycle arrest, elevated DNA damage levels and reduced cell viability. Combined treatment of MCF-7 cells with the high PEITC dose (20 μM) and IR is also characterised by sparing of glucose and reduced lactate abundance, suggesting that the rates of glycolysis are diminished. Glycolysis is the main source of energy and of biosynthetic molecules in cancer cells. Attenuated activity of this pathway further adds to the cancer killing process.

Cellular membranes are a primary target of IR due to the impact ROS can have on lipid bilayers of which phosphocholine is a main constituent. Scavenging of ROS by the higher levels of glutathione observed in MCF-10A cells can explain the apparent increase in their phosphocholine levels following IR. This may reflect the efforts to maintain cell membrane integrity, which can be violated by ROS produced as a result of IR exposure. Conversely, the MCF-7 response to IR is characterised by lower levels of phosphocholine. Phosphocholine can potentially serve as a breast cancer biomarker since higher levels of this molecule have been reported in the clinical setting in breast cancer lesions compared to benign breast cancer lesions [196-198] as well as *in vitro* in comparisons of cancerous cell with normal mammary epithelial cells [199]. Decreases in phosphocholine have been observed in tissues after chemotherapy and radiation treatment and have been correlated with positive therapy outcomes [194, 200-202].

PEITC treatment reduces phosphocholine abundance suggesting an impact on cell membrane integrity that may contribute to radiation induced cancer cell killing. However, this effect is not limited to the tumorigenic landscape. High dose of PEITC combined with IR is genotoxic to healthy cells, characterised by DNA and apparent reduced metabolic activity, providing further evidence to the hormetic behaviour of dietary isothiocyanates [203].

4.5 Conclusions

These results suggest a potential synergistic effect of PEITC and IR towards MCF-7 cell killing and radiosensitisation and that watercress extract, free of PEITC, can rescue healthy cells from collateral damage. It is postulated that glutathione has a principal role in the response of cells to IR challenge and that the inclusion of dietary watercress during RT may enhance the

outcome. Our study examined the acute effects of IR therefore future work could be performed to examine the repair mechanisms of both cell lines subjected to the treatments over time. In addition, better insight into the apoptotic pathways induced by IR combined with watercress and PEITC should be obtained.

6 Effects of domestic processing methods on the phytochemical content of watercress *(Nasturtium officinale)*

Hypothesis

It is hypothesised that common cooking methods will significantly impact the nutrient content of watercress and that the phytochemical profiles obtained will differ according to the cooking method employed.

Aims & Objectives

- The effect of boiling, microwaving, steaming, chopping and blending into smoothie will be examined on the major phytochemical compounds in watercress.
- Flavonols, glucosinolates and carotenoids will be quantified using liquid chromatography and mass spectrometry.
- Total antioxidant activity of watercress following the different processing methods will be evaluated using the Ferric Reducing Antioxidant Power (FRAP) assay.

6.1 Introduction

Watercress (*Nasturtium officinale)* belongs to the family of *Brassicaceae* together with broccoli, cabbage, mustard and Brussels sprouts. Epidemiological studies associate a higher intake of Brassica vegetables, such as watercress, with a reduced risk of various types of cancers [160]. Watercress is an exceptional source of natural, bioactive compounds for which research has highlighted a favourable role in anti-genotoxic and anti-cancer processes both *in vivo* and *in vitro* [53, 57, 58]. The health benefits of watercress have been attributed to phytochemicals including glucosinolates, carotenoids and flavonoid compounds.

Watercress, and essentially all members of the *Brassicaceae* family, has been identified as a rich source of glucosinolates [63]. Glucosinolates are hydrolysed to isothiocyanates by the action of the enzyme myrosinase (β-thiglucoside glucohydrolase; EC 3.2.3.1), upon cell tissue damage such as mastication, chopping or cooking. This group of plant bioactive compounds is responsible for the characteristic pungent taste that Brassica vegetables possess. Gluconasturtiin (2-phelylethyl glucosinolate) is the most prominent glucosinolate in watercress [53, 57] with a range of aliphatic and indole glucosinolates adding to its glucosinolate profile.

High concentrations of carotenoids and flavonol compounds are also contained in watercress. Carotenoids with well established health benefits such as β-carotene, lutein and zeaxanthin are abundant in watercress [76]. Flavonols like quercetin, kaempferol and isorhamnetin, make up the polyphenolic core of watercress [204]. Polyphenols have attracted great importance due to their many health benefits related to cardiovascular function, antioxidant and anticancer activity (Morel, Lescoat, Cillard, & Cillard, 1994 Doostdar, Burke, & Mayer, 2000; Galati, Teng, Moridani, Chan, & O'Brien, 2000).

While watercress is widely consumed raw in salads, it is becoming increasingly popular in cooked foods such as soups, smoothies and also wilted in pasta and meat dishes. Annual retail sales of watercress in the United Kingdom amounted to 40 million pounds in 2015. Sales of food products with cooked or processed watercress as the main ingredient have taken off the last few years, representing approximately 50% of total watercress sales (S. Rothwell, Vitacress salads LTD, personal communication, March 10, 2016). Culinary processing is the source of several complex biochemical and physical alterations, modifying the phytochemical constituents of vegetables, ultimately resulting in nutritional changes [205].

To our knowledge, phytochemical characterisation of watercress subjected to different culinary treatments has not been explored to date. The present research was undertaken to elucidate the effects of five common cooking methods on the phytochemical profile of watercress and formulate suggestions for the most appropriate method for consuming watercress for maximum nutrient ingestion. (The work for this chapter has been published in the Journal of Food Chemistry)

6.2 Materials and methods

6.2.1 Plant Material

Fresh watercress samples were provided from VITACRESS LTD (Andover, Hampshire, UK), transferred to the laboratory and stored at 4 °C for up to 24 hours until all watercress processing analyses were performed. Only samples free from mechanical damage were used in the experiments. All analyses were performed in triplicate using the same batch of plant material to minimise variation in our results.

6.2.2 Reagents & Chemicals

All chemicals were obtained from Sigma Aldrich (Poole, UK), unless otherwise stated.

6.2.3 Domestic Processing

The effect of domestic processing on the phytochemical content and antioxidant activity of watercress was examined by cooking of the plant material by boiling, microwaving, steaming, chopping and blending with water to make a watercress smoothie. Processing treatments and cooking times used were decided upon general consumer preferences and after online search of watercress recipes as well as using past research papers looking at the effects of domestic processing on other types of Brassica vegetables. 100 g portions of watercress were used for each replicate *(n=3).* Temperature data for boiling and steaming treatments were recorded throughout cooking, using a temperature logger (Squirrel OQ610-S, Grant instruments, UK) and a type T thermocouple.

Boiling *(n=3):* 500 ml of tap water was brought to boil (90 °C) in a stainless steel pot and watercress was boiled for 2, 5 and 10 min. Watercress was removed from the boiling water and was kept at -20 °C for analysis.

Microwaving *(n=3):* Fresh watercress was placed in plastic trays, then transferred to a domestic microwave oven (Panasonic, UK) and cooked at full power (1400 W) for 1, 2 and 3 min.

Steaming *(n=3):* A domestic steamer (Russel Hobbs, UK) was pre-heated at 100 °C with 500 ml water at its base. Watercress was placed in the steamer and cooked for 5, 10 and 15 min.

Chopping *(n=3):* 100 g of watercress was transferred to a food processor (Waring Commercial, New York, USA) and chopped for 30 secs at full speed. To study the effect of storage time on the phytochemical content, the chopped watercress was left on the bench at room temperature (21 °C) for 0, 10, 30, 60 and 120 min to replicate how watercress can be treated at home when chopped in salads or other dishes and not consumed immediately after preparation.

Watercress smoothie *(n=3):* 100 g of the plant material was transferred to a juice maker (Vitamix, Total Nutrition Centre, UK), 200 ml of water was added and the watercress was blended for 30 secs at full power. The effect of storage time was also examined by leaving the smoothie on the bench at room temperature (21 °C) for 0, 10, 30, 60 and 120 min.

After processing, all samples were immediately frozen in liquid nitrogen then freeze-dried (Christ A 2-4 LD, Christ, Germany); ground to fine powder using a coffee bean grinder (De'Longhi, Italy), vacuum packed and stored at -20 °C.

6.2.4 Preparation of watercress extracts

Crude methanol (MeOH) extracts: The method used for the preparation of the extracts was adapted from Bell *et al*. [206] Briefly, 40 mg of ground watercress powder was heated in a dry-block at 75 °C for 2 min to inactivate myrosinase enzyme. Preheated (70 °C) 70% (v/v) MeOH

(1 ml) was then added to each sample and placed in a water bath for 20 min at 70 °C. Samples were then centrifuged for 5 min at 6,000 rpm and the supernatant was transferred to fresh tubes. The final volume was adjusted to 1 ml with 70% (v/v) MeOH and stored at -20 °C until the day of analysis. MeOH extracts were used for the FRAP assay, total phenols as well as flavonols and glucosinolates identification and quantification.

Acetone extracts: Total and specific carotenoids were determined in acetone watercress extracts. Watercress powder (25 mg) was weighed out in Falcon tubes (12 ml) previously wrapped in aluminium foil to minimise the degradation of carotenoids by ultra-violet light. Acetone (4 ml) was added to the powder and the samples were shaken for 15 min at 8000 rpm. Following centrifugation at 4000 rpm for 5 min, the supernatant was transferred to a clean tube and the process was repeated (4 ml acetone for the second time and 2 ml the third time) until a colourless supernatant was obtained. The combined supernatants were transferred in fresh tubes and the final volume was adjusted to 10 ml with 100% acetone.

6.2.5 Determination of total phenolics

Total phenols were measured using the method developed by Singleton and Rossi [207] with slight modifications. Briefly, 0.2 ml of the MeOH watercress extract (Section 2.4) or blank was added to 6.0 ml of distilled water in volumetric flasks and mixed with 0.5 ml of Folin - Ciocalteu reagent. A sodium carbonate solution 20% (v/v) (1.5 ml) was added to the mixture and the volume was adjusted to 10 ml. Absorbance was read after incubation of the samples for two hours at room temperature, at 760 nm using a UV-Vis Spectrophotometer (UV-VIS, Perkin Elmers, UK). A standard curve was made using gallic acid in the following

concentrations: 0, 50, 100, 150, 250, 500, 750 &1000 mg/L and total phenols were measured as gallic acid equivalents ($R^2 > 0.99$).

6.2.6 Ferric Reducing Antioxidant Power (FRAP) assay

Antioxidant activity of the samples was determined using the FRAP assay based on an adapted version of the method developed by Benzie and Strain [208]. The FRAP reagent was made by mixing 25 ml of 300 mM acetate buffer (pH 3.6), 2.5 ml 10 mM 2,4,6-tripyridyl-s-triazine solution (TPTZ) and 2.5 ml of freshly prepared ferric chloride hexahydrate ($FeCl_3 \cdot 6H2O$). A standard curve was made using L-Ascorbic acid in the following concentrations: 0, 10, 50, 100, 250, 500, 750, 1000 µmol/L ($R^2 > 0.99$). Each sample (MeOH extracts from Section 2.4) or standard (10 µl) was combined with 300 µl of the FRAP reagent and 100 µl of the mixture was transferred in duplicate in a 96-well plate. Absorbance was measured immediately using a plate reader (Tecan GENios, Geneva, Switzerland) at 595 nm.

6.2.7 Total carotenoids

An aliquot of the acetone extracts prepared as previously described (Section 2.4) was used to quantify the total carotenoid content of the samples spectrophotometrically. Absorbance was measured at 470, 645 and 662 nm in a spectrophotometer (UV-VIS, Perkin Elmers, UK). The total amount of carotenoids was calculated according to the following equations by Lichtenthaler [209].

$$C_a = 11.24\, A_{662} - 2.04\, A_{645}$$

$$C_b = 20.13\, A_{645} - 4.19\, A_{662}$$

$$C_{a+b} = 7.05\, A_{662} + 18.09\, A_{645}$$

$$C_{x+c} = \frac{1000\, A_{470} - 190\, C_a - 63.14\, C_b}{214}$$

*Chlorophyll a (C_a), Chlorophyll b (C_b), Total Chlorophylls (C_{a+b}), Total Carotenoids (C_{x+c}). Equations are based on specific absorption coefficients for 100% acetone. The pigment concentrations obtained by inserting the measures absorbance values are µg/ml plant extract solution.

6.2.8 Quantification of carotenoids via HPLC

To determine the amount of lutein, zeaxanthin and β-carotene present, the acetone extracts were used (Section 2.4). Carotenoids were quantified using the method developed by Guiffrida *et al*. [210] with modifications.10 ml of the extract was mixed with 10 ml of diethyl ether, 10 ml of water and 5ml of 10% (v/v) NaCl. Two layers were formed and the lower - acetone phase was discarded. The upper layer containing the ether was collected in a glass vial and anhydrous Na_2SO_4 was added to it to remove any moisture from the solution. The ether phase was transferred to a clean glass vial, the volume was adjusted to 10ml with diethyl ether and the solution was condensed under nitrogen gas. The dry residue was then reconstituted in 1 ml of methyl tert- butyl ether (MTBE):MeOH (1:1, v/v), filtered using 0.22 µm syringe driven filter unit and analysed by HPLC. The analyses were performed using an YMC30 column (5 µm 250 x 4.6 mm) on a HP Agilent 1050 series HPLC system. The mobile phases used were as follows: Eluent A, consisting of MeOH:MTBE:H_2O (82:16:2 v/v/v) and Eluent B, consisting of MeOH:MTBE:H_2O (23:75:2 v/v/v). The analyses followed a gradient program for the mobile phases, 0 min 0% B, 20 min 0% B, 80 min 70% B, 90 min 70% B. The protocol used a 1 mL/min flow rate and a 100 µL injection volume. UV-vis spectra were gathered in the range of 190-600 nm and the chromatograms were analysed at 450 nm. Identification was based on retention times by comparison with HPLC grade standards of lutein, zeaxanthin and β-carotene (Extrasynthese, France).

6.2.9 Identification and quantification of glucosinolates and flavonols via LC-MS/MS

Methanol extracts, prepared as described above, were used for the quantification of glucosinolates and flavonols in the samples (Section 2.4.1). Each extract (1 ml) was filtered using a 0.22 µm syringe driven filter unit (Millex; EMD Millipore, Billerica, MA, USA) and then diluted using 9ml LC-MS grade water. For the quantification of glucosinolates and flavonols, external calibration curves of 12 mM sinigrin hydrate and isorhamnetin standards were prepared using the following concentrations (56 $ng.\mu l^{-1}$, 42 $ng.\mu l^{-1}$, 28 $ng.\mu l^{-1}$, 14 $ng.\mu l^{-1}$, 5.6 $ng.\mu l^{-1}$, $R^2 > 0.99$). Glucosinolates and flavonols were analysed by LC-MS/MS using an Agilent 1200 LC system coupled to an Agilent 1100 series LC/MS mass trap spectrometer. Separation conditions of samples and MS analysis settings used are identical to those described by Bell, Oruna-Concha [206] . Glucosinolates were quantified at 229 nm and flavonols at 330 nm. The identification was performed using the compounds nominal mass and the analysis of their fragmentation patterns, and also by the comparison with previously published data. All data were analysed using Agilent ChemStation.

6.2.10 Statistical Analysis

The results are presented as the mean of three biological replicates (n = 3) for each sample. One-way ANOVA and Dunnett's multiple comparisons test were used for comparison of all treatments related to the raw watercress. These analyses were carried out using GraphPad Prism version 5.0a for Mac OS X,GraphPad software (Version 5.0a La Jolla, California, USA). Principal component analysis (PCA) and correlation analysis were performed using XL Stat (Version 2016 Addinsoft, New York City, New York, USA).

6.3 Results and Discussion

6.3.1 Total phenols content

Fresh watercress had the highest amount of total phenols (14.86 ± 2.02 mg GAE g^{-1} DW) compared to the processed samples (Fig. 5.1A). Our results are in agreement with that of Aires, Carvalho [211] who found the phenolic content of watercress to be 14.00 ± 0.03 mg GAE g^{-1} DW. In comparison to other vegetables in the Brassica family, watercress is a rich source of phenolic compounds. It has a similar amount to kale (16.67 ± 0.67 mg GAE g^{-1} DW) [212] and it is much higher than broccoli and cabbage which have a lower phenolic content that being 8.86 mg and 5.6 mg GAE g^{-1} DW respectively [213, 214].

Boiling of watercress resulted in a significant decrease ($P<0.05$) in the total phenolic content in comparison with the fresh samples. Total phenolic losses ranged from 49% to 71% in the samples boiled for 2 and 10 minutes respectively. Microwaving and steaming for up to 5 minutes did not significantly affect the phenolic content of watercress ($P>0.05$). Likewise, blending with water to make a watercress smoothie and chopping did not have a significant effect on the total phenolic content in the watercress. However, storage of the smoothies and the chopped watercress samples for 120 minutes at room temperature resulted in a significant reduction of the phenolics from 13.65 ± 1.56 to 10.76 ± 1.15 mg GAE g^{-1} DW and from 10.55 ± 1.48 to 8.65 ± 2.29 mg GAE g^{-1} DW respectively (Figure 1A).

Our results are corroborated by previous studies showing that boiling of Brassica vegetables can lead to significant time dependant losses of phenolics whereas microwaving and steaming led to only minor decreases in the phenolic content of broccoli [215, 216], red cabbage [217] and cauliflower [218]. During the process of cooking, phenolic compounds

appear to be highly reactive undergoing several changes including their release from bound forms, oxidation, degradation and polymerisation [213].

The losses during boiling can be attributed to water-soluble compounds leaching into the water used for boiling or due to breakdown of these compounds during thermal processing. Indeed, analysis of the water used in the boiling experiments (9.35 ± 0.12 mg GAE g^{-1} DW) for total phenolics revealed that phenols had leached into the boiling water. The total amount of phenols in the water used in boiling and the remaining phenol content of watercress was no different from the total phenols in raw watercress. The minimal effect of microwaving and steaming on the phenolic compounds is potentially a result of limited or no contact of the samples with water and also the inactivation of oxidative enzymes preventing the disruption of phenolic biosynthesis and degradation [219]

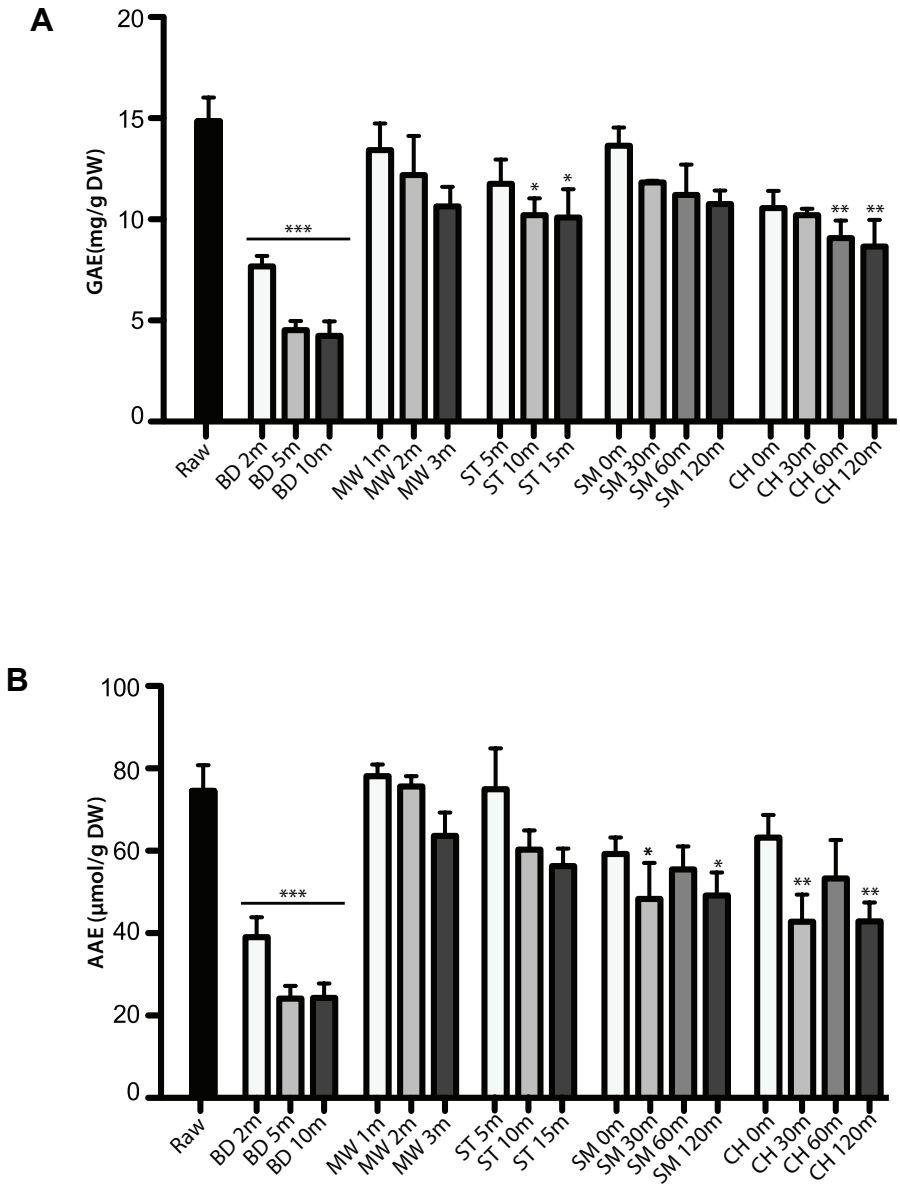

Figure 6.1 (A) Total phenols content in raw and processed samples expressed as gallic acid equivalents (GAE) in mg $g^{-1}$of dry weight (DW). (B) FRAP-assay results for the measurement of the antioxidant activity in raw and cooked watercress samples. Results are presented as ascorbic acid equivalents (AAE) in mg g^{-1} of DW. Data is mean of three biological replicates + SD. Significance: *, $P < 0.05$; **, $P < 0.01$; *** $P < 0.001$ as compared to raw watercress. (BD: Boiled, MW: Microwaved, ST: Steamed, SM: Smoothie, CH: Chopped.

6.3.2 Flavonols identification and quantification

Flavonol profiling of watercress revealed three main derivatives namely kaempferol, quercetin and isorhamnetin as well as feruloyl, ceffeoyl, p-coumaroyl and sinapoyl glucosides attached to kaempferol and quercetin. Kampferol-3-diglucoside-7-glucoside was the most abundant flavonol detected (3.76 ± 0.09 mg g^{-1} DW). The flavonols identified in the fresh watercress leaves are similar to those defined by Martinez-Sanchez, Gil-Izquierdo [204].

Domestic processing of watercress resulted in a significant decrease in the levels of all quantified flavonols (Table 5.1). The only exception was Q 3,4'diGlc-3'-(p.coum-Glc) + K 3,4'-diGlc which appeared to be the most stable of all flavonols and were only significantly affected by boiling ($P<0.05$). Total flavonol losses suggest that these compounds are particularly sensitive to all cooking regimes used. Boiling for 10 minutes nearly depleted all watercress samples of flavonols in a time dependent manner. The unstable nature of flavonols was also apparent in chopped watercress and watercress smoothie with the levels going down to 3.42 ± 0.32 and 4.11 ± 0.36 mg g^{-1} DW respectively as compared to the total amount of flavonols in the fresh samples (10.70 ± 1.07mg g^{-1} DW, $P<0.001$). Similarly to total phenols, the highest retention of flavonols was observed in the microwaved watercress followed by steamed.

Table 5.1 Concentration of individual and average total flavonols in raw and processed watercress samples. Data are presented in mg g-1 of DW (mean ± SD). Experiment was performed with three biological replicates per group. Significance: *, P < 0.05; **, P < 0.01; *** P < 0.001 as compared to flavonoid content of raw watercress. Abbreviations: K, kaempferol; I, isorhamnetin; Q, quercetin; Glc; glucoside, fer, feroloyl; sinp, sinapoyl; p.cisoum, p-coumaroyl; caf, caffeoy

	K 3-diGlc-7-Glc	I 3-Glc	K 3-(fer-triGlc)-7 Glc	Q 3-(fer-Glc)-3'-(sinp-Glc)-4'-Glc + Q 3-p.coum-Glc[a]	Q 3,4'diGlc-3'-(p.coum-Glc) + K 3,4'-diGlc[a]	Q 3-(caf-Glc)-3'-(sinp-Glc)-4'-Glc	Q -3,4'diGlc-3'-(caf-Glc)	K 3-(sinp-triGlc)-7-Glc	K 3-(sinp-Glc)-4'Glc	Total
	mg g^{-1} DW									
Raw	3.76±0.09	1.18±0.03	1.73±0.06	0.52±0.01	0.35±0.02	1.35±0.26	0.76±0.02	0.68±0.14	0.36±0.05	10.70±1.07
Boiled 2m	1.09±0.16***	0.46±0.04***	0.62±0.08***	0.28±0.01***	0.21±0.04	0.29±0.09***	0.36±0.08***	0.20±0.02***	0.15±0.05***	3.66±0.30***
Boiled 5M	0.55±0.04***	0.26±0.02***	0.34±0.03***	0.17±0.02***	0.08±0.01***	0.18±0.09***	0.19±0.05***	0.11±0.06***	0.13±0.06***	2.01±0.15***
Boiled 10m	0.58±0.16***	0.26±0.06***	0.35±0.08***	0.16±0.03***	0.06±0.03***	0.12±0.07***	0.13±0.02***	0.13±0.15***	0.08±0.02***	1.86±0.17***
MW 1m	2.25±0.33**	0.76±0.06***	0.99±0.20***	0.36±0.09*	0.37±0.09	0.63±0.42***	0.61±0.08*	0.36±0.05***	0.20±0.04***	6.53±0.62**
MW 2m	1.57±0.43***	0.54±0.16***	0.74±0.21***	0.25±0.08**	0.23±0.17	0.47±0.19***	0.38±0.23*	0.24±0.10***	0.15±0.04***	4.57±0.44***
MW 3m	1.31±0.22***	0.44±0.09***	0.57±0.10***	0.20±0.04***	0.25±0.04	0.29±0.01***	0.44±0.01*	0.23±0.01***	0.14±0.01***	3.87±0.36**
Steamed 5m	1.50±0.28*	0.53±0.11***	0.68±0.13***	0.27±0.10***	0.28±0.10	0.40±0.08***	0.44±0.16*	0.23±0.05***	0.16±0.03***	4.47±0.41**
Steamed 10m	1.41±0.29***	0.49±0.11***	0.64±0.11***	0.22±0.06***	0.24±0.11	0.36±0.04***	0.41±0.16**	0.21±0.01***	0.15±0.06***	4.12±0.39**
Steamed 15m	1.25±0.19***	0.45±0.06***	0.59±0.11***	0.22±0.07***	0.19±0.06	0.32±0.10***	0.36±0.08***	0.16±0.03***	0.15±0.02***	3.70±0.35***
Smoothie 0m	1.31±0.01***	0.47±0.02***	0.66±0.01***	0.26±0.02***	0.27±0.07	0.44±0.26***	0.37±0.06***	0.21±0.05***	0.11±0.04***	4.11±0.36***
Smoothie 30m	0.92±0.10***	0.35±0.03***	0.49±0.05***	0.14±0.03***	0.18±0.02	0.25±0.14***	0.24±0.04***	0.10±0.02***	0.07±0.01***	2.73±0.27***
Smoothie 60m	1.11±0.16***	0.44±0.09***	0.64±0.11***	0.19±0.03***	0.28±0.04	0.30±0.08***	0.28±0.09***	0.10±0.02***	0.06±0.01***	3.39±0.33***
Smoothie 120m	1.13±0.20***	0.42±0.06***	0.64±0.12***	0.23±0.07***	0.19±0.02	0.26±0.11***	0.29±0.10***	0.11±0.06***	0.06±0.03***	3.34±0.33***
Chopped 0m	1.12±0.17***	0.42±0.07***	0.58±0.09***	0.15±0.04***	0.17±0.10*	0.41±0.14***	0.30±0.11***	0.16±0.03***	0.11±0.01***	3.42±0.32***
Chopped 30m	0.96±0.13***	0.44±0.07***	0.53±0.07***	0.13±0.02***	0.24±0.04	0.24±0.03***	0.40±0.04**	0.16±0.01***	0.10±0.01***	3.21±0.27***
Chopped 60m	0.78±0.07***	0.41±0.04***	0.49±0.06***	0.10±0.01***	0.20±0.02	0.19±0.02***	0.42±0.10**	0.13±0.02***	0.09±0.01***	2.80±0.23**
Chopped 120m	0.72±0.14***	0.38±0.11***	0.49±0.14***	0.06±0.03***	0.11±0.08**	0.34±0.17***	0.26±0.09***	0.11±0.02***	0.08±0.03***	2.56±0.22***

Carotenoid content

In contrast to the previous assays, boiling of watercress resulted in an increased concentration of total measurable carotenoids, from 2.35 ± 0.22 mg g^{-1} DW in the fresh samples to 3.13 ± 0.20 mg g^{-1} DW after 2 minutes of cooking and up to 3.28 ± 0.30 mg g^{-1} DW after 5 minutes of boiling (Table 5.2). Microwaving and steaming did not have a significant impact on the level of total carotenoids ($P>0.05$). On the other hand, the watercress smoothie had significantly lower total carotenoid content, with the levels decreasing from 1.54 ± 0.21 to 1.11± 0.08 mg g^{-1} DW after 60 minutes of storage at ambient temperature. A similar decreasing trend was observed in the chopped watercress samples.

The individual carotenoids identified and quantified in our watercress samples were β-carotene, lutein and zeaxanthin and they all resulted in distinct responses upon domestic processing. β-carotene was the most abundant of the three quantified carotenoids (0.95 ± 0.08 mg g^{-1} DW) and its levels significantly increased after thermal treatment of the watercress samples. Boiling for 5 minutes resulted in β-carotene being significantly increased up to 1.75 ± 0.09 mg g^{-1} DW as compared to the raw samples ($P<0.001$). In the microwaved watercress samples β-carotene was increased up to 1.48 ± 0.26 mg g^{-1} DW ($P<0.01$) and in the samples steamed for 15 minutes levels went up to 1.54 ± 0.07 mg g^{-1} DW ($P<0.001$). β-carotene was decreased in the watercress smoothie only after storage for 30 and 60 and 120 minutes ($P<0.01$) therefore, immediate consumption of a watercress smoothie ensures sufficient intake of β-carotene. No significant differences were found in the chopped samples.

Lutein content of fresh watercress samples was 0.24 ± 0.02 mg g^{-1} DW and it exhibited the highest degree of stability after watercress processing. It was significantly

increased only after 5 minutes of boiling going up to 0.36 ± 0.02 mg g^{-1} DW ($P<0.05$). Significant decreases in lutein were only observed in the smoothie after 120 minutes of storage ($P<0.05$). Zeaxanthin concentration in fresh watercress was notably lower than β-carotene and lutein (0.02 ± 0.00 mg g^{-1} DW). It was dramatically affected by boiling with increases higher than 6 and 3 times, as compared to fresh watercress, after boiling for 5 minutes and steaming for 10 minutes respectively.

Increases in the carotenoid contents of other Brassica vegetables such as broccoli, Brussels sprouts, cabbage and cauliflower upon boiling and steaming have been reported by a number of research groups [76, 213, 220]. Elevations in the measurable carotenoid concentrations after thermal treatments can be explained by changes in the plant cell wall due to the breakdown of cellulose as well as improved extractability of carotenoids from the plant as a result of the denaturation of carotenoid-protein complexes due to thermal processing [221].

Table 6.2 Quantification of total and specific carotenoids, in raw and processed watercress samples. Data is presented as absolute carotenoid concentration in mg g-1 of DW (mean ± SD). Experiment was performed with three biological replicates per group. Significance: *, P < 0.05; **, P < 0.01; ***P < 0.001 as compared to carotenoid content of raw watercress. [a] Total amount of carotenoids measured spectrophotometrically.

	β-carotene	Lutein	Zeaxanthin	Total [a]
	mg g^{-1} DW			
Raw	0.95±0.08	0.24±0.02	0.02±0.00	**2.35±0.22**
Boiled 2m	1.42±0.27**	0.30±0.06	0.09±0.03***	**3.13±0.20****
Boiled 5M	1.75±0.09***	0.36±0.02*	0.13±0.01***	**3.28±0.30*****
Boiled 10m	1.29±0.20	0.24±0.05	0.10±0.03***	**3.00±0.17***
MW 1m	1.47±0.26**	0.32±0.04	0.04±0.01	**2.53±0.15**
MW 2m	1.19±0.09	0.28±0.04	0.04±0.01	**2.57±0.13**
MW 3m	1.48±0.26**	0.26±0.06	0.05±0.00	**2.65±0.33**
Steamed 5m	1.34±0.10*	0.26±0.02	0.05±0.01	**2.33±0.23**
Steamed 10m	1.45±0.10**	0.18±0.03	0.06±0.01*	**2.27±0.12**
Steamed 15m	1.54±0.07***	0.17±0.10	0.05±0.01	**2.31±0.47**
Smoothie 0m	0.61±0.15	0.24±0.02	0.02±0.01	**1.54±0.21****
Smoothie 30m	0.39±0.01**	0.18±0.05	0.03±0.01	**1.14±0.17*****
Smoothie 60m	0.36±0.14***	0.16±0.05	0.02±0.00	**1.11±0.08*****
Smoothie 120m	0.31±0.28***	0.11±0.09*	0.01±0.01	**1.57±0.36****
Chopped 0m	0.81±0.05	0.23±0.04	0.02±0.02	**1.94±0.23**
Chopped 30m	0.62±0.23	0.17±0.08	0.02±0.01	**1.65±0.15***
Chopped 60m	0.71±0.11	0.22±0.01	0.03±0.01	**1.57±0.25****
Chopped 120m	0.67±0.10	0.18±0.02	0.02±0.01	**1.79±0.17**

6.3.3 Glucosinolate identification and quantification

Gluconasturtiin was the most abundant glucosinolate in fresh and cooked watercress samples followed by the indole glucosinolates: glucobrassicin, 4-methoxyglucobrassicin, 4-hydroxyglucobrassicin and the aliphatic glucosinolate glucoibarin (Table 5.3). The profile characterised here is similar to that previously defined by Boyd, McCann [53], Gill, Haldar [57].

Glucosinolate quantification revealed a major impact of cooking on the levels of these phytochemicals. Boiling reduced the levels of total glucosinolates by up to 63% and led to significant loses of all the individual glucosinolates identified in this study ($P<0.001$). Considerable glucosinolate losses after boiling of Brassica vegetables like broccoli, cauliflower and Brussels sprouts, have also been observed in other studies performed by a number of research groups [222, 223]. Heat application combined with cooking in water can result in depletion of glucosinolates in Brassica as a result of enzyme activity modification and thermally induced breakdown processes [205, 224]. Boiling of watercress in water caused significant loss of glucosinolates that most likely have leached into the cooking water. Similar conclusions were drawn by Song and Thornalley [222] who showed that boiling of Brassica vegetables leads to significant leaching of glucosinolates in the boiling water. Jones [224] have shown that the glucosinolate losses in Brassica vegetables are positively correlated with the cooking time.

Microwaving and steaming had a subtle effect on glucosinolate concentrations with minor losses at the longest cooking duration, as compared to the other treatments. Microwaving and steaming for 2 or 5 minutes did not result in major losses of total glucosinolates suggesting that these cooking methods will ensure a higher retention rate of these phytochemicals. Our results are in agreement with that of Song and Thornalley

[222] who examined the impact of different cooking methods on broccoli, brussels sprouts, cauliflower and green cabbage. This observation is likely due to denaturation and subsequent deactivation of the myrosinase enzyme, which depletes glucosinolates in favour of their hydrolysis to isothiocyanates, after application of high temperatures during cooking [225]. We found that cooking by steaming resulted in a slight increase in gluconasturtiin concentrations from 1.76 to 2.04 mg g^{-1} DW ($P<0.05$) and it can therefore be considered as the preferred method of watercress consumption to maximise gluconasturtiin levels. Elevated gluconasturtiin concentrations upon steaming are also reported by Gliszczynska-Swiglo, Ciska [213] in broccoli. Increases in other glucosinolates in Brassica vegetables subjected to steaming have been also been noted in a number of studies [223, 226]. The inactivation of myrosinase at the high temperatures such as the ones reached during steaming, can temporarily cease the conversion of glucosinolates to isothiocyanates [223] a process which can be undertaken post ingestion*, in vivo*, by the action of the endogenous bacterial myrosinase in the gut [227]. Furthermore, heat application leads to plant cell structure disintegration allowing glucosinolates to be released from their bound forms on the plant cell wall making these compounds more recoverable during extraction [213]. Steaming is performed without direct contact of the plant material and water, preventing the leaching of glucosinolates into it.

Homogenisation by blending watercress with water to create a smoothie resulted in dramatic reductions in glucosinolates stemming mainly from the complete loss of gluconasturtiin ($P<0.001$). Upon chopping losses ranged from 35% to 46% after 120 minutes of storage at room temperature. Chopping of vegetables before consumption is a regular practise and this can lead to decreased glucosinolate content since they are exposed to myrosinase for conversion to isothiocyanates. This was reflected in our results

and those of others [222, 228], and it was particularly apparent in the gluconasturtiin quantification. When watercress was homogenised to create a smoothie, gluconasturtiin was completely lost and the levels of other glucosinolates were significantly diminished. Our results are comparable with results from a study performed by Smith, Mithen [228] where homogenisation for juice extraction from Brussels sprouts led to loss of glucosinolates which were converted to isothiocyanates and other breakdown products due to the exposure of glucosinolates to myrosinase enzyme. Song and Thornalley [222] observed that shredding of Brassica vegetables and subsequent storage at ambient temperature results in major losses of glucosinolates with concurrent formation of isothiocyanates. Isothiocyanates such as PEITC are highly volatile compounds therefore they are prone to evaporation as observed by Rose, Faulkner [58] who did not detect PEITC in watercress aqueous extracts. However, Ji, Kuo [229] noted that PEITC remains stable in aqueous buffers with a half-life of 56 h at ambient temperature. This suggests that smoothies or juices made from watercress, which is rich in PEITC, should be freshly consumed after preparation to ensure adequate ingestion.

Table 6.3 Concentration of individual and average total glucosinolates in raw and processed watercress samples. Data is presented in mg g^{-1} of DW (mean ± SD). Experiment was performed with three biological replicates per group. Significance: *, $P < 0.05$; **, $P < 0.01$; ***, $P < 0.001$ as compared to carotenoid content of raw watercress.

	Gluconasturtiin	Glucobrassicin	4-hydroxy-glucobrassicin	4-methoxy-glucobrassicin	Glucoibarin	Total
	mg g^{-1} DW					
Raw	1.76±0.07	0.47±0.04	0.22±0.01	0.26±0.01	0.08±0.00	**2.79±0.09**
Boiled 2m	1.02±0.05***	0.18±0.02***	0.08±0.01***	0.09±0.01***	0.06±0.00	**1.44±0.06*****
Boiled 5M	0.81±0.09***	0.13±0.02***	0.07±0.01***	0.08±0.01***	0.06±0.00	**1.16±0.11*****
Boiled 10m	0.71±0.06***	0.10±0.00***	0.08±0.01***	0.08±0.00***	0.06±0.00	**1.03±0.07*****
MW 1m	1.97±0.22	0.41±0.06	0.18±0.04	0.18±0.06**	0.05±0.04	**2.78±0.40**
MW 2m	1.59±0.19	0.32±0.07	0.17±0.00	0.16±0.01**	0.06±0.00	**2.30±0.22****
MW 3m	1.57±0.09	0.38±0.04	0.12±0.03**	0.15±0.02**	ND	**2.22±0.17****
Steamed 5m	2.04±0.09*	0.35±0.01**	0.18±0.04	0.14±0.03**	0.06±0.00	**2.77±0.06**
Steamed 10m	1.98±0.06	0.35±0.02**	0.19±0.01	0.17±0.01**	ND	**2.69±0.08**
Steamed 15m	1.61±0.31	0.30±0.05***	0.10±0.03***	0.12±0.02***	ND	**2.13±0.34***
Smoothie 0m	ND	0.27±0.05***	0.03±0.05***	0.04±0.05***	ND	**0.34±0.11*****
Smoothie 30m	ND	0.30±0.01***	ND	ND	ND	**0.30±0.01*****
Smoothie 60m	ND	0.28±0.04***	ND	ND	ND	**0.28±0.04*****
Smoothie 120m	ND	0.29±0.01***	ND	ND	0.02±0.04*	**0.31±0.01*****
Chopped 0m	1.06±0.09**	0.52±0.05	0.11±0.03**	0.11±0.01***	ND	**1.80±0.06****
Chopped 30m	1.16±0.05**	0.39±0.04	0.10±0.02*	0.10±0.00***	ND	**1.75±0.02*****
Chopped 60m	1.03±0.06**	0.39±0.05	0.10±0.02*	0.10±0.00***	ND	**1.62±0.11*****
Chopped 120m	1.01±0.06**	0.34±0.06**	0.08±0.01***	0.08±0.01***	0.01±0.02*	**1.52±0.14****

6.3.4 Antioxidant activity

The antioxidant activity of all watercress samples was determined using the FRAP assay (Figure 1B). Fresh watercress had an antioxidant activity of 74.54 ± 10.81 μmol AAE g^{-1} DW. Watercress was found to have the highest antioxidant activity when compared to spinach, rocket and mizuna [204, 230].

Boiling dramatically decreased the antioxidant capacity of watercress over time as compared to raw watercress, with losses reaching 67% of total antioxidant activity for samples cooked for 10 minutes (Fig. 5.1B). Antioxidant activity analysis of the cooking water showed that the losses observed during boiling are due to leaching of antioxidant compounds in the water (46,03 ± 9.42 μmol AAE g^{-1} DW). In contrast, microwaving and steaming of watercress did not result in any significant losses. Chopping and blending to smoothie had no significant impact on the antioxidant activity of the samples, however storage of these samples at room temperature for 30 or 120 minutes resulted in a significant decrease in antioxidant activity. Chopping and blending to smoothie reduced the antioxidant activity to 42.84 ± 8.00 and 48.47 ± 9.63 μmol AAE g^{-1} DW at 120 minutes of storage respectively. The antioxidant activity of raw and cooked samples followed a similar trend to that found for total phenols with a significant correlation between these measures ($R^2 = 0.759$, $P<0.05$).

In a study carried out by Ismail, Marjan [231] it was found that boiling for 1 minute significantly decreased the antioxidant activity of kale, but not that of cabbage. Zhang and Hamauzu Zhang and Hamauzu [215] showed that after boiling and microwaving, broccoli lost 65% and 65.3% of its total antioxidant activity respectively.

Since the antioxidant activity of plants may be defined by the concentration of phenols and ascorbic acid in combination with other phytochemicals, leaching of these

compounds into the boiling water, or oxidation and degradation of them during cooking, can lead to lower antioxidant activity of watercress [213, 219].

6.3.5 Watercress phytochemical profile modifications upon cooking

PCA revealed distinct phytochemical profiles for watercress cooked using different regimes (Fig. 5.2). The profiles obtained from microwaved and steamed watercress closely resembled that of fresh watercress with these cooking methodologies positively correlating with the phenolics, carotenoids and glucosinolate concentrations. In stark contrast, boiled watercress has a phytochemical profile very different from that of fresh watercress characterised by elevated carotenoid amounts (R^2= 0.668) and significant losses in glucosinolates and flavonols, which essentially result in compromised antioxidant activity (R^2= -0.596). Chopped watercress and watercress smoothie samples have similar phytochemical profiles and separate from the fresh samples on the first principal component characterised by losses of all the phytochemicals quantified in our study. Cooking time appears to be negatively correlated with microwaving, boiling and steaming but exposure of chopped samples and watercress smoothie to ambient temperature for extended time periods does not appear to have a particular impact on the measureable phytochemicals in these samples, expect in the total phenolic content of stored chopped watercress. Antioxidant activity as measured by the FRAP assay, exhibits a significant positive correlation with microwaving (R^2= 0.452) driven by higher concentrations of glucosinolates and flavonols suggesting that it should be the preferred method of watercress preparation when it is not consumed raw.

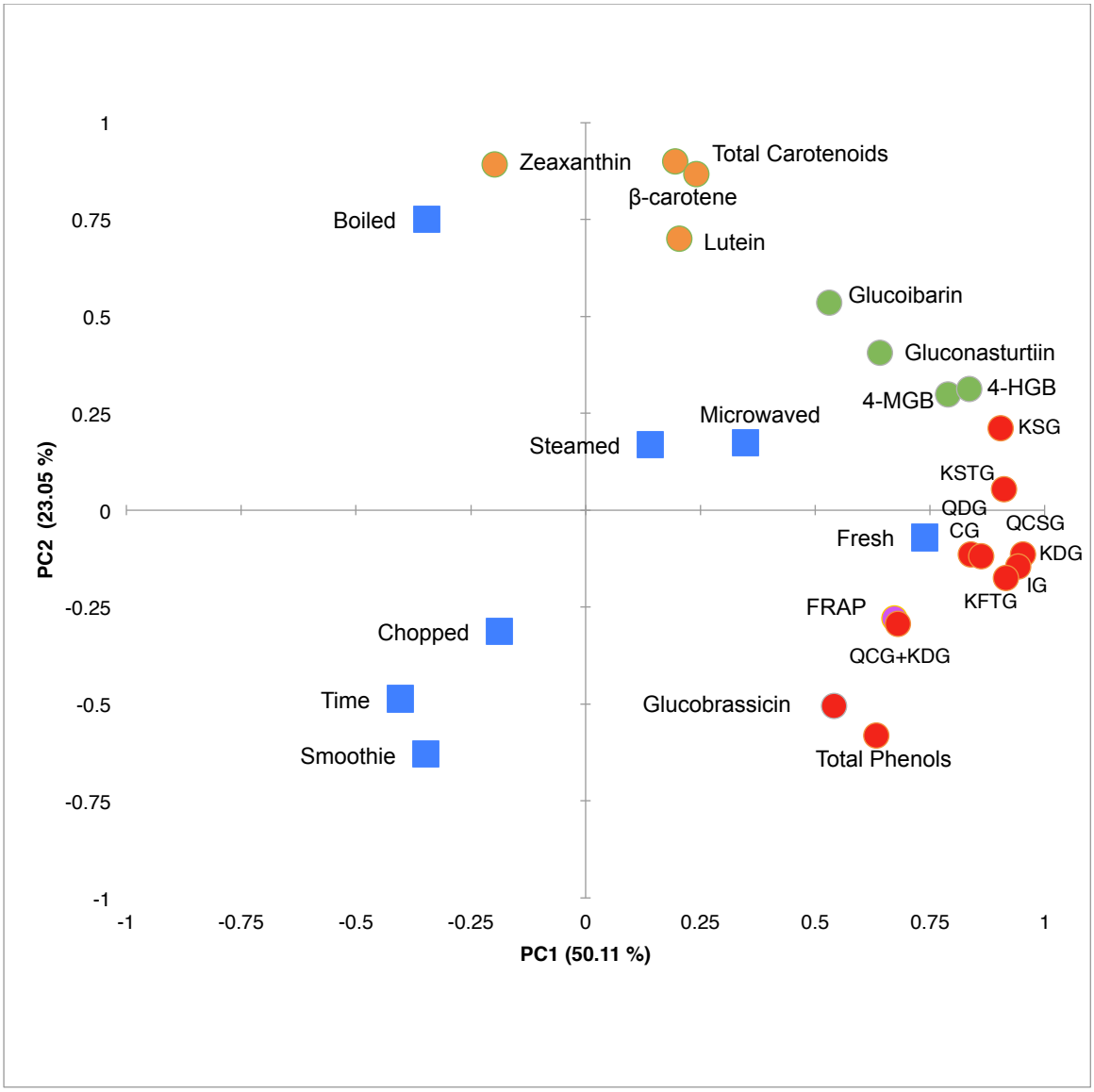

Figure 6.2 PCA scores of all cooked samples (□) and loadings plot for all quantified phytochemicals (O). Abbreviations: 4-MGB, 4-methoxyglucobrassicin; 4-HGB, 4-hydroxyglucobrassicin; KSG, K 3-(sinp-Glc)-4'Glc; KSTG, K 3-(sinp-triGlc)-7-Glc; QDGCG, QCSG, Q 3-(caf-Glc)-3'-(sinp-Glc)-4'-Glc; KDG, K 3-diGlc-7-Glc; IG, I 3-Glc; KFTG, K 3-(fer-triGlc)-7 Glc; QCG+KDG Q 3,4'diGlc-3'-(p.coum-Glc) + K 3,4'-diGlc.

6.4 Conclusions

This study clearly demonstrates that health-promoting compounds in watercress are significantly influenced by domestic processing methods. Cooking by microwaving and steaming preserves the levels of most phytochemicals in watercress. Domestic processing can have a detrimental effect on the bioactives, which may be responsible for the health promoting properties of watercress. Satisfactory retention of beneficial phytochemicals in watercress may be achieved by avoiding boiling which results in a compromised phytochemical profile.

6 Plasma and urinary metabonomic responses to watercress intervention in breast cancer - A pilot study

Hypothesis

It is hypothesised that watercress consumption during radiotherapy treatment can help in limit radiation induced damage in healthy cells, whilst potentially enhancing the response of breast cancer patients to the treatment

Aim

- To explore the ability of watercress intake to modulate the metabolism of breast cancer patients undergoing radiotherapy

Objectives

- ^{1}H NMR metabonomic profiling of plasma and urine samples will be used to identify biochemical differences between breast cancer patients consuming watercress throughout the duration of radiotherapy and breast cancer patients maintain their habitual diet during treatment.

6.1 Introduction

RT works by significantly increasing ROS formation, damaging the DNA of the targeted cancer tissue. It aims in the cease of cancer cell proliferation and ultimately cancer cell death. Non-cancerous cells, including blood cells, are unavoidably affected in the course of radiotherapy treatment. Side effects include skin reactions, nausea, anorexia and generalised pain are extremely common among patients receiving radiotherapy [14]. More severe side effects include hyperpigmentation, skin fibrosis and potential influence on lung and heart tissues. [15, 21]. The need for radio-protective agents is of paramount importance for oncologists especially in cases of radio-resistant tumours where higher doses of radiation have to be administered to the patient.

Of note, the role of nutrition intervention in medium and long-term outcomes in cancer has been demonstrated. It is today acknowledged as grade A evidence that individualised nutritional counselling and education plays a central role in improving long-term outcomes in cancer, by prolonging survival, reducing late radiotherapy toxicity and improving quality of life [232, 233]. The present pilot clinical trial of nutritional supplementation in cancer, intends to further explore the effects of therapeutic diets supplemented with phytonutrients *via* watercress that may prove useful in global disease prognosis.

Building upon the *in vitro* data (previously described in Chapter 3 and 4) supporting a role of watercress and its components -particularly PEITC- against various steps in carcinogenesis, a human intervention study was conducted to explore the potential of watercress to reduce DNA damage levels. A randomised crossover study was carried out by Gill *et al*. in 60 healthy volunteers that were instructed to consume one pack (85g) of raw watercress daily for 8 weeks [57]. Compared to the control phase, watercress

supplementation increased lymphocyte DNA resistance to free radicals, thus reducing DNA damage. The hypothesis set out was that watercress might reduce cancer risk *via* decreased damage to DNA and possible effects on antioxidant status by increasing levels of plasma carotenoids. Additional evidence was obtained from a study performed by Fogarty *et al.* where acute and chronic watercress attenuated DNA damage and lipid peroxidation and decreased H_2O_2 accumulation following exhaustive exercise [52].

Watercress is the richest dietary source of PEITC, to which a number of anti-cancer properties are attributed. A recognised mechanism by which PEITC inhibits the growth and survival of established cancer cells is through the inhibition of angiogenesis [61]. Alwi *et al.* performed a study in twelve healthy women who had previously been treated for breast cancer, where dietary intake of 80 g watercress significantly reduced hypoxia-inducible factor (HIF) signalling activity in peripheral blood cells. HIF is a major positive regulator of angiogenesis and its inhibition by watercress consumption suggests that diet-derived PEITC may be sufficient to modulate angiogenesis [107]. These findings are justifiably interesting for potential cancer prevention by watercress.

Metabolic profiling of bio-fluids obtained from cancer patients undergoing RT can provide important information on treatment efficacy and disease prognosis. However, RT-specific metabolic biomarkers can be difficult to obtain since they are naturally confounded by cancer-specific biomarkers. Limited data from human studies are available regarding prognostic and predictive metabolic biomarkers in RT. In a recent study, metabolomic profiling of urine samples obtained from cancer patients undergoing whole-body RT before receiving hematopoietic stem-cell transplantation, revealed seven metabolic markers differing between pre and post radiation (octanoylcarnitine, hypoxanthine, xanthine, trimethyl-lysine, acetyl-carnitine, decanoylcarnitine and uric

acid). The metabolites identified were directly related to RT targets such as mitochondria-related lipid damage and β-oxidation perturbations (carnitines and trimethyllysine), oxidative stress and radiation-induced DNA damage (purine catabolism: xanthine, hypoxanthine and uric acid) [234].

In this thesis, Chapter 3 has provided *in vitro* data on the potential of watercress extract and PEITC to interact with the metabolome of breast cancer and healthy cells, influencing phospholipid metabolism as well as modulating the antioxidant status of these cells. These observations were accompanied by mitochondrial damage, cell cycle arrest and DNA damage. Subsequently, in Chapter 4 it was shown that through its ability to deplete glutathione, PEITC sensitises breast cancer cells to radiation induced damage whereas the watercress extract appeared protect healthy cells from IR toxicity by influencing intracellular levels of glutathione. To validate these observations *in vivo*, the present study seeks to investigate and analyse the ability of watercress to act as a nutritional adjuvant intervention during radiotherapy treatment, in that it can potentially alleviate radiotherapy derived systemic side effects and improve the treatment outcomes in breast cancer patients.

6.2 Materials and Methods

6.4.1 Subjects

The study was conducted in 47 female volunteers aged between 40-71 years old. All subjects were early-stage breast cancer patients referred for radiotherapy with curative intent at the University Hospital of Santa Maria (Lisbon, Portugal). Exclusion criteria were pregnancy, cognitive impairment, and patients carrying implantable electronic devices (*e.g.* pacemaker). Information regarding family history of was collected from all participants in the study. Ethical review and approval was provided by the ethics committee of both the Lisbon University Hospital and the Faculty of Medicine of the University of Lisbon. The clinical trial was registered at http://clinicaltrials.gov (NCT02468882).

6.4.2 Study design

The study was designed as a non-blinded, prospective randomised controlled trial. The volunteers were assigned to either the control or the intervention group. The control group received standard care, maintaining their *ad libitum* diet. The intervention group was asked to consume 100 g of watercress per day alongside their habitual diet from the onset and for the total duration of the radiotherapy treatment. Breast cancer patients participating in the study were prescribed 60-70 Gy of radiotherapy treatment with fractionated delivery over a 6-7 week period.

Patients received detailed recommendations on how to consume watercress with suggestions for preparation including watercress eaten fresh as a salad, or gently cooked by steaming or microwaving or stirred into hot food before serving. These suggestions were given to the volunteers on the basis of the results obtained in Chapter 5.

Spot urine and blood samples were obtained at baseline and at the end of the RT treatment. Blood samples were collected in heparin containing tubes and centrifuged at 12,000 *g* for 10 min. Plasma aliquots and urine samples were stored at -80 °C until analysed.

6.4.3 Statistical analysis

Statistical analysis of clinical characteristics was carried out using GraphPad Prism version 5.0a for Mac OS X,GraphPad software (Version 5.0a La Jolla, California, USA). P-values were calculated by unpaired t-test with Welch's correction for continues variables and by chi-squared test for categorical variables.

6.4.4 ^{1}H NMR spectroscopy and data processing

Metabonomic profiling was performed on all urine samples. A 400 µl aliquot was added to 200 µl of phosphate buffer (pH 7.4, 100% D_2O, 0.2M Na_2HPO_4/NaH_2PO_4) containing 1mM of the internal standard, 3-(trimethylsilyl)-[2,2,3,3,-$^{2}H_4$]-propionic acid (TSP) and 2mM sodium azide (NaN_3) as a bacteriocide. Samples were vortexed and spun at 13,000 *g* for 10 min and 550µl of the supernatant were transferred into 5mm NMR tubes. Spectroscopic analysis was performed on a 600 MHz Bruker Avance™ NMR spectrometer at 300K using a Bruker TXI probe (Bruker Biospin, Rheinstetten, Germany). ^{1}H NMR spectra of the urine samples were acquired using a standard one-dimensional pulse sequence [recycle delay (RD) -90°-t_1–90°-t_m-90°-acquire free induction decay (FID)]. The water signal was suppressed during the RD of 4 s with a mixing time of (t_m) 100 ms, t_1 was 11.25 µs. For each spectrum, 32 scans were obtained into 64K data points using a spectral width of 12.001 ppm.

Aliquots of 200 µl plasma were combined with 400 µl of saline buffer (100% D_2O, 0.9% NaCl). The samples were mixed by vortexing and were then centrifuged at 13,000 *g* for 10 min and 550 µl of the resulting supernatant were transferred to 5 mm NMR tubes. ^{1}H

NMR spectra were acquired on a 600 MHz Bruker AvanceTM NMR spectrometer at 300K using a Bruker TXI probe (Bruker Biospin, Rheinstetten, Germany) in a random order. Spectra were acquired using a one-dimensional technique using a standard pulse sequence with water pre-saturation and Carr-Purcell-Meiboom-Gill (CPMG) spin echo sequences to minimise the broader peaks occurring from lipids and proteins

The acquired NMR spectra were manually phased, corrected for baseline distortions and referenced to TSP for urine samples or glucose resonance (α anomeric proton) (δ 5.23) for plasma samples (TopSpin 3.0, Bruker, Rheinstetten, Germany) and then imported into MatLab (version R2012a, The Mathworks, Inc.; Natwick, MA). The region containing the water peak was removed as well as the TSP peak region. The urea resonance region was also removed from the urinary spectra. ^{1}H NMR spectra were then aligned manually using a recursive segment-wise peak method (RSPA) algorithm to minimise chemical shift variation due to residual pH differences within samples. Urine spectra were then normalised to unit area to account for inter-sample concentration variation.

MatLab was used for multivariate modelling. Analysis included principal component analysis (PCA) using pareto scaled data to observe clustering in the datasets and identify outliers. Orthogonal projection to latent structures (OPLS) models were constructed using unit variance scaling to maximise any differences between the groups and to identify metabolites driving any potential differences between them. Metabolites were identified using an in-house database of standards and Chenomx NMR suite (version 7.7, Chenomx Inc).

6.3 Results

Clinical information was obtained from the participants in each group. Statistical analysis for the comparison of the clinical characteristics between the control and intervention group are presented in Table 1. Significant differences with age, BMI and blood pressure were observed between the two groups at baseline.

Table 6.1 Baseline clinical characteristics (mean ± SD)

	Control (*n*=25)	**Watercress (*n*=22)**	**P value**
Age (y)	58 ± 9	54 ± 8	**0.047**
BMI (kg/m²)	30.78 ± 6.96	27.27 ± 4.57	**0.044**
High blood pressure*	15	4	**0.003**
Smoker	1	4	0.178
Diabetes Mellitus	2	1	1.000
Oestrogen receptor (-)	3	1	0.612
Progesterone receptor (-)	4	0	0.112
Family History –Breast cancer	6	6	1.000
Family History – Other cancers	13	16	0.223

*Numerical data not available for blood pressure. Data was collected in a binomial form

6.4.5 Plasma metabonomic profiling

Metabolic profiles were measured from the plasma and urine samples of participants in the control and watercress intervention groups. Principal component analysis (PCA) was applied to these profiles to reveal sources of variation within the metabolic data.

The PCA scores plot obtained from the model built on all the baseline plasma profiles revealed separation in the first principal component by treatment group (control or watercress-treatment; PC1 R^2 = 44%; Fig. 6.1A). This indicates that before watercress consumption occurred the participants in this group were metabolically different from those in the control group. The loadings plot for PC1 from this model (Fig. 6.1B) shows that increased levels of VLDL in the control group and higher glycerol content in the

watercress intervention group explained the variation. The PCA model built on the plasma profiles at the end of RT returned similar results (Fig. 6.2). Inclusion of all four experimental groups in one PCA model (control baseline and end of RT, watercress baseline and end of RT) showed that plasma metabolic profiles differed between the two treatment groups along PC1 but there was not observable clustering by RT (baseline vs. RT) (Fig. 6.3) These results suggest that the differences between the two groups are most likely to arise from the differences in their baseline clinical characteristics.

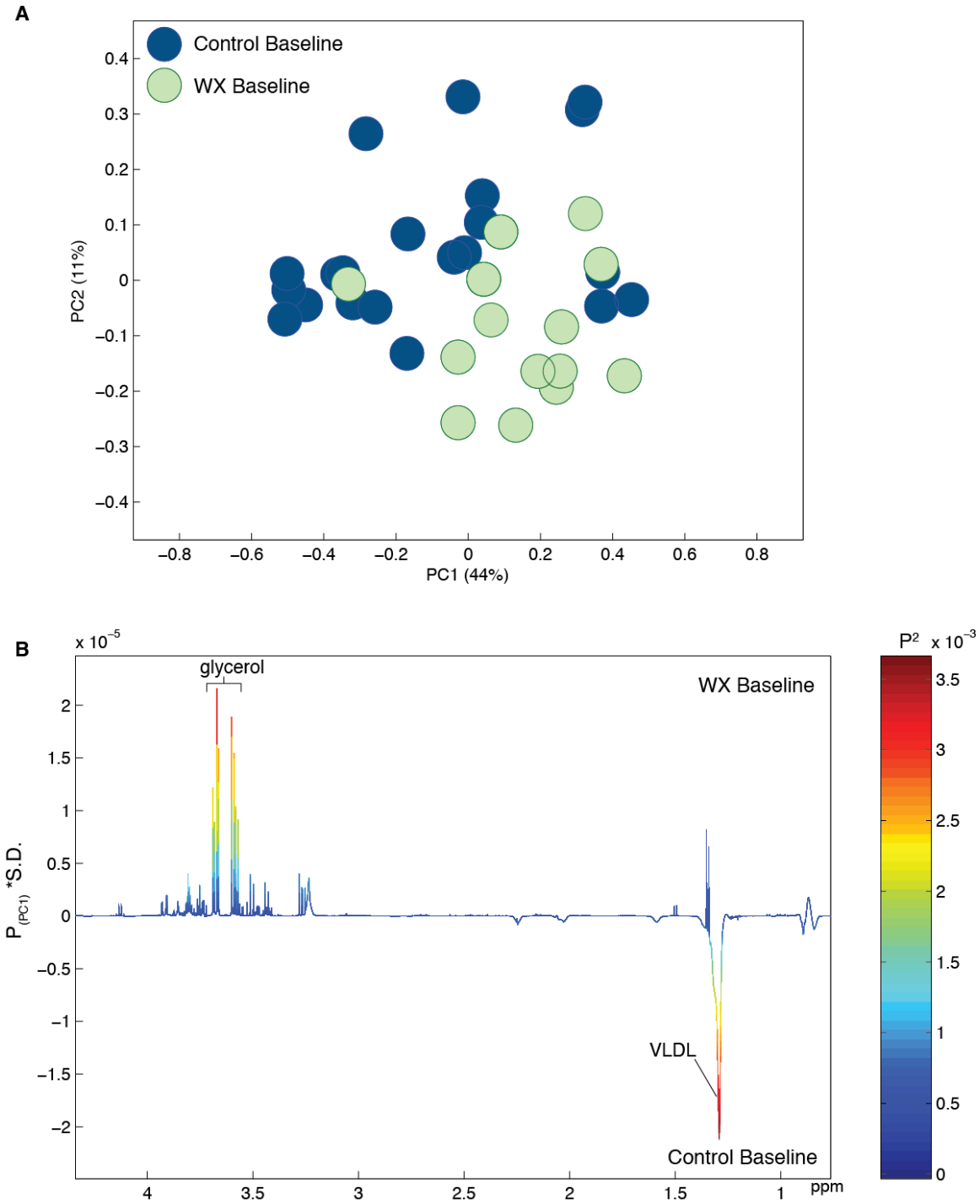

Figure 6.1 (A) PCA scores plot obtained from the plasma metabolic profiles of control and watercress consuming patients at baseline (B) PCA loadings plot for PC1.

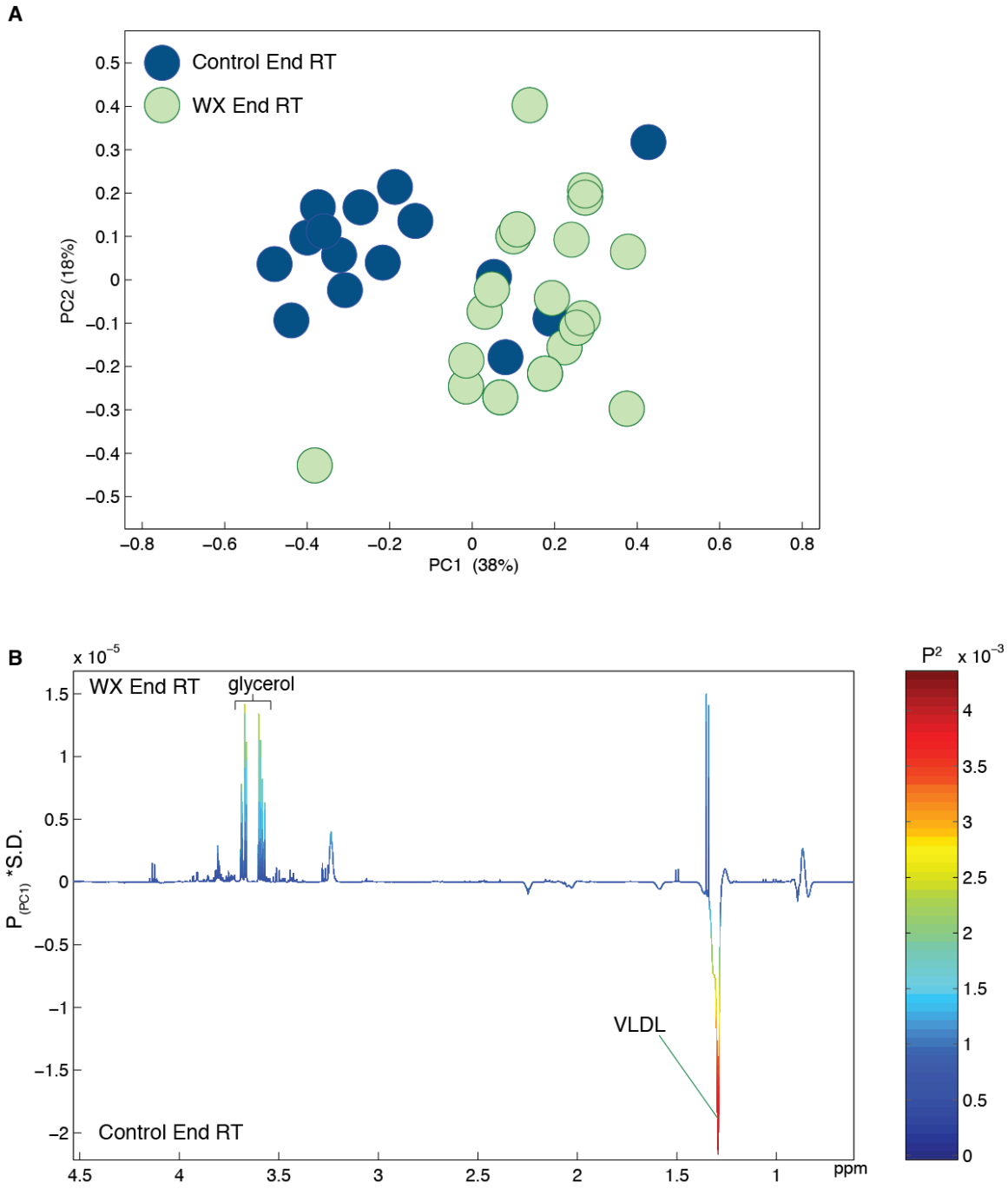

Figure 6.2 (A) PCA scores plot obtained from the plasma metabolic profiles of control and watercress consuming patients at the end of RT (B) PCA loadings plot for PC1.

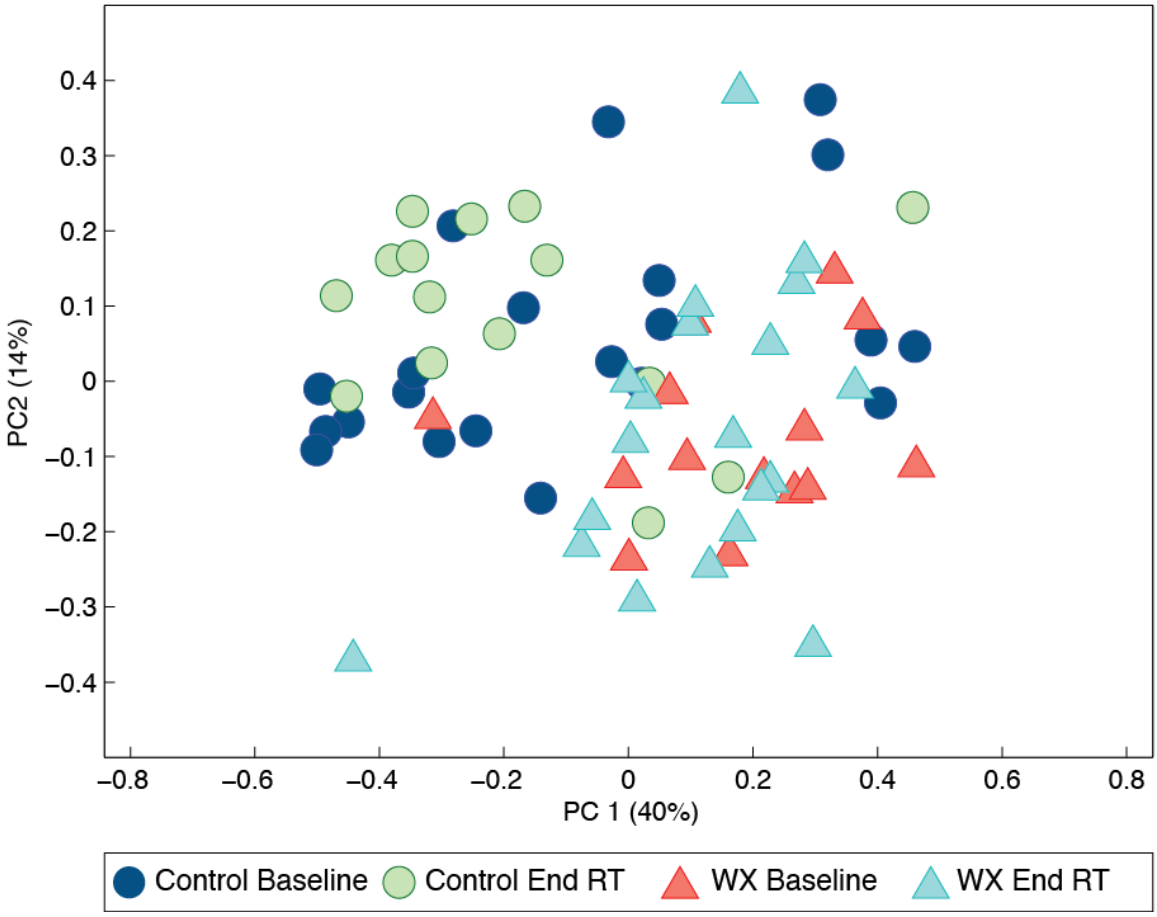

Figure 6.3 PCA scores plot comparing the plasma metabolic profiles of patients in the control group and those whose diet was supplemented with watercress (WX) at baseline and at the end of the radiotherapy treatment (RT). Profiles observed to cluster by treatment group.

Pairwise comparisons were performed between the treatment groups (control versus watercress) before and after RT using OPLS-DA models (Fig. 6.4). OPLS-DA models with good predictive ability were obtained comparing the two groups at baseline ($Q^2\hat{Y}$ = 0.18; p = 0.0110) and at the end of RT ($Q^2\hat{Y}$ = 0.26; p=0.0002). The metabolic variation between the control and watercress treated patients was found to be greater high-density lipoproteins (HDL) in the plasma from watercress treated-patients and higher VLDL in the control patients. These differences were present both at baseline (before watercress consumption) and after radiotherapy indicating that watercress intake was not driving these differences.

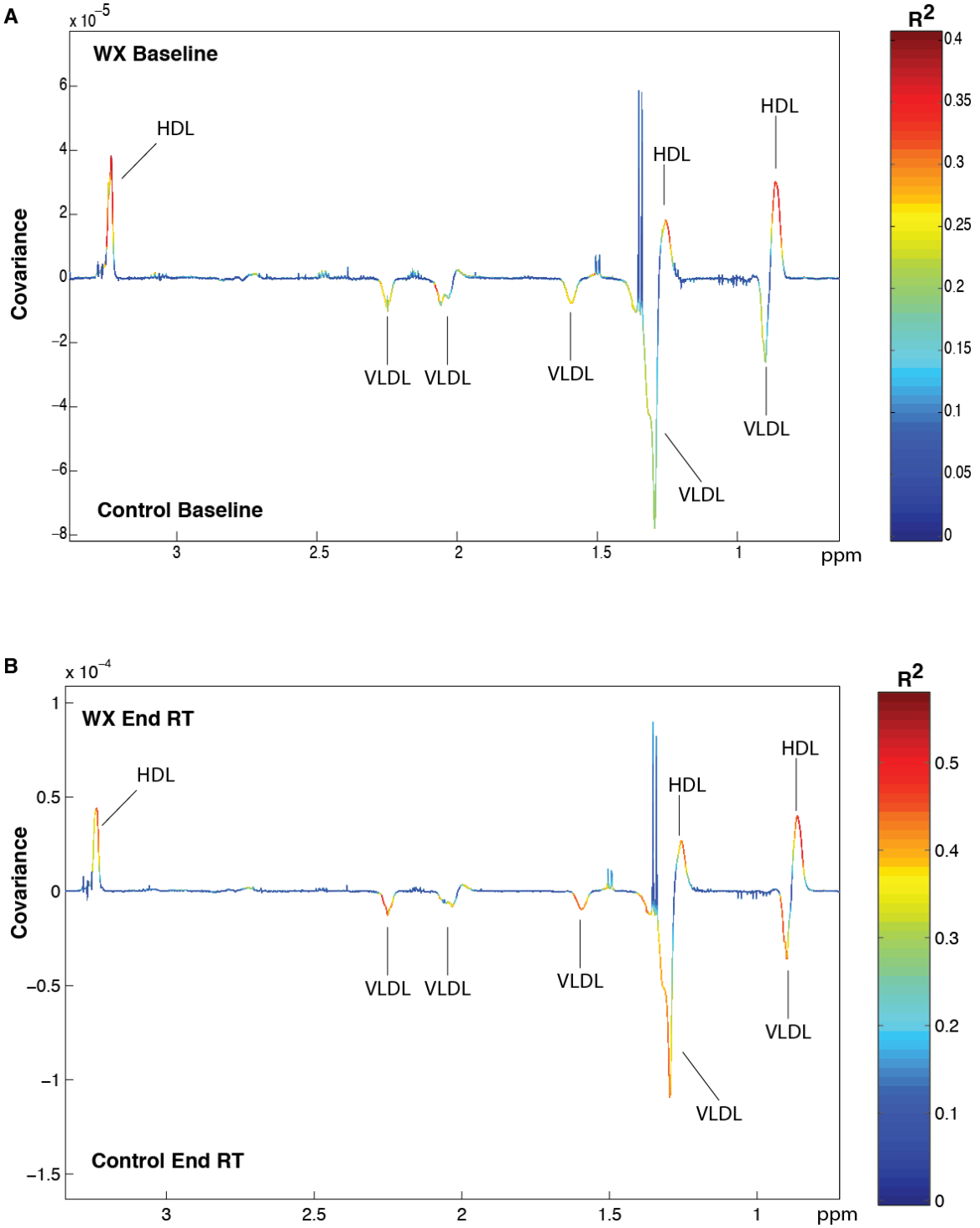

Figure 6.4 OPLS-DA models comparing the plasma metabolic profiles of control and watercress intervention groups at baseline ($Q^2\hat{Y}$ = 0.18; p = 0.0110) (A) and at the end of RT ($Q^2\hat{Y}$ = 0.26; p=0.0002). (B).

6.4.6 Urinary metabolic profiles

The PCA scores plot comparing all the urinary metabolic phenotypes from the study did not reveal any clustering in the dataset (Fig. 6.5A). The variance in the first component of this model was dominated by creatinine and hippurate (Fig. 6.5B) and trimethylamine-*N*-oxide exerted the greatest influence on the second principal component (Fig. 6.5C). The OPLS-DA model constructed to compare the the two groups at baseline was not valid ($Q^2\hat{Y}$ = -0.29, p = 0.89).

PCA analysis of the urinary metabolic profiles at the end of RT revealed clustering along the second principal component by treatment group (Fig. 6.6A). This component explained 12 % of the metabolic variation within the dataset. The biochemical signature of watercress consumption is characterised by higher excretion of hippurate (Fig. 6.6C). An OPLS-DA model was constructed to compare the urinary profiles of control volunteers and those consuming watercress post IR. This model identified significant metabolic variation between the two groups ($Q^2\hat{Y}$ = 0.2010, p = 0.01). Watercress consumption during RT correlated with increased excretion of hippurate and *N*-methyl-nicotinic acid (NMNA) (Fig.6.7).

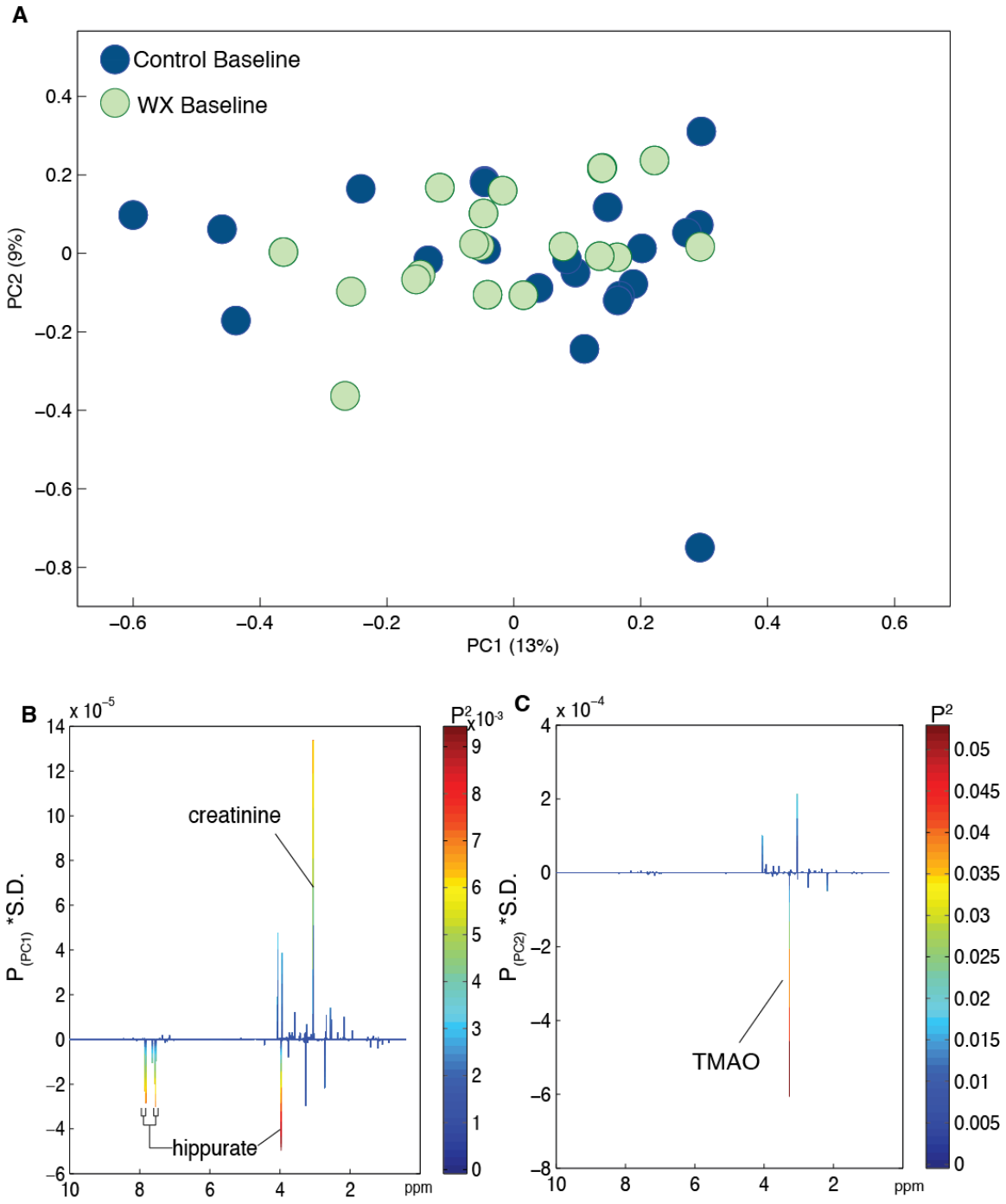

Figure 6.5 (A) PCA scores plot obtained from the urine metabolic profiles of control and watercress consuming patients at baseline. PCA loadings plot for PC1 (B) and PC2 (C).

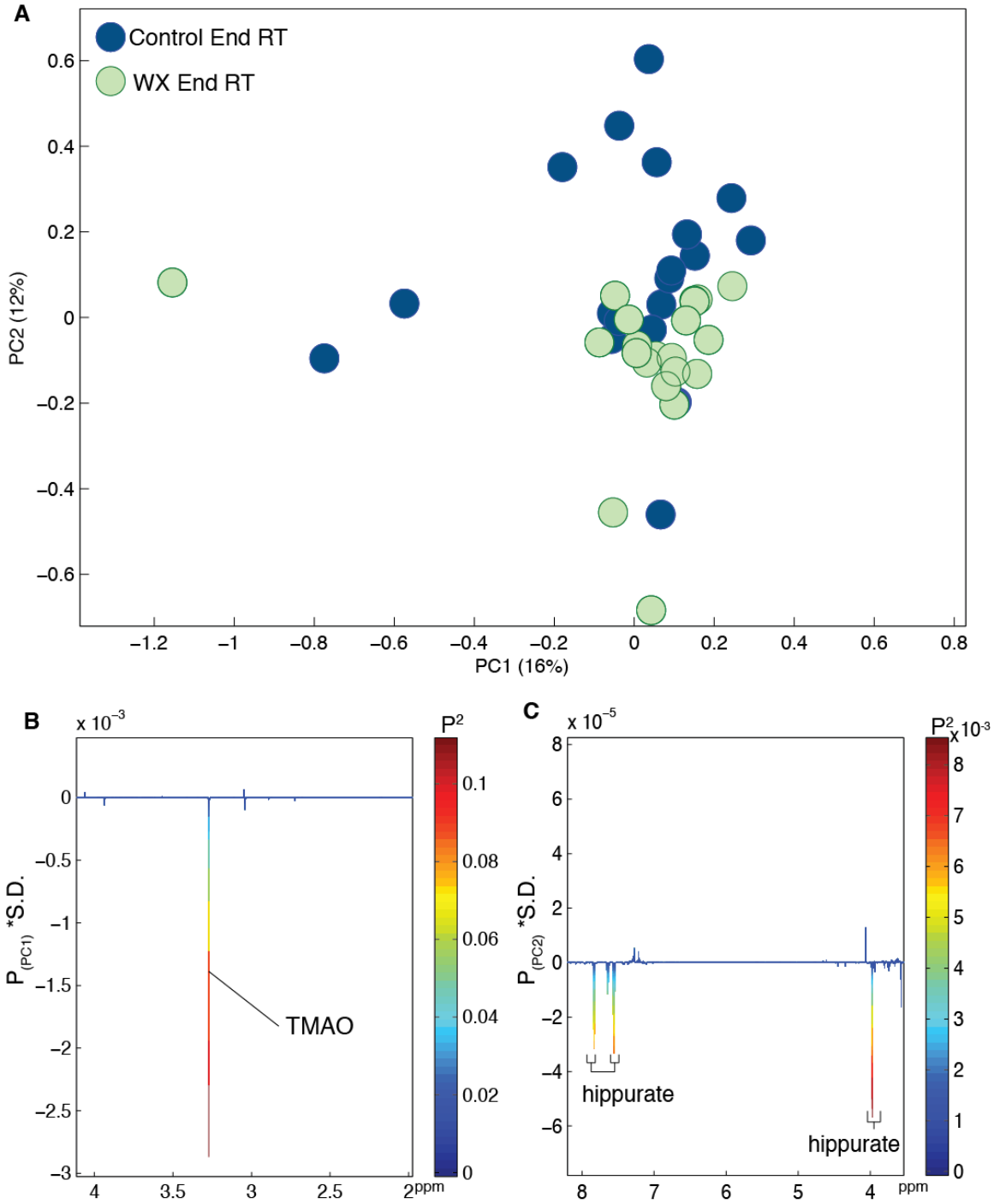

Figure 6.6 (A) PCA scores plot obtained from the urine metabolic profiles of control and watercress-consuming patients at the end of RT. PCA loadings plot for PC1 (B) and PC2 (C).

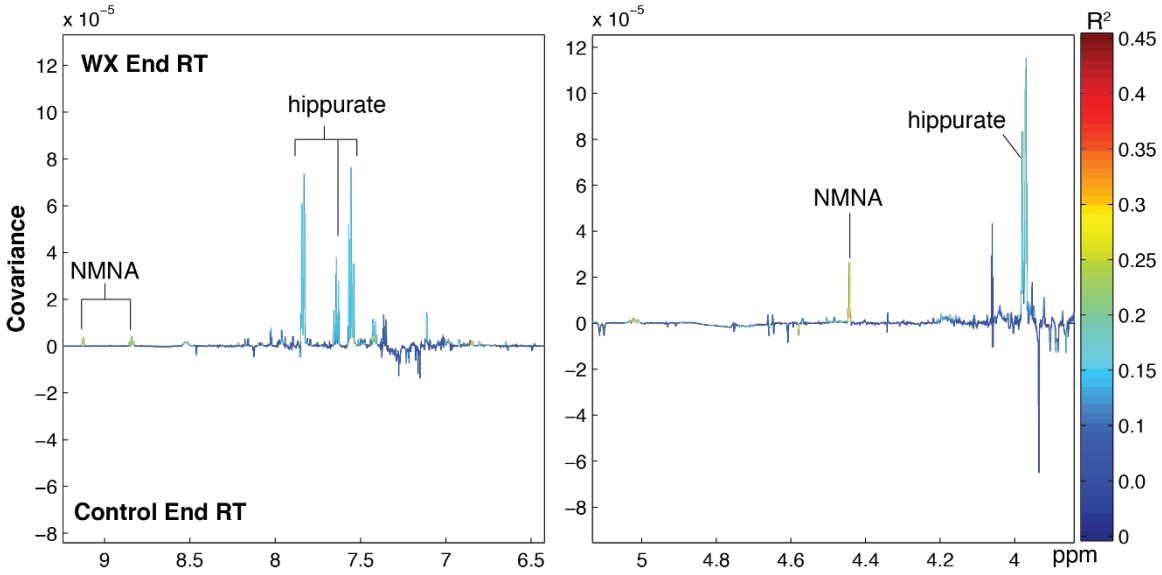

Figure 6.7 OPLS-DA model comparing the urine metabolic profiles of control and watercress intervention groups at the end of RT.

Table 6.2 Summary of the OPLS-DA models returned for the comparisons between the two treatment groups at baseline and at the end of RT.

Group Comparison	Plasma		Urine	
	Q^2Y	P value	Q^2Y	P value
Control Baseline vs WX Baseline	0.18	0.01	-0.29	0.89
Control End RT vs WX End RT	0.26	0.0002	0.20	0.01
Control Baseline vs Control End RT	-0.17	0.53	-0.20	0.59
WX Baseline vs WX End RT	-0.33	0.76	-0.57	0.99

6.4 Discussion

This prospective pilot clinical trial investigated the impact of watercress consumption on the response of early stage breast cancer patients to RT. ^{1}H NMR spectroscopy was employed to characterise the urinary and plasma metabolic profiles of breast cancer patients consuming 100 g/day of watercress (watercress group) and those with no watercress consumption (control group) before and after RT. Multivariate data analysis identified baseline metabolic variation between the participants assigned to the two treatment groups. Those in the control group had higher amounts of circulating VLDL whilst those in the watercress group had higher amounts of HDL cholesterol. These differences remained after watercress consumption and RT. VLDL carries fat from the liver to other parts of the body via the blood and is raised with a high-fat diet. In contrast, HDL collects excess cholesterol in the blood and returns it to the liver where it is broken down and removed. Hence, these lipoproteins can be associated with dietary intake and metabolic health. A significant difference in the BMI values of the two treatment groups was found with the control group having an average BMI of 30.78 kg/m^2 at baseline classifying them as 'moderately obese'. The watercress intervention group had a BMI of 27.27 kg/m^2, classified as overweight. BMI values remained significantly different at the end of the radiotherapy treatment. As a result of this major confounding factor comparisons between the two groups must be treated with considerable caution. These features also suggest that the watercress intervention group was likely already conscious about a healthy lifestyle of which a diet rich in fruits and vegetables is an essential element. Following breast cancer diagnosis, these women might have modified their usual habits towards a healthier well-being. As a result, any observations made here cannot necessarily be attributed to watercress.

Hippurate was found in higher concentrations in the urine of the watercress-consuming group at the end of RT. This is a gut microbial-mammalian co-metabolite and it is formed in the liver from the conjugation of dietary or microbially derived benzoic acid with glycine [235]. Watercress is a rich dietary source of phytochemicals including polyphenolic compounds. Metabolism of phenolic compounds such as chlorogenic acid, quinic acid and cinnamic acid results in a range of aromatic compounds like phenylpropionate, which can be further metabolised to benzoic acid and essentially, increase the amount of urinary hippurate [236]. In studies examining the metabolism and absorption of such polyphenols, hippurate was identified as the predominant urinary metabolite [237-240]. Further to this, a study comparing the urinary profiles from participants consuming either a low phytochemical diet without fruits and vegetables or a standard phytochemical diet, showed that the standard phytochemical diet was associated with increased hippurate excretion further substantiating the link between phytochemicals and hippurate [241].

Hippurate perturbations might also be attributed to potential modulation of the gut microbiota by watercress. Germ free animals do not excrete hippurate demonstrating the importance of the gut microbial activity in the production of hippurate [242, 243]. Cruciferous vegetables have the potential to modify the gut bacterial composition [244] and since certain bacterial species have been linked to specific reactions during the metabolism of particular phytochemicals [245] this can result in changes in the microbially derived urinary metabolites like hippurate.

It should be noted that hippurate can be considered as a potential biomarker of 'health' and conditions like high blood pressure and obesity have been correlated with the lower excretion of hippurate [246-249]. It is certainly of great interest observing increased

hippurate upon watercress consumption, but this result has to be treated with caution considering the differences in the clinical characteristics of the two groups at baseline. Hippurate is known to be inversely related to BMI and blood pressure Further to this, no significant shifts in hippurate concentrations were observed when comparing pre and post radiotherapy urine samples therefore no link between this metabolite and radiation induced damage can be established.

Urinary profiles of the cancer patients consuming watercress during their radiotherapy treatment exhibited an elevation in the excretion of NMNA (trigonelline). NMNA is a product of niacin metabolism and watercress is a good source if niacin and other vitamins of the B-complex. Other dietary sources of trigonelline are coffee as well as plants like fenugreek and garden peas. Trigonelline has been found to have anti-invasive activity against cancer cells *in vitro* and has also been shown to have beneficial anti-diabetic actions.

Several limitations in the study should be discussed. The small number of subjects in each group is likely to under-power the study, particular in a metabolic profiling study where the high number of variables increases the amount of inter-individual variability across the study. Also the sample size was too small for subgroup analyses and most importantly affected the randomisation efficacy for allocation of the volunteers in the treatment groups. Flawed randomisation resulted in significantly different baseline characteristics between the two groups, as discussed above, preventing us from drawing unbiased and meaningful conclusions from the analyses. Additionally, no direct therapeutic outcomes were recorded such as tumour size or patient survival that could be used as a measure of treatment and/or watercress efficacy.

In summary, this study provides some initial [236]indications that watercress could potentially induce metabolic perturbations in biomarkers of health in breast cancer patients possibly aiding in the management of RT induced DNA damage and subsequent side effects. Undoubtedly, further studies with larger intervention groups and better randomisation strategies are required to verify our observations and explore the possible mechanism for watercress' anti-cancer effect.

7 Final discussion

The framework for this thesis was developed from the work of Boyd *et al.* [53] that provided initial data on the direct anti-cancer effects of watercress *in vitro* as well as from two human trials [57] [52] that demonstrated the potential of watercress consumption to reduce DNA damage and increase antioxidant status in adults. As discussed in **Chapter 1** watercress and Brassica vegetables in general, have received great attention for their anti-cancer properties. Most of the health properties attributed to Brassica are due to their high content of glucosinolate-derived bioactives ITCs, and more specifically, in the case of watercress, gluconasturtiin-derived PEITC. PEITC has been extensively shown to inhibit established hallmarks of cancer, supported by a great number of published *in vitro* and animal studies. The effects of watercress and PEITC on cellular energetics and metabolism, which represent essential processes in cancer progression, are largely unexplored. As such, the main aim of this thesis was to investigate the impact of watercress on breast cancer development as well as to examine how watercress interacts with cancer and radiotherapy and understand the different outcomes and biochemical mechanisms underlying this interaction. To address the knowledge gap regarding the lack of metabolic data, a substantial part of this thesis is dedicated to profiling the biochemical effects that watercress and PEITC can have in cancer, using ^{1}H NMR metabonomics.

In **Chapter 3** the metabolic signature of breast cancer *in vitro* was defined by comparing the metabolic phenotypes of breast cancer and healthy cell lines. The profile obtained for the breast cancer cells was consistent with that of rapidly proliferating cells as indicated by the high amount of phosphocholine and glycolytic characteristics. The distinct metabolic perturbations induced by increasing doses of a watercress extract and PEITC were then examined and compared between the two cell lines. Untargeted

metabolic profiling enabled a vast range of metabolites to be screened allowing a broad overview of the metabolic state to be captured. Through this approach, watercress and PEITC were found to perturb a range of pathways and processes, such as oxidative phosphorylation, glycolysis, and one-carbon metabolism. This also provided further evidence supporting the major role of PEITC in the inhibition of mRNA translation in cancer models contributing to its chemopreventive and anti-cancer effects [250].

The results obtained from **Chapter 3** confirmed PEITC as a GSH depleting agent. Interestingly, this effect was specific to the breast cancer cell line. Glutathione depletion by PEITC is the main mechanism through which excessive ROS are formed intracellularly leading to substantial DNA damage and eventually leading to cell death. On the basis of these results oxidative stress and the pro-oxidant phenotype induced by PEITC is hypothesised to increase the sensitivity of the cancer cells to radiation induced damage, which is ROS mediated. Indeed, this is supported by results in **Chapter 4** where a concomitant increase in DNA damage and GSH depletion was observed in the cancer cell model treated with IR and PEITC. This highlights the radiosensitising potential of this compound.

Watercress pre-treatment protected the healthy breast cells from radiation-induced damage as observed by lower levels of DNA damage. This observation was parallel to an increased glutathione content in these cells. Higher abundance of GSH antioxidant is likely to rescue the cells from ROS-induced damage. Findings from human intervention studies with watercress have provided considerable evidence for a prophylactic effect of watercress under pro-oxidant conditions similar to radiotherapy, such as smoking [57] and exhaustive exercise [52]. These effects were explained by shifts in lipophilic compounds like carotenoids, of which watercress is a very rich source, and by

reducing the amount of DNA damage in lymphocytes. It should be noted though, that ITCs bioavailability or excretion was not measured in these studies, therefore it is unknown if any of the protective effects observed were mediated by these compounds. Further to this, the interaction between watercress and the glutathione related detoxification enzymes (GPX, GST) is inconclusive and depends highly on the individual's genotype. The rescuing effect of watercress in the healthy breast cell observed here is unlikely to be a result of PEITC, since the watercress extract used is devoid of this compound. ITCs are highly volatile compounds and do not survive the extraction process. Therefore, we can speculate that the prophylactic effect of watercress *in vitro* is a result of other phytochemicals like carotenoids and polyphenols. Extensive phytochemical profiling of watercress performed in **Chapter 5** further supported this observation.

While watercress did not appear to induce any genotoxicity **(Chapter 3)** in either of the two cell lines under study, PEITC at high doses caused significant DNA damage in both breast cancer and healthy cells. This observation generates further evidence for the hormetic properties of phytochemicals that is, being beneficial at low doses but leading to toxicity when ingested at high doses. It is unlikely though that these toxic exposures will be reached through the human diet.

Findings from **Chapter 5** were used to formulate suggestions for participants in the human trial reported in **Chapter 6** regarding the preferable ways of cooking watercress before consumption to preserve phytochemical density. Cooking of Brassica is known to inactivate the myrosinase enzyme, which is responsible for the conversion of glucosinolates to bioactive ITCs. However, bacteria in the gut possess myrosinase activity and present a potential means through which ITCs can arise in circulation and possibly mediate the health benefits of glucosinolates to the host. The degree to which this is

occurring is unclear and merits further investigation [251]. The significant role of the gut microbiome was also apparent from the increased urinary excretion of the hippurate, a gut-derived metabolite associated with the consumption of polyphenols and a general biomarker of health, in the group of volunteers consuming watercress. These observations highlight the importance of incorporating metagenomic and metabonomic data in the interpretation of clinical trials and epidemiological studies examining the anti-cancer potential of Brassica vegetables.

Results from *in vitro* (and animal) studies examining the impact of whole plant extracts or specific phytochemicals on health and disease can be highly informative. However, caution should be taken when interpreting these observations and drawing conclusions about the potential benefits they can confer to humans. Evidence derived from such studies regarding the mechanisms of action of phytochemicals in Brassica vegetables might not translate to the human. These studies ignore the role of the food matrix in the observed effects since they only use whole juice extracts from the plant under study. More work focusing on the processes of absorption, metabolism, and excretion upon watercress ingestion, has to be undertaken. Phytochemicals contained in watercress like glucosinolates and their hydrolysis products as well as flavonols, undergo complex modifications and conjugations when in the system. The form and quantity at which they reach the target site are poorly understood and they are affected by multi-organ interactions, the gut microbiome and variations in individual's genotype. **Chapter 5** has also highlighted the importance of preparation and cooking methods on the quality and quantity of the ingested phytochemicals.

Study limitations and future perspectives

The work described in this thesis, has addressed a number of research questions, while highlighting some opportunities for future research. Further work would advance our understanding regarding the molecular mechanisms of action of watercress and PEITC in cancer and provide further data on the relevance of watercress consumption during breast cancer therapy *in vivo*.

Breast cancer is a highly heterogeneous disease, with distinct molecular subtypes leading to differential responses to target therapies. The experiments in this thesis were carried out using MCF-7 breast cancer cells and MCF-10A healthy cells. MCF-10A cells are the most commonly used healthy breast cells and represent the best model for the study of normal human mammary epithelial function available to date. On the other hand, MCF-7 cells represent only one molecular subtype of breast cancer. Consequently, further work should be carried out to examine whether the findings from the experiments carried out in this thesis are consistent with other *in vitro* models of breast cancer, which represent different degrees of sensitivity, endocrine responsiveness, metastatic potential and immunoprofile.

In **Chapter 3** significant shifts in the levels of lactate were observed upon treatment with watercress and PEITC in both cells lines suggestive of disruptions in oxidative and glycolytic metabolism. Increased lactate is postulated to arise from a compromised ability for oxidative phosphorylation due to mitochondrial membrane damage and a switching of cells to glycolysis as a last resort for energy acquisition. As discussed previously glycolysis is a key pathway in cancer cell metabolism, therefore further work is recommended to elucidate the mechanism behind our observation. Real-time rates of oxidative phosphorylation and glycolysis can be studied using Seahorse Cell

Analysis™, which provides functional cellular metabolic data. Furthermore, experiments using radiolabeled glucose isotopes to study glucose uptake and metabolism combined with glucose and lactate transporters expression data could provide a more mechanistic overview on the impact of watercress and PEITC on glucose cellular energetics.

In **Chapter 4** a protective effect of watercress against radiation induced damage in healthy breast cells was observed parallel to a radiosensitising impact of PEITC in breast cancer cells. Cell cycle and Comet assay data supported these observations, however additional experiments are required to further explore these effects. Transcriptomics for the interrogation of DNA damage, apoptosis, as well as repair pathways would further our understanding of the chemoprotective effect of watercress and the genotoxic effect of PEITC. Information obtained from such an exploratory approach could be integrated with metabonomic data and provide a better picture of the interactions between genetic, metabolic and physiological shifts in an irradiation-perturbed system.

Despite obtaining encouraging results from the *in vitro* work performed; the results could not be validated *in vivo* **(Chapter 6)** therefore the relevance of our observations remains to be examined. This was a consequence of a flawed study design, characterised by low participant numbers, as well as an incorrect randomisation strategy and no record of treatment endpoints from the patients enrolled in the trial. A revised clinical trial investigating the impact of watercress consumption during radiotherapy should be performed. It is recommended that the new study should be performed at a hospital with a high intake of breast cancer patients to allow for the recruitment of enough volunteers to adequately power the study. The study design should consist of four treatment groups: a) healthy individuals on their habitual diet, b) healthy individuals consuming watercress, c) breast cancer patients undergoing radiotherapy without consuming watercress and d)

breast cancer patients consuming watercress throughout their radiotherapy treatment. Collection of plasma and urine samples from volunteers in these groups would help draw meaningful conclusions on the metabolic fingerprint of breast cancer, radiotherapy and a nutritional intervention through watercress ingestion. Pre-screening of the participants prior to their participation in the clinical trial is of paramount importance to avoid the introduction of bias from differences in anthropometric and physiological factors. In addition, a proper randomisation method should be employed to ensure the acquisition of valid and interpretable results. Additionally, treatment endpoints such as radiotherapy efficacy as described by tumour size and histopathological measures, as well as cancer recurrence, should be recorder for all participants in the trial. This will allow for the correlation of metabonomic measures with cancer treatment outcomes and the generation of meaningful results.

Concluding remark

This thesis has provided evidence for the potential of watercress and PEITC to induce significant metabolic perturbations in breast cancer, a previously unexplored area. Novel preliminary evidence have been obtained, for the potential prophylactic impact of watercress during radiotherapy, through protecting healthy tissue from damage as well as enhancing the therapeutic outcomes of the treatment. The systemic impact of watercress against breast cancer should be further explored, for the generation of robust evidence in support of the current, promising findings.

References

1. Hanahan, D. and R.A. Weinberg, *The hallmarks of cancer.* Cell, 2000. **100**(1): p. 57-70.
2. Hanahan, D. and R.A. Weinberg, *Hallmarks of cancer: the next generation.* Cell, 2011. **144**(5): p. 646-74.
3. Zhang, B., et al., *Genetic variants associated with breast-cancer risk: comprehensive research synopsis, meta-analysis, and epidemiological evidence.* Lancet Oncol, 2011. **12**(5): p. 477-88.
4. Boughey, J.C., et al., *Neoadjuvant chemotherapy in invasive lobular carcinoma may not improve rates of breast conservation.* Ann Surg Oncol, 2009. **16**(6): p. 1606-11.
5. Li, C.I., et al., *Risk of invasive breast carcinoma among women diagnosed with ductal carcinoma in situ and lobular carcinoma in situ, 1988-2001.* Cancer, 2006. **106**(10): p. 2104-12.
6. Shou, J., et al., *Mechanisms of tamoxifen resistance: increased estrogen receptor-HER2/neu cross-talk in ER/HER2-positive breast cancer.* J Natl Cancer Inst, 2004. **96**(12): p. 926-35.
7. Smith, I.E. and M. Dowsett, *Aromatase inhibitors in breast cancer.* N Engl J Med, 2003. **348**(24): p. 2431-42.
8. Slamon, D.J., et al., *Use of chemotherapy plus a monoclonal antibody against HER2 for metastatic breast cancer that overexpresses HER2.* N Engl J Med, 2001. **344**(11): p. 783-92.
9. Goldhirsch, A. and R.D. Gelber, *Endocrine therapies of breast cancer.* Semin Oncol, 1996. **23**(4): p. 494-505.
10. Yakes, F.M., et al., *Herceptin-induced inhibition of phosphatidylinositol-3 kinase and Akt Is required for antibody-mediated effects on p27, cyclin D1, and antitumor action.* Cancer Res, 2002. **62**(14): p. 4132-41.
11. Le, X.F., F. Pruefer, and R.C. Bast, Jr., *HER2-targeting antibodies modulate the cyclin-dependent kinase inhibitor p27Kip1 via multiple signaling pathways.* Cell Cycle, 2005. **4**(1): p. 87-95.
12. Anders, C.K., et al., *The Evolution of Triple-Negative Breast Cancer: From Biology to Novel Therapeutics.* Am Soc Clin Oncol Educ Book, 2016. **35**: p. 34-42.
13. Hudis, C.A. and L. Gianni, *Triple-negative breast cancer: an unmet medical need.* Oncologist, 2011. **16 Suppl 1**: p. 1-11.
14. Glover, D. and V. Harmer, *Radiotherapy-induced skin reactions: assessment and management.* Br J Nurs, 2014. **23**(4): p. S28, S30-5.
15. Clarke, M., et al., *Effects of radiotherapy and of differences in the extent of surgery for early breast cancer on local recurrence and 15-year survival: an overview of the randomised trials.* Lancet, 2005. **366**(9503): p. 2087-106.
16. Clinic, M. *Radiation Therapy*. 2016 [cited 2016 13/10/2016]; Available from: http://www.mayoclinic.org/tests-procedures/radiation-therapy/multimedia/radiation-therapy/img-20005977.
17. Houtgraaf, J.H., J. Versmissen, and W.J. van der Giessen, *A concise review of DNA damage checkpoints and repair in mammalian cells.* Cardiovasc Revasc Med, 2006. **7**(3): p. 165-72.
18. Azzam, E.I., J.P. Jay-Gerin, and D. Pain, *Ionizing radiation-induced metabolic oxidative stress and prolonged cell injury.* Cancer Lett, 2012. **327**(1-2): p. 48-60.
19. Drooger, J., et al., *Adjuvant radiotherapy for primary breast cancer in BRCA1 and BRCA2 mutation carriers and risk of contralateral breast cancer with special attention*

to patients irradiated at younger age. Breast Cancer Res Treat, 2015. **154**(1): p. 171-80.
20. Hubenak, J.R., et al., *Mechanisms of injury to normal tissue after radiotherapy: a review.* Plast Reconstr Surg, 2014. **133**(1): p. 49e-56e.
21. Kirova, Y.M., et al., *Risk of second malignancies after adjuvant radiotherapy for breast cancer: a large-scale, single-institution review.* Int J Radiat Oncol Biol Phys, 2007. **68**(2): p. 359-63.
22. Cairns, R.A., I.S. Harris, and T.W. Mak, *Regulation of cancer cell metabolism.* Nat Rev Cancer, 2011. **11**(2): p. 85-95.
23. DeBerardinis, R.J. and N.S. Chandel, *Fundamentals of cancer metabolism.* Sci Adv, 2016. **2**(5): p. e1600200.
24. Hanahan, D. and L.M. Coussens, *Accessories to the crime: functions of cells recruited to the tumor microenvironment.* Cancer Cell, 2012. **21**(3): p. 309-22.
25. Pavlova, N.N. and C.B. Thompson, *The Emerging Hallmarks of Cancer Metabolism.* Cell Metab, 2016. **23**(1): p. 27-47.
26. Lunt, S.J., N. Chaudary, and R.P. Hill, *The tumor microenvironment and metastatic disease.* Clin Exp Metastasis, 2009. **26**(1): p. 19-34.
27. Warburg, O., F. Wind, and E. Negelein, *THE METABOLISM OF TUMORS IN THE BODY.* The Journal of General Physiology, 1927. **8**(6): p. 519-530.
28. Vander Heiden, M.G., L.C. Cantley, and C.B. Thompson, *Understanding the Warburg effect: the metabolic requirements of cell proliferation.* Science, 2009. **324**(5930): p. 1029-33.
29. Krall, A.S., et al., *Asparagine promotes cancer cell proliferation through use as an amino acid exchange factor.* Nat Commun, 2016. **7**: p. 11457.
30. Vaughn, A.E. and M. Deshmukh, *Glucose metabolism inhibits apoptosis in neurons and cancer cells by redox inactivation of cytochrome c.* Nat Cell Biol, 2008. **10**(12): p. 1477-83.
31. Comerford, S.A., et al., *Acetate dependence of tumors.* Cell, 2014. **159**(7): p. 1591-602.
32. Mashimo, T., et al., *Acetate is a bioenergetic substrate for human glioblastoma and brain metastases.* Cell, 2014. **159**(7): p. 1603-14.
33. Schug, Z.T., et al., *Acetyl-CoA synthetase 2 promotes acetate utilization and maintains cancer cell growth under metabolic stress.* Cancer Cell, 2015. **27**(1): p. 57-71.
34. Glunde, K., Z.M. Bhujwalla, and S.M. Ronen, *Choline metabolism in malignant transformation.* Nat Rev Cancer, 2011. **11**(12): p. 835-48.
35. Galons, J.P., C. Job, and R.J. Gillies, *Increase of GPC levels in cultured mammalian cells during acidosis. A 31P MR spectroscopy study using a continuous bioreactor system.* Magn Reson Med, 1995. **33**(3): p. 422-6.
36. Glunde, K., et al., *Hypoxia regulates choline kinase expression through hypoxia-inducible factor-1 alpha signaling in a human prostate cancer model.* Cancer Res, 2008. **68**(1): p. 172-80.
37. Gunther, U.L., *Metabolomics Biomarkers for Breast Cancer.* Pathobiology, 2015. **82**(3-4): p. 153-65.
38. Giannoni, E., et al., *Intracellular reactive oxygen species activate Src tyrosine kinase during cell adhesion and anchorage-dependent cell growth.* Mol Cell Biol, 2005. **25**(15): p. 6391-403.
39. Lee, S.R., et al., *Reversible inactivation of the tumor suppressor PTEN by H2O2.* J Biol Chem, 2002. **277**(23): p. 20336-42.

40. Takahashi, A., et al., *Mitogenic signalling and the p16INK4a-Rb pathway cooperate to enforce irreversible cellular senescence.* Nat Cell Biol, 2006. **8**(11): p. 1291-7.
41. Garrido, C., et al., *Mechanisms of cytochrome c release from mitochondria.* Cell Death Differ, 2006. **13**(9): p. 1423-33.
42. Harris, I.S. and J.S. Brugge, *Cancer: The enemy of my enemy is my friend.* Nature, 2015. **527**(7577): p. 170-1.
43. Schafer, Z.T., et al., *Antioxidant and oncogene rescue of metabolic defects caused by loss of matrix attachment.* Nature, 2009. **461**(7260): p. 109-13.
44. Raderer, M. and W. Scheithauer, *Clinical trials of agents that reverse multidrug resistance. A literature review.* Cancer, 1993. **72**(12): p. 3553-63.
45. Brockmoller, S.F., et al., *Integration of metabolomics and expression of glycerol-3-phosphate acyltransferase (GPAM) in breast cancer-link to patient survival, hormone receptor status, and metabolic profiling.* J Proteome Res, 2012. **11**(2): p. 850-60.
46. Tang, X., et al., *A joint analysis of metabolomics and genetics of breast cancer.* Breast Cancer Res, 2014. **16**(4): p. 415.
47. Budczies, J., et al., *Glutamate enrichment as new diagnostic opportunity in breast cancer.* Int J Cancer, 2015. **136**(7): p. 1619-28.
48. Tenori, L., et al., *Exploration of serum metabolomic profiles and outcomes in women with metastatic breast cancer: a pilot study.* Mol Oncol, 2012. **6**(4): p. 437-44.
49. Tenori, L., et al., *Serum metabolomic profiles evaluated after surgery may identify patients with oestrogen receptor negative early breast cancer at increased risk of disease recurrence. Results from a retrospective study.* Mol Oncol, 2015. **9**(1): p. 128-39.
50. Jobard, E., et al., *A serum nuclear magnetic resonance-based metabolomic signature of advanced metastatic human breast cancer.* Cancer Lett, 2014. **343**(1): p. 33-41.
51. Palaniswamy, U.R. and R.J. McAvoy, *Watercress: A Salad Crop with Chemopreventive Potential.* HortTechnology, 2001. **11**(4): p. 622-626.
52. Fogarty, M.C., et al., *Acute and chronic watercress supplementation attenuates exercise-induced peripheral mononuclear cell DNA damage and lipid peroxidation.* Br J Nutr, 2013. **109**(2): p. 293-301.
53. Boyd, L.A., et al., *Assessment of the anti-genotoxic, anti-proliferative, and anti-metastatic potential of crude watercress extract in human colon cancer cells.* Nutr Cancer, 2006. **55**(2): p. 232-41.
54. Fahey, J.W., A.T. Zalcmann, and P. Talalay, *The chemical diversity and distribution of glucosinolates and isothiocyanates among plants.* Phytochemistry, 2001. **56**(1): p. 5-51.
55. Rask, L., et al., *Myrosinase: gene family evolution and herbivore defense in Brassicaceae.* Plant Mol Biol, 2000. **42**(1): p. 93-113.
56. Dinkova-Kostova, A.T. and R.V. Kostov, *Glucosinolates and isothiocyanates in health and disease.* Trends Mol Med, 2012. **18**(6): p. 337-47.
57. Gill, C.I.R., et al., *Watercress supplementation in diet reduces lymphocyte DNA damage and alters blood antioxidant status in healthy adults.* American Journal of Clinical Nutrition, 2007. **85**(2): p. 504-510.
58. Rose, P., et al., *7-Methylsulfinylheptyl and 8-methylsulfinyloctyl isothiocyanates from watercress are potent inducers of phase II enzymes.* Carcinogenesis, 2000. **21**(11): p. 1983-8.
59. Zhang, Y., S. Yao, and J. Li, *Vegetable-derived isothiocyanates: anti-proliferative activity and mechanism of action.* Proc Nutr Soc, 2006. **65**(1): p. 68-75.

60. Zhang, Y., *Molecular mechanism of rapid cellular accumulation of anticarcinogenic isothiocyanates.* Carcinogenesis, 2001. **22**(3): p. 425-31.
61. Cavell, B.E., et al., *Anti-angiogenic effects of dietary isothiocyanates: mechanisms of action and implications for human health.* Biochem Pharmacol, 2011. **81**(3): p. 327-36.
62. Wu, X., Q.H. Zhou, and K. Xu, *Are isothiocyanates potential anti-cancer drugs?* Acta Pharmacol Sin, 2009. **30**(5): p. 501-12.
63. Bell and C. Wagstaff, *Glucosinolates, Myrosinase Hydrolysis Products, and Flavonols Found in Rocket (Eruca sativa and Diplotaxis tenuifolia).* Journal of Agricultural and Food Chemistry, 2014. **62**(20): p. 4481-4492.
64. Tang, L., et al., *The principal urinary metabolites of dietary isothiocyanates, N-acetylcysteine conjugates, elicit the same anti-proliferative response as their parent compounds in human bladder cancer cells.* Anticancer Drugs, 2006. **17**(3): p. 297-305.
65. Chung, F.L., et al., *Quantitation of human uptake of the anticarcinogen phenethyl isothiocyanate after a watercress meal.* Cancer Epidemiol Biomarkers Prev, 1992. **1**(5): p. 383-8.
66. Seow, A., H. Vainio, and M.C. Yu, *Effect of glutathione-S-transferase polymorphisms on the cancer preventive potential of isothiocyanates: an epidemiological perspective.* Mutat Res, 2005. **592**(1-2): p. 58-67.
67. Spitz, M.R., et al., *Dietary intake of isothiocyanates: Evidence of a joint effect with glutathione S-transferase polymorphisms in lung cancer risk.* Cancer Epidemiology Biomarkers & Prevention, 2000. **9**(10): p. 1017-1020.
68. Wang, L.I., et al., *Dietary intake of Cruciferous vegetables, Glutathione S-transftrase (GST) polymorphisms and lung cancer risk in a Caucasian population.* Cancer Causes & Control, 2004. **15**(10): p. 977-985.
69. Lam, T.K., et al., *Cruciferous vegetable consumption and lung cancer risk: a systematic review.* Cancer Epidemiol Biomarkers Prev, 2009. **18**(1): p. 184-95.
70. Dyba, M., et al., *Metabolism of isothiocyanates in individuals with positive and null GSTT1 and M1 genotypes after drinking watercress juice.* Clin Nutr, 2010. **29**(6): p. 813-8.
71. Morel, I., et al., *Role of flavonoids and iron chelation in antioxidant action.* Methods Enzymol, 1994. **234**: p. 437-43.
72. Doostdar, H., M.D. Burke, and R.T. Mayer, *Bioflavonoids: selective substrates and inhibitors for cytochrome P450 CYP1A and CYP1B1.* Toxicology, 2000. **144**(1-3): p. 31-8.
73. Galati, G., et al., *Cancer chemoprevention and apoptosis mechanisms induced by dietary polyphenolics.* Drug Metabol Drug Interact, 2000. **17**(1-4): p. 311-49.
74. Franke, A.A., et al., *Vitamin C and flavonoid levels of fruits and vegetables consumed in Hawaii.* Journal of Food Composition and Analysis, 2004. **17**(1): p. 1-35.
75. USDA, *USDA Nutrient Data Laboratory.* Choice: Current Reviews for Academic Libraries, 2013. **42**: p. 153-153.
76. Hart, D.J. and K.J. Scott, *Development and Evaluation of an Hplc Method for the Analysis of Carotenoids in Foods, and the Measurement of the Carotenoid Content of Vegetables and Fruits Commonly Consumed in the Uk.* Food Chemistry, 1995. **54**(1): p. 101-111.
77. O'Neill, M.E., et al., *A European carotenoid database to assess carotenoid intakes and its use in a five-country comparative study.* Br J Nutr, 2001. **85**(4): p. 499-507.

78. Wogan, G.N., et al., *Environmental and chemical carcinogenesis.* Semin Cancer Biol, 2004. **14**(6): p. 473-86.
79. Gross-Steinmeyer, K., et al., *Phytochemical-induced changes in gene expression of carcinogen-metabolizing enzymes in cultured human primary hepatocytes.* Xenobiotica, 2004. **34**(7): p. 619-32.
80. Nakajima, M., et al., *Inhibition and inactivation of human cytochrome P450 isoforms by phenethyl isothiocyanate.* Drug Metab Dispos, 2001. **29**(8): p. 1110-3.
81. Yoshigae, Y., et al., *The inactivation of human CYP2E1 by phenethyl isothiocyanate, a naturally occurring chemopreventive agent, and its oxidative bioactivation.* Drug Metab Dispos, 2013. **41**(4): p. 858-69.
82. Gross-Steinmeyer, K., et al., *Sulforaphane- and phenethyl isothiocyanate-induced inhibition of aflatoxin B1-mediated genotoxicity in human hepatocytes: role of GSTM1 genotype and CYP3A4 gene expression.* Toxicol Sci, 2010. **116**(2): p. 422-32.
83. Morris, C.R., et al., *Inhibition by allyl sulfides and phenethyl isothiocyanate of methyl-n-pentylnitrosamine depentylation by rat esophageal microsomes, human and rat CYP2E1, and Rat CYP2A3.* Nutr Cancer, 2004. **48**(1): p. 54-63.
84. Yuan, J.M., et al., *Clinical Trial of 2-Phenethyl Isothiocyanate as an Inhibitor of Metabolic Activation of a Tobacco-Specific Lung Carcinogen in Cigarette Smokers.* Cancer Prev Res (Phila), 2016. **9**(5): p. 396-405.
85. Chung, F.L., M.A. Morse, and K.I. Eklind, *New potential chemopreventive agents for lung carcinogenesis of tobacco-specific nitrosamine.* Cancer Res, 1992. **52**(9 Suppl): p. 2719s-2722s.
86. Hecht, S.S., et al., *Complete inhibition of 4-(methylnitrosamino)-1-(3-pyridyl)-1-butanone-induced rat lung tumorigenesis and favorable modification of biomarkers by phenethyl isothiocyanate.* Cancer Epidemiol Biomarkers Prev, 1996. **5**(8): p. 645-52.
87. Conaway, C.C., Y.M. Yang, and F.L. Chung, *Isothiocyanates as cancer chemopreventive agents: their biological activities and metabolism in rodents and humans.* Curr Drug Metab, 2002. **3**(3): p. 233-55.
88. Cheung, K.L. and A.N. Kong, *Molecular targets of dietary phenethyl isothiocyanate and sulforaphane for cancer chemoprevention.* AAPS J, 2010. **12**(1): p. 87-97.
89. Hu, R., et al., *Identification of Nrf2-regulated genes induced by chemopreventive isothiocyanate PEITC by oligonucleotide microarray.* Life Sci, 2006. **79**(20): p. 1944-55.
90. Konsue, N. and C. Ioannides, *Tissue differences in the modulation of rat cytochromes P450 and phase II conjugation systems by dietary doses of phenethyl isothiocyanate.* Food Chem Toxicol, 2008. **46**(12): p. 3677-83.
91. Konsue, N. and C. Ioannides, *Differential response of four human livers to modulation of phase II enzyme systems by the chemopreventive phytochemical phenethyl isothiocyanate.* Mol Nutr Food Res, 2010. **54**(10): p. 1477-85.
92. Gao, N., et al., *Phenethyl isothiocyanate exhibits antileukemic activity in vitro and in vivo by inactivation of Akt and activation of JNK pathways.* Cell Death Dis, 2011. **2**: p. e140.
93. Loganathan, S., et al., *Inhibition of EGFR-AKT axis results in the suppression of ovarian tumors in vitro and in preclinical mouse model.* PLoS One, 2012. **7**(8): p. e43577.
94. Okubo, T., K. Washida, and A. Murakami, *Phenethyl isothiocyanate suppresses nitric oxide production via inhibition of phosphoinositide 3-kinase/Akt-induced IFN-gamma secretion in LPS-activated peritoneal macrophages.* Mol Nutr Food Res, 2010. **54**(9): p. 1351-60.

95. Cavell, B.E., et al., *Natural product-derived antitumor compound phenethyl isothiocyanate inhibits mTORC1 activity via TSC2.* J Nat Prod, 2012. **75**(6): p. 1051-7.
96. Gupta, P., et al., *Metastasis of Breast Tumor Cells to Brain Is Suppressed by Phenethyl Isothiocyanate in a Novel In Vivo Metastasis Model.* PLoS One, 2013. **8**(6): p. e67278.
97. Gupta, P. and S.K. Srivastava, *Antitumor activity of phenethyl isothiocyanate in HER2-positive breast cancer models.* BMC Med, 2012. **10**: p. 80.
98. Qin, C.Z., et al., *Advances in molecular signaling mechanisms of beta-phenethyl isothiocyanate antitumor effects.* J Agric Food Chem, 2015. **63**(13): p. 3311-22.
99. Cheung, K.L., et al., *PEITC induces G1 cell cycle arrest on HT-29 cells through the activation of p38 MAPK signaling pathway.* AAPS J, 2008. **10**(2): p. 277-81.
100. Chen, P.Y., et al., *Phenethyl Isothiocyanate (PEITC) Inhibits the Growth of Human Oral Squamous Carcinoma HSC-3 Cells through G(0)/G(1) Phase Arrest and Mitochondria-Mediated Apoptotic Cell Death.* Evid Based Complement Alternat Med, 2012. **2012**: p. 718320.
101. Wu, C.L., et al., *Benzyl isothiocyanate (BITC) and phenethyl isothiocyanate (PEITC)-mediated generation of reactive oxygen species causes cell cycle arrest and induces apoptosis via activation of caspase-3, mitochondria dysfunction and nitric oxide (NO) in human osteogenic sarcoma U-2 OS cells.* J Orthop Res, 2011. **29**(8): p. 1199-209.
102. Xiao, D., et al., *Proteasome-mediated degradation of cell division cycle 25C and cyclin-dependent kinase 1 in phenethyl isothiocyanate-induced G2-M-phase cell cycle arrest in PC-3 human prostate cancer cells.* Mol Cancer Ther, 2004. **3**(5): p. 567-75.
103. Hwang, H.J., et al., *Inhibitory effects of caffeic acid phenethyl ester on cancer cell metastasis mediated by the down-regulation of matrix metalloproteinase expression in human HT1080 fibrosarcoma cells.* J Nutr Biochem, 2006. **17**(5): p. 356-62.
104. Yang, M.D., et al., *Phenethyl isothiocyanate inhibits migration and invasion of human gastric cancer AGS cells through suppressing MAPK and NF-kappaB signal pathways.* Anticancer Res, 2010. **30**(6): p. 2135-43.
105. Xiao, D. and S.V. Singh, *Phenethyl isothiocyanate inhibits angiogenesis in vitro and ex vivo.* Cancer Res, 2007. **67**(5): p. 2239-46.
106. Wang, X.H., et al., *Inhibition of hypoxia inducible factor by phenethyl isothiocyanate.* Biochem Pharmacol, 2009. **78**(3): p. 261-72.
107. Syed Alwi, S.S., et al., *In vivo modulation of 4E binding protein 1 (4E-BP1) phosphorylation by watercress: a pilot study.* Br J Nutr, 2010. **104**(9): p. 1288-96.
108. Syed Alwi, S.S., et al., *Differential induction of apoptosis in human breast cancer cell lines by phenethyl isothiocyanate, a glutathione depleting agent.* Cell Stress Chaperones, 2012. **17**(5): p. 529-38.
109. Yeh, C.C., et al., *Phenethyl isothiocyanate enhances TRAIL-induced apoptosis in oral cancer cells and xenografts.* Clin Oral Investig, 2016.
110. Aggarwal, M., et al., *Reactivation of mutant p53 by a dietary-related compound phenethyl isothiocyanate inhibits tumor growth.* Cell Death Differ, 2016. **23**(10): p. 1615-27.
111. Xiao, D., et al., *Phenethyl isothiocyanate-induced apoptosis in PC-3 human prostate cancer cells is mediated by reactive oxygen species-dependent disruption of the mitochondrial membrane potential.* Carcinogenesis, 2006. **27**(11): p. 2223-34.
112. Satyan, K.S., et al., *Phenethyl isothiocyanate (PEITC) inhibits growth of ovarian cancer cells by inducing apoptosis: role of caspase and MAPK activation.* Gynecol Oncol, 2006. **103**(1): p. 261-70.

113. Schriewer, J.M., et al., *ROS-mediated PARP activity undermines mitochondrial function after permeability transition pore opening during myocardial ischemia-reperfusion.* J Am Heart Assoc, 2013. **2**(2): p. e000159.
114. Loor, G., et al., *Mitochondrial oxidant stress triggers cell death in simulated ischemia-reperfusion.* Biochim Biophys Acta, 2011. **1813**(7): p. 1382-94.
115. Trachootham, D., et al., *Effective elimination of fludarabine-resistant CLL cells by PEITC through a redox-mediated mechanism.* Blood, 2008. **112**(5): p. 1912-22.
116. Trachootham, D., et al., *Selective killing of oncogenically transformed cells through a ROS-mediated mechanism by beta-phenylethyl isothiocyanate.* Cancer Cell, 2006. **10**(3): p. 241-252.
117. Xiao, D., et al., *Phenethyl isothiocyanate inhibits oxidative phosphorylation to trigger reactive oxygen species-mediated death of human prostate cancer cells.* J Biol Chem, 2010. **285**(34): p. 26558-69.
118. Tusskorn, O., et al., *Phenethyl isothiocyanate induces apoptosis of cholangiocarcinoma cells through interruption of glutathione and mitochondrial pathway.* Naunyn Schmiedebergs Arch Pharmacol, 2013. **386**(11): p. 1009-16.
119. Lee, J.W. and M.K. Cho, *Phenethyl isothiocyanate induced apoptosis via down regulation of Bcl-2/XIAP and triggering of the mitochondrial pathway in MCF-7 cells.* Arch Pharm Res, 2008. **31**(12): p. 1604-12.
120. Huong le, D., et al., *Effect of beta-phenylethyl isothiocyanate from cruciferous vegetables on growth inhibition and apoptosis of cervical cancer cells through the induction of death receptors 4 and 5.* J Agric Food Chem, 2011. **59**(15): p. 8124-31.
121. Gibson, S.B., et al., *Increased expression of death receptors 4 and 5 synergizes the apoptosis response to combined treatment with etoposide and TRAIL.* Mol Cell Biol, 2000. **20**(1): p. 205-12.
122. Kassie, F., et al., *Effects of garden and water cress juices and their constituents, benzyl and phenethyl isothiocyanates, towards benzo(a)pyrene-induced DNA damage: a model study with the single cell gel electrophoresis/Hep G2 assay.* Chem Biol Interact, 2003. **142**(3): p. 285-96.
123. Gill, C.I., et al., *The effect of cruciferous and leguminous sprouts on genotoxicity, in vitro and in vivo.* Cancer Epidemiol Biomarkers Prev, 2004. **13**(7): p. 1199-205.
124. Hofmann, T., et al., *Modulation of detoxification enzymes by watercress: in vitro and in vivo investigations in human peripheral blood cells.* Eur J Nutr, 2009. **48**(8): p. 483-91.
125. Hecht, S.S., et al., *Effects of watercress consumption on metabolism of a tobacco-specific lung carcinogen in smokers.* Cancer Epidemiol Biomarkers Prev, 1995. **4**(8): p. 877-84.
126. Schuurman, A.G., et al., *Vegetable and fruit consumption and prostate cancer risk: a cohort study in The Netherlands.* Cancer Epidemiol Biomarkers Prev, 1998. **7**(8): p. 673-80.
127. Giovannucci, E., et al., *A prospective study of cruciferous vegetables and prostate cancer.* Cancer Epidemiol Biomarkers Prev, 2003. **12**(12): p. 1403-9.
128. Key, T.J., et al., *Fruits and vegetables and prostate cancer: no association among 1104 cases in a prospective study of 130544 men in the European Prospective Investigation into Cancer and Nutrition (EPIC).* Int J Cancer, 2004. **109**(1): p. 119-24.
129. McCullough, M.L., et al., *A prospective study of whole grains, fruits, vegetables and colon cancer risk.* Cancer Causes Control, 2003. **14**(10): p. 959-70.
130. Michels, K.B., et al., *Prospective study of fruit and vegetable consumption and incidence of colon and rectal cancers.* J Natl Cancer Inst, 2000. **92**(21): p. 1740-52.

131. Flood, A., et al., *Fruit and vegetable intakes and the risk of colorectal cancer in the Breast Cancer Detection Demonstration Project follow-up cohort.* Am J Clin Nutr, 2002. **75**(5): p. 936-43.
132. Voorrips, L.E., et al., *Vegetable and fruit consumption and risks of colon and rectal cancer in a prospective cohort study: The Netherlands Cohort Study on Diet and Cancer.* Am J Epidemiol, 2000. **152**(11): p. 1081-92.
133. Neuhouser, M.L., et al., *Fruits and vegetables are associated with lower lung cancer risk only in the placebo arm of the beta-carotene and retinol efficacy trial (CARET).* Cancer Epidemiol Biomarkers Prev, 2003. **12**(4): p. 350-8.
134. Voorrips, L.E., et al., *Vegetable and fruit consumption and lung cancer risk in the Netherlands Cohort Study on diet and cancer.* Cancer Causes Control, 2000. **11**(2): p. 101-15.
135. Chow, W.H., et al., *A cohort study of tobacco use, diet, occupation, and lung cancer mortality.* Cancer Causes Control, 1992. **3**(3): p. 247-54.
136. Feskanich, D., et al., *Prospective study of fruit and vegetable consumption and risk of lung cancer among men and women.* J Natl Cancer Inst, 2000. **92**(22): p. 1812-23.
137. Gandini, S., et al., *Meta-analysis of studies on breast cancer risk and diet: the role of fruit and vegetable consumption and the intake of associated micronutrients.* Eur J Cancer, 2000. **36**(5): p. 636-46.
138. Smith-Warner, S.A., et al., *Intake of fruits and vegetables and risk of breast cancer: a pooled analysis of cohort studies.* JAMA, 2001. **285**(6): p. 769-76.
139. Ambrosone, C.B., et al., *Breast cancer risk in premenopausal women is inversely associated with consumption of broccoli, a source of isothiocyanates, but is not modified by GST genotype.* J Nutr, 2004. **134**(5): p. 1134-8.
140. Thomson, C.A., et al., *Increase in cruciferous vegetable intake in women previously treated for breast cancer participating in a dietary intervention trial.* Nutr Cancer, 2007. **57**(1): p. 11-9.
141. Nicholson, J.K., J.C. Lindon, and E. Holmes, *'Metabonomics': understanding the metabolic responses of living systems to pathophysiological stimuli via multivariate statistical analysis of biological NMR spectroscopic data.* Xenobiotica, 1999. **29**(11): p. 1181-9.
142. Patti, G.J., O. Yanes, and G. Siuzdak, *Innovation: Metabolomics: the apogee of the omics trilogy.* Nat Rev Mol Cell Biol, 2012. **13**(4): p. 263-9.
143. Holmes, E., I.D. Wilson, and J.K. Nicholson, *Metabolic phenotyping in health and disease.* Cell, 2008. **134**(5): p. 714-7.
144. Beckonert, O., et al., *High-resolution magic-angle-spinning NMR spectroscopy for metabolic profiling of intact tissues.* Nat Protoc, 2010. **5**(6): p. 1019-32.
145. Beckonert, O., et al., *Metabolic profiling, metabolomic and metabonomic procedures for NMR spectroscopy of urine, plasma, serum and tissue extracts.* Nat Protoc, 2007. **2**(11): p. 2692-703.
146. Brindle, J.T., et al., *Rapid and noninvasive diagnosis of the presence and severity of coronary heart disease using 1H-NMR-based metabonomics.* Nat Med, 2002. **8**(12): p. 1439-44.
147. Clayton, T.A., et al., *Pharmaco-metabonomic phenotyping and personalized drug treatment.* Nature, 2006. **440**(7087): p. 1073-7.
148. Claus, S.P. and J.R. Swann, *Nutrimetabonomics:applications for nutritional sciences, with specific reference to gut microbial interactions.* Annu Rev Food Sci Technol, 2013. **4**: p. 381-99.

149. Coen, M., *A metabonomic approach for mechanistic exploration of pre-clinical toxicology*. Toxicology, 2010. **278**(3): p. 326-40.
150. Keeler, J., *Understanding NMR spectroscopy*. 2005, Chichester, England; Hoboken, NJ: Wiley.
151. Reich, H. *5.3 Spin-Spin Splitting: J-Coupling*. 2016 [cited 2016 12/12/2016]; Available from: https://www.chem.wisc.edu/areas/reich/nmr/05-hmr-03-jcoupl.htm.
152. Reusch, W. *Nuclear Magnetic Resonance Spectroscopy*. 2013 6 June 2017]; Available from: https://www2.chemistry.msu.edu/faculty/reusch/virttxtjml/spectrpy/nmr/nmr1.htm.
153. Nicholson, J.K., et al., *750 MHz 1H and 1H-13C NMR spectroscopy of human blood plasma.* Anal Chem, 1995. **67**(5): p. 793-811.
154. Trygg, J., E. Holmes, and T. Lundstedt, *Chemometrics in metabonomics.* J Proteome Res, 2007. **6**(2): p. 469-79.
155. Craig, A., et al., *Scaling and normalization effects in NMR spectroscopic metabonomic data sets.* Anal Chem, 2006. **78**(7): p. 2262-7.
156. Eriksson, L. and A.B. Umetrics, *Multi- and megavariate data analysis*. 2006, UmeÂ, Sweden: Umetrics AB.
157. Cloarec, O., et al., *Evaluation of the orthogonal projection on latent structure model limitations caused by chemical shift variability and improved visualization of biomarker changes in 1H NMR spectroscopic metabonomic studies.* Anal Chem, 2005. **77**(2): p. 517-26.
158. Cloarec, O., et al., *Statistical total correlation spectroscopy: an exploratory approach for latent biomarker identification from metabolic 1H NMR data sets.* Anal Chem, 2005. **77**(5): p. 1282-9.
159. Eriksson, L., et al., *Using chemometrics for navigating in the large data sets of genomics, proteomics, and metabonomics (gpm).* Anal Bioanal Chem, 2004. **380**(3): p. 419-29.
160. Verhoeven, D.T.H., et al., *Epidemiological studies on brassica vegetables and cancer risk.* Cancer Epidemiology Biomarkers & Prevention, 1996. **5**(9): p. 733-748.
161. Boggs, D.A., et al., *Fruit and vegetable intake in relation to risk of breast cancer in the Black Women's Health Study.* Am J Epidemiol, 2010. **172**(11): p. 1268-79.
162. Liu, X. and K. Lv, *Cruciferous vegetables intake is inversely associated with risk of breast cancer: a meta-analysis.* Breast, 2013. **22**(3): p. 309-13.
163. Giallourou, N., M.J. Oruna-Concha, and N. Harbourne, *Effects of domestic processing methods on the phytochemical content of watercress (Nasturtium officinale).* Food Chem, 2016. **212**: p. 411-9.
164. Rose, P., et al., *Broccoli and watercress suppress matrix metalloproteinase-9 activity and invasiveness of human MDA-MB-231 breast cancer cells.* Toxicol Appl Pharmacol, 2005. **209**(2): p. 105-13.
165. Zhang, Y., *Role of glutathione in the accumulation of anticarcinogenic isothiocyanates and their glutathione conjugates by murine hepatoma cells.* Carcinogenesis, 2000. **21**(6): p. 1175-82.
166. Hu, Y., et al., *Mitochondrial manganese-superoxide dismutase expression in ovarian cancer: role in cell proliferation and response to oxidative stress.* J Biol Chem, 2005. **280**(47): p. 39485-92.

167. Xu, C., et al., *Mechanism of action of isothiocyanates: the induction of ARE-regulated genes is associated with activation of ERK and JNK and the phosphorylation and nuclear translocation of Nrf2.* Mol Cancer Ther, 2006. **5**(8): p. 1918-26.
168. Xu, C., et al., *Suppression of NF-kappaB and NF-kappaB-regulated gene expression by sulforaphane and PEITC through IkappaBalpha, IKK pathway in human prostate cancer PC-3 cells.* Oncogene, 2005. **24**(28): p. 4486-95.
169. Jeong, W.S., et al., *Modulatory properties of various natural chemopreventive agents on the activation of NF-kappaB signaling pathway.* Pharm Res, 2004. **21**(4): p. 661-70.
170. Karin, M., *Nuclear factor-kappaB in cancer development and progression.* Nature, 2006. **441**(7092): p. 431-6.
171. Rose, P., et al., *Beta-phenylethyl and 8-methylsulphinyloctyl isothiocyanates, constituents of watercress, suppress LPS induced production of nitric oxide and prostaglandin E2 in RAW 264.7 macrophages.* Nitric Oxide, 2005. **12**(4): p. 237-43.
172. Powolny, A.A. and S.V. Singh, *Differential response of normal (PrEC) and cancerous human prostate cells (PC-3) to phenethyl isothiocyanate-mediated changes in expression of antioxidant defense genes.* Pharm Res, 2010. **27**(12): p. 2766-75.
173. Hong, Y.H., et al., *ROS Accumulation by PEITC Selectively Kills Ovarian Cancer Cells via UPR-Mediated Apoptosis.* Front Oncol, 2015. **5**: p. 167.
174. Moskaug, J.O., et al., *Polyphenols and glutathione synthesis regulation.* Am J Clin Nutr, 2005. **81**(1 Suppl): p. 277S-283S.
175. Hurd, T.R., et al., *Inactivation of pyruvate dehydrogenase kinase 2 by mitochondrial reactive oxygen species.* J Biol Chem, 2012. **287**(42): p. 35153-60.
176. Amelio, I., et al., *Serine and glycine metabolism in cancer.* Trends Biochem Sci, 2014. **39**(4): p. 191-8.
177. Tedeschi, P.M., et al., *Contribution of serine, folate and glycine metabolism to the ATP, NADPH and purine requirements of cancer cells.* Cell Death Dis, 2013. **4**: p. e877.
178. Jain, M., et al., *Metabolite profiling identifies a key role for glycine in rapid cancer cell proliferation.* Science, 2012. **336**(6084): p. 1040-4.
179. Shyh-Chang, N., et al., *Influence of threonine metabolism on S-adenosylmethionine and histone methylation.* Science, 2013. **339**(6116): p. 222-6.
180. Shah, T., et al., *Noninvasive imaging identifies new roles for cyclooxygenase-2 in choline and lipid metabolism of human breast cancer cells.* NMR Biomed, 2012. **25**(5): p. 746-54.
181. Bommareddy, A., et al., *Atg5 regulates phenethyl isothiocyanate-induced autophagic and apoptotic cell death in human prostate cancer cells.* Cancer Res, 2009. **69**(8): p. 3704-12.
182. Azoulay-Alfaguter, I., et al., *Combined regulation of mTORC1 and lysosomal acidification by GSK-3 suppresses autophagy and contributes to cancer cell growth.* Oncogene, 2015. **34**(35): p. 4613-23.
183. Siegel, R.L., K.D. Miller, and A. Jemal, *Cancer statistics, 2016.* CA Cancer J Clin, 2016. **66**(1): p. 7-30.
184. Hoeijmakers, J.H., *Genome maintenance mechanisms for preventing cancer.* Nature, 2001. **411**(6835): p. 366-74.
185. Ohara, M., et al., *Benzyl isothiocyanate sensitizes human pancreatic cancer cells to radiation by inducing apoptosis.* Int J Mol Med, 2011. **28**(6): p. 1043-7.
186. Tripathi, K., et al., *Allyl isothiocyanate induces replication-associated DNA damage response in NSCLC cells and sensitizes to ionizing radiation.* Oncotarget, 2015. **6**(7): p. 5237-52.

187. Katoch, O., et al., *Sulforaphane mitigates genotoxicity induced by radiation and anticancer drugs in human lymphocytes.* Mutat Res, 2013. **758**(1-2): p. 29-34.
188. Hoffman, J.D., W.M. Ward, and G. Loo, *Effect of antioxidants on the genotoxicity of phenethyl isothiocyanate.* Mutagenesis, 2015. **30**(3): p. 421-30.
189. Wang, X., et al., *Phenethyl isothiocyanate sensitizes human cervical cancer cells to apoptosis induced by cisplatin.* Mol Nutr Food Res, 2011. **55**(10): p. 1572-81.
190. Eisa, N.H., et al., *Phenethyl isothiocyanate potentiates anti-tumour effect of doxorubicin through Akt-dependent pathway.* Cell Biochem Funct, 2015. **33**(8): p. 541-51.
191. Gupta, P., et al., *Molecular targets of isothiocyanates in cancer: recent advances.* Mol Nutr Food Res, 2014. **58**(8): p. 1685-707.
192. Janicke, R.U., et al., *Ionizing radiation but not anticancer drugs causes cell cycle arrest and failure to activate the mitochondrial death pathway in MCF-7 breast carcinoma cells.* Oncogene, 2001. **20**(36): p. 5043-53.
193. Moon, Y.J., D.A. Brazeau, and M.E. Morris, *Dietary phenethyl isothiocyanate alters gene expression in human breast cancer cells.* Evid Based Complement Alternat Med, 2011. **2011**.
194. Rainaldi, G., et al., *Metabolomics using 1H-NMR of apoptosis and Necrosis in HL60 leukemia cells: differences between the two types of cell death and independence from the stimulus of apoptosis used.* Radiat Res, 2008. **169**(2): p. 170-80.
195. Rosi, A., et al., *Role of glutathione in apoptosis induced by radiation as determined by 1H MR spectra of cultured tumor cells.* Radiat Res, 2007. **167**(3): p. 268-82.
196. Katz-Brull, R., P.T. Lavin, and R.E. Lenkinski, *Clinical utility of proton magnetic resonance spectroscopy in characterizing breast lesions.* J Natl Cancer Inst, 2002. **94**(16): p. 1197-203.
197. Bolan, P.J., et al., *In vivo quantification of choline compounds in the breast with 1H MR spectroscopy.* Magn Reson Med, 2003. **50**(6): p. 1134-43.
198. Meisamy, S., et al., *Adding in vivo quantitative 1H MR spectroscopy to improve diagnostic accuracy of breast MR imaging: preliminary results of observer performance study at 4.0 T.* Radiology, 2005. **236**(2): p. 465-75.
199. Eliyahu, G., T. Kreizman, and H. Degani, *Phosphocholine as a biomarker of breast cancer: molecular and biochemical studies.* Int J Cancer, 2007. **120**(8): p. 1721-30.
200. Sijens, P.E., et al., *Hydrogen magnetic resonance spectroscopy follow-up after radiation therapy of human brain cancer. Unexpected inverse correlation between the changes in tumor choline level and post-gadolinium magnetic resonance imaging contrast.* Invest Radiol, 1995. **30**(12): p. 738-44.
201. Lindskog, M., et al., *Proton magnetic resonance spectroscopy in neuroblastoma: current status, prospects and limitations.* Cancer Lett, 2005. **228**(1-2): p. 247-55.
202. Podo, F., *Tumour phospholipid metabolism.* NMR Biomed, 1999. **12**(7): p. 413-39.
203. Bao, Y., et al., *Benefits and risks of the hormetic effects of dietary isothiocyanates on cancer prevention.* PLoS One, 2014. **9**(12): p. e114764.
204. Martinez-Sanchez, A., et al., *A comparative study of flavonoid compounds, vitamin C, and antioxidant properties of baby leaf Brassicaceae species.* J Agric Food Chem, 2008. **56**(7): p. 2330-40.
205. Palermo, M., N. Pellegrini, and V. Fogliano, *The effect of cooking on the phytochemical content of vegetables.* Journal of the Science of Food and Agriculture, 2014. **94**(6): p. 1057-1070.

206. Bell, M.J. Oruna-Concha, and C. Wagstaff, *Identification and quantification of glucosinolate and flavonol compounds in rocket salad (Eruca sativa, Eruca vesicaria and Diplotaxis tenuifolia) by LC–MS: Highlighting the potential for improving nutritional value of rocket crops.* Food Chemistry, 2015. **172**: p. 852-861.
207. Singleton, V.L. and J.A. Rossi, *Colorimetry of Total Phenolics with Phosphomolybdic-Phosphotungstic Acid Reagents.* American Journal of Enology and Viticulture, 1965. **16**(3): p. 144-158.
208. Benzie, I.F.F. and J.J. Strain, *The Ferric Reducing Ability of Plasma (FRAP) as a Measure of "Antioxidant Power": The FRAP Assay.* Analytical Biochemistry, 1996. **239**(1): p. 70-76.
209. Lichtenthaler, H.K. and C. Buschmann, *Chlorophylls and Carotenoids: Measurement and Characterization by UV-VIS Spectroscopy*, in *Current Protocols in Food Analytical Chemistry*. 2001, John Wiley & Sons, Inc.
210. Giuffrida, D., et al., *Characterization of 12 Capsicum varieties by evaluation of their carotenoid profile and pungency determination.* Food Chem, 2013. **140**(4): p. 794-802.
211. Aires, A., et al., *Phytochemical characterization and antioxidant properties of baby-leaf watercress produced under organic production system.* CyTA - Journal of Food, 2013. **11**(4): p. 343-351.
212. Hagen, S.F., et al., *Effect of cold storage and harvest date on bioactive compounds in curly kale (Brassica oleracea L. var. acephala).* Postharvest Biology and Technology, 2009. **51**(1): p. 36-42.
213. Gliszczynska-Swiglo, A., et al., *Changes in the content of health-promoting compounds and antioxidant activity of broccoli after domestic processing.* Food Addit Contam, 2006. **23**(11): p. 1088-98.
214. Puupponen-Pimiä, R., et al., *Blanching and long-term freezing affect various bioactive compounds of vegetables in different ways.* Journal of the Science of Food and Agriculture, 2003. **83**(14): p. 1389-1402.
215. Zhang, D.L. and Y. Hamauzu, *Phenolics, ascorbic acid, carotenoids and antioxidant activity of broccoli and their changes during conventional and microwave cooking.* Food Chemistry, 2004. **88**(4): p. 503-509.
216. Turkmen, N., F. Sari, and Y.S. Velioglu, *The effect of cooking methods on total phenolics and antioxidant activity of selected green vegetables.* Food Chemistry, 2005. **93**(4): p. 713-718.
217. Podsedek, A., et al., *Effect of domestic cooking on the red cabbage hydrophilic antioxidants.* International Journal of Food Science and Technology, 2008. **43**(10): p. 1770-1777.
218. Natella, F., et al., *Microwave And Traditional Cooking Methods: Effect Of Cooking On Antioxidant Capacity And Phenolic Compounds Content Of Seven Vegetables.* Journal of Food Biochemistry, 2010. **34**(4): p. 796-810.
219. Vallejo, F., F.A. Tomás-Barberán, and C. García-Viguera, *Phenolic compound contents in edible parts of broccoli inflorescences after domestic cooking.* Journal of the Science of Food and Agriculture, 2003. **83**(14): p. 1511-1516.
220. Bernhardt, S. and E. Schlich, *Impact of different cooking methods on food quality: Retention of lipophilic vitamins in fresh and frozen vegetables.* Journal of Food Engineering, 2006. **77**(2): p. 327-333.

221. Khachik, F., et al., *Separation, Identification, and Quantification of Carotenoids in Fruits, Vegetables and Human Plasma by High-Performance Liquid-Chromatography.* Pure and Applied Chemistry, 1991. **63**(1): p. 71-80.
222. Song, L. and P.J. Thornalley, *Effect of storage, processing and cooking on glucosinolate content of Brassica vegetables.* Food Chem Toxicol, 2007. **45**(2): p. 216-24.
223. Vallejo, F., F.A. Tomás-Barberán, and C. Garcia-Viguera, *Glucosinolates and vitamin C content in edible parts of broccoli florets after domestic cooking.* European Food Research and Technology, 2002. **215**(4): p. 310-316.
224. Jones, R.B., *Effects of postharvest handling conditions and cooking on anthocyanin, lycopene, and glucosinolate content and bioavailability in fruits and vegetables.* New Zealand Journal of Crop and Horticultural Science, 2007. **35**(2): p. 219-227.
225. Verkerk, R., et al., *Effects of processing conditions on glucosinolates in cruciferous vegetables.* Cancer Letters, 1997. **114**(1-2): p. 193-194.
226. Pellegrini, N., et al., *Effect of Different Cooking Methods on Color, Phytochemical Concentration, and Antioxidant Capacity of Raw and Frozen Brassica Vegetables.* Journal of Agricultural and Food Chemistry, 2010. **58**(7): p. 4310-4321.
227. Rouzaud, G., et al., *Influence of plant and bacterial myrosinase activity on the metabolic fate of glucosinolates in gnotobiotic rats.* British Journal of Nutrition, 2003. **90**(2): p. 395-404.
228. Smith, T.K., R. Mithen, and I.T. Johnson, *Effects of Brassica vegetable juice on the induction of apoptosis and aberrant crypt foci in rat colonic mucosal crypts in vivo.* Carcinogenesis, 2003. **24**(3): p. 491-495.
229. Ji, Y., Y. Kuo, and M. Morris, *Pharmacokinetics of Dietary Phenethyl Isothiocyanate in Rats.* Pharmaceutical Research, 2005. **22**(10): p. 1658-1666.
230. Payne, A.C., et al., *Antioxidant assays – consistent findings from FRAP and ORAC reveal a negative impact of organic cultivation on antioxidant potential in spinach but not watercress or rocket leaves.* Food Sci Nutr, 2013. **1**(6): p. 439-44.
231. Ismail, A., Z.M. Marjan, and C.W. Foong, *Total antioxidant activity and phenolic content in selected vegetables.* Food Chemistry, 2004. **87**(4): p. 581-586.
232. Ravasco, P., et al., *Impact of nutrition on outcome: a prospective randomized controlled trial in patients with head and neck cancer undergoing radiotherapy.* Head Neck, 2005. **27**(8): p. 659-68.
233. Ravasco, P., et al., *Dietary counseling improves patient outcomes: a prospective, randomized, controlled trial in colorectal cancer patients undergoing radiotherapy.* J Clin Oncol, 2005. **23**(7): p. 1431-8.
234. Laiakis, E.C., et al., *Development of a metabolomic radiation signature in urine from patients undergoing total body irradiation.* Radiat Res, 2014. **181**(4): p. 350-61.
235. Swann, J.R., et al., *Microbial-mammalian cometabolites dominate the age-associated urinary metabolic phenotype in Taiwanese and American populations.* J Proteome Res, 2013. **12**(7): p. 3166-80.
236. Lees, H.J., et al., *Hippurate: the natural history of a mammalian-microbial cometabolite.* J Proteome Res, 2013. **12**(4): p. 1527-46.
237. Pero, R.W., H. Lund, and T. Leanderson, *Antioxidant metabolism induced by quinic acid. Increased urinary excretion of tryptophan and nicotinamide.* Phytother Res, 2009. **23**(3): p. 335-46.
238. Gonthier, M.P., et al., *Chlorogenic acid bioavailability largely depends on its metabolism by the gut microflora in rats.* J Nutr, 2003. **133**(6): p. 1853-9.

239. Nutley, B.P., P. Farmer, and J. Caldwell, *Metabolism of trans-cinnamic acid in the rat and the mouse and its variation with dose.* Food Chem Toxicol, 1994. **32**(10): p. 877-86.
240. Peters, M.M. and J. Caldwell, *Studies on trans-cinnamaldehyde. 1. The influence of dose size and sex on its disposition in the rat and mouse.* Food Chem Toxicol, 1994. **32**(10): p. 869-76.
241. Walsh, M.C., et al., *Influence of acute phytochemical intake on human urinary metabolomic profiles.* Am J Clin Nutr, 2007. **86**(6): p. 1687-93.
242. Claus, S.P., et al., *Systemic multicompartmental effects of the gut microbiome on mouse metabolic phenotypes.* Mol Syst Biol, 2008. **4**: p. 219.
243. Nicholls, A.W., R.J. Mortishire-Smith, and J.K. Nicholson, *NMR spectroscopic-based metabonomic studies of urinary metabolite variation in acclimatizing germ-free rats.* Chem Res Toxicol, 2003. **16**(11): p. 1395-404.
244. Li, F., et al., *Human gut bacterial communities are altered by addition of cruciferous vegetables to a controlled fruit- and vegetable-free diet.* J Nutr, 2009. **139**(9): p. 1685-91.
245. Peppercorn, M.A. and P. Goldman, *Caffeic acid metabolism by bacteria of the human gastrointestinal tract.* J Bacteriol, 1971. **108**(3): p. 996-1000.
246. Holmes, E., et al., *Human metabolic phenotype diversity and its association with diet and blood pressure.* Nature, 2008. **453**(7193): p. 396-400.
247. Friedrich, N., et al., *Short-term changes of the urine metabolome after bariatric surgery.* OMICS, 2012. **16**(11): p. 612-20.
248. Calvani, R., et al., *Gut microbiome-derived metabolites characterize a peculiar obese urinary metabotype.* Int J Obes (Lond), 2010. **34**(6): p. 1095-8.
249. Alberti, K.G., et al., *The metabolic syndrome--a new worldwide definition.* Lancet, 2005. **366**(9491): p. 1059-62.
250. Yeomans, A., et al., *PEITC-mediated inhibition of mRNA translation is associated with both inhibition of mTORC1 and increased eIF2alpha phosphorylation in established cell lines and primary human leukemia cells.* Oncotarget, 2016.
251. Traka, M. and R. Mithen, *Glucosinolates, isothiocyanates and human health.* Phytochemistry Reviews, 2009. **8**(1): p. 269-282.

Appendix

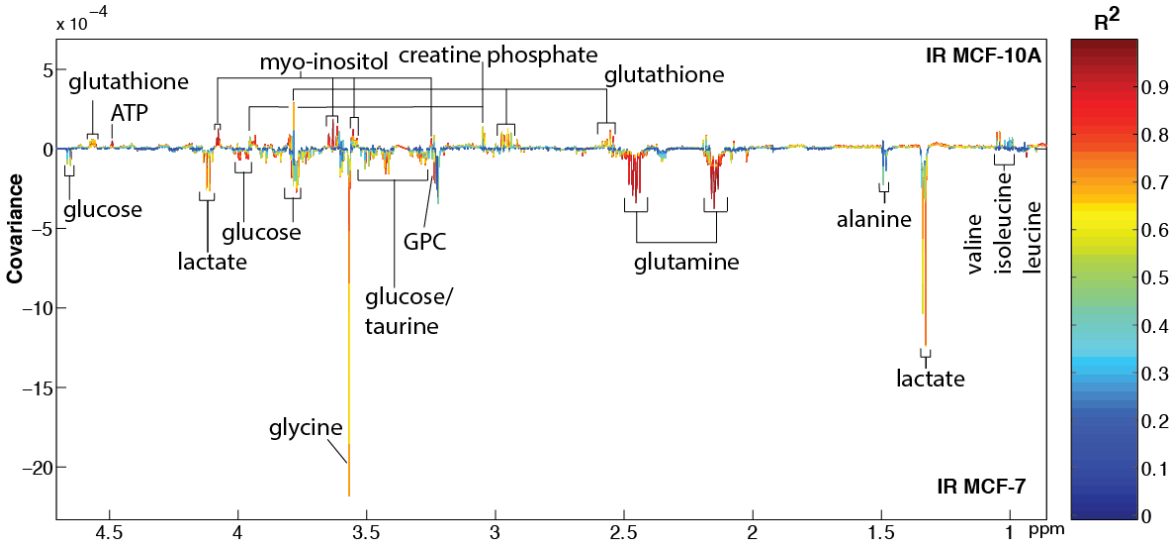

Figure S1 OPLS-DA model comparing the metabolic response of MCF-7 and MCF-10A cells exposed to 5 Gy IR. GPC, glycerophosphocholine

List of Publications

- Omairi, S, A Matsakas, H Degens, O Kretz, KA Hansson, AV Solbrå, JC Bruusgaard, B Joch, R Sartori, **N Giallourou**, R Mitchell, H Collins-Hooper, K Foster, A Pasternack, O Ritvos, M Sandri, V Narkar, JR Swann, TB Huber, and K Patel. "Enhanced Exercise and Regenerative Capacity in a Mouse Model That Violates Size Constraints of Oxidative Muscle Fibres". *Elife*. 5 (2016)

- **Giallourou, N**, MJ Oruna-Concha, and N Harbourne. "Effects of Domestic Processing Methods on the Phytochemical Content of Watercress (Nasturtium Officinale)". *Food Chemistry*. 212 (2016): 411-9

- Kiilerich, P, L S. Myrmel, E Fjære, Q Hao, F Hugenholtz, S B. Sonne, M Derrien, L M. Pedersen, R K. Petersen, A Mortensen, TR Licht, MU Rømer, UB Vogel, LJ Waagbø, **N Giallourou**, Q Feng, L Xiao, C Liu, B Liaset, M Kleerebezem, J Wang, L Madsen and K Kristiansen "Effect of a Long-Term High-Protein Diet on Survival, Obesity Development, and Gut Microbiota in Mice". *American Journal of Physiology*. 310.6 (2016).

- Matsakas, A, D.A Prosdocimo, M.K Jain, R Mitchell, H Collins-Hooper, K Patel, **N Giallourou**, J.R Swann, P Potter, T Epting, and K Patel. "Investigating Mechanisms Underpinning the Detrimental Impact of a High-Fat Diet in the Developing and Adult Hypermuscular Myostatin Null Mouse". *Skeletal Muscle*. 5.1 (2015)

- Collins-Hooper, H, R Sartori, **N Giallourou**, A Matsakas, Robert Mitchell, Helen Mararenkova, Hannah Flasskamp, Raymond Macharia, Steve Ray, Jonathan R. Swann, Marco Sandri, Ketan Patel and A Musaro. "Symmorphosis Through Dietary Regulation: a Combinatorial Role for Proteolysis, Autophagy and Protein Synthesis in Normalising Muscle Metabolism and Function of Hypertrophic Mice After Acute Starvation." *Plos One*. 10.3 (2015)

- Jiang, X, S Jones, BY Andrew, A Ganti, OV Malysheva, **N Giallourou**, PM Brannon, MS Roberson and MA Caudill. "Choline Inadequacy Impairs Trophoblast Function and Vascularization in Cultured Human Placental Trophoblasts." *Journal of Cellular Physiology*. 229.8 (2014): 1016-27.